EXPERIMENTAL AND NUMERICAL EVALUATION OF A MULTI-PAD EVAPORATIVE COOLER

BY

VICTOR CHIJIOKE OKAFOR, B. ENG (HONS.), M. ENG
REG. NO: 20114842788

A THESIS SUBMITTED TO POSTGRADUATE SCHOOL
FEDERAL UNIVERSITY OF TECHNOLOGY, OWERRI.

IN PARTIAL FULFILLMENT OF THE REQUIREMENTS FOR THE AWARD OF DOCTOR OF PHILOSOPHY (Ph.D) IN POWER AND MACHINERY ENGINEERING OF THE DEPARTMENT OF AGRICULTURAL AND BIO-RESOURCES ENGINEERING

MAY, 2021

CERTIFICATION

We certify that this research work and write-up on *"Experimental and Numerical Evaluation of a Multi-Pad Evaporative Cooler"* was carried out by **Okafor, Victor Chijioke (B.Eng., M.Eng)** with Registration Number, **20114842788** is a thesis submitted to the Postgraduate School, Federal University of Technology, Owerri, in partial fulfillment for the award of Doctor of Philosophy in Power and Machinery Engineering in the Department of Agricultural Engineering of the Federal University of Technology, Owerri.

..... **Engr. Prof. G.I. Nwandikom** (Principal Supervisor)	13/05/2021 ..... **Date**
..... **Engr. Prof. N.A.A. Okereke** (Co-supervisor)	17/05/2021 ..... **Date**
..... **Engr. Dr. N.C. Ezeanya** (Co-supervisor)	17/05/2021 ..... **Date**
..... **Engr. Dr. N.C. Ezeanya** (Ag. Head of Department)	17/05/2021 ..... **Date**
..... **Engr. Prof. J.C. Ezeh** (Dean, S.E.E.T.)	17/05/2021 ..... **Date**
..... **Prof. C.C. Eze** (Dean, Postgraduate School)	..... **Date**
..... **Engr. Prof. V.I.O. Ndirika** (External Examiner)	17th May, 2021 ..... **Date**

DEDICATION

To my sister, **Mrs Happiness C. Anokute** and her husband, **Mr Sunday E. Anokute**

ACKNOWLEDGEMENTS

I would like to express my sincere and heartfelt gratitude to GOD Almighty who gave me the strength and unlimited support during the entire period of my study. A great many thanks go to my main supervisor Engr. Prof. G. I. Nwandikom for his continuous support, guidance and motivation. I would also like to thank my other supervisors, Engr. Prof. N.A.A. Okereke and Engr. Dr. C. N. Ezeanya for their support and contributions.

I am indebted to many of my supportive colleagues. They are Engr. Prof. S. N. Asoegwu, Engr. Dr. K. N. Nwaigwe, Engr. Prof. C. C. Egwuonwu, Engr. Dr. K. O. Chilakpu, Engr. Dr. N. R. Nwakuba, Engr. Dr. O. Chukwuezie, Engr. Maxwell Chikwue and Engr. Mrs. G. U. Asonye for their advice, assistance, and moral support.

I am also very grateful to the Federal University of Technology, Owerri for the study fellowship offered to me for this programme.

Finally, I wish to thank my one and only sister, Mrs. Happiness Anokute and her husband Mr. Sunday Anokute for their unselfish, endless love, care and encouragement. I could never have accomplished so much without them.

TABLE OF CONTENTS

LIST OF FIGURES

LIST OF TABLES

LIST OF PLATES

ABSTRACT

An automated open circuit multi-pad wind tunnel controlled by Arduino microprocessor was constructed. The multi-pad test rig is made up of four identical chambers insulated from each other. Each chamber has three zones (air inlet, measurement and air outlet) and consists of 12V dc suction fans, 12V dc water pumps, and pressure, temperature/humidity sensors connected to a programmable circuit board (micro-controller) with a piece of software (integrated development environment, IDE) known as Arduino microprocessor which controls and automates the overall operation of the cooler system through its relay and receives signals from the sensors placed at the measurement zone of the wind tunnel. The inlet and exit temperatures, humidity and static pressure of the air passing through the wetted pad were measured, recorded and displayed on the liquid crystal display (LCD) and transferred to a microcomputer via a universal serial board (USB) cord. The experiment was conducted using the Randomized Complete Block (RCBD) layout. Four (4) cooling pad materials were used for the evaluation of the multi-pad evaporative cooler. The selected cooling pad materials are: (1) Imported rigid media (Celdek), (2) Jute fibre (3) Coconut fibre and (4) Pop sponge. Cooling pad saturation efficiency and static pressure drop across the wetted pad form the two major performance criteria while pad face air velocity (v), pad thickness (t) and water flow rate (w) formed the major treatments (ie factors VTW). Each of the three factors had five levels. For pad face air velocity (v): 0.5, 1.0, 1.5, 2.0 and 2.5m/s; For pad thickness (t): 50, 100, 150, 200 and 150mm and for water flow rate (w): 1.0, 1.25, 1.5, 1.75, and 2.0l/min. Results obtained show that saturation efficiency increases with increasing pad thickness and pad face air velocity for all the pad except for Celdek that showed a slight decrease in saturation efficiency with increasing pad face air velocity. The results of the tests conducted to evaluate the effects of the water flow rate on the saturation efficiency of pad materials indicated that the range of water flow rate chosen had little effect on the saturation efficiency. Saturation efficiency ranged from 51.3% to 80.7%; 56.3% to 83.9%; 54.7% to 80.6%; 46.8% to 71.9% for Celdek, Jute fibre, Coconut fibre and Pop sponge respectively. While Pressure drop ranged from 2.3Pa to 63.2Pa; 11.1Pa to 150.5Pa; 8.3Pa to 130.6Pa and 5.5Pa to 104.7Pa for Celdek, Jute fibre, Coconut fibre and Pop sponge respectively. Central Composite Design in Design Expert 6.0. Statistical Software was used for the statistical analysis while online Tukey's honestly significant difference (HSD) test was used for means separation. Model equations-based on Buckingham π - theorem using multiple regression analysis was developed.

Keywords: Saturation efficiency; Pressure drop; evaporative cooling; cooling pads.

CHAPTER ONE

INTRODUCTION

1.1 Background Information

Evaporative cooling is a process of heat and mass transfer based on the conversion of sensible heat into latent heat by evaporation of water in the air stream (Velasco *et al*., 2010). During the process, as the incoming air passes through the wetted cooling pad, the sensible heat content of the air is utilized to evaporate the water. This brings about a reduction in the dry bulb temperature of air and a corresponding increase in the relative humidity. It is an adiabatic conversion of sensible heat to latent heat.It has numerous applications of environmentcontrol in agriculture, which require more cooling than can be provided by ventilation alone.Where its application is suitable, evaporative cooling systems have the advantage of low energy consumption. It is friendlyto the environment and having low capital and maintenance costs. However, despite all the great potentials exhibited by evaporative cooling systems, it has not been accepted worldwide due to some technical problems.Due to its importance in reducingtheemissionsofcarbon dioxide (CO_2) and chlorofluorocarbons (CFCs) in our environment,it is necessary to improve on the technology.Evaporative cooling utilizes fresh air to replace the air inside our homes many times while the conventional air conditioning systems re-cycle the indoor air. It is cheaper to maintain an evaporative cooling system than conventional air conditioning systems. It is up to 50% cheaper to install and seven times cheaper to run than refrigerated cooling (Vivek, 2011). Since it uses less electricity than other forms of cooling it is more kind to our environment since its greenhouse gas contribution is very low. With the risingsstandard of living, air-conditioning system has become more popular and even a necessity in life to create comfortable environment,and consumed a large amount of energy at the same time. Considering the increasing desire in energy conservation, a more efficient air conditioning technology is highly needed. Evaporative cooling has been regarded as an attractive option, when compared to other existing ones

like vapor compression, absorption/adsorption and thermoelectric refrigeration systems, due to its low cost and high efficiency.

The need for energy is rapidly increasing, and a lot of energy is being spent on everything we do. Energy comes in different forms, like heat, electricity, nuclear energy, light, etc. The increasing demand for world energy causes the depletion of energy resources which adversely affect our environment resulting in global climatic change. Carbon dioxide emissions from burning fossil fuel contribute to global warming of theearth.Pérez-Lombard et al. (2008) stated that in 2004, European countries used about 37%, 28% and 32% of total energy use, on buildings, industry and transportation respectively, while United Kingdom, used about 39% of total energy use on buildings. According to Jiang (2008), 50% of the energy consumption in buildings is used for heating ventilation and air conditioning (HVAC) systems in developed countries. When compared to other sectors, the building sector consumes a large amount of the total primary energy. Energy consumption in buildings stand at between 30–40% of the total primary energy use globally(Pérez-Lombard et al., 2008). Figure 1.1 shows the world energy consumption pattern. From the figure the environmentally friendly renewable energy sources are used much less than fossil fuels. The high demand for fossil fuels will lead to increased CO_2 emission which will have negative impacton our environment.However, energy efficient systems that will reduce energy consumption and CO2 emissions are highly needed. One of these is evaporative cooling systems.

Renewable energies are now receiving attention because of the falling trend in their costs as shown in figure 1.2 as well as being environmentally friendly (Muazu, 2008).Population growth and increasing demand for improvement in living standards, have resulted to increased demand for air conditioning system and as a result newer power generating plant are built to reduce severe strain on electricity grids caused by using more air conditioning systems. Building more power generating plant means more carbon dioxide emission to our environment and the resulting climate change.

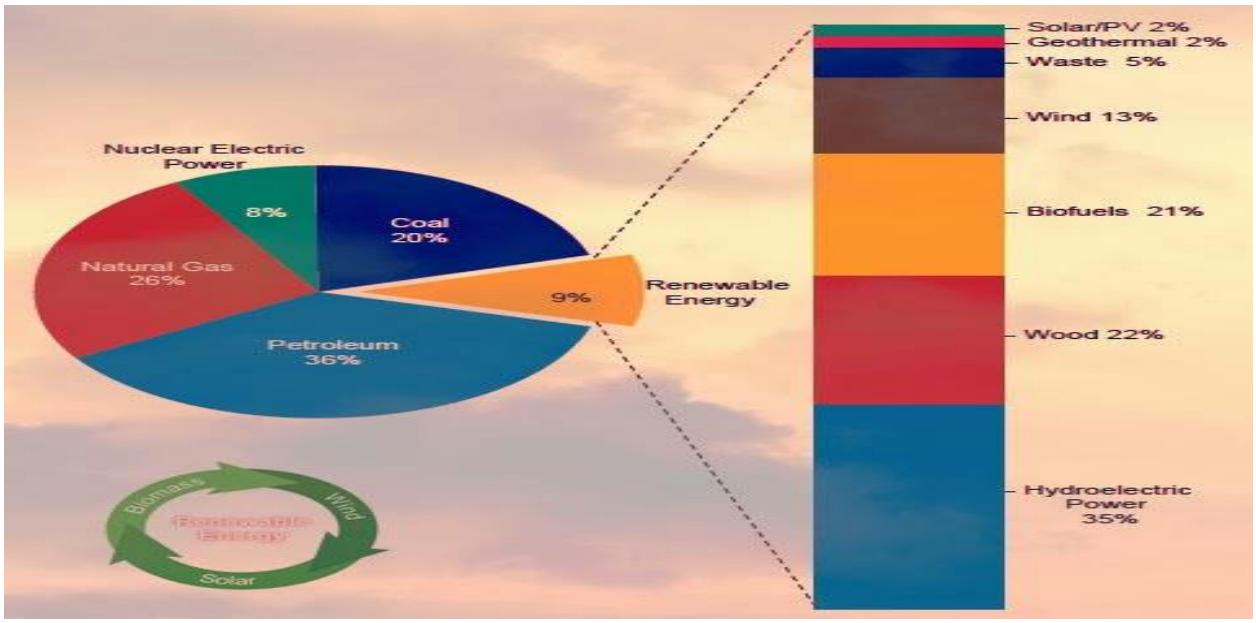

Figure 1.1 Graphical representation of the world energy consumption

Source: Renewable Energy Sources(2018)

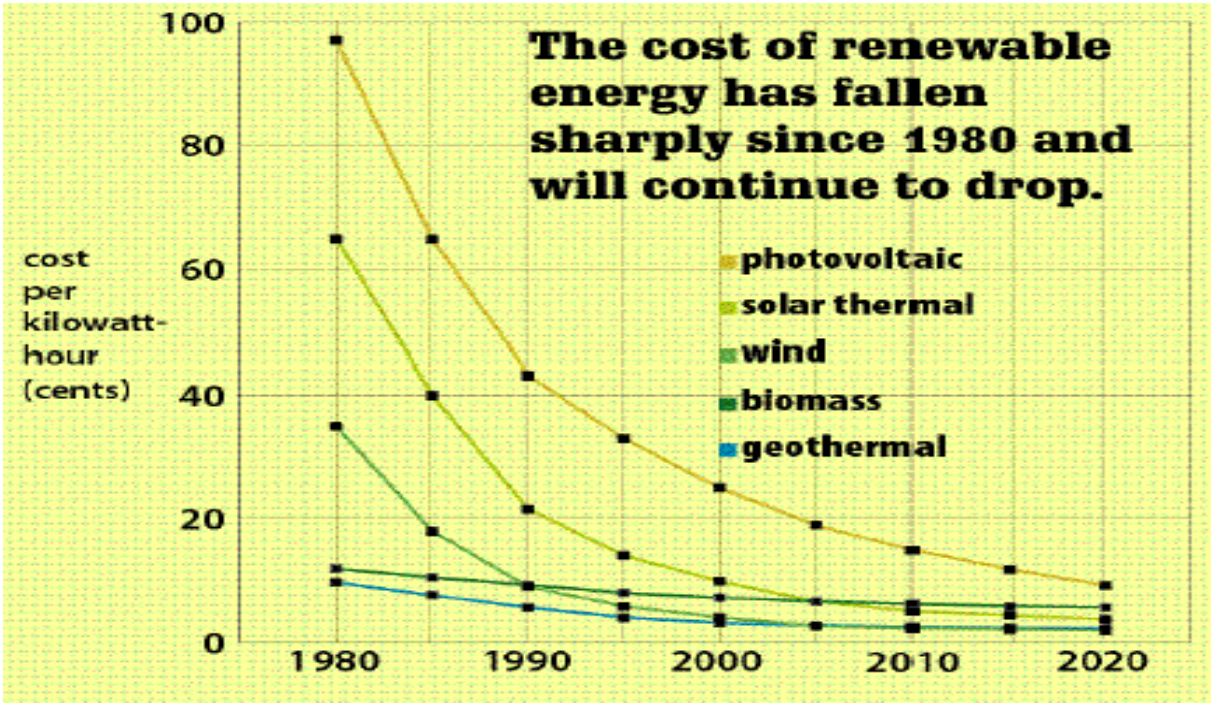

Figure 1.2 Falling trend of renewable energy costs Muazu (2008)

In 1992 at the Environment and Development conference in Rio de Janeiro the European Union discussed about how to stabilize and reducethe emission of carbon dioxide (CO_2) and chlorofluorocarbons (CFCs) into the environment (Muazu, 2008). Majority of the

energy consumption in building for cooling or heating is derived from fossil fuels. It is therefore very vital to provide a less energy intensive system for space cooling in order to reduce dependency on the conventional vapour compression air conditioning systems.

Reducing heat generated while operating engineering systems has become a great concern and have been undercontinuous investigation. Evaporative cooling is an alternative cooling system for the cooling of engineering systems in operation because of its simplicity and power saving benefits (Chukwueke et al., 2012). Evaporative cooling is economical, energy efficient and friendly to the environment.

While vapor compression cooling systems decreases both temperature and humidity, evaporative cooling decreases less temperature and increases humidity. However, evaporative cooling system is more suitable with agricultural activity which does not require much lower temperature.

The quality and quantity of agricultural production is mainly limited due to constraints imposed on the products by the environmental conditions of agricultural buildings. Some of the environmental conditions are relative humidity, temperature, light intensity, and some harmful gases in the ambient air (Al-Amri, 2000).

In hot weather the temperature of air inside agricultural buildings may exceed 40^0 C resulting heat stress. In greenhouses, heat stress affects stem strength, fruit set and size and flowering. In animal buildings, heat stress reduces feed consumption, decreases weight gain, milk and egg yields (Al-Amri, 2000). However, various systems have been designed to reduce air temperature and minimize heat stress of plants and animals. The application of evaporative coolers can reduce such temperatures within the range of 4^0C–13 ^{0}C (Ugurlu and Kara, 2000; O¨ztu¨rk, 2003).Thus, evaporative cooling is generally more efficient where the relative humidity is low the air temperature is high (Dzivama et al., 1999).

Evaporative cooling is one of the common ways that can be usedto reduce heat stress inside the agricultural structures (Darwesh et al., 2009). The application of evaporative cooling systems in agricultural buildings isincreasing in most countries, but this increase has been hindered due to high cost of commercial pad materials. The performance of

evaporative cooling is mainly dependent on such factorsaswater flow rate, pad material,pad thickness and density, pad face-air velocity and weather conditions (Darwesh et al., 2009).High flow rate of water increases the pressure drop. This is because water tends to fill the pore spaces on the pad and consequently retard the flow of air.Padporosity is improved by increasing the pad density resulting in more uniform distribution of water. Increasing pad thickness increases the pressure drop as well as increasing the air-water contact time of air passing across the pad. As air passes through morepad thickness, its water content increases thus decreasing the vapor pressure difference and consequently decreasing the evaporation rate.Air velocity passing across the pads varies at different points within the pad and it is difficult to measure. The velocity entering or exiting from the padis much easier to measure and is commonly used to define pad velocity. Generally, an evaporative cooling pad system must reduce the air temperature to the preferred point using the least power consumption and expenses. Thus, the suitable pad media must have the highest evaporative cooling efficiency and lowest airflow resistance.

1.2 **Problem Statement**

High air temperatures in agricultural buildingscause thermal stress on plants and animals. In animal houses thermal stress reduces feed consumption, decreases weight gain, milk and egg yields. In greenhouses thermal stress affect stem strength, fruit set and size as well as poor flowering.However, the most appropriate cooling system in use today is the commercial vapour compression systems that are intensively power-consuming. These systems consume a lot of energy and produce harmful effect on environment by damaging ozone layer.Therefore, an alternative source of cooling system that is energy efficient and friendly to our environment is highly desirable. Evaporative cooling system is a good option but the high cost of commercial cooling pad has been a major factor limiting the use of evaporative cooling to mitigate the negative effect of thermal

stress.The low cost and easy-to-find materials, that have potential of being used as wetted pad for evaporative cooling system, are necessary for agriculture. However, there is need to develop an evaporative cooler test rig for evaluating the suitability of local pad materials.This study investigated the evaporative cooling efficiency and pressure drop of some locally available materials to be used as alternative cooling pads.

1.3 **Objectives of Study**

The main objective of this work is numerical and experimental evaluation of a multi-pad evaporative cooler.

The specific objectives include:

(1) Construction of test rig and its instrumentation.

(2)Evaluation of pad materials in terms of saturation efficiency and static pressure drop using different treatments of pad thickness, pad-face air velocity and water flow rate.

(3)To develop simple mathematical correlations for predicting the saturation efficiency, pressure drop of the various cooling pads at any desired mass flow rate, pad thickness,pad face air velocity, water flow rate and given ambient condition.

(4) To validate the models with experimental data.

1.4 **Justification of Study**

With the rising living standard, air-condition system has become more popular and even a necessity in life to create comfortable environment, and consumed a large amount of energy at the same time. Given the ever-increasing urgency in energy conservation, a more efficient air conditioning technology is obviously highly desirable. Due to its low cost and potential high efficiency, evaporative cooling has been viewed as an alternative option, when compared to vapor compression air-conditioning systems. Through ECS superior cooling and ventilation can be provided with minimal energy consumption and without the use of chlorofluorocarbons (CFCs). Around the globe, evaporative air-

cooling residential units can save at least 118 million pounds of HCFC-22. These residential coolers save approximately 60 million barrels of oil annually and 27 billion pounds of annual CO_2emissions in lieu of using vapor-compression air-conditioning systems (Foster, 1995). Therefore, there is a need to develop a multi-pad evaporative cooling test rig for evaluating the suitability of our locally available cheap materials that can be used as cooling media. A multi - pad test rig incorporated with electronically controlled units and microprocessors that control and automate the overall operation of the cooling system in which the water flow rate, air flow rate as well as other cooling parameters of temperature, relative humidity, and static pressure drop across the cooling pad media can be displayed and monitored on-screen, measured and recorded for efficient and effective cooling operation justify its usage for evaluating the suitability of alternative local materials for use as evaporative cooling media. Furthermore, the ability to use the data generated using the multi - pad test rig to model the cooling process and predict the cooling efficiency and static pressure drop for each of the selected cooling pad media also justify the study.

1.5**Scope of Study**

This study covered the development of a multi- pad test rig and evaluation of the cooling efficiencies and static pressure drop across some selected evaporative cooling pad media.Evaluation of the selected pad materials to establish the optimum design specification, and development of simple model equations for predicting the performance parameters. It will further consider the effect of air flow rate, water flow rate and pad thickness on the performance parameters (Saturation efficiency and Pressure drop). Also, model validation with experimental data to achieve better understanding of the interaction of the factors on the performance of the cooling pads will be studied.

CHAPTER TWO

LITERATURE REVIEW

2.1 **Evaporative Cooling Process**

When non saturated air-vapour mixtures come in contact with water, heat and mass transfer occur. The rate of this transferdepends on the temperature difference and vapour pressure difference between the water and air-vapour mixture. Since the vapour pressure of the water is higher than that of the unsaturated air, vapour moves from the water to the air. The transfer involves a change of state from liquid to vapour requiring heat of vaporization. The sensible heat of the air is used for the evaporation of the water, thus changing from sensible heat to latent heat of vaporization (i.e., heat transfer). However, as water changes to vapourduring the process, the air carries away the vapour and becomes more humid (i.e. mass transfer). When air becomes saturated with water vapourat the prevailing temperature, dynamic equilibrium will result. The underlying principle of evaporative cooling is based on the conversion of sensible heat into latent heat by evaporation of water in the air stream (Velasco *et al*., 2010). There is no gained or lost of energy, however, as the air provides the energy to evaporate water its temperature decreases. Since no external heat is addedthe process is known as adiabatic saturation which is achieved by converting the sensible heat of the air to latent heat.The enthalpy or total heat remains the same and since the amount of heat removed from the air cannot be greater than the latent heat required to saturate the air with water vapour at the prevailing temperature, there should be a limit to the cooling achieved by adiabatic saturation of air. Thus, the cooling potential is influenced by the water content of the air and is limited to the wet-bulb temperature of the incoming air (Velasco *et al*., 2010). In order to evaporate water, the heat need is gotten from whatever surface the water comes in contact with. Removing heat from an object will make the temperature of that object to

decrease.Muazu(2008) reported that the amount of heat required to evaporate one gallon(4.547liters) is about 9179.022KJand that evaporative cooling can remove tremendous amount of heat from the air. Typical evaporative cooling process is shown in figure 2.1.

2.2 **Methods of Evaporative Cooling System.**

Basically, three main methods of evaporative cooling exist: 1) Directevaporative cooling (DEC), (2) Indirect evaporative cooling (IEC) and (3)Direct/ indirector hybrid evaporative cooling.

2.2.1**Direct evaporative cooling (DEC):**

In this method,non-saturated air-vapor mixtures is drawn across porous wetted pads and during the process the air sensible heat energy is used to evaporates some water, reducing the air's dry-bulb temperaturewhile its moisture content increases. In this process, the energy in the air does not change. The latent heat follows the water vapour and diffuses into the air.Twotypesof direct evaporative cooling systems are: The passive direct evaporative cooling systemin which natural wind velocity provide the means of air movement across the wetted pad and non-passive direct evaporative cooling systemthat uses either a blower or a suction fan to force the air across the wetted pad. In direct evaporative cooling system moisture is added to the cool air, thus creating uncomfortable conditions for human being (Maheshwari *et al.,* 2001). Figure 2.2 shows the detailed components of direct evaporative cooler. During operation, as the blower blows air to the house to be cooled the pressure inside the cooler decreases causing ambient air to traverse across the wetted cooling pads. The temperature of air is lowered in the process as its sensible heat content is used to evaporate water. The float is used to maintain the water level in the sump while the recirculation pump pumps water from the sump via the distribution linesto the top of the cooling pad. The water drips through the evaporative pads by gravity back to the sump. Figure 2.3 shows the direct evaporative cooling process on a psychometric chart. Point A represents theinlet air condition before entering the cooling pad. Point B^* represents the actual air condition after leaving the cooling pad.

Point B represents the theoretical/idealair condition after leaving the cooling pad corresponding to 100% cooling efficiency.

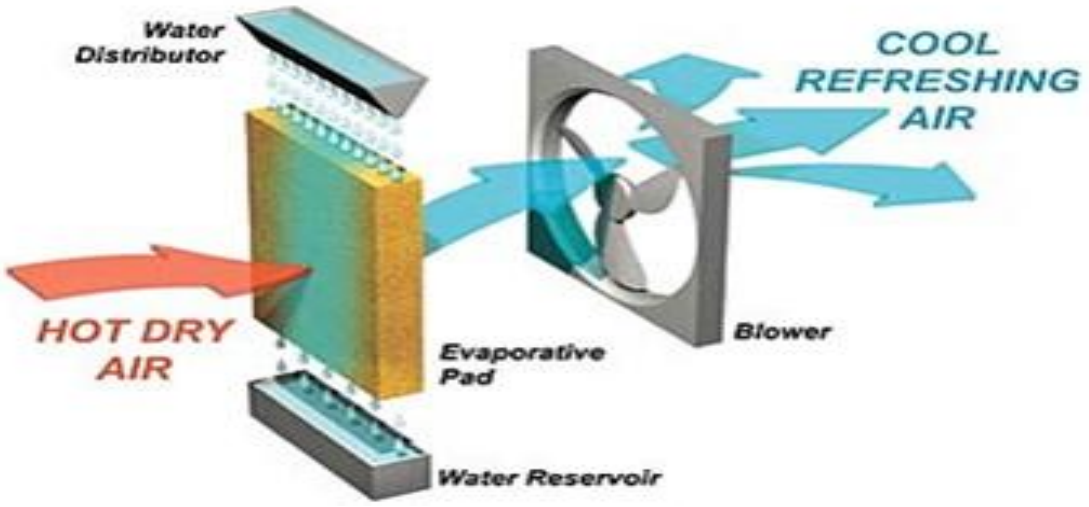

Figure 2.1 Basic evaporative cooling processes (Sreeram, 2014)

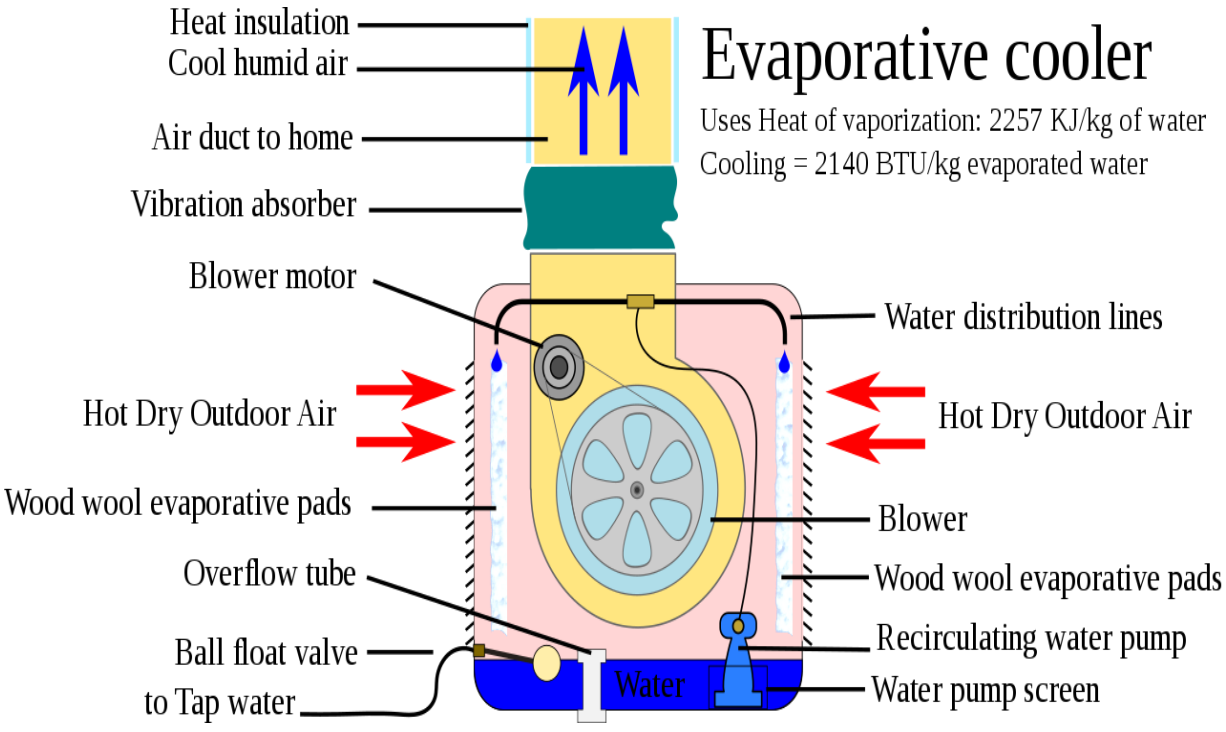

Figure 2.2 Detailed components of direct evaporative cooler(Givoni, 1994)

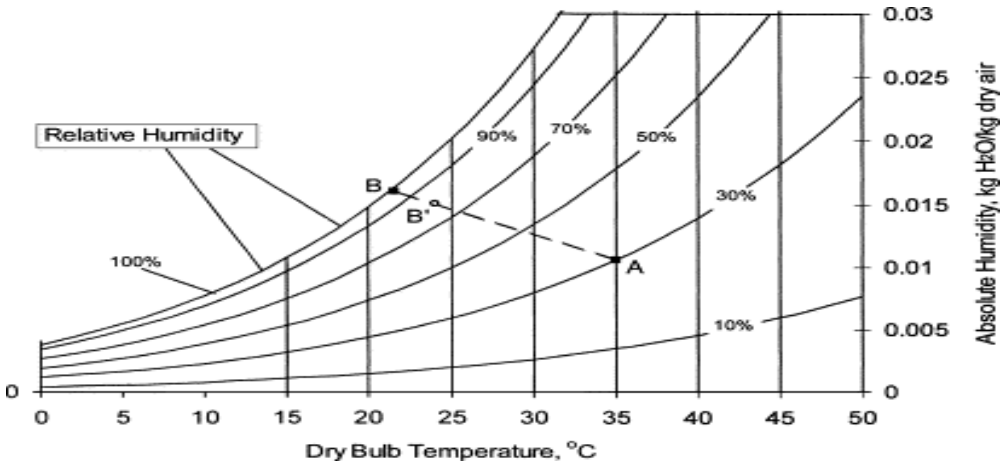

Figure 2.3Direct evaporative cooling process on a psychometric chart(Muazu, 2008)

2.2.2**Indirect evaporative cooling (IEC)**

On the other hand, an indirect evaporative cooling system provides cooling without addinganymoisture making it more attractive than direct evaporative system. However, the cooling effectiveness is generally low, around 40–60% (Maheshwari *et al.*, 2001). It uses direct evaporative cooling in combination with heat exchanger to transfer the cool energy to the supply air. The cooled moist air from the direct evaporative cooling does not come in direct contact with the supply air. The Maisotsenko cycle employs a multi-step heat exchanger to reduce the temperature of the air below the wet-bulb temperature.

Figure 2.4 shows a simple schematic of an indirect evaporative cooler. From figure 2.5 the primary (product) air passes through the dry channel of the heat exchanger, and the secondary (working) air passes through the wet channnel. The heat energy required for evaporation on the wet surface is absorbed from the dry side air and thus the dry side air temperature decreases. At the same time the latent heat of the vaporized water diffuses into the working air in the wet-sideand is prevented from entering the building space to be cooled (Zhiyin *et al.*, 2012). However since the temperature of the air falls, its relative

humidity will increase but cannot be as that under the direct evaporative cooling process.

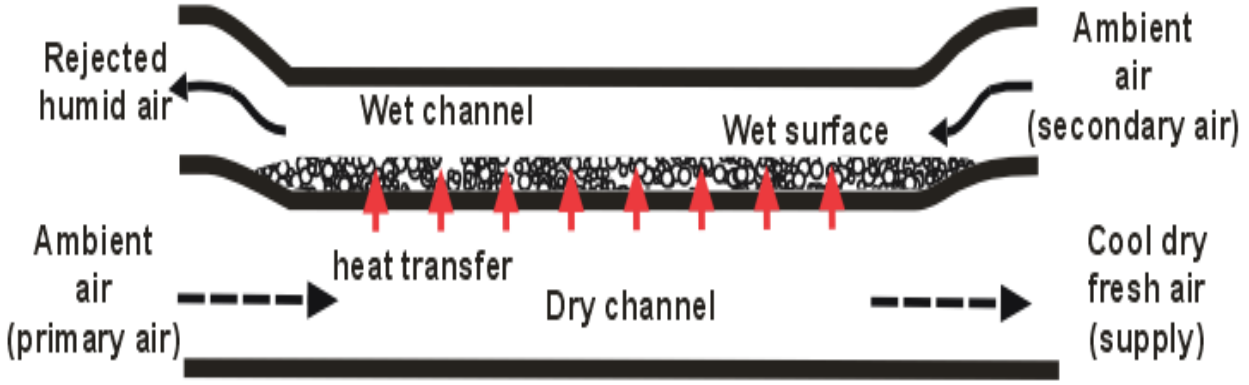

Figure 2.4 A simple schematic of an indirect evaporative cooler (Boukhanouf *et al.*,2014)

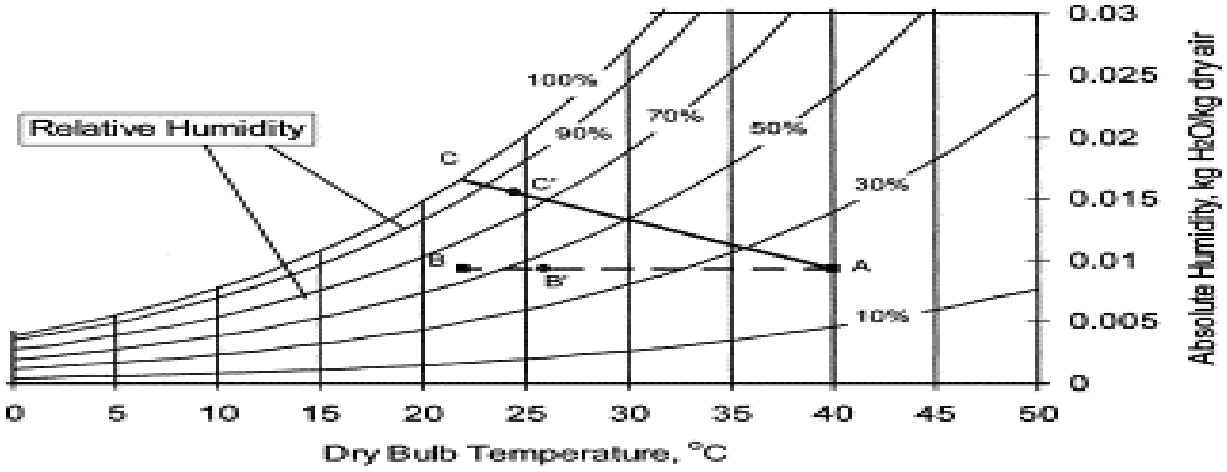

Figure 2.5Indirect evaporative cooling processes on a psychometric chart (Muazu, 2008).

Figure 2.5 shows theindirect evaporative cooling processes on a psychometric chart.Line (AC') shows the secondary air actual path while line (AC) represents the secondary air ideal path. Line (AB')shows the primary air actual path while line (AB) represents the primary air ideal path. It can be seenthat path (AB') follows approximately the line of the moisture content of the air which remains constant between point A and point B', whilethedry bulb air temperature decreases from 40 ^{0}C to 26 ^{0}C without increasing its water content. The effectiveness of indirect evaporative coolers is much lower in comparison with direct evaporative cooler, and even in a well-designed indirect evaporative cooler, the supply air could be cooled to within 2 to 5^{0}C of the wet bulb

temperature. This constitutes a severe thermodynamic limitation. The effectiveness of indirect evaporative cooler may range from 40% to 80% and this limitation has led several researchers to develop and modify the thermal process of indirect evaporative cooling system.

2.2.3**Indirect / direct evaporative cooling**

In this method the hot air is first pre-cooled indirectly without adding moisture by passing through a heat exchanger which is being cooled on the outsideby evaporation. During the direct stage, the pre-cooled air passes across a wetted pad and moisture is added to the air as it cools. Since the air supply is pre-cooled in the first stage without adding moisture, less moisture is added in the direct stage, to reach the desired cooling temperatures.

Depending on the weather conditions and the intended use, indirect / direct evaporative coolers might be usedto increase the cooling effect(Abbouda and Almuhanna, 2012). In places where the higher ambient humidity does not permitlow indoor temperatures from a direct evaporative air-conditioner, combining indirect and direct processes can be more appropriate. Figure 2.6 shows an Indirect/direct evaporative cooling system.

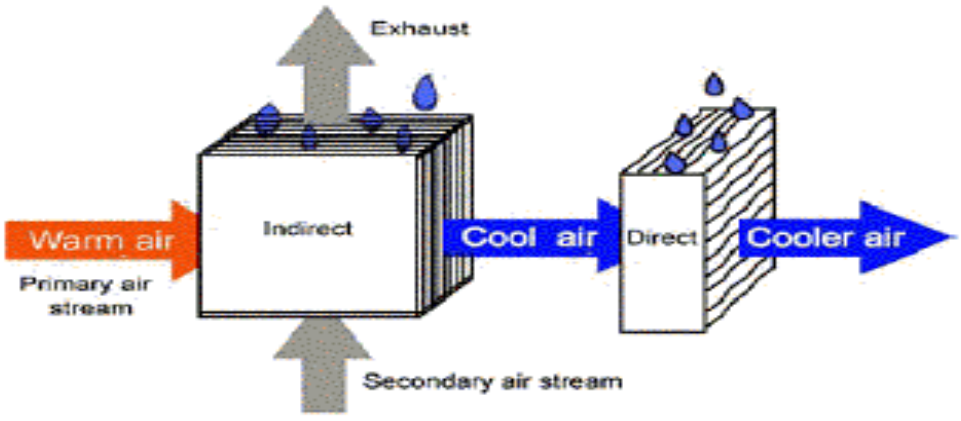

Figure 2.6: Indirect/direct evaporative cooling system. Muazu (2008)

In hot weather air conditions, the supply air from the indirect evaporative coolers presents a dry bulb temperature over 21ºC and its relative humidity below 50 %. Thus, it may be necessary to introduce direct evaporative cooling process that will further decrease the temperature.

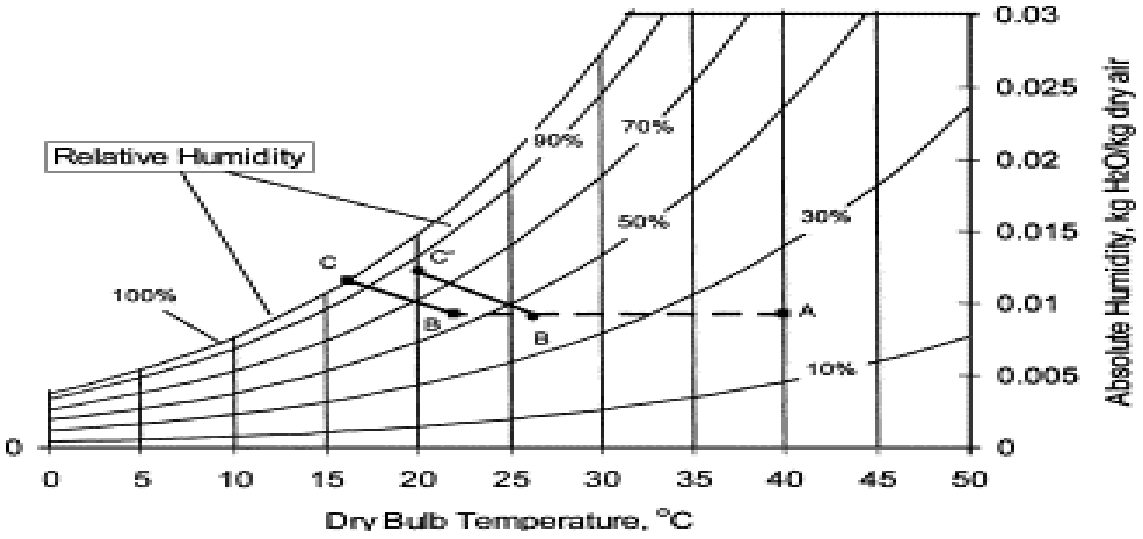

Figure 2.7: Cooling path indirect/direct evaporative cooler on psychrometric chart (Muazu, 2008)

From figure 2.7, line AB indicates the ideal path for the indirect stageand line BC the ideal path for the direct stageboth corresponding to 100% efficiency. LineAB'is the actual path for the indirect line B'C'is the actual path for the direct stagebothcorresponding to actual operating efficiency.

2.2.3.1 **Dew point evaporative cooling based on Maisotsenko-cycle (M cycle)**

In order to improve the effectiveness of wet-bulb temperature a novel thermodynamic cycle,wasinventedby Maisotenko(i.e. Maisotenko-cycle). The designconsistsofmulti-perforated cross-flow plate heat exchanger and can reduce theairtemperature below the wet bulb and above the dew point of the cooling air, without adding humidity to the supply medium hence, the name" dew point evaporative cooling (Maisotsenko et al., 2003)".

The heat and mass transfer process ofthis heat exchanger are shown in figure 2.8.

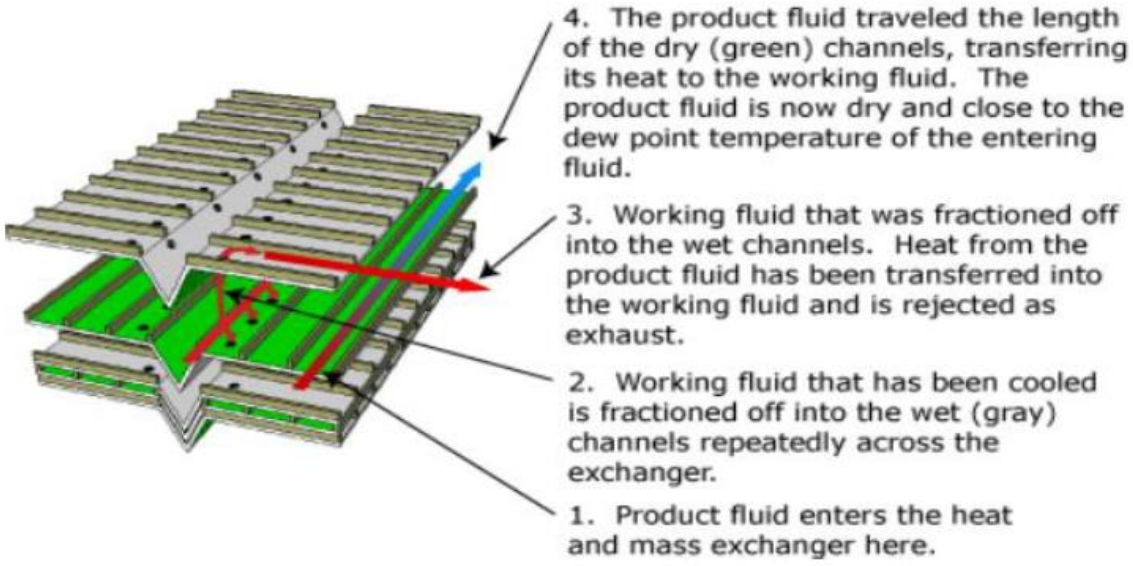

Figure 2.8The heat and mass transfer process of heat exchanger, (M-cycle)(Maisotsenko et al., 2003)

Figure 2.9shows the principle and psychometric representation of an ideal M-cycle. Both the working and product air have the same inlet condition. At stage 1 the intake and working air passes through the dry side of a perforated plate. As the working air passes across the dry side it's temperature decreases and is partially diverted to the wet side via the perforations thus changing from state1 to state 3'. Only small amount of the working air reaches the end of thedry working air channel and is also diverted to the wet side. The wet side temperature is lowerand as a result it absorbs heat from its two adjacent sides for evaporatingthe water, thus changing from state 3' to 3''. The working air undergoes an isothermal humidification process from state 3' to 3''and another change from 3'' to 3 as a result of transfer of sensible heat from the adjacent air streams.At the same time, the product air is cooled from state 1 to 2 as it passes through over the other adjacent dry side.

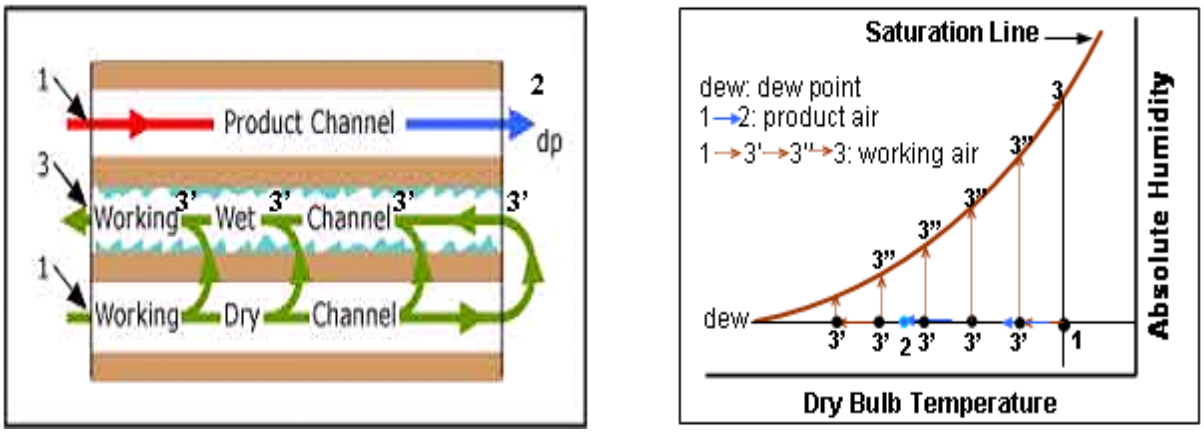

Figure. 2.9 Principle of the heat and mass exchanger based on M-cycle and its representation on psychrometric chart (Coolerado, 2006).

2.2.3.2 **Desiccant based evaporative cooling**

A desiccant material is one that absorbs and holds water vapour. The process by which moisture is absorbed in the desiccant material can be classified as absorption or adsorption depending on whether the process goes through a chemical or a physical change (Amir and Ali, 2006). This system involves placing the adsorptive material like silica gel on the desiccant wheel. This adsorptive material removes water vapour from the ambient air thus decreasing the specific humidity while the dry bulb temperature remains almost unchanged. During the process the dried air become hot and has to be cooled to a lower dry bulb temperature by removing the excess heat. This can be achieved by using indirect evaporative cooling and by passing it through a direct evaporative cooling the air becomes cooler and re-humidified. For continuous operation the desiccant material must be regenerated (i.e. water must be removed from it constantly). This can be done by heating in an unsaturated air stream. The material is then cooled so that it will be able to absorb moisture again for the process to continue (Amir and Ali, 2006).

2.2.3.3 **Dehumidification**

In some application theincrease in moisture content of the cool air associated with direct evaporative cooling can be undesirable. However, it may be necessary to remove the excess moisture. Dehumidification is amethod for decreasing the level of moisture from a direct evaporative cooling system. It can be achievedin the following ways.

a) By injectingdrier air into the space in order to dilute the higher humid air.

b) By extracting the latent heat in the form of water vapour from the air while an equal amount of sensible heat in the form of raised temperature is added.

2.3 **Evaporative Pad Materials**

Evaporative cooling pad has a cross-flow arrangement structure that is used for cooling purposes. It is a permeable screen of porous material that is saturated with water by an irrigation-like system installed at the top. A good pad material should be porous enough to allow free flow of air with minimal resistance. It should be able to absorb water and release it for evaporation. It should have maximum amount of wetted surface area for an adequate period of air water contact time to achieve near saturation. As air and water come in contact, the air loses its sensible heat that changes the temperature and gains an equal amount of latent heat of vapour. The main functions of the cooling pads are: (i) to provide the surface area for cross flowof water and air (ii) to regulate the downward movement of water ensuring that the exchange process last longer and to provide more latent heat flow.The structural setup is so designed that it facilitates easy contact of air and water. Cooling pads come in different shapes and sizes and also vary in its material types. Some of them include Aspen pads, Cellulose pads Glasdek pads etc.

A wide range of material types can be used as a cooling medium to evaporate water, i.e. metal, fibre, ceramics, zeolite and carbon. Several commercially available pad designs can be classified as either rigid or non-rigid media. Non-rigid media include pads made of hog hair, rubberized hog hair, and aspen shavings etc. Rigid media include pads made of aluminum, plastic fibre, and corrugated cellulose paper glued in such a way that air flows through small tunnels or flutes. The main characteristics used to rate a pad are: (i)

cost, (ii) life, (iii) pressure drop, and (iv) efficiency. The more efficient a pad at a given air velocity, the more cooling it will provide. Evaporation (saturation) effectiveness is a property that determines how close the air being conditioned is to the state of saturation. Pad efficiency is defined by equation (2.1) as the ratio of the actual temperature drop across the pad to the maximum temperature drop possible across the pad, or percentage change in saturation level of air as it passes through the pad (ASHRAE, 2007). This can be expressed as:

Saturation Efficiency $(\dot{\eta}_{sat}) = \frac{T_{db} - T_c}{T_{db} - T_{wb}} \times 100$(ASHRAE, 2007) 2.1

where,

T_c = dry-bulb temperature of air exiting from pad, (^{0}C)

T_{db} = dry-bulb temperature of air entering the pad, (^{0}C)

T_{wb} = wet-bulb temperature of air entering the pad,(^{0}C)

Two major types of commercial pad in use are Aspen Pad and Rigid Medium Cellulose Pad. There are many studies on locally available materials evaluated to provide alternative pad media.Dagtekin et al. (1998) studied on somelocally available materials like cardboard, hazelnut rind and wood shavings and got efficiencies of (79%), (48%) and (69%) respectively for the studied materials.

Al- Sulaiman(2002) worked on palm fibreandjute and got efficiencies of 38.9%, and 62.1% respectively. Tinoco et al. (2001) worked on expanded clay, sawdust, vegetable fiber and coal. Mekonnen (1996) carried out research on clay particles, wood shavings and sack. Dzivama et al.(1999) worked on ground sponge, stem sponge, jute fiber and charcoal. Their results revealed that stem sponge showed superior pad material qualities compared to the ground sponge, jute fiber and charcoal.

Tinoco et al. (2001)reported that when compared with the cellulose pads,expanded clay

and vegetable fiber were recommended as pad materials for evaporative cooling systems.Figure 2.10 shows some evaporative cooling pads.

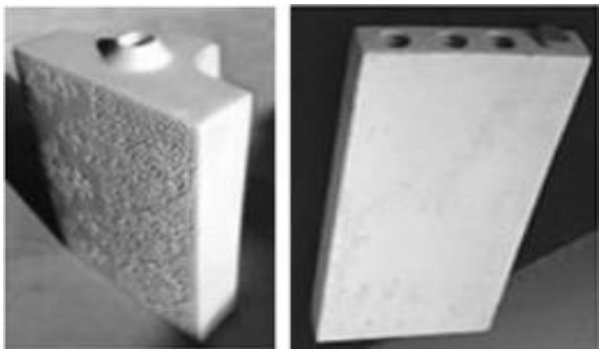

(1) Porous ceramic (Schiano-phan, 2009)

(2) cellulose pad(Amer et al., 2015)

(3) Luffa sponge (Al-Sulaiman, 2002)

(4) Palm dates fibers (Al-Sulaiman, 2002)

(5) Aspen pad(Amer et al., 2015)

Figure 2.10. Some evaporative cooling pads

2.3.1**Porous ceramic materials**

Porous ceramic structures developed by combining various chemical elements and binders such as alumina ($Al_2 O_3$), silicon oxides (SiO_2), silicon nitrides ($Si_3 N_4$) and non-silicate glasses, are widely used in evaporative cooling applications. Being corrosion-resistant, lightweight, widely available and inexpensive as well as having accurately controlled porosity, elevated temperature capability, they can be produced in a variety of shapes and sizes to specific requirements.They can withstand harsh conditions and they were mainly designed to be a fully integrated and functional building element.

Figure 2.12 shows a ceramic container used by Schiano-Phan, who investigated the cooling properties as an integral part of a building's fabric. In a similar way, Ibrahim et al. (2003)applied porous ceramic samples for direct evaporative cooling in buildings. Furthermore, both authors Schiano-Phan (2009) and Ibrahim et al.(2003) measured the porosity of ceramic container prototypes by using the following mathematical expressionasstated in equation 2.2.

$$P = \frac{\mathrm{W-D}}{\mathrm{W-I}} \quad 2.2$$

Where,

P = porosity; w= wetted weight; D = dry weight of each prototype; and I= immersed weight (i.e. weight of water displaced when immersed in water) of each prototype.

The effect of porosity on the cooling performance of the ceramic evaporative cooler was investigated byIbrahim et al.(2003). Their results show that high porosity materials can achieve superior cooling capacities. Its availability makes it possible to be used widely in evaporative cooling applications. Figure 2.11shows the porous ceramic samples used by Schiano-Pha while figure 2.12shows porous ceramic panel installed in a building.

2.3.2 **Application of cooling pads**.

Evaporative cooling pads are mainly applied on evaporative coolers that can be installed on a window of a building as shown in figure2.13.

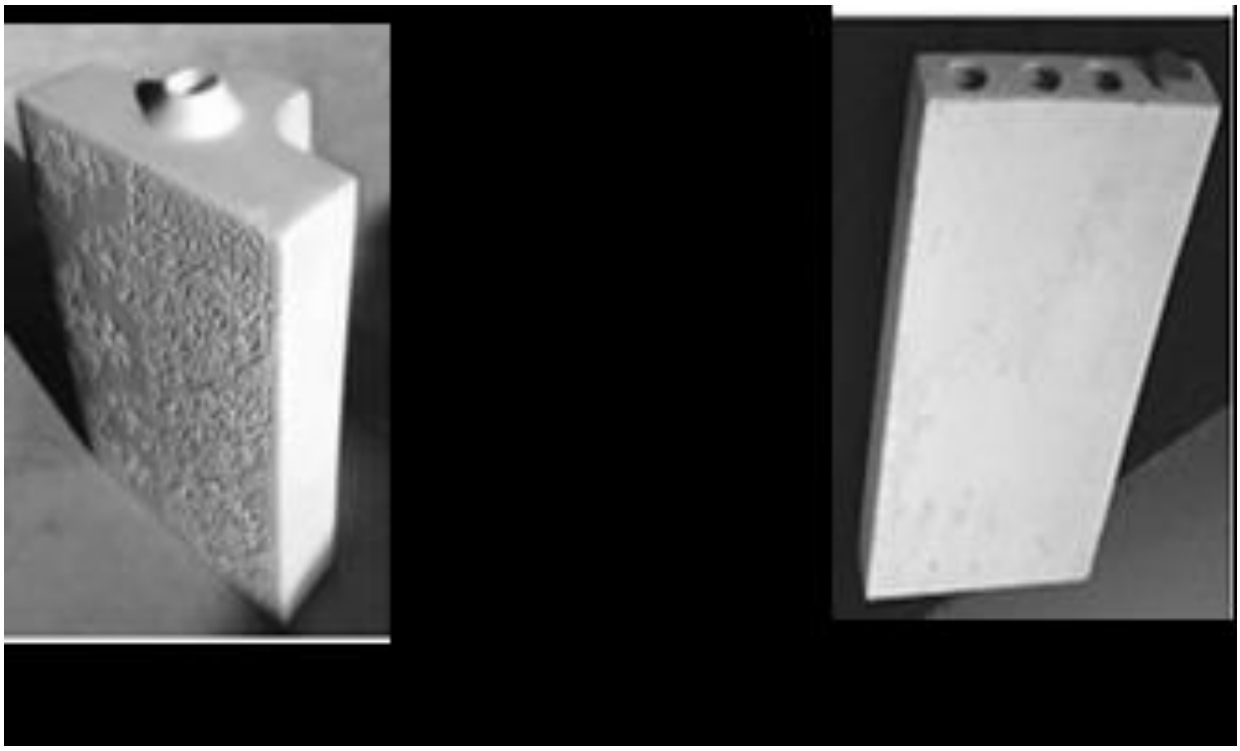

Figure 2.11 Porous ceramic samples for evaporative cooling. (Schiano-Phan, 2009)

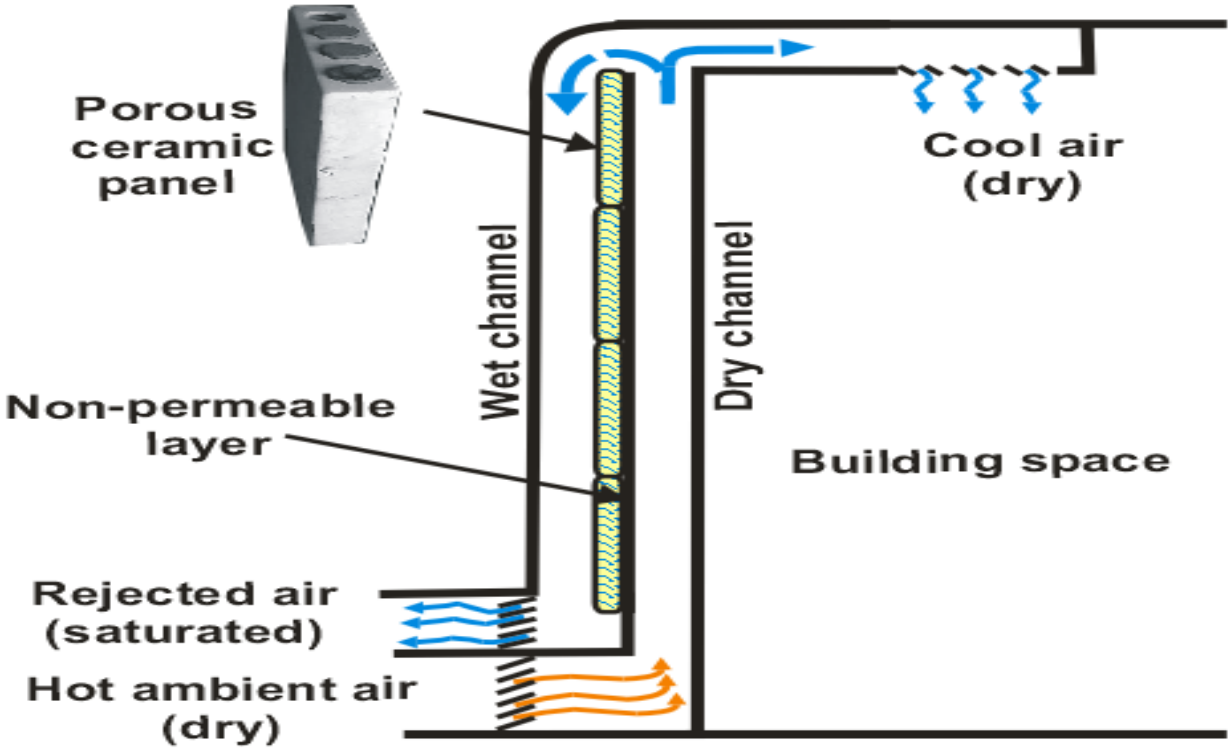

Figure 2.12 Porous ceramic panel installed in a building(Ibrahim et al., 2003)

Figure 2.13 Multiple evaporative coolers installed on a factory building (Muazu, 2008).

Figure 2.14 Green houses with a pad evaporative cooling unit (Muazu, 2008)

Evaporative coolers withcooling pad can be used in greenhouse systems. Figure 2.14 shows an evaporative cooler installed at the air inlet to the green house. While operating in warm weather, the pads are wetted to make the incoming air cool as it traverses through the cooling pad water evaporates into the incoming air.

Many factors affect the performance of pad-fan evaporative cooling system. Such factorsas: (i) weather conditions, (ii) pad material, (iii) pad thickness and density, (iv)water flow rate and (v) pad face air velocity.

2.3.3 **Pad thickness and density**

The cooling efficiency of an evaporative cooling system is affected immensely by the thickness of the evaporative cooling pad. As pad thickness is increased, the contact time for air and water is increased as well as the resistance to the flow of air. The increasein the contact time allows for more evaporation resulting in higher saturation efficiency. When air passes through additional thickness of pad, the vapor pressure differencebetween the water and non-saturated air decreases. This reduces the evaporation rate indicating that there should be an optimal thickness for every pad material. Pad density is defined as the mass per unit volume of the pad material. Increasing pads density improves the overallporosityallowing for more uniform distribution of water. This, however, increases resistance to air flow.

2.3.4**Water flow rate**

The cooling efficiency of an evaporative cooling system is affected immensely by the flow rate of water.Insufficient water leads to reduction insurface area for evaporation, hence,reduction in heat and mass transfer. This results in lowered saturation efficiency.In addition, at very low flow rates of water, almost all of the water reaching a pad is evaporated, leaving salt deposits on the pad, further reducing saturation efficiency. With increased flow rates, water tends to occupy the pore spaces, preventing some of the surface from coming in contact with air thus reducing evaporation. This reduced space also restricts air flow, increasing static pressure loss.To maximize operating efficiency, adequate water supply and distribution systems are required. The amount of water needed will vary with the type of system used. When sheet of water flow down the pad surfacetheresistance to air flow increases and transfer of free water into the house may result.

2.3.5 **Air velocity**

As the velocity of air increases the contact time decreases.At very low air flow rate the air exhibit laminar flow behavior and only the air in the viscous layer surrounding the pad get saturated with moisture. As air velocity increases, the flow tends to be more turbulent, breaking the viscous layer. This results in more evaporation and saturation efficiency.At higher velocity, water droplets from the cooling pap are carried-overinto the interior. Depending on the type of pad and the applied water flow rate, Franco et al, (2010) recommended a range of air speeds through a cellulose evaporative cooling pads of 1 to 1.5ms^{-1} at which the pressure drop was between 3.9Pa and 11.25Pa. ASAE (2000), recommended that face velocities passing acrossthe corrugated cellulose pad with thickness of 10 and 15 cm should be 1.25 and 1.75 m/s, respectively.

2.3.6 Problems associated with evaporative cooling pad.

Impurities in the water and salt depositon the pad can restrict the flow of air and reduce evaporation. When algae grow on the pad, it can decay causing air to pass through thedecayed area without making contact with water.This will greatly reduce the efficiency of the cooling pad material.

2.4**Applications of Evaporative Cooling**

The application of evaporative cooling techniques mainly depends on whether additional moisture in the supply air to the space is tolerable. Direct system is used where high humidity is required. Evaporative cooling systems are commonly applied for cooling of agricultural buildings due to the low power requirement. Evaporative cooling has been reported for achieving a favorable environment for greenhouses crops (Kittas*et al.*, 2001); poultry and dairy houses for reducing heat stress on animal (Zabeltitz, 2002 and Chen, 2003) and storage structure for fruits and vegetables.

2.4.1 **Preservation of fruits and vegetables**

The quality and storage life of fruits and vegetables may be seriously compromised within a few hours of harvest unless the crop has been cooled quickly to control deterioration.Vegetablesandfruits need to be properly stored so as to extend their shelf life. Proper storage involves controlling both the temperature and relative humidity of the storage area. To greatly improve theproduct storability proper management of aeration, temperature and relative humidity and moisture loss are very essential. Odesola and Onyebuchi (2009) reported that evaporative cooling is an efficient and economical means for reducing temperature and increasing the relative humidity of an enclosure, and has been applied for extending the shelf life of plant produce which is needed for maintaining the freshness of the commodities.

A porous wall (pot in pot) evaporative cooler for preservation of fruits and vegetables. was developed by Anyanwu (2004). He obtained a storage life of less than four days (93hours) on tomato.In Nigeria the study conducted by Ndukwu(2011),using evaporative cooler constructed with clay reduced ambient temperatures from 32-40 ^{0}C to 24-29 ^{0}C throughout the day. This cooler was found to have a cooling capacity from 870-1207 W and was able to store tomatoes for 19 days.

2.4.2 **Environment control in greenhouse**

Greenhouses often become too warm during hot weather conditions. The interior temperatures need to be below outside ambient temperatures. Evaporative cooling systems for cooling greenhouses have been developed to provide the desired growing conditions in the greenhouse during the hot season. To reduce interior greenhouse temperatures, water evaporation systems, which not only cool the air but also increase the humidity, are more feasible than mechanical cooling systems. The humidity is important due to its effect on the rate of water loss from plants. Kittas *et al.*(2001) reported that

evaporative cooling systems are commonly used for cooling of agricultural structures with comparatively low investment and less power input and has been used for achieving a favorable environment for greenhouses crops. Greenhouses are used to improve the environmental conditions in which plants are grown. The main parameters affecting the growing of plants inside greenhouse are temperature and relative humidity.Sethi and Sharma(2007a), reported that the choice of the crops to be grown, maintenance, ease of operation and economic viability are considered the key factors for selecting appropriate technology for cooling systems.Due to itssimplicity of operation and control evaporative cooling system has been used in greenhouses. Fans combined with wetted pads are the most widely used for greenhouses cooling (Jain and Tiwari, 2002). Kittas *et al.* (2001) observed that a fan-pad cooling system during summer in a commercial greenhouse producing cut roses and a half–shaded plastic roof reached 80% efficiency and succeeded in maintaining greenhouse temperatures that were cooler (up to 10 ^{0}C lower) than outside. By applying a partially shading to a large greenhouse equipped with cooling pads Kittas *et al*. (2003) were able to eliminate the temperature gradients between inlet and outlet associated with fan-pad system. Bymeans of regenerating the desiccation of the incoming air.

2.4.3: **Environment control in animal buildings**

It has been reported by several researchers that evaporative cooling improved milk production and fertility for cows during summertime climates (Ali*et al*., 1999). Animalsrequiredenergy to maintain the life functions and always need to get rid of heat. Animals lose body heat in two ways. (1)By sensible heat loss through conduction, convection, and radiation and (2) By evaporation. The sensible heat transfer is driven by the temperature differencewhile evaporative heat transfer is governedby the vapor pressure difference between the animal and its surroundings. As the ambient temperature rises, evaporative heat transfer becomes the more dominant pathway of heat loss to maintain homoeothermic. Al-Amri(2000) reported that high air temperatures in animal

houses reduces feed consumption, decreases weight gain, milk and egg yields.However,evaporativecooling systems can be used in poultry houses in hot climates, for eliminating the negative effects of heat at inner environment.

2.4.4**Cooling for human thermal comfort**

The riseinliving standard has made air-condition system more popular and a necessity in life in order to create comfortable environment for man.Air conditioning increases the efficiency of man during working period, especially in hot weather.Conventional air conditioning system has high power requirement and high capital investment. Because of this a more efficient air conditioning technology is highly desirable.Evaporative cooling offers an economical, energy efficient and practical means of cooling and can be used to maximum advantage in areas of high dry bulb temperatures, with low outdoor relative humidity. Maisotsenko and Reyzin (2005) introduced the (M-cycle) which is a new design of the heat exchanger of IEC system to overcome some of the disadvantages of DEC systems and enhance the effectiveness of wet-bulb temperature IEC. The performance of an early-2005 model Coolarado cooler indirect evaporative cooling was evaluated by Elberling (2006). The author indicated that, although theoretically the wet bulb effectiveness of the unit can be greater than 100%, the wet-bulb effectiveness over the test conditions ranged from 81% to 91%.

2.4.5**Evaporative pre-cooling**

Evaporative pre-cooling involves reducing the air conditioner load by cooling the air that surrounds air conditioner condensers.ThisIncreases the temperature difference between the condenser coil and the surrounding environment and this increases the heat transfer efficiency, making the system to run efficiently during hot climate. Indirect evaporative cooling system can be used as a pre-cooling unit before mechanical cooling systems forming a hybrid evaporative/mechanical cooling system. Evaporative condenser pre-coolingcan be applied to gas turbines to increase the thermal efficiency. An evaporative

cooling system can also be used to pre-cool fresh air for air-conditioned space to reduce the cooling capacity and saves energy especially in hot climate countries.

2.5**Energy Saving Potential of Evaporative Cooling System**

Air-conditioning is very important in ensuring thermal comfort of man. Nowadays, energy bills have become unaffordable. Yet the dominant cooling systems still remainsintensively power-consuming ones, i.e. vapour compression systems. They also produce harmful effect on environment by damaging ozone layer. Vapour compression refrigeration-based air conditioners are being used for comfort cooling throughout the world. Luis et al. (2008) reported that heating, ventilation and air conditioning (HVAC) is the major energy user in a building and consumes around 50% of the total supplied energy and that air-conditioning as an important function of the HVAC system, is becoming increasingly crucial for many buildings as it contribute around 30–40% of world total energy consumption and similar proportion of global carbon emission. El-Dessonky et al.(2004) also reported that during the hottest summer period when air conditioning is in full operation, many cities in China, Kuwait etc, experienced unwanted grid 'cut-off resulting frompower-over- loads. In order to reduce high dependency on the vapour compression refrigeration-based air conditioners an alternative method of cooling is required. For building located in hot and dry regions, evaporative cooling can be an alternative method of cooling. It is an environmentally friendly and energy efficient method for achieving thermal comfort in places where ambient air humidity is low.

Jiang and Zhang (2006)calculated the energy saving potentials of using direct evaporative cooling for air pre-cooling in air-cooled water chiller units in 15 typical cities in China. The results showed that by using DEC, the COP of the chillers can be enhanced by 15–25% in most of those cities.

You et al. (1999) analyzedthe energy saving potentials of usingdirect evaporative coolingin air-cooled chiller units. The results of their analysis indicate that the energy efficiency ratio (EER) of air-cooled chiller units in Tianjing can be increased by 14%.

Tilahun(2010), investigated the feasibility and economic evaluation of low-cost evaporative cooling system with 100mmpad thickness used in a fruit and vegetables storage. The evaporative air cooler is able to decrease the air temperature from 36 °C to 16.4 °C and increase the relative humidity from 25.4 % to 91.1 %. The cooling efficiency obtained ranged between 55 % and 84 %. The power consumption recorded is 1.13 kWh and energy efficiency of 26.3 was obtained. The experiment was conducted at a fixed mass flow rate of air of 4.3 kg/s.

A methodology for energy saving potential of an indirect evaporative cooling system to pre-cool fresh air was developed by Maheshwari et al. (2001). The method was used to reduce cooling capacity of the conventional air conditioning equipment. They demonstrated a reductioninenergy consumption of a conventional air conditioning system of nearly 30% and peak power demand of 40%, achieving nearly 100% more saving of electricity compared with the same system used in the coastal area.

Evaluation of the performances of an indirect evaporative cooler as apre-cooling unit for mechanical cooling systems in Iran was carried out by Delfani et al. (2010). The results showed that about75% of cooling load and about 55% savings in electrical energyconsumption can be obtained when using an evaporative cooling system beforemechanical cooling systems.

The performance of counter flow dew point cooler installedin a residential building was evaluated by Frank (2011). The results of a performance characteristic of this cooler with respect to its outlet temperatures and electrical energy efficiency showed that the averagecooling capacity was 10.5 kW and the average energy efficiency ratio was 8.0. Table 2.4 shows the results of energy savings for each year from 2001 to 2005 and the annual energy saving associated with cooling the outside fresh air between 52 to 56%.
Wasin et al. (2010) investigated the energy consumption of evaporative air conditions in different parts of Australia. Hecalculatedthe total annual electricity consumption to provide cooling during all hours when the outside temperature is above 27°C.

2.6**Economic and Environmental Analysis of Evaporative Cooling System**

Evaporative cooling systems have manyeconomicand environmental advantages when compared with mechanical compression refrigeration system. The economic advantages of evaporative cooling over mechanical compression systems are mainly due to low initial investment, low installation and maintenance costs, as well as reduction in insulation requirements.Theenvironmentaladvantages are mainly the reduction in carbon dioxide (CO_2) and chlorofluorocarbons (CFCs) emissions which have been proven to reduce the earth's ozone layer. Foster (1995), reported thataround the globe evaporative air cooler residential units directly obviate at least 118 million pounds of HCFC-22 and save approximately 60 million barrels of oil annually and 27 billion pounds of annual CO_2 emissions in lieu of using vapour-compression air-conditioning systems. He alsoreportedthat the 4 million evaporative air cooler units in operation in the United States provide an estimated annual energy savings equivalent to 12 million barrels of oil and an annual reduction of 5.4 billion bounds of CO_2 emissions as well as avoiding the need for 24 million pounds of refrigerant traditionally used in residential vapour compression refrigeration systems.

Many research works have been done on economic and environmental analyses of the evaporative cooling systems by comparing their performance againstconventionalvapour compression systems. Maheshwari et al. (2001) studied the energy saving potential and economic comparison by calculating payback period and life cycle cost of the indirect evaporative cooling system. Steeman et al. (2009) carried out feasibility studiesusing the static or dynamic calculations methods to examine the thermal performance, thermal comfort level and economic features of the IEC/combined systems in residential buildings with arid climates.

The feasibility and economics of reducing the indoor temperature and raising the relative humidity of the evaporative cooled fruit and vegetables storage chamber by using direct

evaporative cooling was investigated byTilahun (2010). He built an experimental forced ventilation evaporative cooler for the study. The economic computation was based on the number of months each fruit or vegetable was available in market. It was found that the evaporative cooling system was capable of significantly reducing the temperature and increasing the relative humidity as required for short time storage of selected fruits and vegetables.

Taking the same sized conventional air conditioner as the reference, Navon and Arkin (1994) investigated the economic benefit and thermal comfort of using a combined direct and indirect evaporative cooling system in a residential building in Israel. Annual equivalent costs method was used tocalculate the life cycle cost of the combined evaporative cooling system and the conventional airconditioner. The results indicated that the economic benefit relating to use of the combined evaporative cooling system is very promising owing to its significant energy cost saving over the conventional air conditioner.

Jaber and Ajib (2011) designed an indirect evaporative air-conditioning for the typical Mediterranean residential buildings.Theyreported that most of the cooling load of the buildings could be matched by using an indirect evaporative cooling unit with the air

flow rate of 1100 l/s. They also reported that if such an IEC system were mounted in 500,000 Mediterranean residential buildings, as replacements for conventional mechanical vapour compression refrigeration systems, the estimated annual energy saving and CO 2 emission reduction would be around 1084 GWh and 637,873 tons per annum, respectively. The payback time of the implementation would be less than two years.

2.7**Advantages and Disadvantages of Evaporative Cooling System**

2.7.1 **Advantages of evaporativecooling system**.

The following are some of the advantages of evaporative cooling systems:

Evaporative cooling systems have fewer moving parts and thus simple to construct and maintain. The evaporative cooling system Lowers the air temperature and filters the air using water as the working fluid, hence, reducing environmental pollution and global warming. The energy requirements for running a fan and pump or only a fan in evaporative cooling system is low making the system to save energy. The system is associated with continuous circulating of fresh air in the building as it works by displacing the warm indoor air with the fresh cold air.

2.7.2 **Disadvantages of evaporative cooling**

Evaporative cooling systems have some disadvantages which can be prevented if the system is properly designed, operated and well maintained. It increases the relative humidity level in the building space. Building should not have excess moisture in order to prevent dampness in the building. However, in some applications like storage of fruits and vegetables it may not be a disadvantage. In some area where there is water scarcity, its operation may experience some difficulty since the system consumes a lot of water.

2.8 **Instrumentation and Measurement**

2.8.1**Sensors**

(A) Temperature sensor

A Temperature Sensor, as the name suggests, senses the temperature i.e., it measures the changes in the temperature. There are different types of Temperature Sensors like Temperature Sensor ICs, Thermocouples, RTD (Resistive Temperature Devices), etc. Temperature Sensors can be analog or digital. In an Analog Temperature Sensor, the changes in the Temperature correspond to change in its physical property like resistance or voltage. Temperature Sensors are used everywhere like computers, mobile phones, automobiles, air conditioning systems, industries etc.

(A) Humidity sensors

Humidity is one of the most commonly measured physical quantities and is of great importance in a wide variety of commercial and industrial applications, including those associated with building ventilation control, clean rooms in the semiconductor and automotive industries, environmental chambers for the testing of electronics, industrial drying, and process monitoring in the chemicals, electronics, food/beverage, pharmaceutical, cosmetics and biomedical analysis industries.Humidity Sensors/Detectors/Transducers are electronic devices that measure the amount of water in the air and convert these measurements into signals that can be used as inputs to control or display devices.

(C) Pressure sensors

Pressure Sensors are electro-mechanical devices that detect forces per unit area in gases or liquids and provide signals to the inputs of control and display devices. A pressure sensor/transducer typically uses a diaphragm and strain gage bridge to detect and measure the force exerted against a unit area.

(D) Force sensors

Force Sensors/Transducers are electronic devices that measure various parameters related to forces such as weight, torque, load, etc. and provide signals to the inputs of control or display devices. A force sensor typically relies on a load cell, a piezoelectric device whose resistance changes under deforming loads. Force sensors are used in load measuring applications of all kinds, from truck scales to bolt tensioning devices..

(E)Leak sensors

Leak Sensors/Detectors are electronic devices used for identifying or monitoring the unwanted discharge of liquids or gases. Some leak detectors rely on ultrasonic means to detect air leaks.

2.8.2 **Air velocity meters**

Air velocity meters, commonly called anemometers, are used to measure the speed and/or volume of air movement. Air velocity is measured using a vane anemometer. It utilizes the kinetic energy of an airstream to drive its windmill like impeller. The rotation of the impeller blade is proportional to the air velocity and translation of the impeller rotation speed will give a measure of the air velocity. Depending on the velocities measured, different types of anemometers are used.

2.8.3 **Differential pressure meter**

Differential pressure is simply the difference between two applied pressures, often referred to as delta p (Δp). A differential pressure meter is used to measure differential pressure in pneumatic, compressor and pump installations, valves, tanks and heating, ventilation and air conditioning (HVAC) systems.Differential pressure meters are generally used for measurements before and after a specific point, for example, the input and output points of a pump. The sensor is generally composed of two measurement chambers that are separated by a membrane. The deviation of the membrane due to the pressure shows the measurement of the differential pressure.

2.8.4 **Arduinomicroprocessor**

Arduino is an open-source electronics platform based on easy-to-use hardware and software. Arduino boards are able to read inputs and turn it into an output. You can tell your board what to do by sending a set of instructions to the microcontroller on the board. To do so you use the Arduino programming language (based on Wiring), and the Arduino Software (IDE), based on Processing.

2.8.4.1 **Elements of arduino**

The Arduino mainly has two components, its hardware and software. For the hardware part of the Arduino, it consists of the physical board and also sensors and shields used to interact with the board

(A) Hardware

An Arduino board consists of a microcontroller with complementary components that facilitate programming and incorporation into other circuits. An important aspect of the Arduino is its standard connectors, which means users connect the CPU board to a variety of interchangeable add-on modules called shields. Some shields communicate with the Arduino board directly over various pins, but most of the shields are individually addressable via an I²C serial bus. An Arduino microcontroller is the heart of the development board, which works as a mini computer and can receive as well as send information or command to the peripheral devices connected to it. It has built in "I/O" (input/output) capabilities and can read and write digital and analog values, as well as connect directly to the "real world".

Plate 2.1 An Arduino development board. Source:Rajan, et al (2015)

B. Software

The Arduino integrated development environment (IDE) is a cross-platform application written in Java and which is obtained from the IDE for the Processing programming language and the Wiring projectsRajan et al. (2015). It is sketched to introduce programming to artists and other newcomers unfamiliar with software development. It comprises a code editor with features such as syntax spotlighted, brace matching, and automated indentation and is also capable of compiling and uploading programs to the board with a single click. A program or codes written for Arduino is called a sketch. The Arduino programs are written in C or C++. An Arduino IDE comes with a software library called "Wiring" from the original Wiring projects, which makes many common input/output operations much simple.

2.8.5. **Fans**

Fans provide air for ventilation and industrial process requirements. Fans generate a pressure to move air against a resistance caused by ducts, dampers, or other components in a fan system. The fan rotor receives energy from a rotating shaft and transmits it to the air. Fans provide solutions to various industrial processes within a vast range of industries including mining, electrical power production, building heating and ventilation (HVAC), metals production and processing, cement production, petrochemical and many more. From combustion processes or cooling, to dust collection, material handling, air conditioning, extracting waste gasses, and chemical processing, industrial fans are the backboneofmanyindustrialprocesses.There are two primary types of fans: centrifugal and axial. These types are characterized by the path of the airflow through the fan. Centrifugal fans use a rotating impeller to increase the velocity of an airstream. As the air moves from the impeller hub to the blade tips, it gains kinetic energy. This kinetic energy is then converted to a static pressure increase as the air slows before entering the discharge. Centrifugal fans are capable of generating relatively high pressures.The capability to generate low to medium flow rates at medium to high pressures makes

centrifugal fans ideal for applications with higher system pressure losses such as cooling and heating systems, dust control, transporting materials, boiler and chemical production processes.

Axial fansmove an airstream along the axis of the fan. The air is pressurized by the aerodynamic lift generated by the fan blades. Axial fans are commonly used in low-pressure, high-volume applications. Axial fans tend to have higher rotational speeds.The flow rate is parallel to the axis of the fan and these fans are often used for cooling and ventilation

2.8.6. **Pumps**

A pump is a device that moves fluids (liquids or gases), or sometimes slurries, by mechanical action, typically converted from electrical energy into hydraulic energy. water pump is an electrical device designed to take the already existing water and increase the rate at which that water is moving. When the water is speeding up in the pump, the device is creating low pressure at the intake, therefore creating a vacuum.As the water is coming from the low-pressure side, the water outlet undergoes a higher pressure and pushes the water with that force. The working principle of a water pump mainly depends upon the positive displacement principle as well as kinetic energy to push the water. These pumps use AC power or DC power for energizing the motor of the water pump. The water pump is a portable device and can be applied in several household applications. Water pumps are classified into two types namely positive displacement and centrifugal. These pumps are mainly designed for supplying water from one location to another constantly.

2.8.7. **Automation and control**

Automation is the creation and application of technology to monitor and control the production and delivery of products and services.Automation, includes the use of various control systems for operating equipment such as machinery, processes in factories, boilers, and heat-treating ovens, switching on telephone networks, and other applications

and vehicles with reduced human intervention. It describes a wide range of technologies that reduce human intervention in processes. Human intervention is reduced by predetermining decision criteria, sub-process relationships, and related actions — and embodying those predeterminations in machinesGroover (2014). Automation covers applications ranging from a household thermostat controlling a boiler, to a large industrial control system with tens of thousands of input measurements and output control signals.Process automation and control is an industrial system in which processes are controlled and monitored automatically so that only a few people are needed to carry them out.Industrial automation is the use of control systems, predominately computer based, to control industrial machinery and processes.Advantages commonly attributed to automation include higher production rates and increased productivity, more efficient use of materials, better product quality, improved safety, shorter workweeks for labour, and reduced factory lead times. Higher output and increased productivity have been two of the biggest reasons in justifying the use of automation. Despite the claims of high quality from good workmanship by humans, automated systems typically perform the manufacturing process with less variability than human workers, resulting in greater control and consistency of product quality.

2.9 **Developments in Evaporative Cooling Research**

Because of the increasing interests and the significant potential of evaporative cooling technology, various methods of evaporative cooling incorporating other heat transfer devices have been investigated. Many studies were carried out to establish the functional features of evaporative cooling pad in different weather conditions. Al-Sulaiman (2002) evaluated the performance of local fibers in evaporative cooling using date palm fibers, jute and “Luffa” as wetted pads in evaporative cooling. He considered the thermal efficiency, material performance and reduction in cooling efficiency. His results gave cooling efficiencies of 62.1%, 55.1%, 49.9% and 38.9% for Jute, “Luffa”, commercial pads and date fibers respectively. He carried out material performance tests which comprised of salt deposition and bio-degradation and the result showed that “Luffa” has

an advantage over commercial fibres. However, he concluded that if jute surface can be treated to offer higher mould resistance and also maintain uniform distribution after wetting they will be suitable options. An experiment set developed by Koca etal. (1991) was used to assess the performance of three different cellulose pads. A study to determine the most suitable pad material for evaporative cooling system was carried out byDagtekin et al. (1998).In their study they compared pads made of sawdust, nutshell and cellulose. Dai and Sumathy (2002),evaluated a cross-flow direct evaporative cooler with wet honeycomb paper as the packing material. They presented a mathematical model which was experimentally validated for theoretical prediction of the system performance. The unit was found to reduce air temperature by 9^0C and raise humidity ratio by 50%. In designing an indirect evaporative cooling system modeling and simulation is vital to obtain the optimum parameters. Heat and mass transfer model were developed based on the basic principles for evaporative cooling (Alonso et al.,1998). The model can be used for systems energy analyses and product optimization. In addition to various achievements made in evaporative cooling,Ibrahim et al., (2003) carried out a study on porous ceramic evaporators for building cooling applications under direct as well as indirect types of evaporative cooling. The prototype porous ceramic evaporators used were classified as low, medium and high porosity evaporators based on firing temperatures of 1110 ^{0}C, 1130 ^{0}C and 1170 ^{0}C respectively. Experimental results showed that the high porosity ceramic evaporator consistently performed better 6 ^{0}C - 8 ^{0}C drops in dry-bulb temperatures, 30% rise in relative humidity and 224W/m^2 maximum cooling was reported. These formed a very good basis for the choice of ceramic evaporators based on porosity considerations. Finally, the investigation revealed that porous ceramic has demonstrated significant potential for possible integration into building under direct evaporative cooling (Ibrahim et al., 2003).

A study on thermal performance of a non-conditioned building equipped with an indirect Evaporative Cooling (IEC) system in three different climatic conditions of India was undertakenbyTulsidasani et al. (1997, Part 2). They investigated the effects of various design parameters of the indirect Evaporative Cooling (IEC) on the discomfort standards.

The analysis shows that the IEC system is effective in providing thermal comfort to buildings in dry, hot and combined climates.

El-Dessouky et al.(2004)evaluated the performanceof an experimental unit of indirect evaporative cooling system followed by a directevaporative system for indoor air conditioning in the hot and humid environment ofKuwait. The results of this experiment showed that the range of the efficiency for anindirect evaporative cooling system followed by a direct evaporative cooling system is90%–120%. They obtained a range of 20%–40% and 63%–93%efficiency for indirect and direct evaporative cooling systems respectively.

The experiment carried out by Al-Sulaiman (2002) gave saturation efficiency of 62.1% for jute. Since jute fibre is one of the material that will be used in this research,this research will further ascertain the suitability of jute to be used as a cooling pad

2.10**Conclusion from The Literature Review**

From the above review, the following are the major conclusions:

1) Evaporative coolers provide excellent ventilation by using 100% fresh air.

2) The performance of evaporative cooling systems mainly depends on the pad material, pad thickness, air velocity and water flow rate.

3) Evaporative cooling systems have many advantages. It is simple to construct and maintain, inexpensive, energy efficient and potentially attractive.

4) As wet bulb depression increases, the effectiveness of evaporative cooling increases.

5) The effectiveness of the indirect evaporative cooler depends on type of heat exchanger and characteristics of wet media material.

6) Indirect evaporative cooling can achieve high thermal efficiencies without increasing the humidity of air.

7) The environmental benefits of evaporative cooling technology are impressive due to its low noise from components and reduced CO_2 emission.

CHAPTER THREE

MATERIALS AND METHODS

3.1**Materials**

3.1.1 **Evaporative cooling test rig:**

A low-speedopen-circuit multi-pad wind tunnel was developed to simulate pad-fan evaporative cooling systems and to provide direct measurements of system performance. The Evaporative cooling test rig is of rectangular cross-section and consists of four separate wind tunnels. Each tunnel has 3 zones: (i) the air inlet zone (12), (ii) the measurement zone (13) and (iii) the air outlet zone (14) as shown in figure 3.1. The measurement zone was designed to accommodate 50, 100, 150, 200 and 250-mm thickness of the test pads.In the front and the back of the pad frame were the measurement sections as shown in figure 3.1. Each measurement section contained the measuring points, temperature and relative humidity sensors (2) and static pressure sensors (1). By installing the suction fan (9) at the end of the air outlet zone (14), air from the air inlet zone was drafted through the wetted pad and exited this zone to environment.ENGR. OKAFORPHD THESSIS MAIN WORK 1JUNE 2021ENGR. OKAFORPHD THESSIS MAIN WORK 1JUNE 2021The wind tunnel is made of galvanized iron sheets and 25mm thick marine ply wood. Each tunnel is insulated from each other. The cooling pad frame was made from a galvanized steel frames to create an evaporative cartridge. It was designed such that one side of the cartridge can be adjusted to accommodate different levels of pad thicknesses. The active surface area of these cartridges was 300mm by 300mm. The front and the back faces of the cartridges were covered with galvanized wire sieve. The water distribution system consist of a 2mm flexible tube (6) with one end fitted to a perforated hollow rectangular aluminum profile (11) and the other end connected to a direct current (dc) pump (5) that was connected to the water sump (3) via 2mm flexible tube. Several small holes were provided on the aluminum profile (11) to insure uniform distribution of the water. A drainage hole is

provided at the bottom of the pad frame and a return pipe (4) connected to the hole. The water sump (3) was made long enough to coverthe entire drainage holes on each chamber.

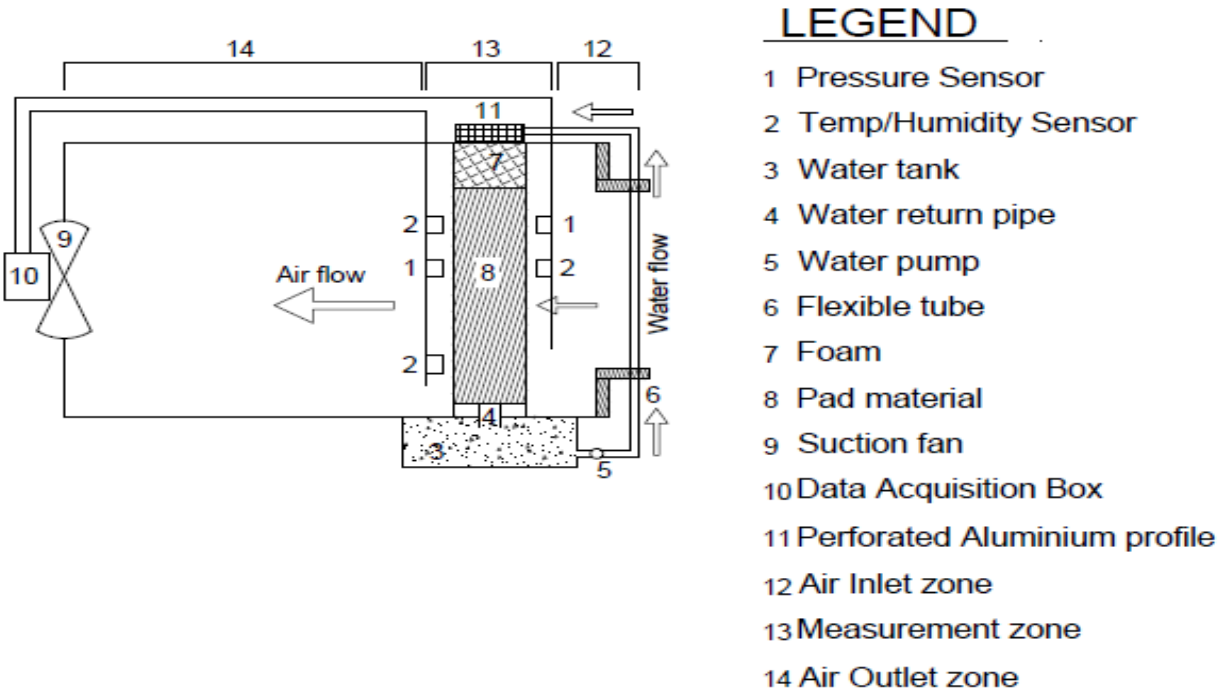

Figure 3.1. Schematic diagram of the single chamber/tunnel evaporative cooling test rig

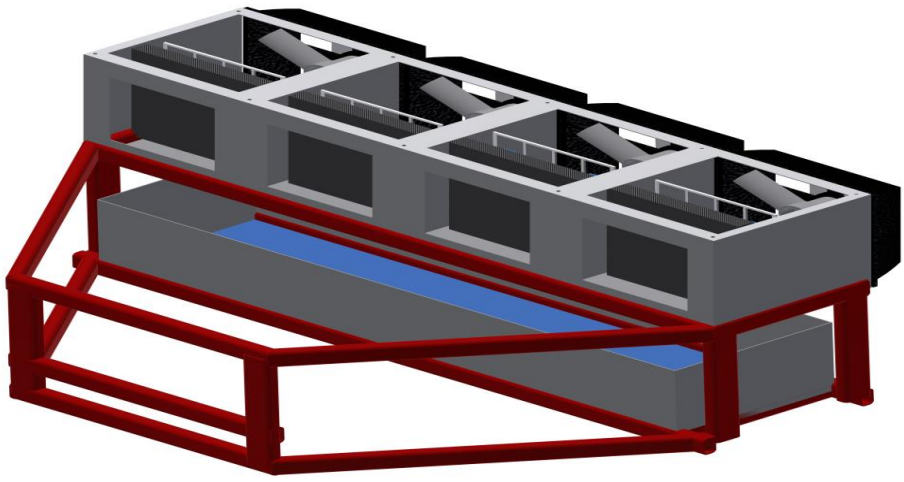

Figure 3.2 Pictorial view of the evaporative cooling test rig

Plate 3.1: Front view picture of evaporative test rig. (1. Data acquisition/control and display box; 2. Suction fan;.3. Pump transformer; 4. Fan transformer; 5.USB Cable; 6.Water sump)

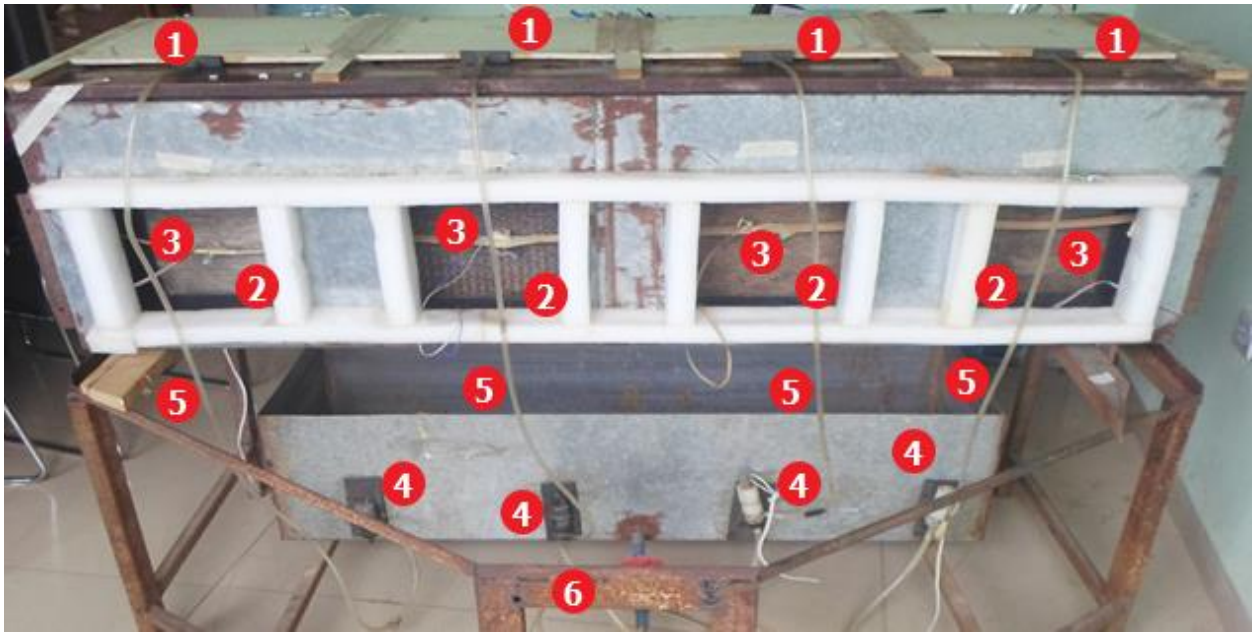

Plate 3.2: Back view picture of evaporative test rig (1. Perforated aluminum profile; 2. Pad materials; 3. Temperature / Pressure Sensors; 4.12Vdc Pumps; 5. Water distribution hose; 6. Supporting Frame.)

During the experiment, the fan draws in warm outside air through the wetted media, cooling the air. The water pump was used to lift the water from the sump through the distribution system to the top of the pads from where it trickleddown by gravity back to the water sump. The system is shown schematically in figure 3.1. Figure 3.2 shows the pictorial view of the evaporative cooling test rig with the top cover removed. plate 3.1 3.2 and 3.3 are the photographs of the front, back, and top views respectively. Figure 3.3 shows the circuit diagram of the evaporative test rig.

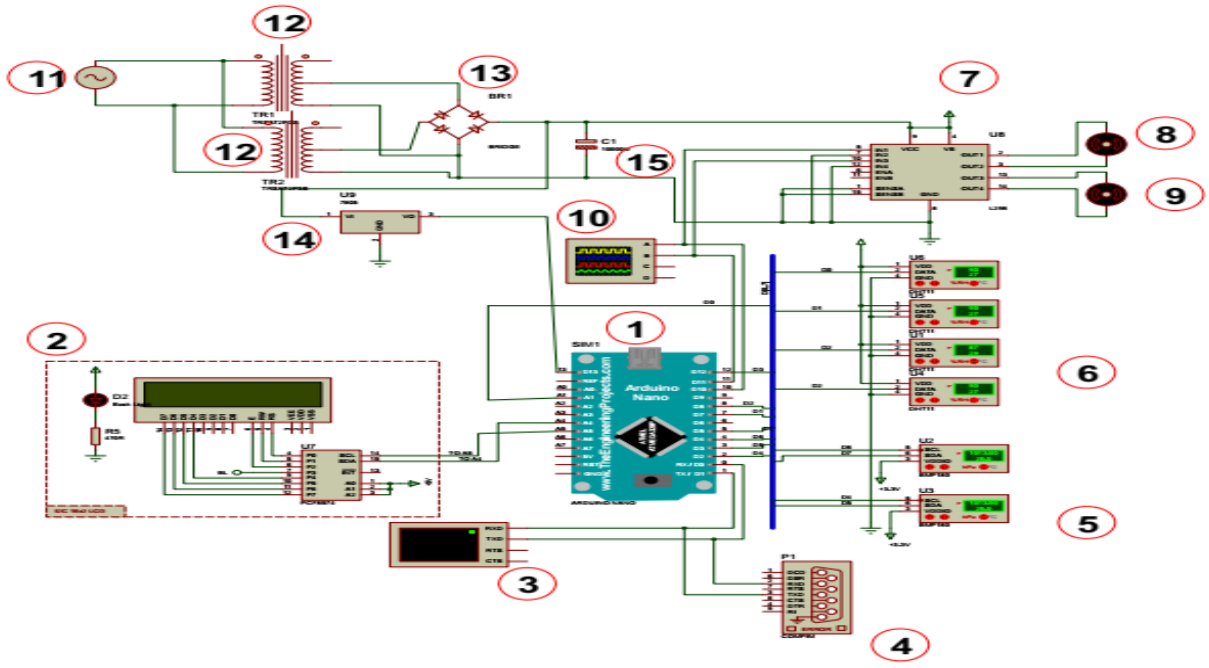

LEGEND		LEGEND	
1.	ARDUINO MICROPROCESSOR BOARD	**9.**	12V DC PUMP
2.	LCD DISPLAY UNIT	**10.**	DIGITAL MULTI METER
3.	SERIAL MONITOR INTERFACE	**11.**	AC MAINS POWER SOURCE
4.	SERIAL TO USB ADAPTER PORT	**12.**	STEP DOWN TRANSFORMERS
5.	BMP180 PRESSURE/ TEMP SENSORS	**13.**	BRIDGE RECTIFIER
6.	DHT11 TEMP/ HUMIDITY SENSORS	**14.**	5V DC VOLTAGE REGULATOR
7.	DC FAN / PUMP SPEED CONTROLLER	**15.**	SMOOTHING CAPACITOR
8.	12V DC FAN		

Figure 3.3 Circuit diagram of the evaporative test rig.

3.1.2**Pad materials used for the experiment**

The pads are the most important element in the exchange of heat and mass, fulfilling two main functions. First, they provide the surface for the exchange and cross flows of water and air. Second, they delay the down flow of water, ensuring that the exchange process lasts longer. This leads to an increase in the heat given off by the water to the non saturated air. The cooling capacity of an evaporative pad depends on its thickness and the material it is made of and on the air and water flow through it.

A good pad material should provide a greater transfer surface, greater mechanical resistance, and low resistance to the passage of air and water. Four different pad materials were employed in the study. They are: (a) Rigid cellulose media(Celdek), (b) Jute fibre, (c) Cocoanut fibre and (d) Plaster of Paris (POP) sponge. Plate3.1 shows the experimental pad materials.

(a) Celdek (b) Jute fibre

(c) Coconut fibre (d) POP sponge

Plate 3.3 Experimental pad materials

3.2 **Methods**

3.2.1 **Experimental procedure**

The experiments to determine the effects of pad thickness, water flow rate and pad face air velocity on the performance of the selected pad materials were carried out at five levels of pad-face air velocity i.e. 0.5, 1.0, 1.5, 2.0 and 2.5m/s, five levels of pad thickness i.e. 50, 100, 150, 200 and 250mm, and five levels of water flow rate i.e. 1.0, 1.25, 1.5, 1.75 and 2.0 L/min. At first, Before the experiment both the fan motor and the pump motor were calibrated to the five levels of pad-face air velocities and five levels of water flow rates respectively. The calibration was done for each level of pad thickness by using a programmable dc motor controller circuit that varies the motor speed by changing the voltage supplyas well as converting the motor speed to a numerical value. By setting the controller to a value (e.g. 50) the motor automatically run at a speed corresponding to that value. Before the calibration of the fan and pump dc motors for 50mm pad thickness the pad cartridge was adjusted to accommodate 50mm thickness of the pad material and about 0.15kg (150g) of each local pad materials was carefully placed in the cartridge to occupy a fixed volume of $0.0045m^3$ ($0.3m \times 0.3m \times 0.05m = 4500000mm^3$). This gives a uniform packing density of approximately $33.3kg/m^3$ for all the local pad materials. During the calibration of the fan motor, the anemometer was placed at the inlet zone of the cooling chamber and the numerical value of the controller was varied by trial and error until the anemometer reading becomes constant at the particular level of pad-face air velocity and the value of the controller circuit corresponding to the fan speed that gave the level was recorded. The procedure was repeated until all the values corresponding to the various fan speeds that gave all the five levels of pad-face air velocities have been determined. In a similar manner the calibration of the pump motor was done but in this case a calibrated container and a stop watch was used. The stop watch was set to stop at 60seconds for each trial and the controller varied until the pump motor pumps litres of water corresponding to the level of water flow rate we want to determine. At this point the numerical value of the controller circuit that gave the pump speed for that level of water flow rate was recorded.The procedure was repeated until all

the values corresponding to the various pump speeds that gave all the five levels ofwater flow rates have been determined. During the tests, the water inlet was fitted on the top of the pad frame and the water was distributed over the upper face of the evaporative pad through the perforated aluminum profile at a constant flow rate corresponding to the particular level of water flow rate under study. The evaporative pads were wetted before each test and the recording of the measured data wasstarted at least 5 min after each test run started.The pressure, temperature and humidity of the air before and after passing through the wetted pad were measured using digital sensors. The sensors were located 25mm upstream and downstream from the sample to be tested. They were mounted on a rubberized wire mesh. Measurement of all points were centralized and logged on a data-acquisition system. Pump control, fan control and data acquisition as well as the general supervision of the unit start-up and shutdown were all done through theAudiuno relay output board and data-acquisition software. The values of the wet bulb temperature (T_{wb}) for each dry bulb temperature (T_{db}) and relative humidity of incoming air were determined by using on- line psychometric chart.

The evaporative saturation efficiencies of the pad media were determined by using the expression in equation (2.1).

3.2.2 **Experimental design and statistical analyses:**

Factorial experiments are used when little is known concerning the optimum levels of the factors or which of the factors are of greatest importance. The experiments were conducted using the Randomized Complete Block (RCBD) layout. Pad thickness (T), pad face air velocity (V) and water flow rate (W) formed the major treatments (i.e. Factors TVW). Each of the three factors has five (5) levels. For pad thickness (T): 50, 100, 150 and 200 and 250mm; for air velocity (V): 0.5, 1.0, 1.5, 2.0 and 2.5ms^{-1}; and for water flow rate (W): 1.0, 1.25, 1.5, 1.75 and 2.0 $Lmin^{-1}$. Each set of data was replicated three times for each pad material.The treatments and levels were combined in a randomized set as presented in table 3.1, and their interaction effect studied. The analysis of the number of experimental points was thus carried out:

Table 3.1: Experimental layout of a factorial treatment design

PAD MATERIAL TYPE:								
Water flow rate (l/min)	Pad face Air vel. (m/s)	Pad Thickness (mm)					TOTAL	MEAN
		T_1	T_2	T_3	T_4	T_5		
W_1	V_1	$W_1T_1V_1$	$W_1T_2V_1$	$W_1T_3V_1$	$W_1T_4V_1$	$W_1T_5V_1$		
	V_2	$W_1T_1V_2$	$W_1T_2V_2$	$W_1T_3V_2$	$W_1T_4V_2$	$W_1T_5V_2$		
	V_3	$W_1T_1V_3$	$W_1T_2V_3$	$W_1T_3V_3$	$W_1T_4V_3$	$W_1T_5V_3$		
	V_4	$W_1T_1V_4$	$W_1T_2V_4$	$W_1T_3V_4$	$W_1T_4V_4$	$W_1T_5V_4$		
	V_5	$W_1T_1V_5$	$W_1T_2V_5$	$W_1T_3V_5$	$W_1T_4V_5$	$W_1T_5V_5$		
TOTAL								
MEAN								
W_2	V_1	$W_2T_1V_1$	$W_3T_2V_1$	$W_3T_3V_1$	$W_3T_4V_1$	$W_3T_5V_1$		
	V_2	$W_2T_1V_2$	$W_3T_2V_2$	$W_3T_3V_2$	$W_3T_4V_2$	$W_3T_5V_2$		
	V_3	$W_2T_1V_3$	$W_3T_2V_3$	$W_3T_3V_3$	$W_3T_4V_3$	$W_3T_5V_3$		
	V_4	$W_2T_1V_4$	$W_3T_2V_4$	$W_3T_3V_4$	$W_3T_4V_4$	$W_3T_5V_4$		
	V_5	$W_2T_1V_5$	$W_3T_2V_5$	$W_3T_3V_5$	$W_3T_4V_5$	$W_3T_5V_5$		
TOTAL								
MEAN								
W_3	V_1	$W_3T_1V_1$	$W_3T_2V_1$	$W_3T_3V_1$	$W_3T_4V_1$	$W_3T_5V_1$		
	V_2	$W_3T_1V_2$	$W_3T_2V_2$	$W_3T_3V_2$	$W_3T_4V_2$	$W_3T_5V_2$		
	V_3	$W_3T_1V_3$	$W_3T_2V_3$	$W_3T_3V_3$	$W_3T_4V_3$	$W_3T_5V_3$		
	V_4	$W_3T_1V_4$	$W_3T_2V_4$	$W_3T_3V_4$	$W_3T_4V_4$	$W_3T_5V_4$		
	V_5	$W_3T_1V_5$	$W_3T_2V_5$	$W_3T_3V_5$	$W_3T_4V_5$	$W_3T_5V_5$		
TOTAL								
MEAN								
W_4	V_1	$W_4T_1V_1$	$W_4T_2V_1$	$W_4T_3V_1$	$W_4T_4V_1$	$W_4T_5V_1$		
	V_2	$W_4T_1V_2$	$W_4T_2V_2$	$W_4T_3V_2$	$W_4T_4V_2$	$W_4T_5V_2$		
	V_3	$W_4T_1V_3$	$W_4T_2V_3$	$W_4T_3V_3$	$W_4T_4V_3$	$W_4T_5V_3$		
	V_4	$W_4T_1V_4$	$W_4T_2V_4$	$W_4T_3V_4$	$W_4T_4V_4$	$W_4T_5V_4$		
	V_5	$W_4T_1V_5$	$W_4T_2V_5$	$W_4T_3V_5$	$W_4T_4V_5$	$W_4T_5V_5$		
TOTAL								
MEAN								
W_5	V_1	$W_5T_1V_1$	$W_5T_2V_1$	$W_5T_3V_1$	$W_5T_4V_1$	$W_5T_5V_1$		
	V_2	$W_5T_1V_2$	$W_5T_2V_2$	$W_5T_3V_2$	$W_5T_4V_2$	$W_5T_5V_2$		
	V_3	$W_5T_1V_3$	$W_5T_2V_3$	$W_5T_3V_3$	$W_5T_4V_3$	$W_5T_5V_3$		
	V_4	$W_5T_1V_4$	$W_5T_2V_4$	$W_5T_3V_4$	$W_5T_4V_4$	$W_5T_5V_4$		
	V_5	$W_5T_1V_5$	$W_5T_2V_5$	$W_5T_3V_5$	$W_5T_4V_5$	$W_5T_5V_5$		
TOTAL								
MEAN								

For each pad material: TVW × 3 replications = 5×5×5×3 = 375 data points

For the four different pad materials (celdek, coconut fibre, jute fibre and pop sponge), it becomes: 375×4 = 1500 experimental points (treatment combinations).

Statistical analysis:

An analysis of variance was conducted to determine the significanceof the factors and interaction between the factors. Analysis of the collected data was carried out using Central Composite Design in Design Expert 6.0. Statistical Software. Microsoft Office Excel Package 2007 Version was used for the multiple regression analysis while on-line Tukey HSD test was used to separate treatment means.

3.2.3 **Performance evaluation**

The evaluation of the cooling performance of the selected pad media was done according to the two main criteria. The first criterion was the saturation efficiency and second was the static pressure drop. The evaporative saturation efficiencies of the pad media were determined by using equation 2.1

The static pressure drop was determined by obtaining the difference in pressure between the air inlet pressure and pressure of the air after passing through the pad thickness.

3.2.4**Model development approach**

The mathematical model used for this work is based on semi-experimental numerical model known as the Buckingham pi group models. Buckingham pi theorem states that an equation involving a number of physical variables which are expressible in terms of independent fundamental physical quantities can be expressed in term of N = n - m dimensionless parameters. The dimensionless π - group is determined by substituting the number of fundamental dimensions from the number of quantities (i.e. variables) to be modeled.

Number of dimensionless π - group (Nπ) is given by

$N\pi = n - m$ 3.1

where,

n is the number of quantities and m is the number of fundamental dimensions.

3.2.4.1 Model development for saturation efficiency (η_{Sat})

The modeling of saturation efficiency is based on the fundamental dimensions MLTK.

where M, L,T and K are mass, length, time and temperature respectively.

For this work the parameters to be modeled are shown in table 3.2 below.

Table 3.2 Modeling parameters for Saturation Efficiency.

No	Parameters	Dimensions	S.I. Units
1	Pad thickness (t)	L	m
2	Mass flow rate of air (m_a)	MT^{-1}	kg/sec.
3	Enthalpy at inlet (h_{v1})	L^2T^{-2}	KJ/kg
4	Air inlet duct cross-sectional area (A_s)	L^2	m^2
5	Saturation Efficiency (η_{sat})	------	-------
6	Wet bulb temperature (T_{wb})	k	^0C
7	Dry bulb temperature (T_{db})	k	^0C
8	Specific volume (s_v)	L^3M^{-1}	m^3/kg

Number of fundamental dimension, m = 4

Number of quantities, n = 8

Number of π - group, n - m = 8 - 4 = 4

Hence, we have four (4) π- groups.

The general model of the π groups is given by:

$\boldsymbol{\pi_i} = x_j x_i^a x_z^c x_w^d$

Where a,c and d are dimensionless coefficients.

$\pi_1 = f(\pi_2, \pi_3, \text{------} \pi_{k-r})$,

Thus:

$\boldsymbol{\pi_1} = t^a m_a^b S_v^c T_{db} h_{V1}$ 3.2

$$\boldsymbol{\pi_1} = \frac{t^4 h_{v1}}{m_a^2 S_v^2} \qquad 3.3$$

$\boldsymbol{\pi_2} = t^a m_a^b S_v^c T_{db}^d A_s$ 3.4

$$\boldsymbol{\pi_2} = \frac{A_s}{t^2} \qquad 3.5$$

$\boldsymbol{\pi_3} = t^a m_a^b S_v^c T_{db} \eta_{sat}$ 3.6

$\boldsymbol{\pi_3} = \eta_{sat}$ 3.7

$\boldsymbol{\pi_4} = t^a m_a^b S_v^c T_{db}^d T_{wb}$ 3.8

$$\boldsymbol{\pi_4} = \frac{T_{wb}}{T_{db}} \qquad 3.9$$

Summary of the dimensionless π - groups for the modeling of saturation efficiency (η_{sat}) are as follows:

$$\boldsymbol{\pi_1} = \frac{t^4 h_{v1}}{m_a^2 S_v^2}, \qquad \boldsymbol{\pi_2} = \frac{A_s}{t^2}, \qquad \boldsymbol{\pi_3} = \eta_{sat}, \qquad \boldsymbol{\pi_4} = \frac{T_{wb}}{T_{db}}$$

3.2.4.2 **Model development for pressure drop across the pad (ΔP)**

Modeling of pressure drop across the pad is based on the fundamental dimensions MLT.

where M, Land T are mass, length and time respectively.

For this work the parameters to be modeled are shown in table 3.3 below.

Table 3.3 Modeling parameters for Pressure Drop.

No	Parameters	Dimensions	S.I. Units
1	Pad depth (d)	L	m
2	Geometric Length (L_e)	L	m
3	Volumetrc flow rate of water (Q_w)	L^3T^{-1}	m^3/sec
4	Volumetrc flow rate of air (Q_a)	L^3T^{-1}	m^3/sec.
5	Pressure drop (ΔP)	$ML^{-1}T^{-2}$	N/m^2
6	Air velocity (V_a)	LT^{-1}	m/sec.
7	Density of air (ρ_a)	$M L^{-3}$	kg/ m^3

Number of fundamental dimension, m = 3

Number of quantities, n = 7

Number of π - group, n - m = 7 - 3 = 4

$\boldsymbol{\pi_1} = \rho_a^a Q_a^b d^c L_e$ 3.10

$\boldsymbol{\pi_1} = d^{-1}L_e = L_e / d$ 3.11

$\boldsymbol{\pi_2} = \rho_a^a Q_a^b d^c Q_w$ 3.12

$\boldsymbol{\pi_2} = Q_a^{-1}Q_w = Q_w / Q_a$ 3.13

$\boldsymbol{\pi_3} = \rho_a^a Q_a^b d^c \Delta P$ 3.14

$\boldsymbol{\pi_3} = \rho_a^{-1} Q_a^{-2} d^4 \Delta P = d^4 \Delta P / \rho_a Q_a^2$ 3.15

$\boldsymbol{\pi_4} = \rho_a^a Q_a^b d^c V_a$ 3.16

$\boldsymbol{\pi_4} = Q_a^{-1} d^2 V_a = d^2 V_a / Q_a$ 3.17

Summary of the dimensionless π - groups for the modeling of Pressure drop (ΔP) are as follows:

$\boldsymbol{\pi_1} = L_e / d$, $\boldsymbol{\pi_2} = Q_w / Q_a$, $\boldsymbol{\pi_3} = d^4 \Delta P / \rho_a Q_a^2$, $\boldsymbol{\pi_4} = d^2 V_a / Q_a$

However, since $\boldsymbol{\pi_3}$ is a function of pressure drop, ie $\boldsymbol{\pi_3} = (d^4 / \rho_a Q_a^2) \times \Delta P$ multiplying all the π – groups by $(\rho_a Q_a^2 / d^4)$ will give :

$\boldsymbol{\pi_1} = L_e \rho_a Q_a^2 / d^5$, $\boldsymbol{\pi_2} = \rho_a Q_w Q_a / d^4$, $\boldsymbol{\pi_3} = \Delta P$, $\boldsymbol{\pi_4} = V_a \rho_a Q_a / d^2$

3.2.5 **Model validation**

Under the varying factors of pad thickness, pad–face air velocity and water flow rate, the saturation efficiency and pressure drop of the various pad materials were determined experimentally. Central Composite Design in Design Expert 6.0. Statistical Software and Microsoft Office Excel Package 2007 Version were used to analysis the numerical data which involve graphical computations, modeling and optimization. The validity or suitability (goodness of fit) of the models was tested by comparing with the experimental data, while the modeling efficiency was estimated using the coefficient of determination (R^2).When a straight line is obtained, it indicate the suitability of the models to describe the saturation efficiency and pressure drop of the various pad materials.

CHAPTER FOUR

RESULTS AND DISCUSSION

4.1 **Results**

Table 4.1 Average values of ambient temperature, cooler temperature, saturation efficiency and pressure drop for 50mm pad thickness

PAD THICK-NESS (mm)	WATER FLOW RATE (L/min)	AIR FLOW RATE (m/s)	AMBIENT TEMP.T (^{0}C)		COOLER TEMP. T_C (^{0}C)				SAT. EFFICIENCY η_{sat} (%)				PRESSURE DROP ΔP (pa)			
			T_{db}	T_{wb}	CE	JU	CO	SP	CE	JU	CO	SP	CE	JU	CO	SP
50	1.0	0.5	34.3	24.1	28.2	28.6	28.1	29.2	60.2	56.3	54.7	46.8	1.4	6.5	4.9	3.2
		1.0	33.4	23.4	27.7	27.5	27.3	28.3	56.9	57.4	55.1	48.2	2.5	11	7.8	5.5
		1.5	35.0	24.6	29.3	28.6	28.8	29.7	54.4	61.3	59.5	50.8	4.1	17.6	12.5	9.4
		2.0	34.2	24.0	28.8	27.8	27.8	28.8	52.6	63.1	62.3	53.1	6.8	26.4	20	15.5
		2.5	35.5	24.8	30.0	28.9	28.7	29.5	51.4	62.0	63.9	55.7	11.1	37	29	24
	1.25	0.5	34.8	23.9	28.2	28.6	28.9	29.4	60.9	56.8	55.1	49.2	2.2	10.1	7.6	5.0
		1.0	32.9	23.6	27.5	27.3	27.5	28.2	57.3	59.9	57.6	50.8	3.9	16.1	12.1	8.5
		1.5	34.7	23.6	28.6	27.8	28.1	28.8	54.8	61.9	59.8	52.9	6.2	24.6	18.1	12.8
		2.0	35.2	24.6	29.6	28.5	28.6	29.3	52.8	63.2	62.5	55.7	10.2	34.8	28	21.7
		2.5	32.5	23.5	27.9	26.8	26.9	27.5	51.3	63.7	62.7	56.1	14.3	46.6	37.7	31.2
	1.50	0.5	34.7	23.6	27.9	28.4	28.5	29.2	61.3	56.9	55.6	49.9	3.4	15.7	11.8	7.5
		1.0	33.8	23.1	27.7	27.3	27.6	28.3	57.4	60.3	58.1	51.2	6.1	23.9	18.8	13.2
		1.5	34.2	24.0	28.6	27.9	28.0	28.8	55.0	61.9	60.3	52.9	9.3	34.9	27.2	19.2
		2.0	32.8	23.4	27.8	26.3	26.4	27.1	53.0	63.5	62.8	56.1	15.3	47.7	39.2	30.4
		2.5	33.3	23.6	28.3	27.1	27.3	27.9	51.7	63.7	62.1	55.9	20	58.6	48.7	38.9
	1.75	0.5	34.1	24.3	28.1	28.5	28.6	29.2	61.5	56.9	55.8	50.2	5.3	22	16.5	10.5
		1.0	33.0	23.6	27.6	27.3	27.5	28.2	57.8	60.6	58.6	51.3	9.5	31.5	26.3	18.5
		1.5	35.0	24.5	29.2	28.5	28.6	29.4	55.1	61.8	60.5	53.1	13.9	42.4	35.4	25
		2.0	34.3	24.1	28.9	27.8	27.9	28.5	53.1	63.8	61.2	56.7	22.9	57.6	49	36
		2.5	35.1	24.2	29.4	28.1	28.2	28.9	52.3	63.9	61.7	57.0	28	68.7	58.8	45.8
	2.00	0.5	35.5	24.8	28.9	29.4	29.5	30.1	61.9	57.1	56.0	50.1	7.4	28.6	23.1	14.7
		1.0	32.5	23.5	27.3	27.1	27.2	27.9	57.9	60.5	58.9	51.4	13.3	40.9	34.2	24.1
		1.5	36.0	24.0	29.3	28.6	28.7	29.6	55.6	62.0	61.0	53.6	18.1	53	42.5	30
		2.0	33.3	23.6	28.1	27.1	27.1	27.9	53.3	64.1	63.8	56.0	27.5	69.1	56.4	41
		2.5	34.1	24.4	29.0	27.9	27.9	28.6	52.9	64.1	63.9	57.2	33.6	79	67.6	52.7

T_{db}= Dry bulb temp. T_{wb}= Wet bulb temp; CE= Celdek; JU= Jute; CO= Coconut; SP = Sponge

Table 4.2Average values of saturation efficiency and pressure drop for various pad materials at 1.75 l/min pad water flow rate.

Water Flow Rate:		1.75 l/min							
Pad Thick-ness (mm)	Pad Face Air Velocity (m/sec.)	SATURATION EFFICIENCY				PRESSURE DROP			
		CELDEK	JUTE FIBER	COCONUT FIBER	POP SPONGE	CELDEK	JUTE FIBER	COCONUT FIBER	POP SPONGE
50	0.5	61.5	56.9	55.8	50.2	5.3	22	16.5	10.5
	1.0	57.8	60.6	58.6	51.3	9.5	31.5	26.3	18.5
	1.5	55.1	61.8	60.5	53.1	13.9	42.4	35.4	25
	2.0	53.1	63.8	61.2	56.7	22.9	57.6	49	36
	2.5	52.3	63.9	61.7	57.0	28	68.7	58.8	45.8
100	0.5	71.8	63.7	60.7	54.1	6.9	28.6	21.5	13.7
	1.0	68.9	67.2	63.5	56.9	11.9	39.4	32.9	23.1
	1.5	66.3	71.3	65.7	58.9	16.7	50.9	42.5	30.2
	2.0	64.5	73.1	67.8	61.5	27.5	69.1	58.8	43.7
	2.5	63.9	74.3	68.5	61.3	33.6	79	67.6	53.8
150	0.5	77.9	70.7	66.8	60.7	9	37.2	28	17.8
	1.0	74.8	73.8	69.6	62.8	14.9	49.3	41.1	28.9
	1.5	73.3	78.0	72.1	63.9	20	61.1	51.1	36.2
	2.0	72.6	80.3	75.6	66.8	31.1	82.9	70.6	52.8
	2.5	71.4	80.7	76.0	67.0	40.3	94.8	81.1	66.1
200	0.5	80.7	72.9	69.2	62.9	11.7	48.4	36.4	23.1
	1.0	79.1	76.9	72.6	65.9	18.6	61.6	49.3	36.1
	1.5	77.5	82.5	76.3	66.2	24	73.3	61.3	43.4
	2.0	77.1	82.6	80.3	70.7	37.3	99.5	84.7	63.4
	2.5	76.7	81.7	79.9	70.1	48.4	113.8	97.3	79.3
250	0.5	79.8	73.5	70.8	63.4	15.2	62.9	47.3	30.1
	1.0	78.6	77.2	73.3	66.5	23.3	77	61.6	45.1
	1.5	77.3	80.9	77.4	67.3	28.8	90.1	73.6	52.1
	2.0	76.1	82.5	79.5	69.3	44.8	119.4	101.6	76.1
	2.5	76.3	82.3	80.3	71.6	58.1	136.6	116.8	95.2

Table 4.1 shows the average values of ambient temperature, cooler temperature, saturation efficiency and pressure drop for 50mm pad thickness while table 4.2 shows the average values of saturation efficiency and pressure drop for various pad materials at 1.75 l/min pad water flow rate. Other tables are shown in appendix 4.1 to 4.14.

4.1.1**Effect of Pad Face Air Velocity on the Saturation Efficiency and Pressure Drop of Different Pad Types:**

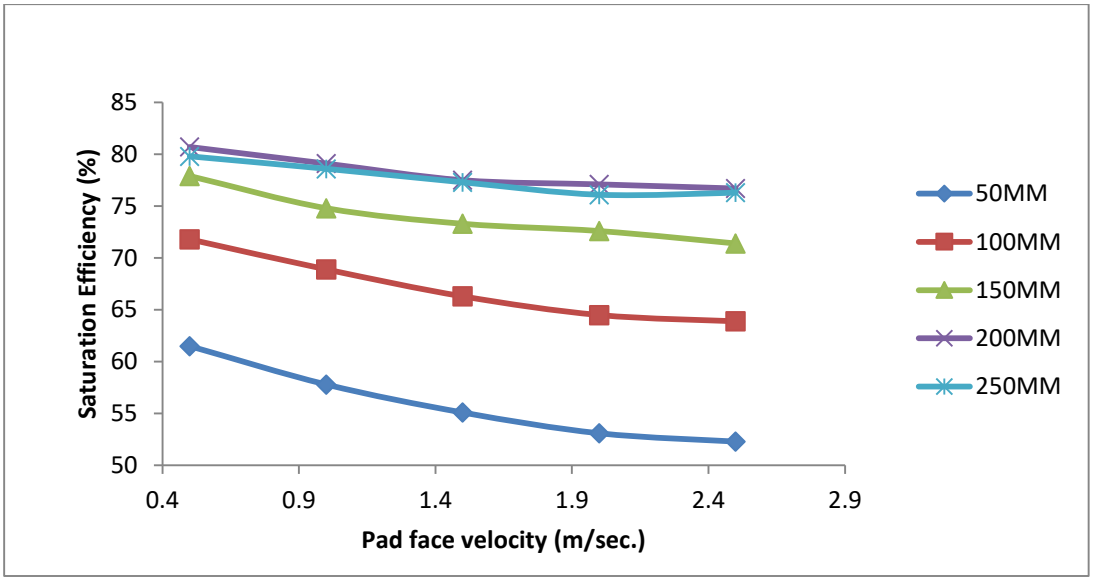

Figure 4.1 (a) Effect of pad face air velocities (pfav) at constant pad thickness and 1.75 l/min. water flow rate on saturation efficiency ofCeldek

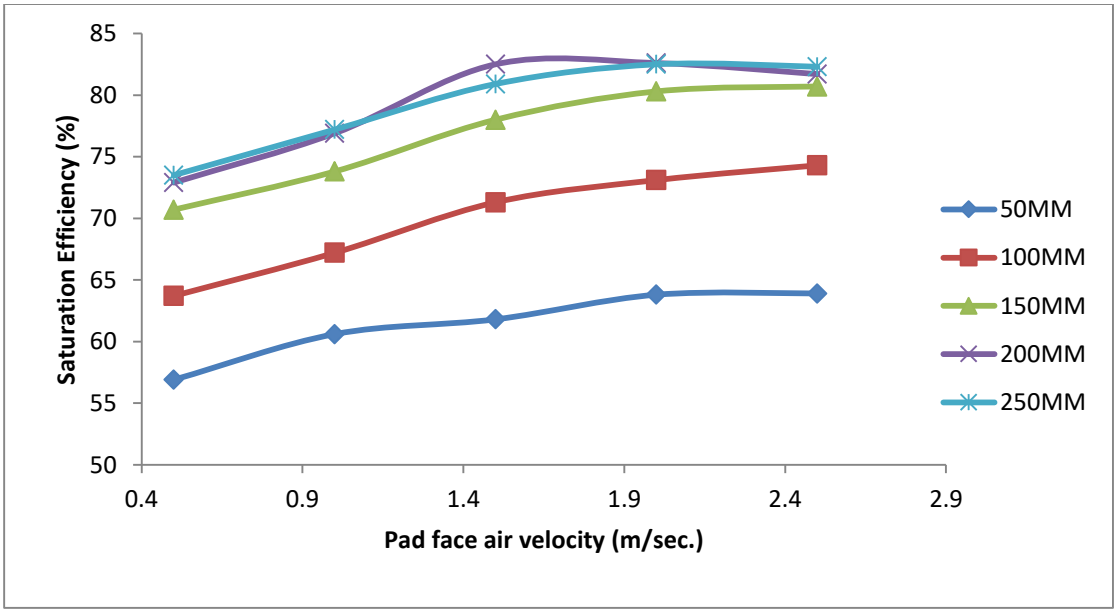

Figure 4.1 (b)Effect of pad face air velocities (pfav) at constant pad thickness and 1.75 l/min. water flow rate on saturation efficiency ofJutefibre.

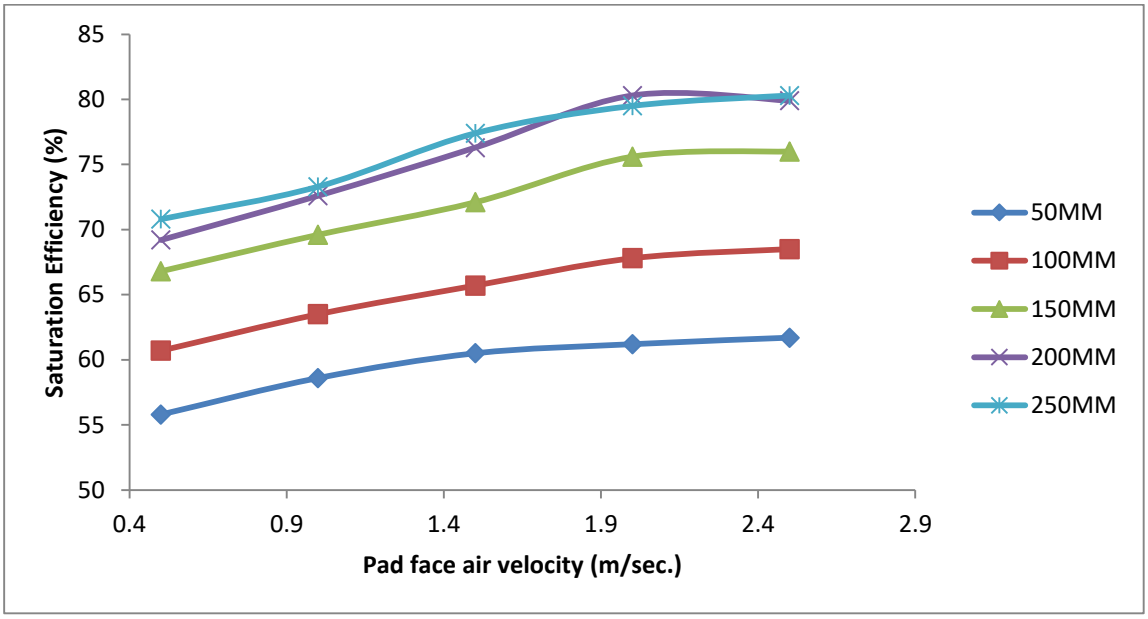

Figure 4.1 (c) Effect of pad-face air velocities (pfav) at constant pad thickness and 1.75 l/min. water flow rate on saturation efficiency of Coconut fiber.

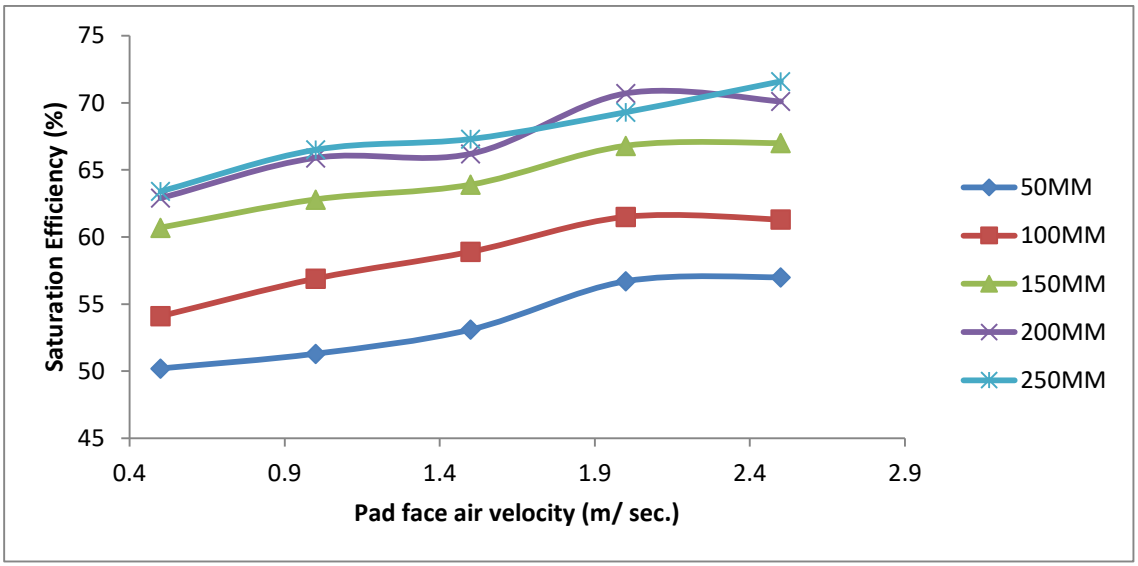

Figure 4.1 (d) Effect of pad face air velocities (pfav) at constant pad thickness and 1.75 l/min. water flow rate on saturation efficiency of Pop sponge.

Figure 4.1 (a) to (d) show the effect of pad face air velocities at constant pad thickness and 1.75 l/min. water flow rate on saturation efficiency of Celdek, Jute fibre, Coconut fibre and POP Sponge respectively. While figure 4.1 (e) and (f) show the effect of pad face air velocities on saturation efficiency and pressure drop of pad types at 150mm pad thickness and 1.75 l/min. water flow raterespectively.

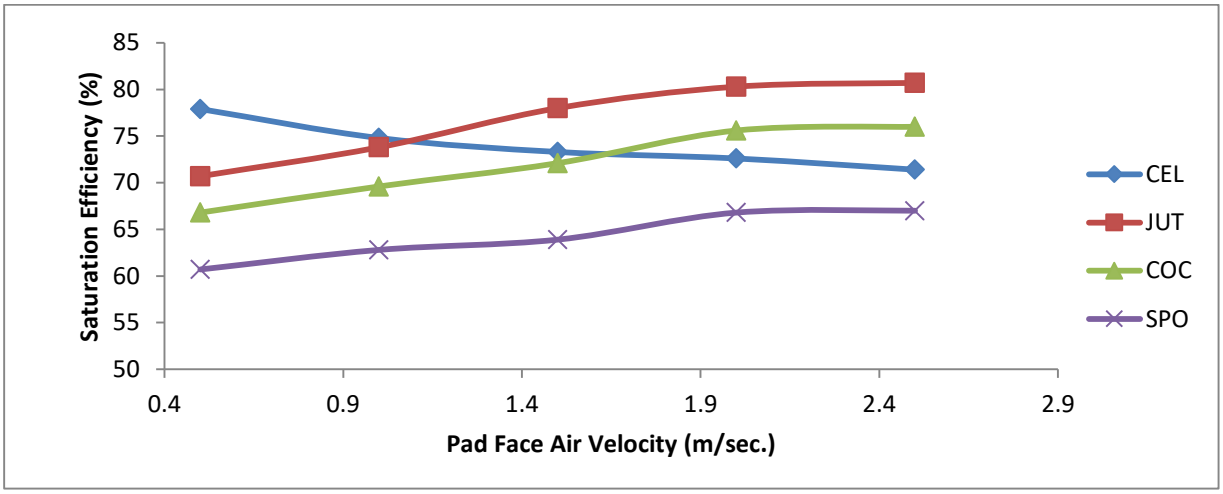

Figure 4.1 (e) Effect of pad face air velocities on the saturationefficiency of pad types at 150mm pad thickness and 1.75 l/min. water flow rate.

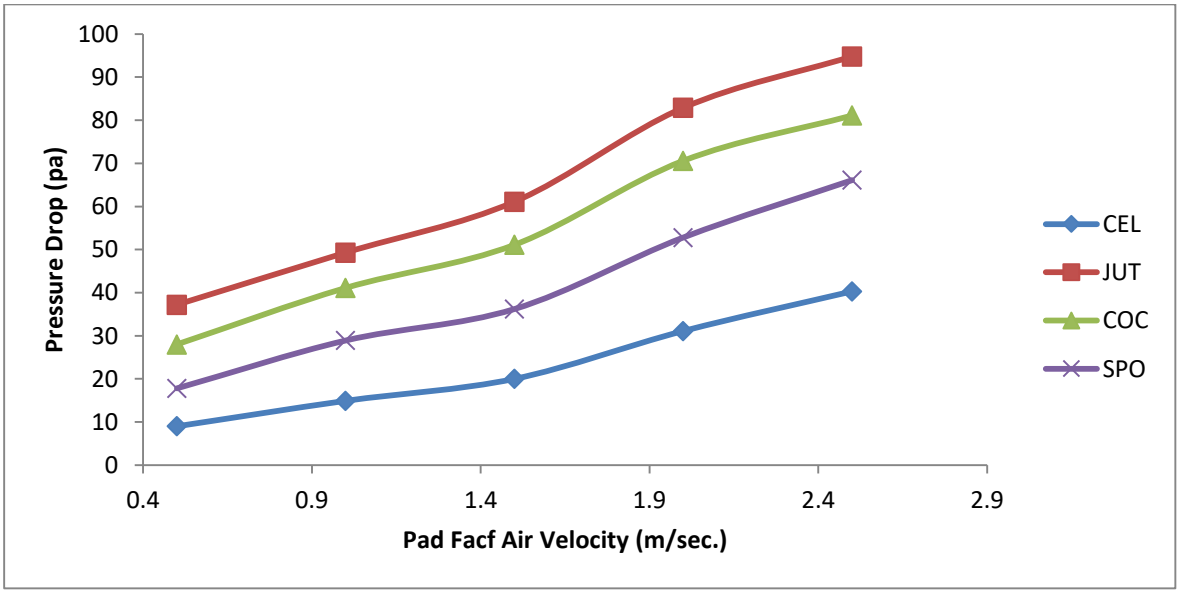

Figure 4.1 (f) Effect of pad face air velocity on the pressure drop of pad types at 150mm pad thickness and 1.75 l/min. water flow rate.

4.1.2**Effect of Pad Thickness on the Sat. Efficiency and Pressure Drop of Pad Types:**

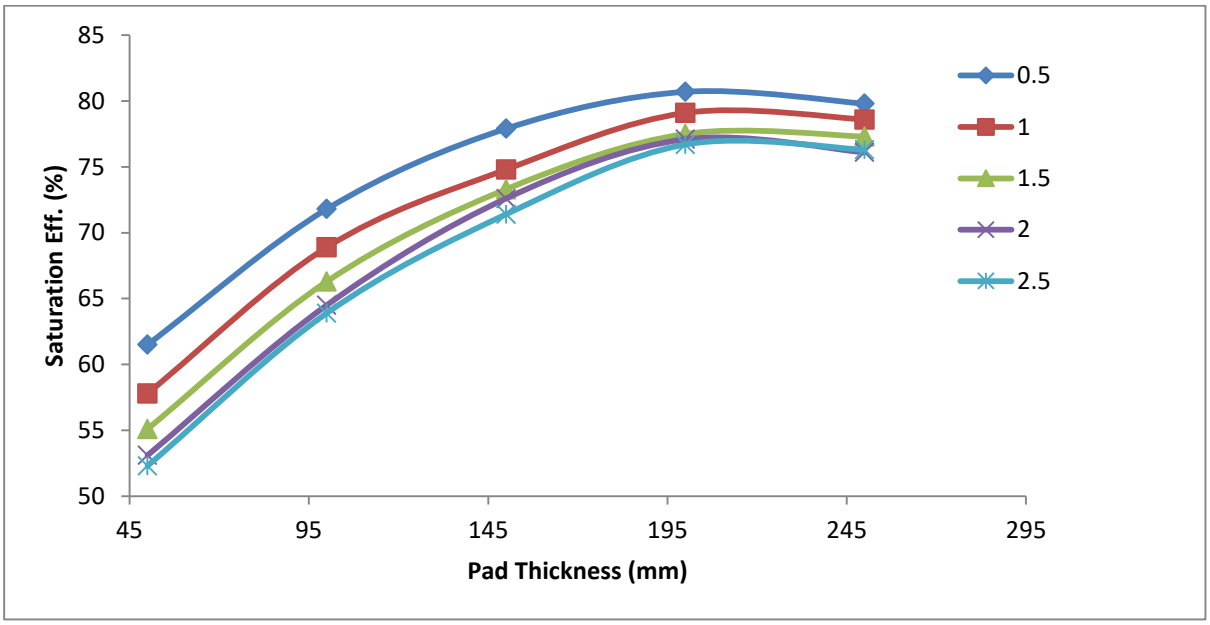

Figure 4.1 (g) Effect of pad thickness at constantpad face air velocities and 1.75 l/min. water flow rate on saturation efficiency of Celdek

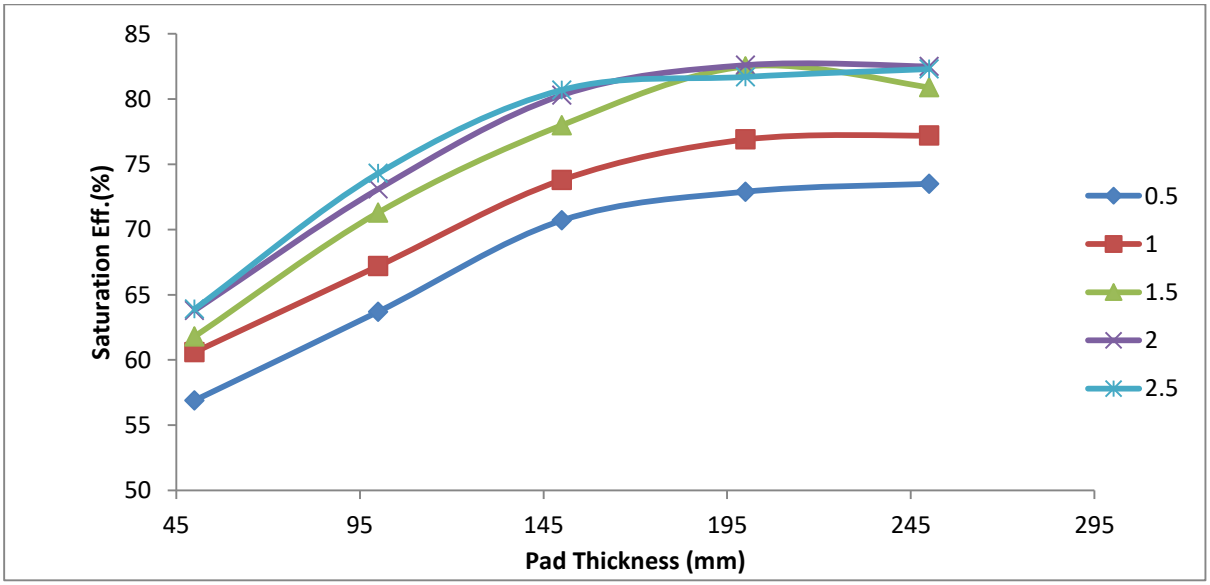

Figure 4.1 (h) Effect of pad thickness at constantpad face air velocities and 1.75 l/min. water flow rate on saturation efficiency of Jute fibre.

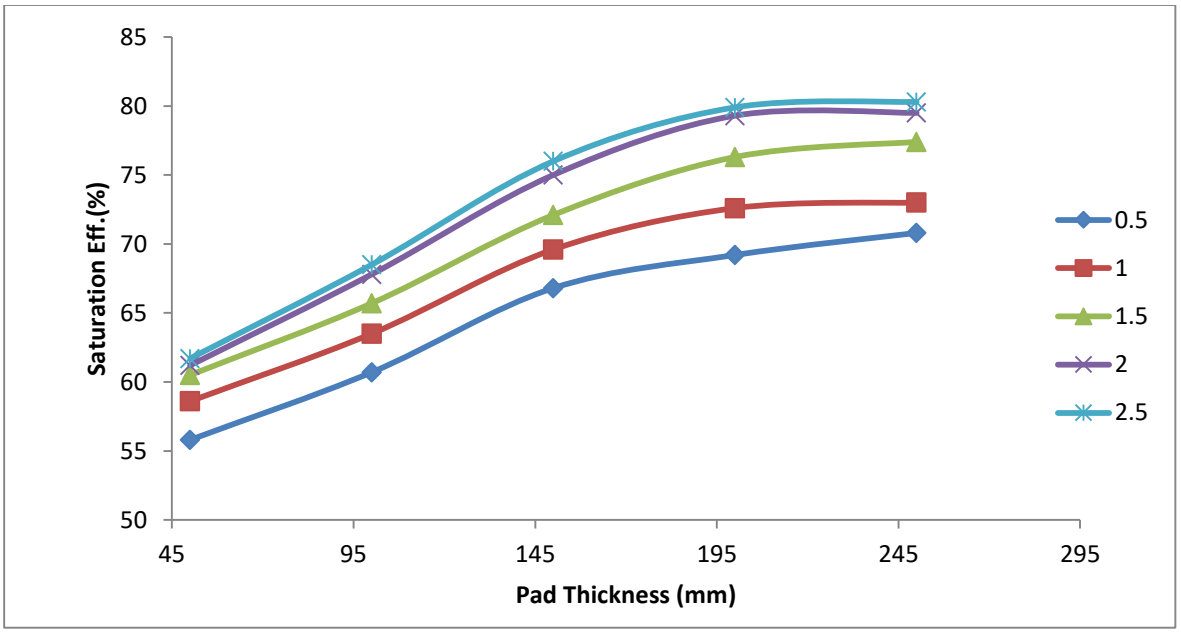

Figure 4.1 (i) Effect of pad thickness at constantpad face air velocities and 1.75 l/min.water flow rate on saturation efficiency of Coconut fibre.

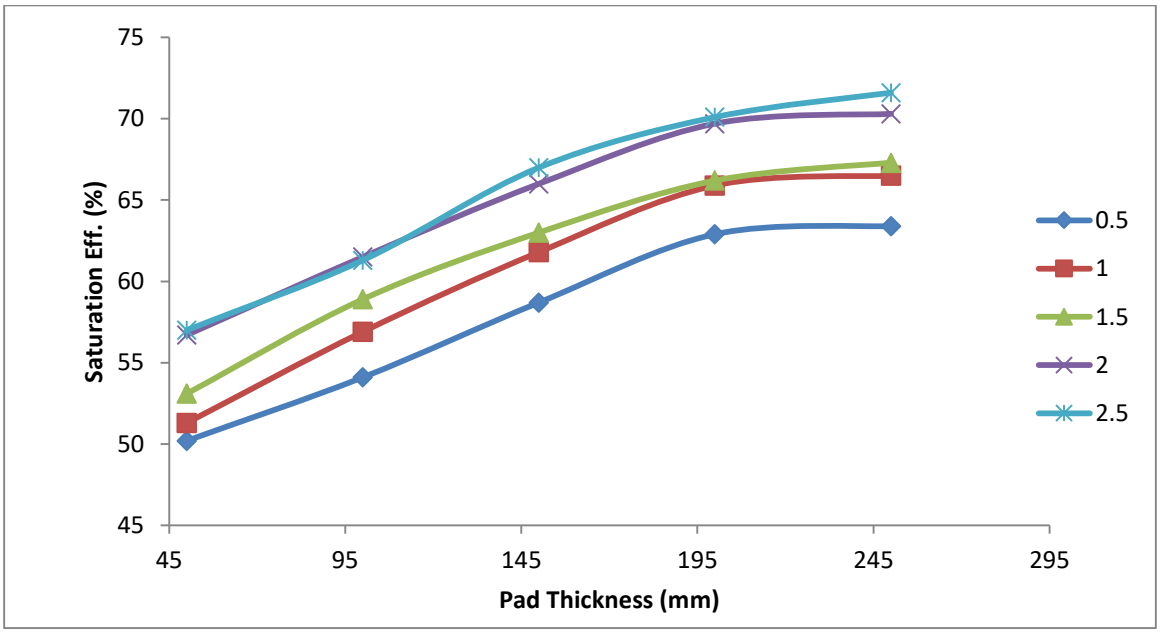

Figure 4.1 (j) Effect of pad thickness at constantpad face air velocities and 1.75 l/min. water flow rate on saturation efficiency of POP Sponge

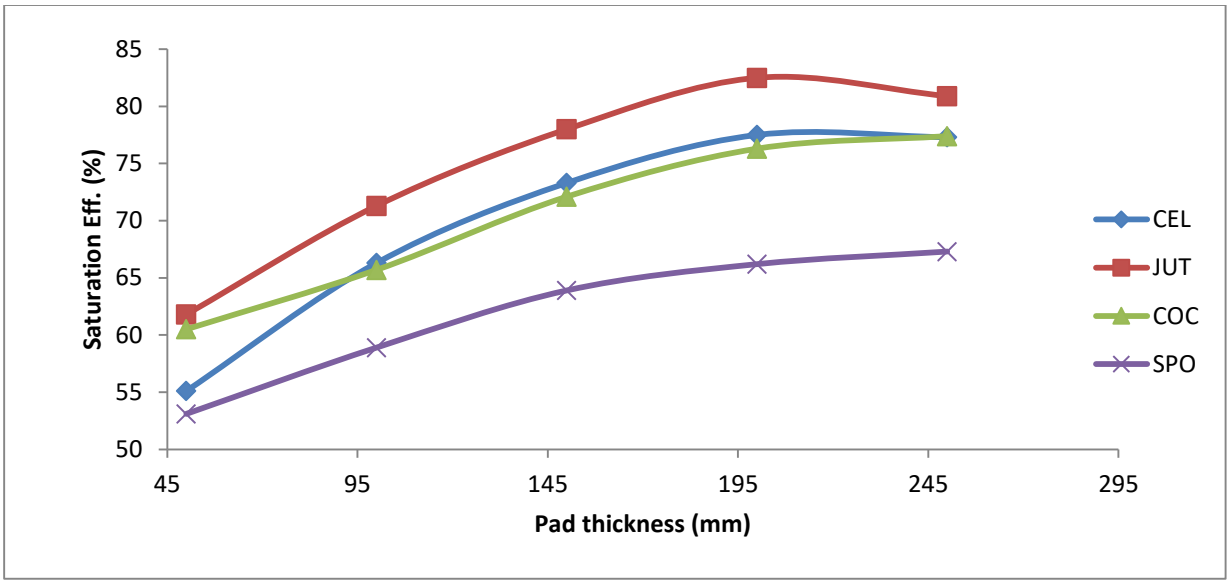

Figure 4.1 (k) Effect of pad thickness on saturation efficiency of pad types at 1.5 m/sec.pad face air velocity and 1.75 l/min. water flow rate.

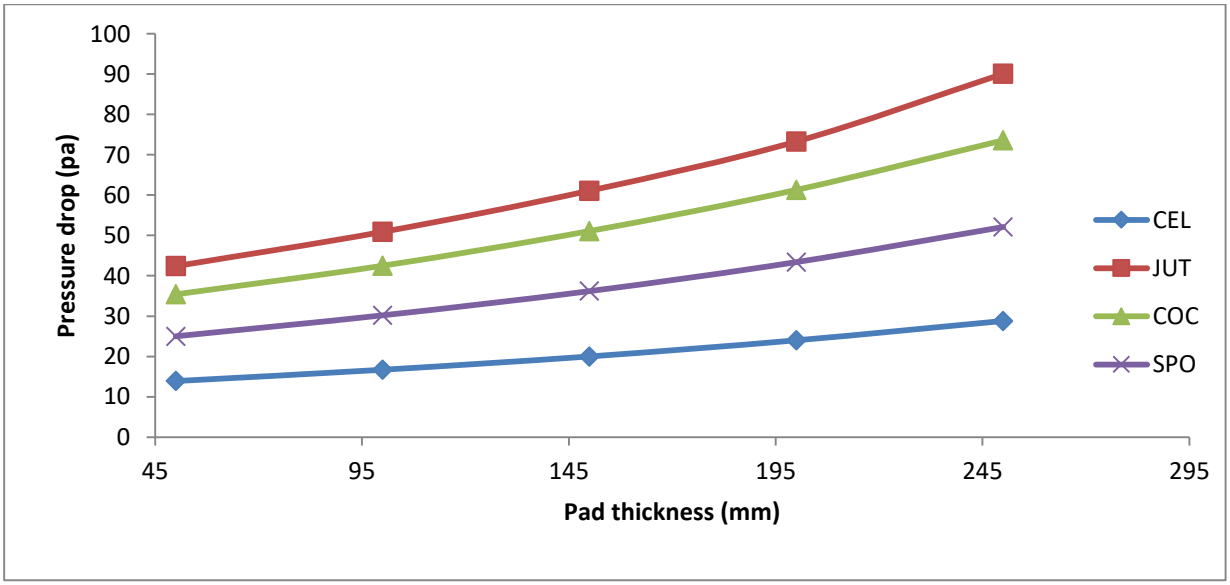

Figure 4.1 (l) Effect of pad thickness on Pressure drop of pad types at 1.5 m/sec.pad face air velocity and 1.75 l/min. water flow rate.

Figure 4.1 (g) to (j) show the effect of pad thicknessesat constant pad face air velocity and 1.75 l/min. water flow rate on saturation efficiency of Celdek, Jute fibre, Coconut fibre and POP Sponge respectively. While figure 4.1 (k) and (l) show the effect of pad thickness on the saturation efficiency and pressure drop of pad types at 1.5m/sec. pad face air velocity and 1.75 l/min. water flow raterespectively.

4.1.3 **Effect of Water flow rate on the Saturation Efficiency and Pressure Drop of Pad Types:**

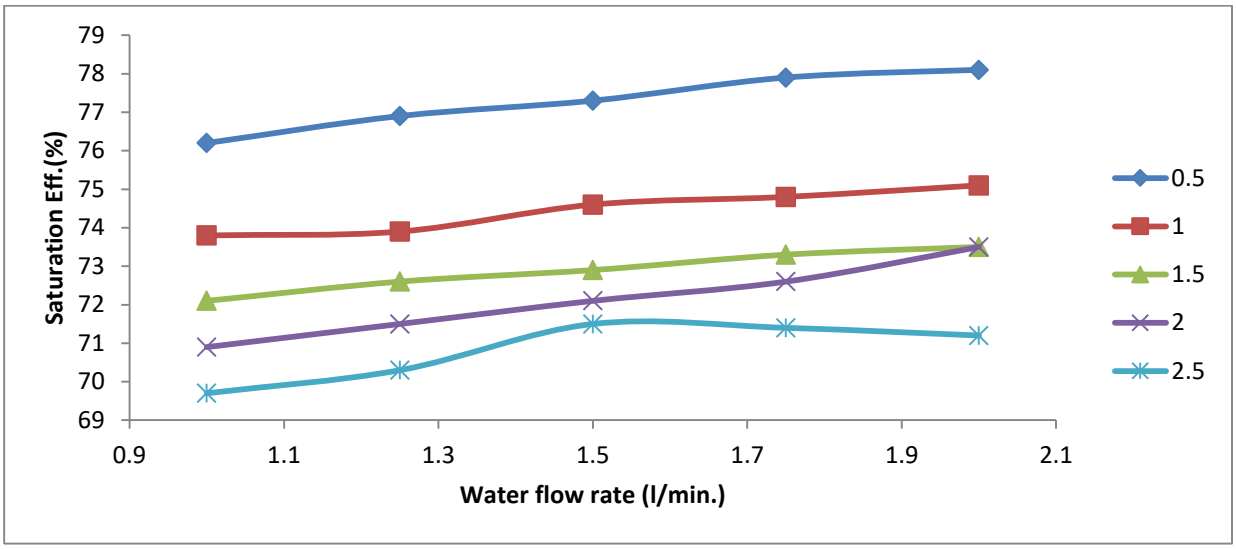

Figure 4.1(m) Effect of water flow rate on thesaturation efficiency of Celdek at constant pad face air velocity and150mm pad thickness.

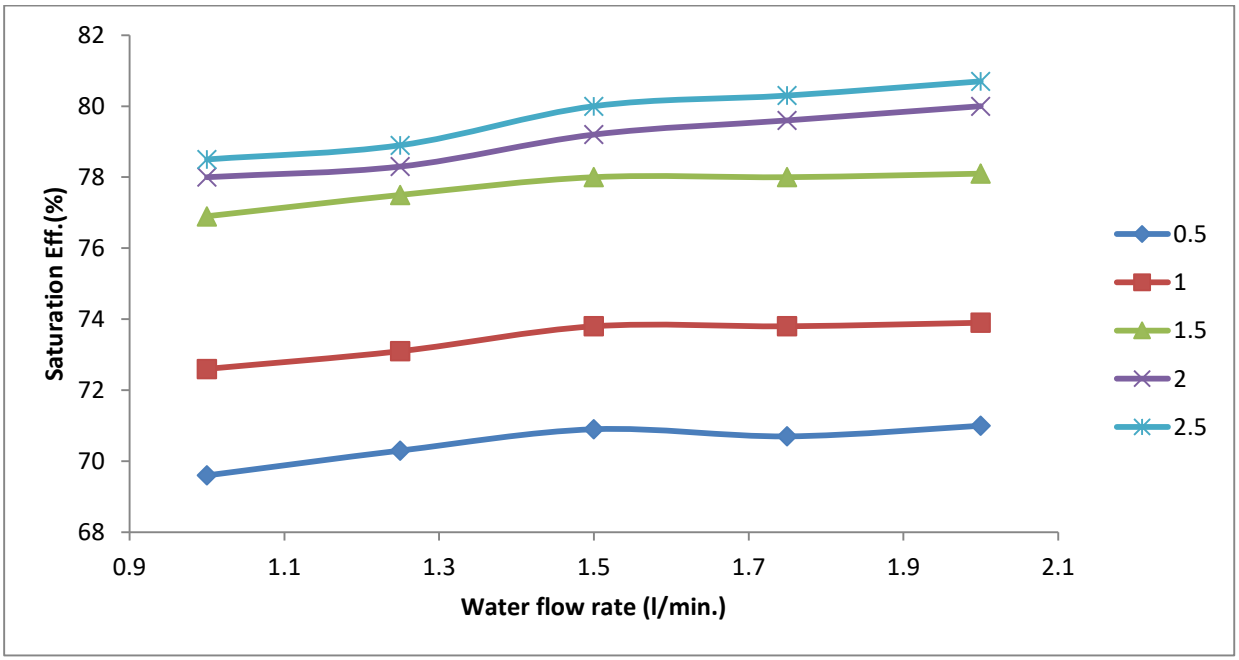

Figure 4.1(n) Effect of water flow rate on the saturation efficiency of Juteat constant pad face air velocity and150mm pad thickness.

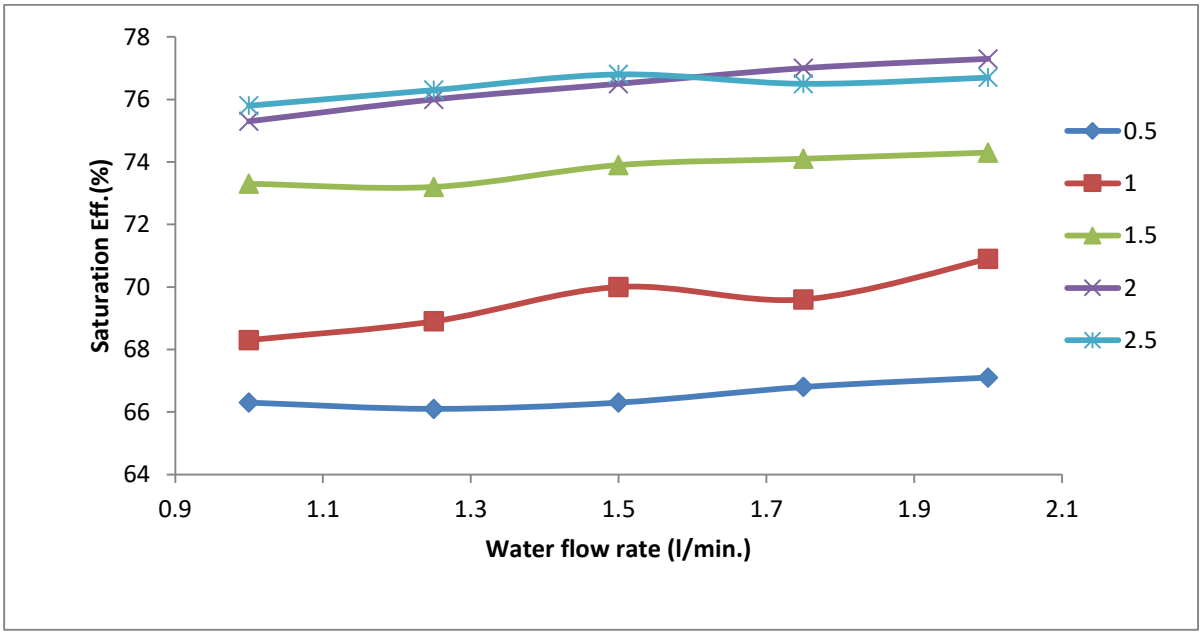

Figure 4.1(o) Effect of water flow rate on thesaturation efficiency of coconutat constant pad face air velocity and150mm pad thickness.

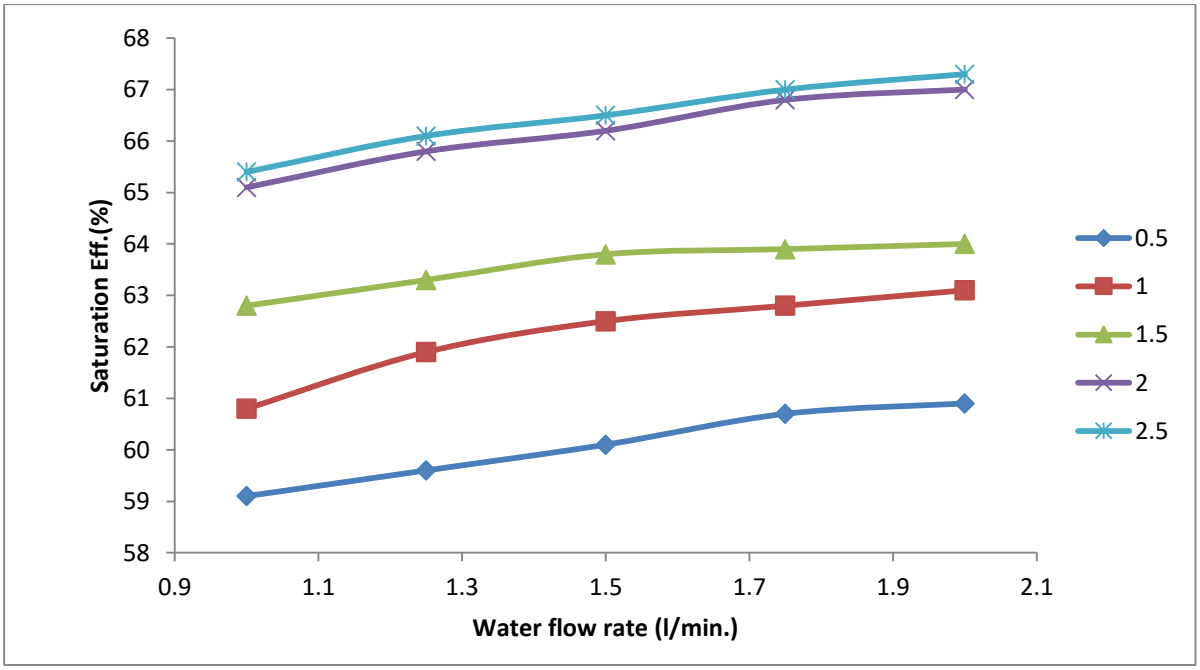

Figure 4.1(p) Effect of water flow rate on thesaturation efficiency of POP Spongeat constant pad face air velocity and 150mm pad thickness.

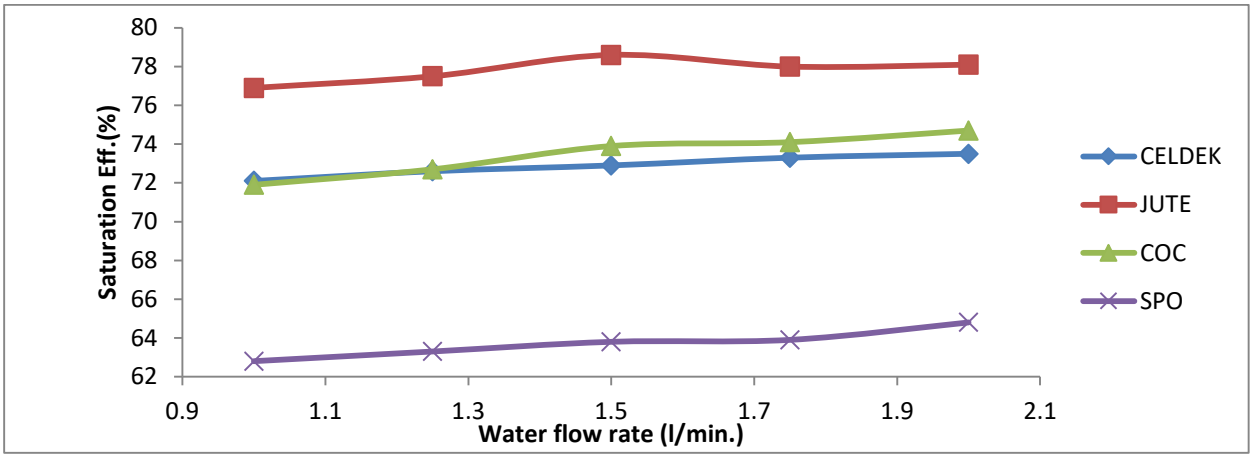

Figure 4.1(q) Effect of water flow rate on the saturation efficiency of pad types at 1.5 m/sec.pad face air velocity and and150mm pad thickness.

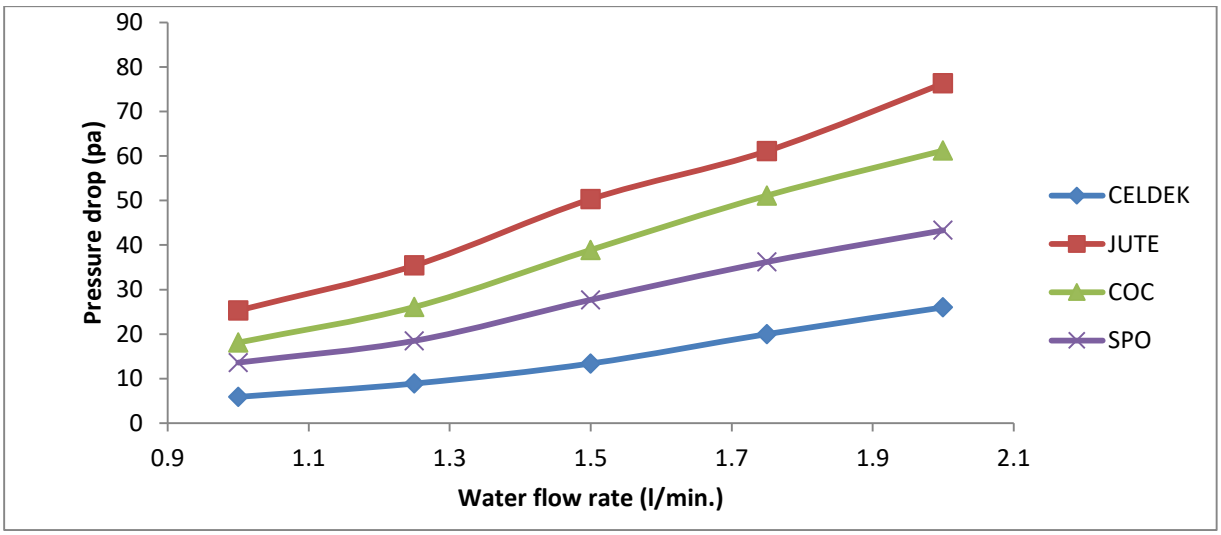

Figure 4.1(r) Effect of water flow rate on pressure drop of pad types at 1.5 m/sec.pad face air velocity and and150mm pad thickness.

Figure 4.1 (m) to (p) show the effect of water flow rate at constant pad face air velocity and 150mm pad thicknesson saturation efficiency of Celdek, Jute fibre, Coconut fibre and POP Sponge respectively. While figure 4.1 (q) and (r) show the effect of water flow rate on the saturationefficiencyand pressure drop of pad types at 1.5m/sec. pad face air velocity and 150mm pad thicknessrespectively.

4.1.4 **Statistical analysis for the effect of pad thickness, water flow rate and pad face air velocity on saturation efficiency and pressure drop.**

4.1.4.1 **Statistical analysis for celdekpadmaterial**

The effects of pad thickness, water flow rate and airflow rate on the efficiency and presure drop of Celdek was understudied using Central Composite Design in Design Expert 6.0. Statistical software. The design consists of twenty (20) treatment combinations as shown in table 4.3.

Table 4.3: Central composite design of efficiency and pressure drop for Celdek

S/N	Pad thickness (mm)	Water flowrate (l/s)	Air Vel (m/s)	Experimental Efficiency (%)	Predicted efficiency (%)	Experimental Pressure drop (Pa)	Predicted Pressure drop (Pa)
1	200	1.75	2.0	77.1	76.98	37.3	36.44
2	250	1.5	1.5	76.9	76.60	19.3	19.68
3	150	1.5	1.5	72.9	72.86	13.4	13.38
4	200	1.25	2.0	76.2	76.06	17.5	17.32
5	200	1.25	1.0	78.1	78.05	7.6	7.85
6	150	2.0	1.5	73.5	74.05	26	26.94
7	100	1.75	1.0	68.9	68.13	11.9	11.67
8	150	1.0	1.5	72.1	72.83	5.9	5.54
9	150	1.5	1.5	72.9	72.86	13.4	13.38
10	150	1.5	1.5	72.9	72.86	13.4	13.38
11	200	1.75	1.0	79.1	79.18	18.6	18.42
12	150	1.5	1.5	72.9	72.86	13.4	13.38
13	50	1.5	1.5	55	56.59	9.3	9.50
14	100	1.25	2.0	64.3	63.31	12.2	11.96
15	150	1.5	1.0	77.3	77.77	9.5	9.13
16	150	1.5	1.5	72.9	72.86	13.4	13.38
17	150	1.5	2.5	71.5	72.31	28.9	29.85
18	150	1.5	1.5	72.9	72.86	13.4	13.38
19	100	1.25	1.0	68.4	67.61	4.9	5.34
20	100	1.75	2.0	64.5	63.64	27.5	26.84

For example the first treatment combination is made up of 200mm pad thickness, 1.75

l/min. water flow rate and 2.0m/s produced 77.1% and 37.3Pa saturation efficiency and pressure drop respectively. Results of other treatment combinations are also shown in table 4.3. A quadratic model shown in equation 4.1 was generated by the software using the experimental values to predict the efficiency of Celdeck

η_{sat}= 65.62 +0.11t - 4.65v- 2.22× $10^{-4}t^2$+ $0.77v^2$4.1

The model validation was understudied using analysis ofvariance (ANOVA) as shown in table 4.4. While figure 4.3 shows the graph of predicted and actual efficiency for Celdek pad.

Table 4.4:Anova for Response Surface Quadratic Model Sat.Efficiency of Celdek

	Sum of		Mean	F		Remarks
Source	Squares	DF	Square	Value	Prob > F	
Model	610.52	9	67.84	92.63	< 0.0001	significant
t	483.17	1	483.17	659.76	< 0.0001	significant
w	1.80	1	1.80	2.45	0.1483	non-sig
v	35.94	1	35.94	49.07	< 0.0001	significant
t × t	70.85	1	70.85	96.74	< 0.0001	significant
w × w	0.60	1	0.60	0.82	0.3854	non-sig
v × v	8.55	1	8.55	11.68	0.0066	significant
tw	0.18	1	0.18	0.25	0.6308	non-sig
tv	2.65	1	2.65	3.61	0.0866	non-sig
wv	0.02	1	0.02	0.03	0.872	non-sig
Residual	7.32	10	0.73			
Lack of Fit	7.32	5	1.46			
Pure Error	0.00	5	0.00			
Cor Total	617.85	19				

Std. Dev.	0.86	R-Squared	0.9881
Mean	72.02	Adj R-Squared	0.9775
C.V.	1.19	Pred R-Squared	0.9103
PRESS	55.44	Adeq Precision	37.332

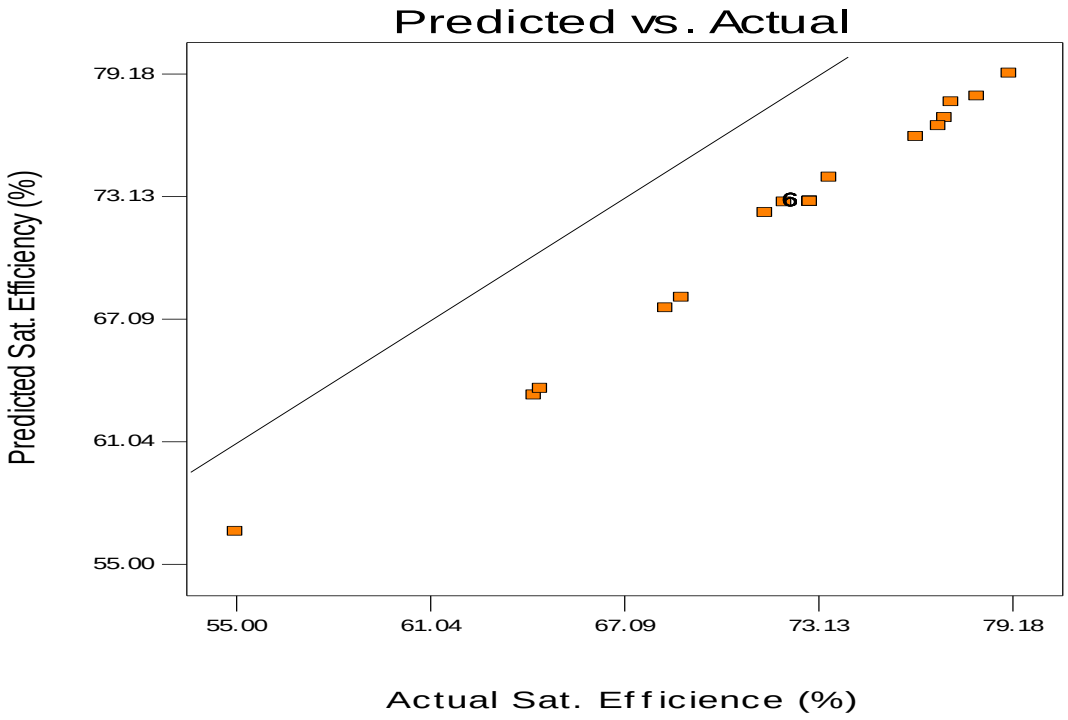

Figure 4.2: Graph of predicted and actual efficiency for Celdek pad.

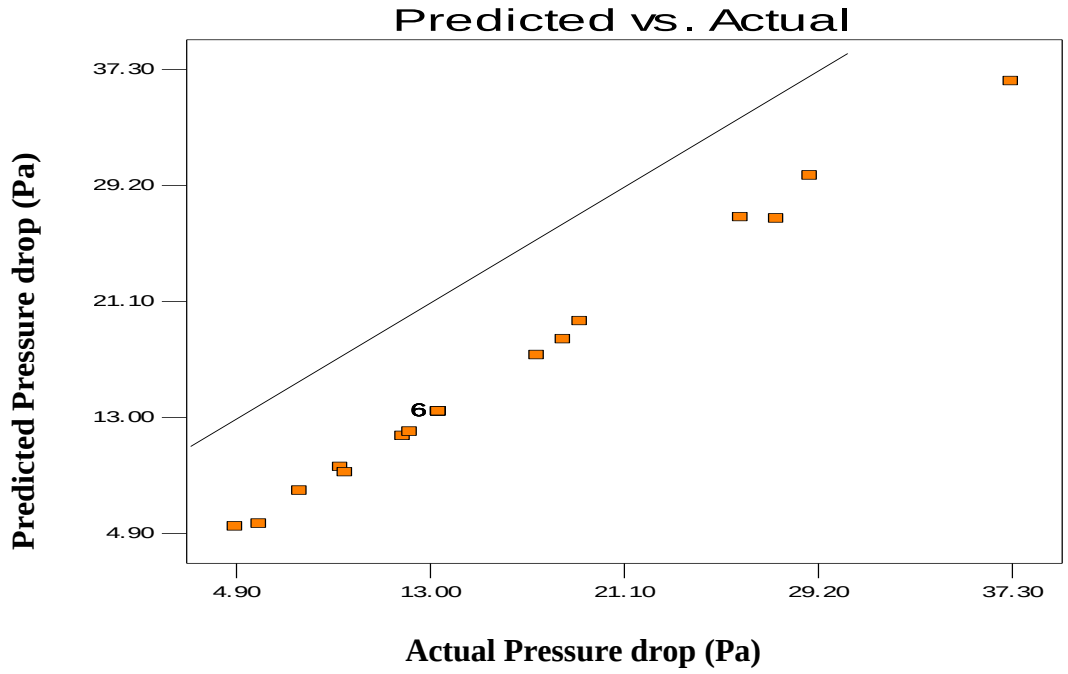

Figure 4.3: Graph of predicted and actual pressure drop for Celdek pad

Also generated by the software is the model equation for the prediction of pressure drop across Celdelk pad as shown in equation 4.2.

$$\Delta P = +11.44 - 0.03t - 9.00w - 7.80v + 4.27 \times 10^{-5}t^2 + 4.04w^2 + 2.16v^2 + 0.02tw$$

$$+7.13 \times 10^{-3}tv + 4.28wv \quad 4.2$$

The model equation 4.2 was validated using ANOVA and the results shown in table 4.5.

The interaction among pad thickness, airflow rate and water flow rate and the effects on pressure drop are represented in the response surface plots shown in figures 4.5 (a) to (c).

Table 4.5 :Anova for response surface quadratic model pressure drop of Celdek

Source	Sum of Squares	DF	Mean Square	F Value	Prob > F	
Model	1322.6	9	146.96	381.73	< 0.0001	significant
t	125.0	1	125.00	324.71	< 0.0001	significant
w	553.0	1	553.01	1436.47	< 0.0001	significant
v	518.2	1	518.22	1346.12	< 0.0001	significant
t × t	2.6	1	2.63	6.84	0.0258	significant
w × w	14.7	1	14.72	38.24	0.0001	significant
v × v	67.2	1	67.22	174.61	< 0.0001	significant
tw	9.0	1	9.03	23.46	0.0007	significant
tv	4.1	1	4.06	10.55	0.0088	significant
wv	36.6	1	36.55	94.94	< 0.0001	significant
Residual	3.8	10	0.38			
Lack of Fit	3.8	5	0.77			
Pure Error	0.0	5	0.00			
Cor Total	1326.5	19				

Std. Dev.	0.62	R-Squared	0.9971
Mean	15.84	Adj R-Squared	0.9945
C.V.	3.92	Pred R-Squared	0.9779
PRESS	29.25	Adeq Precision	70.8807

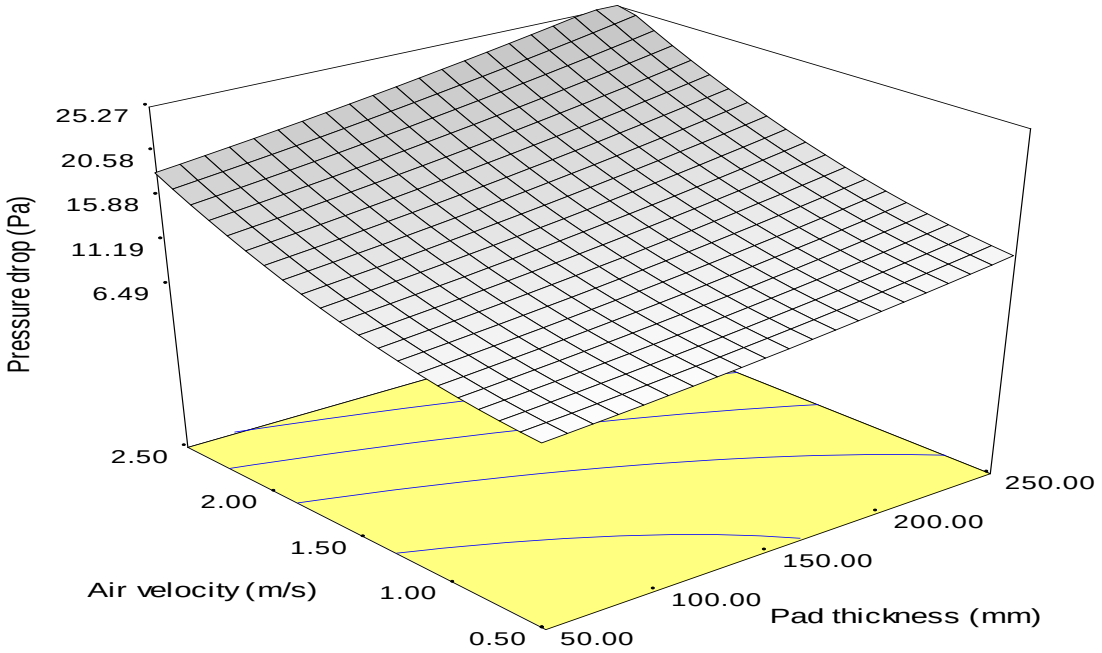

Figures 4.4(a) Response surface plot of the interaction effect of air velocity and pad thickness on pressure drop of Celdek pad.

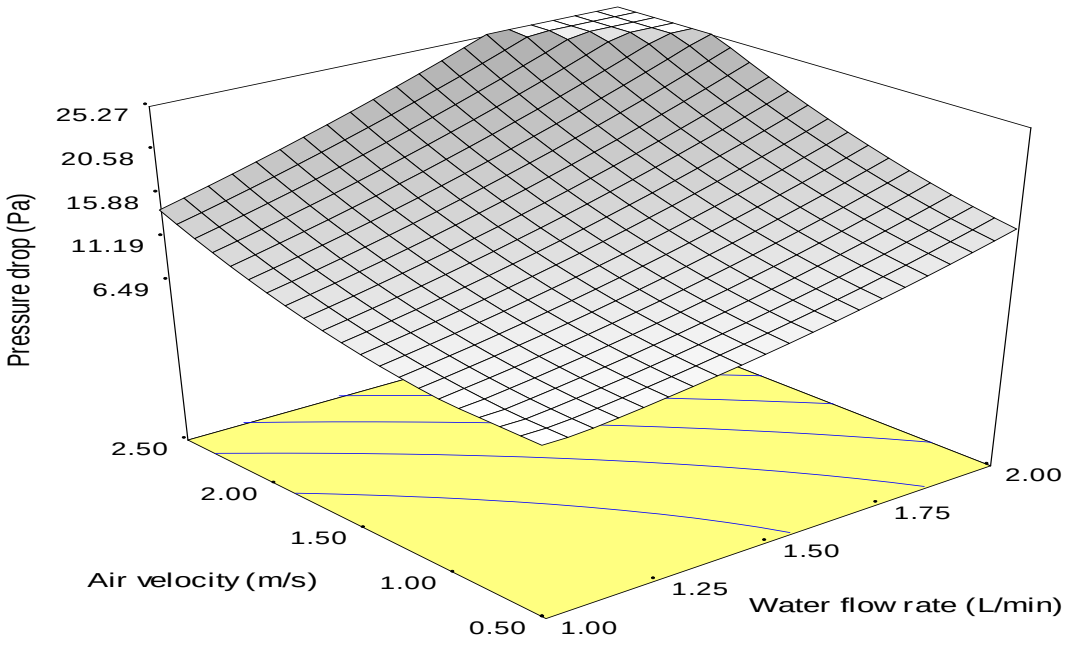

Figure4.4(b) Response surface plot of the interaction effect of air velocity and water flow rate on the pressure drop of Celdek pad.

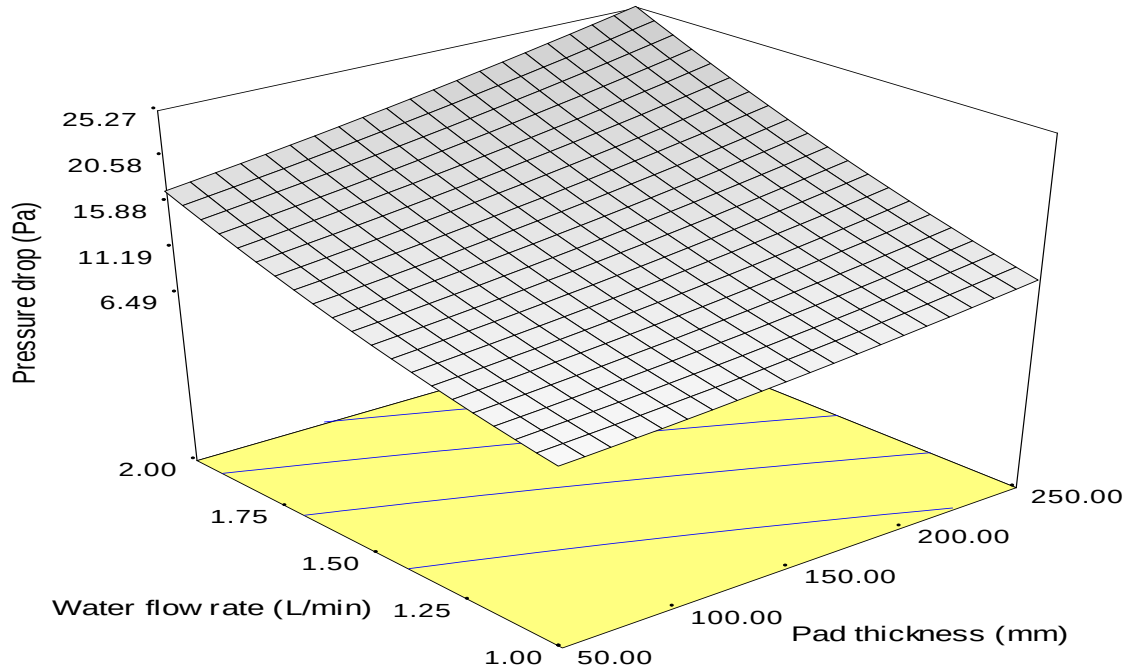

Figure4.4(c) Response surface plot of the interaction effect of water flow rate and pad thickness on the pressure drop of Celdek pad

4.1.4.1.1:**Optimization of the efficiency and pressure drop of celdek pad**

The efficiency and pressure drop of celdek pad was optimized under the conditions stated in table 4.6

Table 4.6 Conditions for sat. efficiency and pressure drop of celdek pad optimization

Constraints						
		Lower	Upper	Lower	Upper	
Name	Goal	Limit	Limit	Weight	Weight	Importance
Thickness	is in range	50	250	1	1	3
wat.flwrate	is in range	1	2	1	1	3
air.vel	is in range	0.5	2.5	1	1	3
efficiency	maximize	55	79.1	1	1	3
pressure drp	minimize	4.9	37.3	1	1	3

From table 4.6, the pad thickness, water flow rate and pad face air velocity are within range, whereas efficiency and pressure drop are at maximum and minimum respectively.

From the software, the following optimization values were obtained

Table 4.7 Optimization of the sat. efficiency and pressure drop of celdek pad

No.	Thickness	water florate	AIR VEL	efficiency	pressure Drop	Desirability
1	197	1	0.5	77	6.9	0.927
2	195	1	0.5	76.9	6.8	0.926
3	185	1	0.5	76.6	6.7	0.921
4	174	1	0.5	76.2	6.5	0.914
5	161	1	0.5	75.6	6.3	0.904

The desirability plot for saturation efficiencyand pressure drop is shown in figure 4.5 (d)

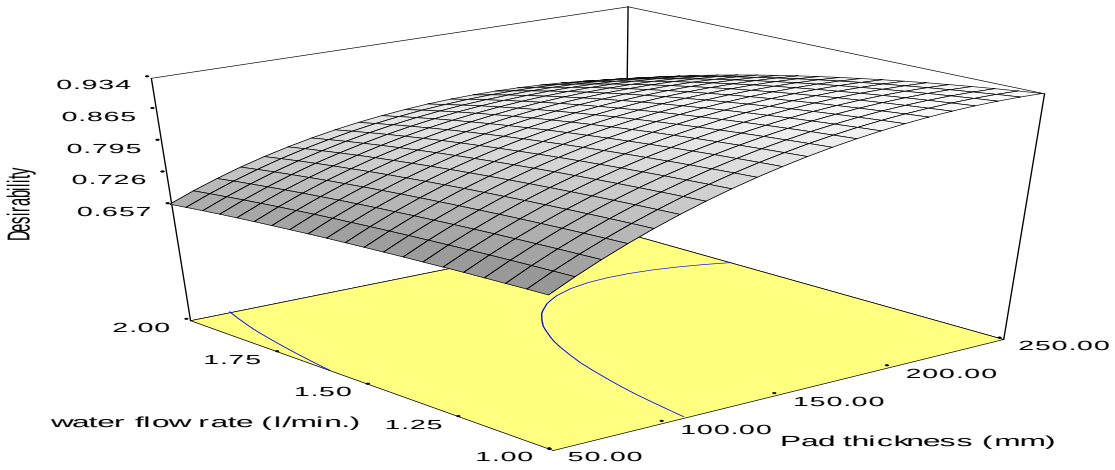

Figure: 4.4 (d)Desirability plot for Saturation efficiency of Celdek pad.

4.1.4.2 **Statistical analysis for jute fibrepad material**

The effects of pad thickness, water flow rate and airflow rate on the efficiency and presure drop of Jute fibre was understudied using Central Composite Design in DesignExpert 6.0. statistical software. The design consists of twenty (20) treatment combinations as shown in table 4.8. For example, the first treatment combination is made up 150mm pad thickness, 1.5 l/min. water flow rate and 1.5m/s produced 78.6% and

50.3Pa efficiency and pressure drop respectively. Results of other treatment combinations are also shown in table 4.8. A quadratic model shown in equation 4.3was generated by the software using the experimental values to predict the efficiency of Jute fibre pad.

Table 4.8: Central composite design of efficiency and pressure drop jute fibre

S/N	Pad thiclness (mm)	Water flow rate (l/s)	Air velocity (m/s)	Experimental Efficiency (%)	Predicted efficiency (%)	Experimental Pressure drop (Pa)	Predicted Pressure drop (Pa)
1	150	1.5	1.5	78.6	78.61	50.3	50.3
2	150	1.5	0.5	70.9	71.04	26.5	27.89
3	150	1.0	1.5	76.9	76.53	25.3	25.94
4	150	1.5	2.5	81.3	80.79	80.9	79.51
5	200	1.75	2.0	82.6	83.27	99.5	100.58
6	150	1.5	1.5	78.6	78.61	50.3	50.3
7	200	1.25	1.0	75.7	76.25	31.4	30.74
8	150	2.0	1.5	78.1	78.09	76.3	75.66
9	100	1.25	2.0	71.7	71.79	41.8	41.61
10	150	1.5	1.5	78.6	78.61	50.3	50.3
11	150	1.5	1.5	78.6	78.61	50.3	50.3
12	200	1.25	2.0	81.3	81.90	60.2	61.02
13	100	1.75	1.0	67.2	66.87	39.4	38.58
14	150	1.5	1.5	78.6	78.61	50.3	50.3
15	100	1.25	1.0	66.8	66.40	20.1	19.01
16	100	1.75	2.0	73.1	72.82	69.1	69.72
17	150	1.5	1.5	78.6	78.61	50.30	50.30
18	250	1.5	1.5	80.7	79.65	72.50	71.63
19	50	1.5	1.5	61.9	62.58	34.9	35.78
20	200	1.75	1.0	76.9	77.07	61.6	61.79

$$\eta_{sa} = +54.16 + 0.13t + 5.75w + 5.26v - 2.66\times10^{-4}t^2 - 1.83w^2 - 0.95v^2 \quad 4.3$$

The model validation was understudied using analysis of variance (ANOVA) as shown in table 4.9

Table 4.9:Anova for response surface quadratic model efficiency of jute fiber

Source	Sum of Squares	DF	Mean Square	F Value	Prob > F	
Model	578.27	9	64.25	184.01	< 0.0001	significant
t	351.80	1	351.80	1007.52	< 0.0001	significant
w	2.92	1	2.92	8.37	0.016	significant
v	114.76	1	114.76	328.67	< 0.0001	significant
t × t	101.29	1	101.29	290.09	< 0.0001	significant
w × w	3.02	1	3.02	8.66	0.0147	significant
v × v	13.09	1	13.09	37.50	0.0001	significant
tw	0.06	1	0.06	0.18	0.6842	non signif.
tv	0.03	1	0.03	0.09	0.7709	non signif.
wv	0.15	1	0.15	0.43	0.5253	non signif.
Residual	3.49	10	0.35			
Lack of Fit	3.49	5	0.70			
Pure Error	0.00	5	0.00			
Cor Total	581.7655	19				

Std. Dev.	0.59	R-Squared	0.994
Mean	75.84	Adj R-Squared	0.989
C.V.	0.78	Pred R-Squared	0.954
PRESS	26.66	Adeq Precision	49.504

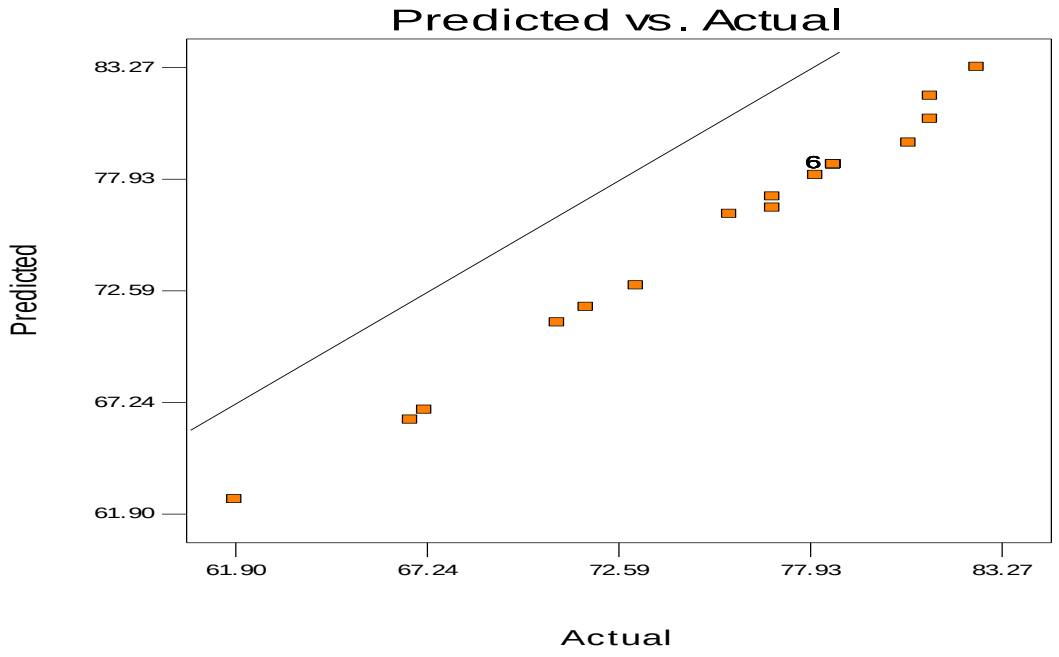

Figure 4.5: Graph of predicted and actual efficiency for Jute fibre.

Also generated by the software is the model equation for the prediction of pressure drop across the Jute fibre pad as shown in equation 4.4.

$$\Delta P = +0.74 - 0.04t + 12.45w + 2.46v + 1.20\times10^{-4}t^2 + 1.20v^2 + 0.06tw + 0.02tv + 4.28wv \quad 4.4$$

The model equation 4.4 was validated using anova and the results shown in table 4.10.

Table 4.10:Anova for response surface quadratic model pressure drop of jute fiber

Source	Sum of Squares	DF	Mean Square	F Value	Prob > F	
Model	7920.52	9	880.06	795.23	< 0.0001	significant
t	1550.84	1	1550.84	1401.37	< 0.0001	significant
w	2983.93	1	2983.93	2696.33	< 0.0001	significant
v	3216.38	1	3216.38	2906.37	< 0.0001	significant
t × t	20.85	1	20.85	18.84	0.0015	significant
w × w	0.45	1	0.45	0.41	0.5371	non signif
v × v	20.85	1	20.85	18.84	0.0015	significant
tw	65.55	1	65.55	59.23	< 0.0001	significant
tv	29.26	1	29.26	26.44	0.0004	significant
wv	36.55	1	36.55	33.03	0.0002	significant
Residual	11.07	10	1.11			
Lack of Fit	11.07	5	2.21			
Pure Error	0.00	5	0.00			
Cor Total	7931.59	19				

Std. Dev.	1.052	R-Squared	0.999
Mean	52.065	Adj R-Squared	0.997
C.V.	2.021	Pred R-Squared	0.989
PRESS	84.292	Adeq Precision	109.704

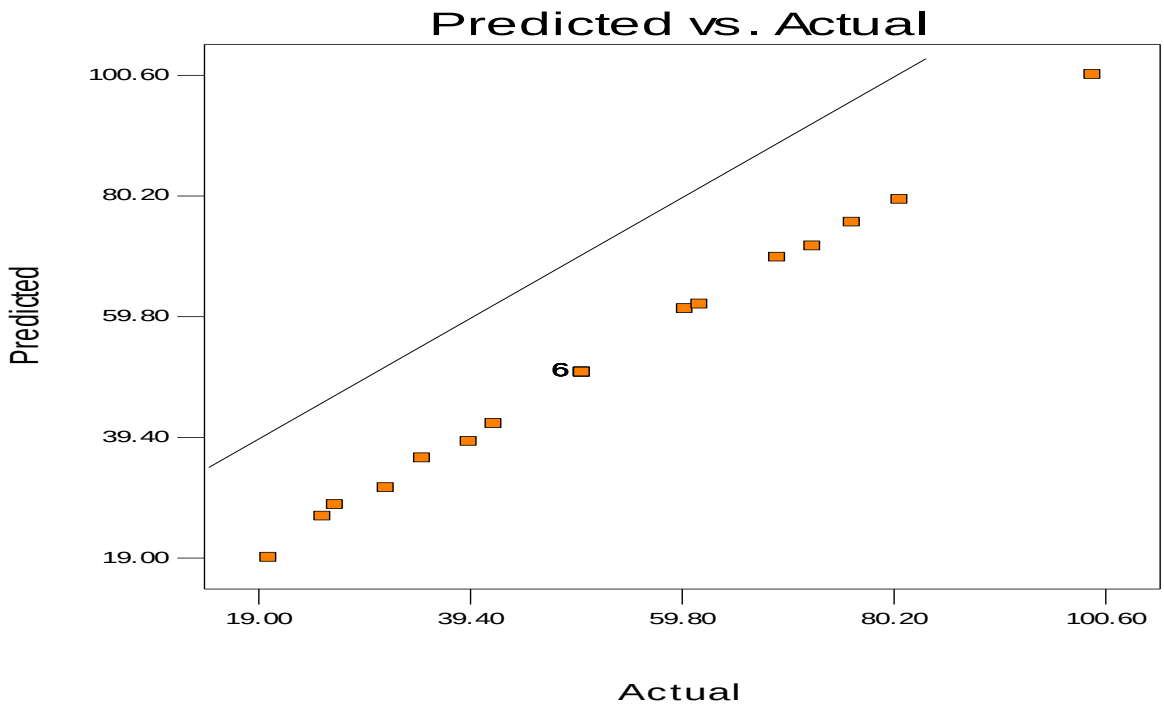

Figure 4.6: Graph of predicted and actual pressure drop for jute fiber pad

The interaction among pad thickness, airflow rate and water flow rate and the effects on pressure drop are represented in the response surface plots shown in figures.4.8(a) to (c).

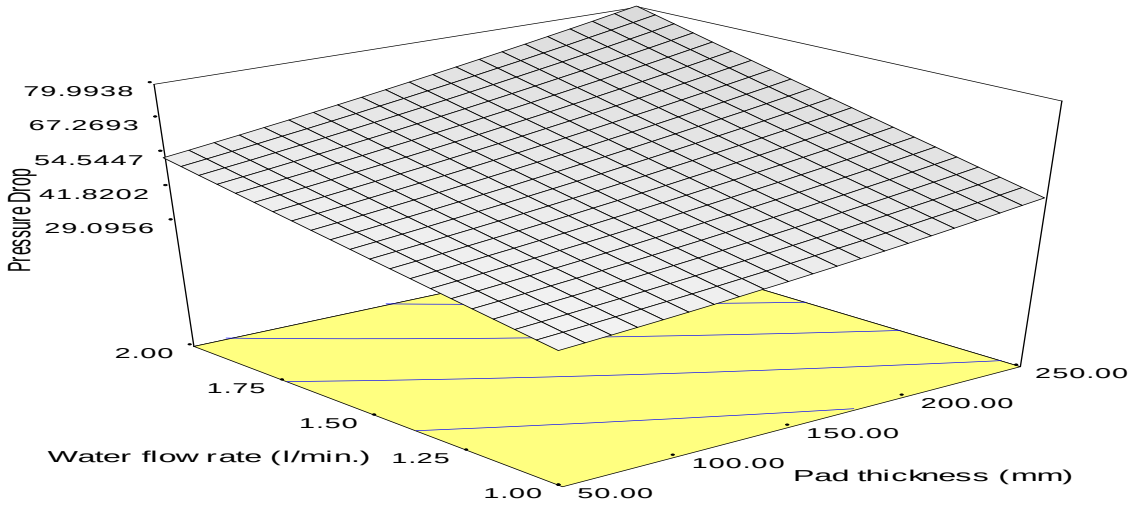

Figure 4.7 (a) Response surface plot of the interaction effect of water flow rate and pad thickness on pressure drop of Jute fibre pad.

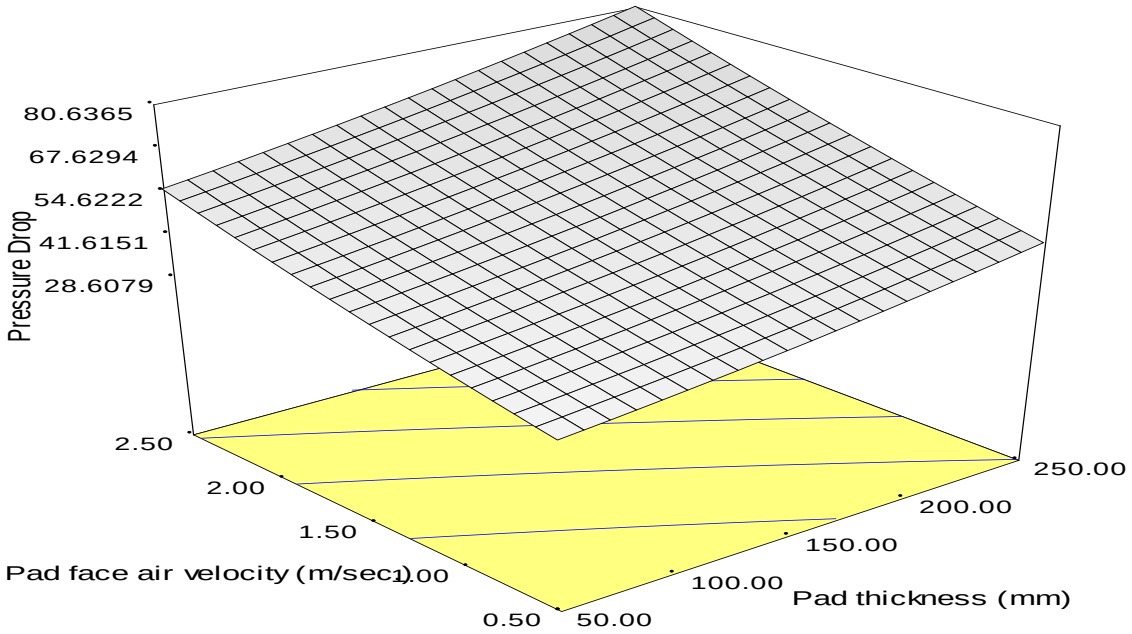

Figure4.7 (b) Response surface plot of the interaction effect of pad face air velocity and pad thickness on the pressure drop of Jute fibre pad.

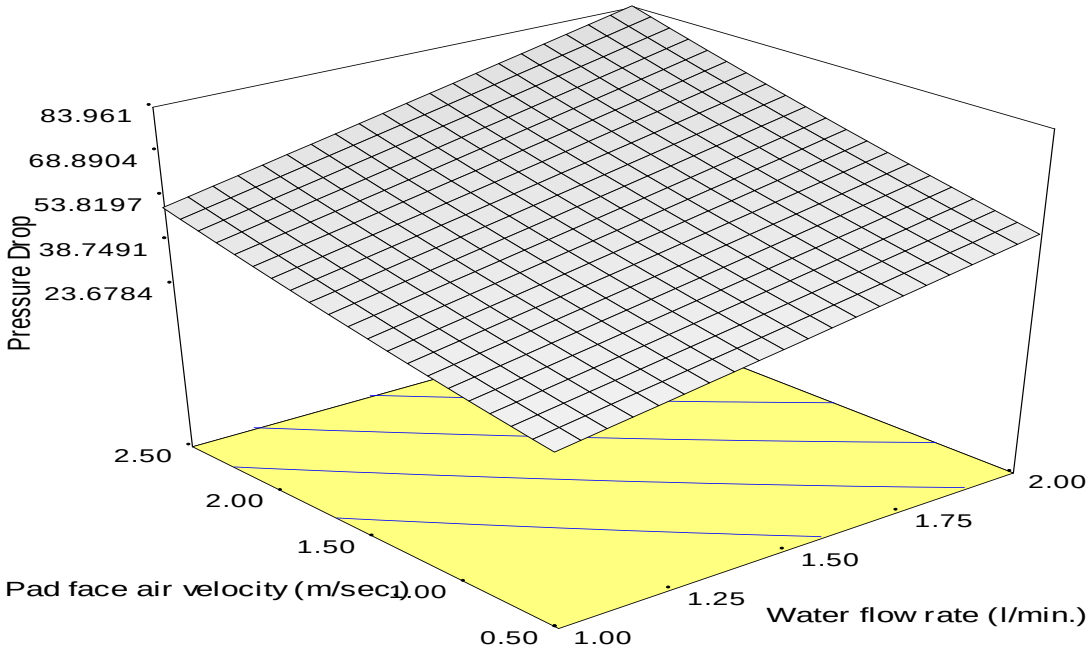

Figure4.7 (c) Response surface plot of the interaction effect of water flow rate and pad face air velocity on the pressure drop of Jute fibre pad

4.1.4.2.1**Optimization of the saturation efficiency and pressure drop of Jute fibre**

Table 4.11 Conditions for optimization of Sat. efficiency and pressure drop of Jute fibre

Constraints						
		Lower	Upper	Lowe	Upper	
Name	Goal	Limit	Limit	Weigl	Weight	Importance
Pad Thickness	is in range	50	250	1	1	3
Water flow rate	is in range	1.0	2.0	1	1	3
Pad Air Velocity	is in range	0.5	2.5	1	1	3
Sat. Efficiency	maximize	61.9	82.6	1	1	3
Pressure Drop	minimize	20.1	99.5	1	1	3

From table 4.11, the pad thickness, water flow rate and pad face air velocity are within range, whereas efficiency and pressure drop are at maximum and minimum respectively.

From the software, the following optimization values were obtained as shown in table 4.12

Table 4.12 Optimization of the Sat. efficiency and pressure drop of Jute fiber pad

No.	Thickness	water florate	AIR VEL	efficiency	pressure Drop	Desirability
1	200	1	1.2	78.6	35.8	0.805
2	204	1	1.2	78.7	36.3	0.805
3	203	1	1.4	79.2	38.4	0.802
4	157	1	1.5	77.9	35.7	0.789
5	151	1	2	78.8	42	0.769

The desirability plot for saturation efficiency and pressure dropis shown in figure 4.7 (d).

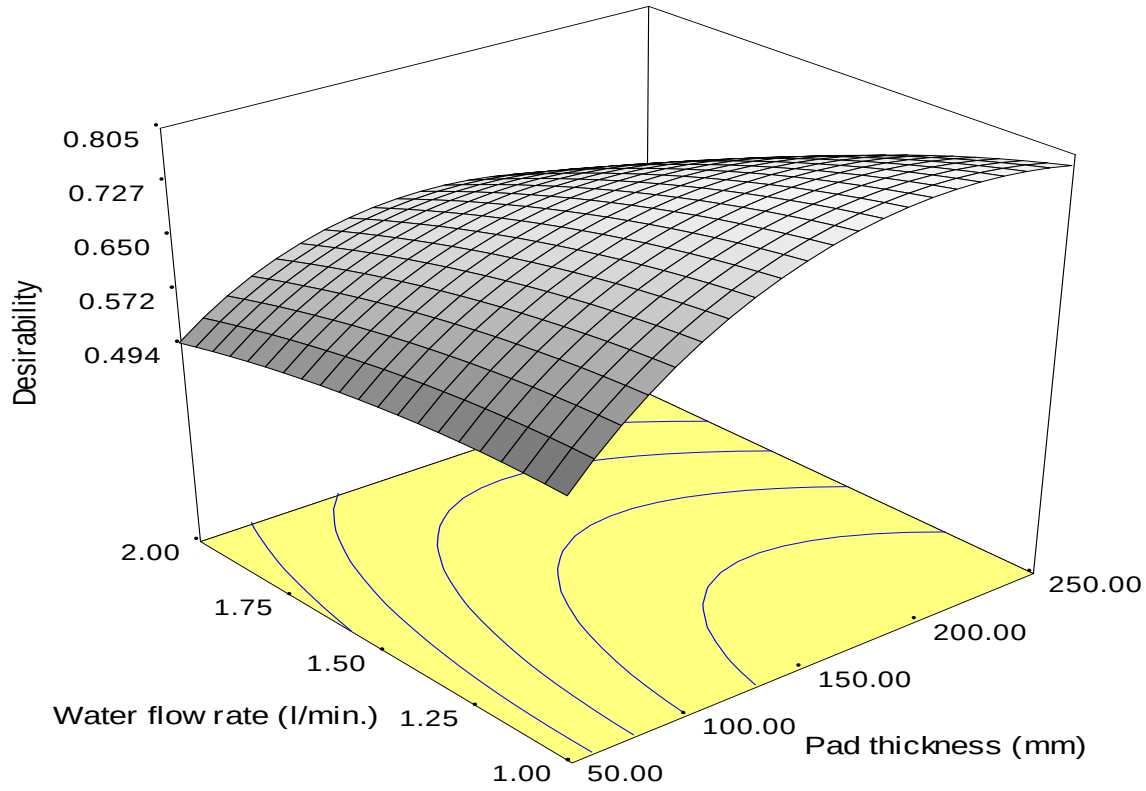

Figure4.7 (d)Desirability plot for saturation efficiency of Jute fibre pad.

4.1.4.3**Statistical analysis for coconut fibrepad material**

The effects of pad thickness, water flow rate and airflow rate on the efficiency and pressure drop of coconut fibre was understudied using Central Composite Design inDesignExpert 6.0. statistical software. The design consists of twenty (20) treatment combinations as shown in Table 4.13. For example, the first treatment combination is made up 150mm pad thickness, 1.5 l/min. water flow rate and 1.5m/s produced 73.9% and 38.9Pa efficiency and pressure drop respectively. Results of other treatment combinations are also shown in table 4.13. A quadratic model shown in equation 4.5was generated by the software using the experimental values to predict the efficiency of coconutfibre pad.

$$\eta_{sa} = + 57.12 + 0.07t + 5.52v - 1.72 \times 10^{-4}t^2 - 1.22v^2 + 7.63 \times 10^{-3}\, tv \qquad 4.5$$

Table 4.13 Central composite design of efficiency and pressure drop coconut fibre

S/N	Pad thiclness (mm)	Water flow rate (l/s)	Air velocity (m/s)	Experimental Efficiency (%)	Predicted efficiency (%)	Experimental Pressure drop (Pa)	Predicted Pressure drop (Pa)
1	150	1.5	1.5	73.9	73.9	38.9	38.7
2	200	1.25	1.0	71.3	71.6	23.6	24.0
3	150	1.0	1.5	73.3	73.2	18.1	21.5
4	200	1.75	2.0	80.3	79.5	84.7	78.7
5	150	1.5	1.5	73.9	73.9	38.9	38.7
6	150	1.5	1.5	73.9	73.9	38.9	38.7
7	250	1.5	1.5	77.1	77.3	56.1	59.4
8	100	1.25	2.0	68.9	68.4	33.6	27.5
9	150	1.5	0.5	66.3	66.3	19.9	16.3
10	100	1.75	1.0	63.5	63.3	32.9	32.7
11	150	1.5	1.5	73.9	73.9	38.9	38.7
12	150	1.5	1.5	73.9	73.9	38.9	38.7
13	100	1.25	1.0	63.9	64.2	15.1	15.9
14	50	1.5	1.5	60.3	60.7	27.2	31.3
15	100	1.75	2.0	67.8	67.1	58.8	53.2
16	150	1.5	1.5	73.9	75.1	38.9	49.9
17	200	1.25	2.0	79.0	78.7	48.4	43.4
18	150	2.0	1.5	72.3	73.1	61.2	65.2
19	200	1.75	1.0	72..6	72.7	49.3	50.2
20	150	1.5	1.5	73.9	73.9	38.9	38.7

The model validation was understudied using analysis of variance (ANOVA) as shown in table 4.14

Table 4.14 :Anova for response surface quadratic model efficiency of coconutfibre

Source	Sum of Squares	DF	Mean Square	F Value	Prob > F	
Model	500.34	9	55.59	136.11	< 0.0001	significant
t	332.18	1	332.18	813.26	< 0.0001	significant
w	0.02	1	0.02	0.06	0.8104	non signif
v	102.87	1	102.87	251.85	< 0.0001	significant
t × t	42.41	1	42.41	103.82	< 0.0001	significant
w × w	1.02	1	1.02	2.49	0.1455	non signif
v × v	21.46	1	21.46	52.55	< 0.0001	significant
tw	2.10	1	2.10	5.14	0.051	non signif
tv	4.65	1	4.65	11.39	0.0071	significant
wv	0.06	1	0.06	0.15	0.7067	non signif
Residual	4.08	10	0.41			
Lack of Fit	4.08	5	0.82			
Pure Error	0.00	5	0			
Cor Total	504.43	19				

Std. Dev.	0.639	R-Squared	0.9919
Mean	71.7	Adj R-Squared	0.9846
C.V.	0.891	Pred R-Squared	0.9384
PRESS	31.07	Adeq Precision	41.5251

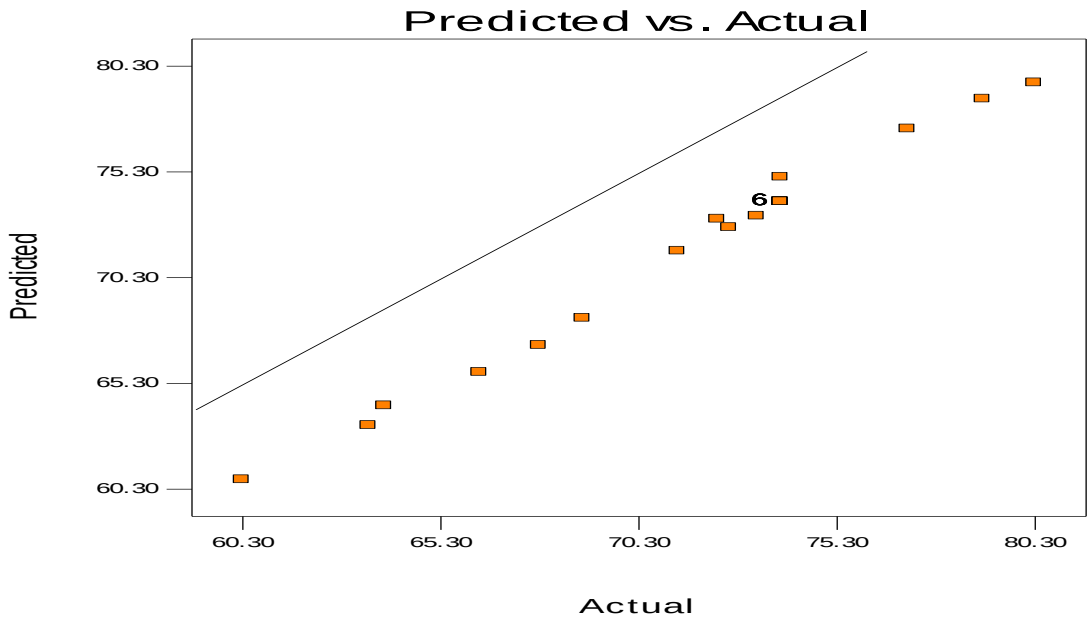

Figure 4.8: Graph of predicted and actual efficiency for Coconutfibre.

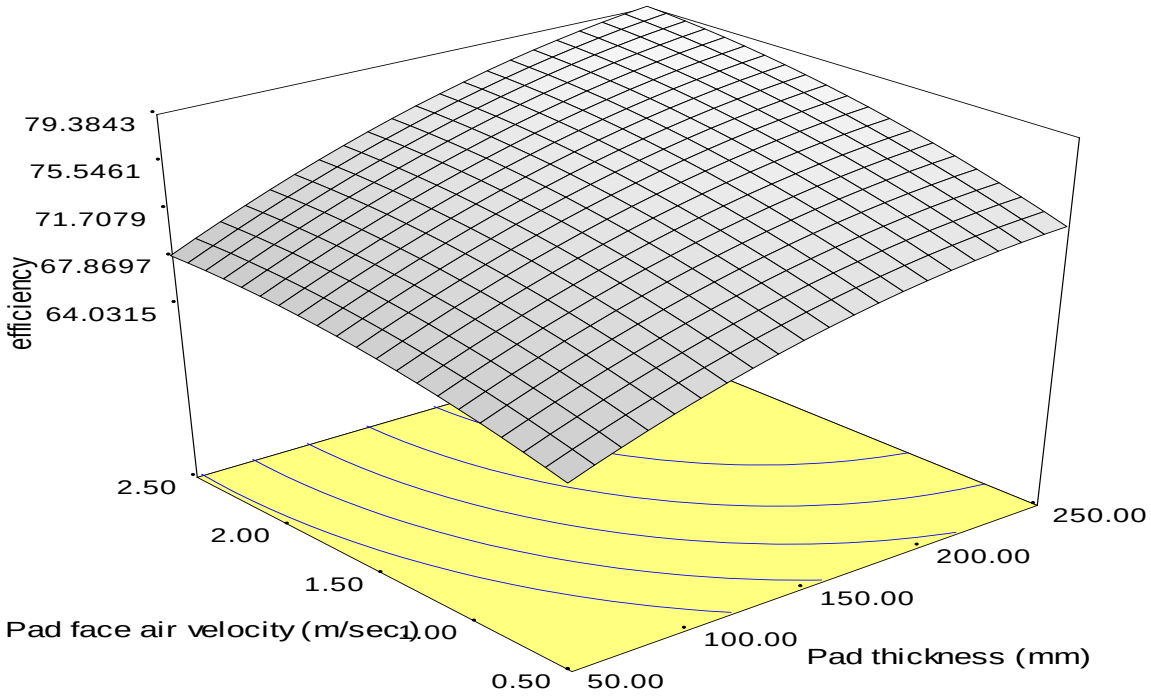

Figure4.9 Response surface plot of the interaction effect of pad face air velocity and pad thickness on the efficiencyofCoconutfibre pad.

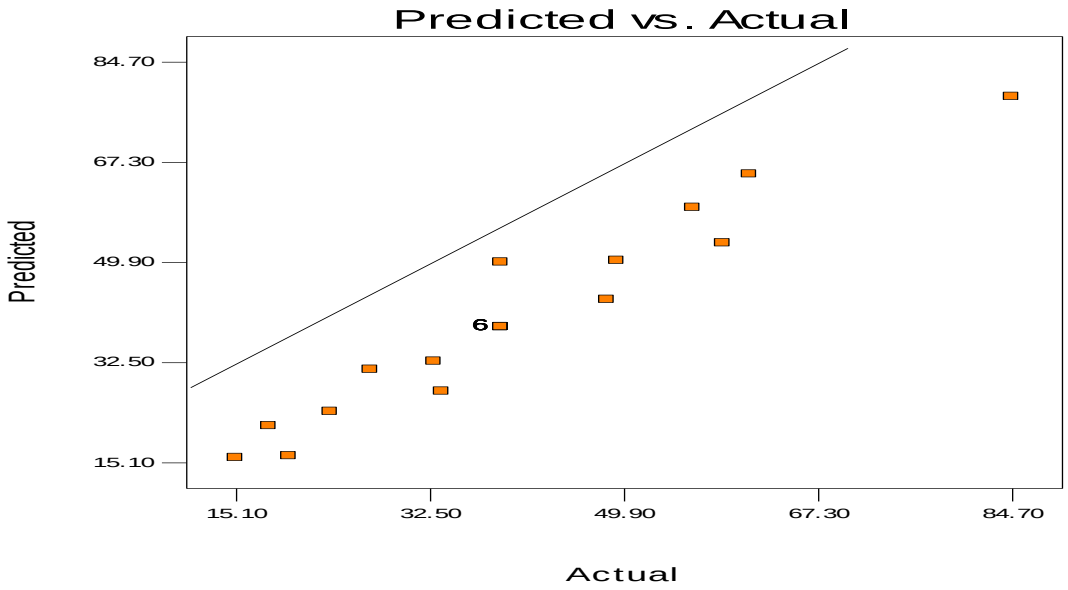

Figure 4.10: Graph of predicted and actual pressure drop for coconut fibre pad

Also generated by the software is the model equation for the prediction of pressure drop across the Coconut fibre pad as shown in equation 4.6

$$\Delta P = 13.01 - 0.09t - 7.58w + 6.23v \qquad 4.6$$

The model equation 4.6 was validated using anova and the results shown in table 4.15.

Table 4.15 Anova for response surface quadratic model pressure drop of Coconutfibre

Source	Sum of Squares	DF	Mean Square	F Value	Prob > F	
Model	4932.75	9	548.08	17.09	< 0.0001	significant
t	955.02	1	955.02	29.78	0.0003	significant
w	2306.61	1	2306.61	71.93	< 0.0001	significant
v	1365.40	1	1365.40	42.58	< 0.0001	significant
t × t	79.48	1	79.48	2.48	0.1465	non signif
w × w	38.82	1	38.82	1.21	0.297	non signif
v × v	56.65	1	56.65	1.77	0.2133	non signif
tw	45.12	1	45.12	1.41	0.2629	non signif
tv	31.20	1	31.20	0.97	0.3472	non signif
wv	40.50	1	40.50	1.26	0.2873	non signif
Residual	320.68	10	32.07			
Lack of Fit	320.68	5	64.14			
Pure Error	0.00	5	0			
Cor Total	5253.43	19				

Std. Dev.	5.66	R-Squared	0.939
Mean	40.06	Adj R-Squared	0.884
C.V.	14.14	Pred R-Squared	0.537
PRESS	2431.37	Adeq Precision	15.662

The relationship between the experimental and predicted efficiencies is shown in figure 4.11. The straight line indicates the suitability of the model to describe the Pressure drop of the Coconutfibre pad.

4.1.4.3.1**Optimization of the efficiency and pressure drop of coconut fiber pad**

Table 4.16 Conditions for optimization of efficiency and pressure drop of coconut pad

Constraints						
		Lower	Upper	Lower	Upper	
Name	Goal	Limit	Limit	weight	Weight	Importance
Pad thickness	Is in range	50	250	1.0	1.0	3
Water flow rate	Is in range	1.0	2.0	1.0	1.0	3
Air velocity	Is in range	0.5	2.5	1.0	1.0	3
Efficiency	maximize	60.3	80.3	1.0	1.0	3
Pressure drop	minimize	15.1	84.7	1.0	1.0	3

From table 4.16, the pad thickness, water flow rate and pad face air velocity were within range, whereas efficiency and pressure drop were at maximum and minimum respectively.

From the software, the following optimization values were obtained

Table 4.17 Optimization of the sat. efficiency and pressure drop of Coconutfibre pad

No.	Pad thickness (mm)	Water flow rate (l/min)	Pad face air vel. (m/s)	Sat. Efficiency (%)	Pressure drops (Pa)	Desirability
1	194	1	1.9	76.3	33.5	0.767
2	195	1	2.1	76.8	34.9	0.767
3	192	1	1.7	75.8	31.8	0.766
4	185	1	1.6	75.1	30.1	0.763
5	156	1	1.6	74.1	28.2	0.748

The desirability plot for saturation efficiencyis shown in figure 4.11.

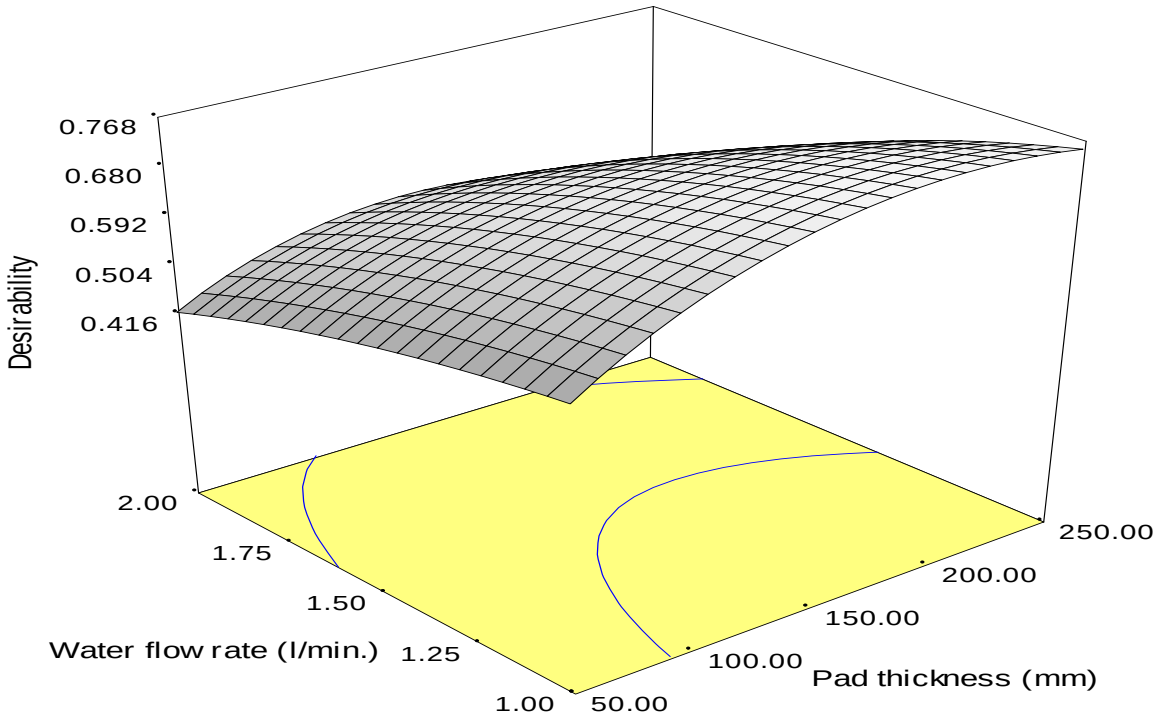

Figure4.11 Desirability plot for saturation efficiency of Coconutfibre pad.

4.1.4.4**Statisticalanalysis for popspongepad material**

The effects of pad thickness, water flow rate and airflow rate on the efficiency and presure drop of POP sponge pad material was understudied using Central Composite Design in design expert 6.0. statistical software. The design consists of twenty (20) treatment combinations as shown in table 4.18. For example the first treatment combination is made up 250mm pad thickness, 1.5 l/min. water flow rate and 1.5m/s produced 67.2% and 39.8Pa efficiency and pressure drop respectively. Results of other treatment combinations are also shown in table 4.18

Table 4.18 Central composite design of efficiency and pressure dropofpopsponge

S/N	Pad thickness (mm)	Water flowrate (l/s)	Air Vel (m/s)	Experimental Efficiency (%)	Predicted efficiency (%)	Experimental Pressure drop (Pa)	Predicted Pressure drop (Pa)
1	250	1.5	1.5	67.2	67.22	39.8	40.83
2	150	1.5	1.5	63.8	63.79	27.7	27.65
3	200	1.75	2.0	70.7	70.44	63.4	62.97
4	150	2.0	1.5	65.8	66.30	43.3	44.82
5	200	1.25	1.0	63.4	63.82	16.6	15.33
6	150	1.5	1.5	63.8	63.79	27.7	27.65
7	150	1.5	2.5	66.5	67.14	53.6	52.87
8	200	1.25	2.0	68.9	68.65	37.4	37.82
9	100	1.25	2.0	60.9	60.81	26.0	26.21
10	50	1.5	1.5	52.9	53.2	19.2	19.96
11	100	1.75	2.0	61.5	6085	43.7	43.71
12	100	1.75	1.0	56.9	56.93	23.1	21.42
13	150	1.5	1.5	63.8	63.79	27.7	27.65
14	150	1.5	1.5	63.8	63.79	27.7	27.65
15	150	1.5	0.5	60.1	59.78	12.7	15.22
16	150	1.0	1.5	64.8	64.63	13.6	13.87
17	200	1.75	1.0	65.9	65.77	36.1	34.63
18	150	1.5	1.5	63.8	63.79	27.7	27.65
19	100	1.25	1.0	56.7	56.73	10.6	9.77
20	150	1.5	1.5	63.8	63.79	27.7	27.65

. A quadratic model shown in equation 4.7was generated by the software using the experimental values to predict the efficiency of POP sponge pad.

η_{sa} = + 57.19 + 0.06t - 7.29w + 2.37v - 1.27× $10^{-4}t^2$+ 2.36w^2+ 8.75× 10^{-3}tw4.7

The model validation was understudied using (ANOVA) as shown in table 4.19

Table 4.19 Anova for response surface quadratic model efficiency of POP Sponge

Source	Sum of Squares	DF	Mean Square	F Value	Prob > F	
Model	338.57	9	37.62	229.88	< 0.0001	significant
t	237.48	1	237.48	1451.2	< 0.0001	significant
w	3.38	1	3.37	20.58	0.0011	significant
v	65.3	1	65.3	399.06	< 0.0001	significant
t × t	23.09	1	23.09	141.09	< 0.0001	significant
w × w	5.02	1	5.02	30.7	0.0002	significant
v × v	0.2	1	0.2	1.2	0.2992	non signif
tw	1.53	1	1.53	9.36	0.0121	significant
tv	0.28	1	0.28	1.72	0.2192	non signif
wv	0.01	1	0.01	0.07	0.7985	non signif
Residual	1.64	10	0.16			
Lack of Fit	1.64	5	0.33			
Pure Error	0	5	0			
Cor Total	340.21	19				

Std. Dev.	0.4	R-Squared	0.9952
Mean	63.25	Adj R-Squared	0.9908
C.V.	0.64	Pred R-Squared	0.9628
PRESS	12.66	Adeq Precision	60.2774

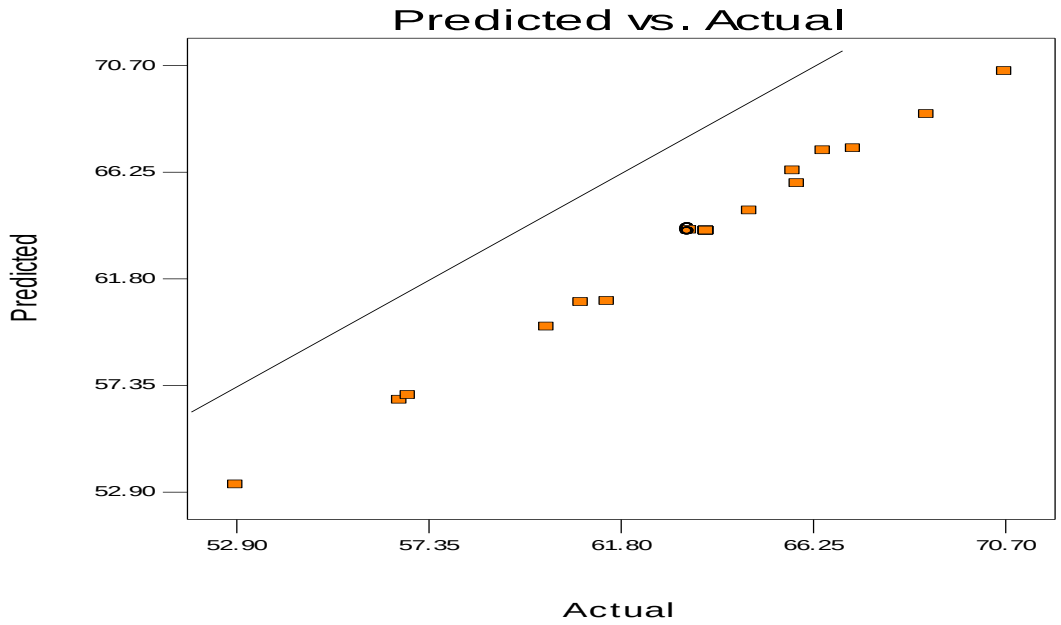

Figure 4.12: Graph of predicted and actual efficiency for POP Sponge.

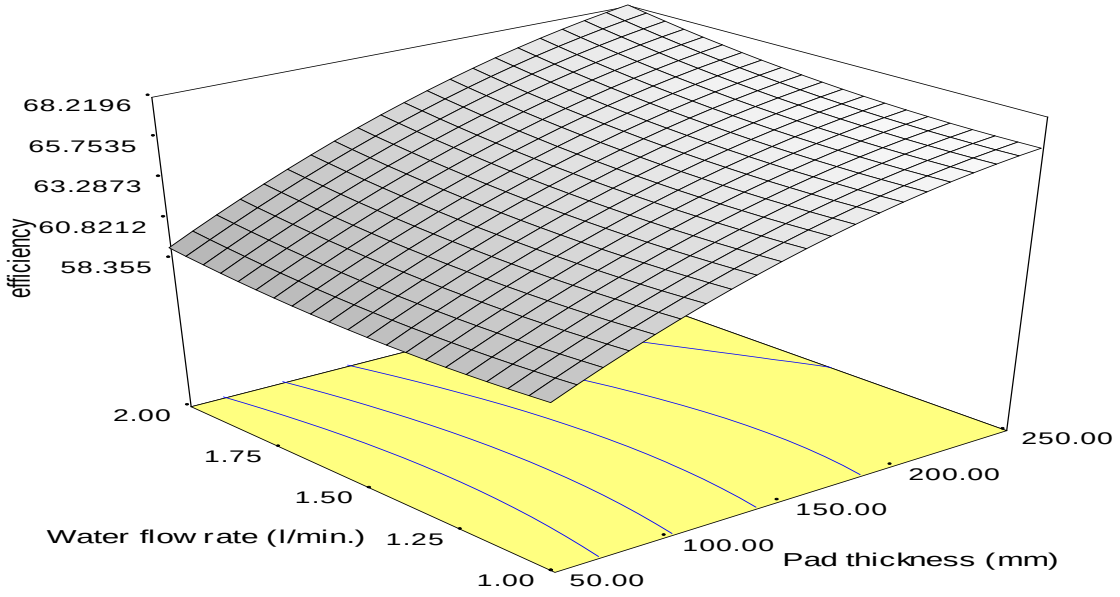

Figure4.13 Response surface plot of the interaction effect of water flow rate and pad thickness on the efficiency of pop sponge.

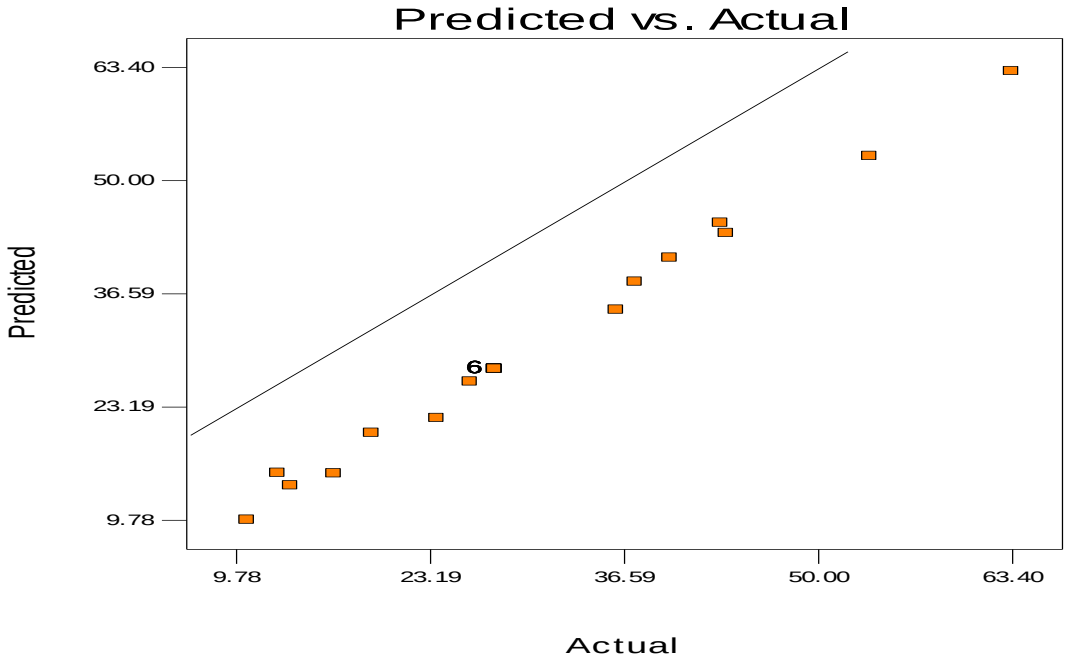

Figure 4.14: Graph of predicted and actual pressure drop for POP Sponge pad

Also generated by the software is the model equation for the prediction of pressure drop across the Pop Sponge pad as shown in equation 4.8

$$\Delta P = 4.91 - 0.05t + 1.43w - 2.22v + 9.87 \times 10^{-5}t^2 + 2.28v^2 + 0.04tw + 0.02tv + 2.78wv \quad 4.8$$

The model equation 4.8 was validated using anova and the results shown in table 4.20.

The relationship between the experimental and predicted pressure drop is shown in figure 4.14. The straight line indicates the suitability of the model to describe the pressure drop of the POP Sponge pad

Table 4.20 Anova for response surface quadratic model pressure drop of POP Sponge

	Sum of		Mean	F		
Source	Squares	DF	Square	Value	Prob > F	
Model	3530.87	9	392.32	189.14	< 0.0001	significant
t	518.45	1	518.45	249.95	< 0.0001	significant
w	1167.1	1	1167.1	562.66	< 0.0001	significant
v	1698.11	1	1698.1	818.67	< 0.0001	significant
t × t	14.02	1	14.02	6.76	0.0265	significant
w × w	5.46	1	5.46	2.63	0.1359	non signifi
v × v	74.72	1	74.72	36.02	0.0001	significant
tw	27.01	1	27.01	13.02	0.0048	significant
tv	20.16	1	20.16	9.72	0.0109	significant
wv	15.4	1	15.4	7.43	0.0214	significant
Residual	20.7	10	2.07			
Lack of Fit	20.74	5	4.15			
Pure Error	0	5	0			
Cor Total	3551.61	19				

Std. Dev.	1.4402	R-Squared	0.9941
Mean	30.295	Adj R-Squared	0.9889
C.V.	4.754	Pred R-Squared	0.9556
PRESS	157.85	Adeq Precision	52.1541

. The interaction among pad thickness, airflow rate and water flow rate and the effects on pressure drop are represented in the response surface plots shown in Figures 4.15 (a) to (c).

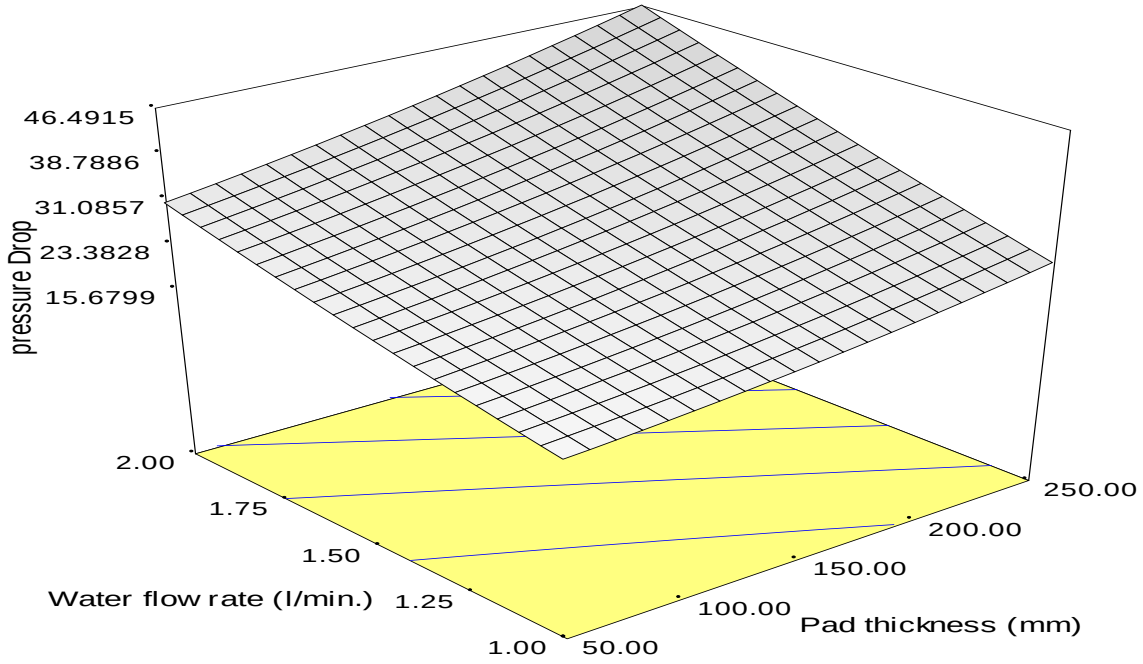

Figure 4.15 (a) Response surface plot of the interaction effect of water flow rate and pad thickness on pressure drop of Pop Sponge pad.

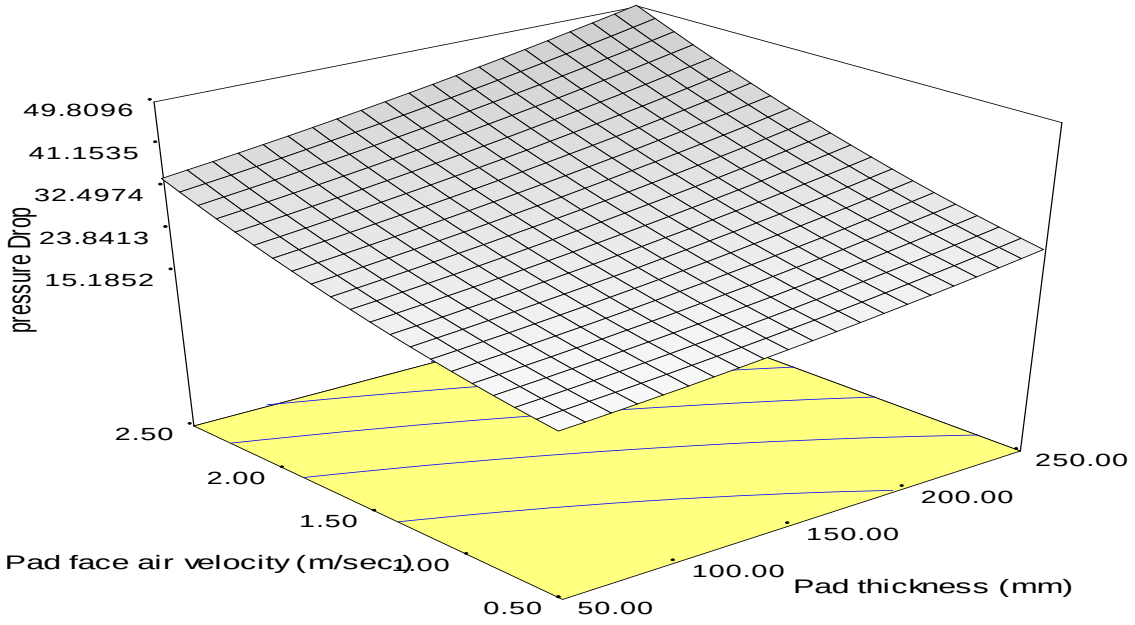

Figure4.15 (b) Response surface plot of the interaction effect of pad face air velocity and pad thickness on the pressure drop of POP Sponge pad.

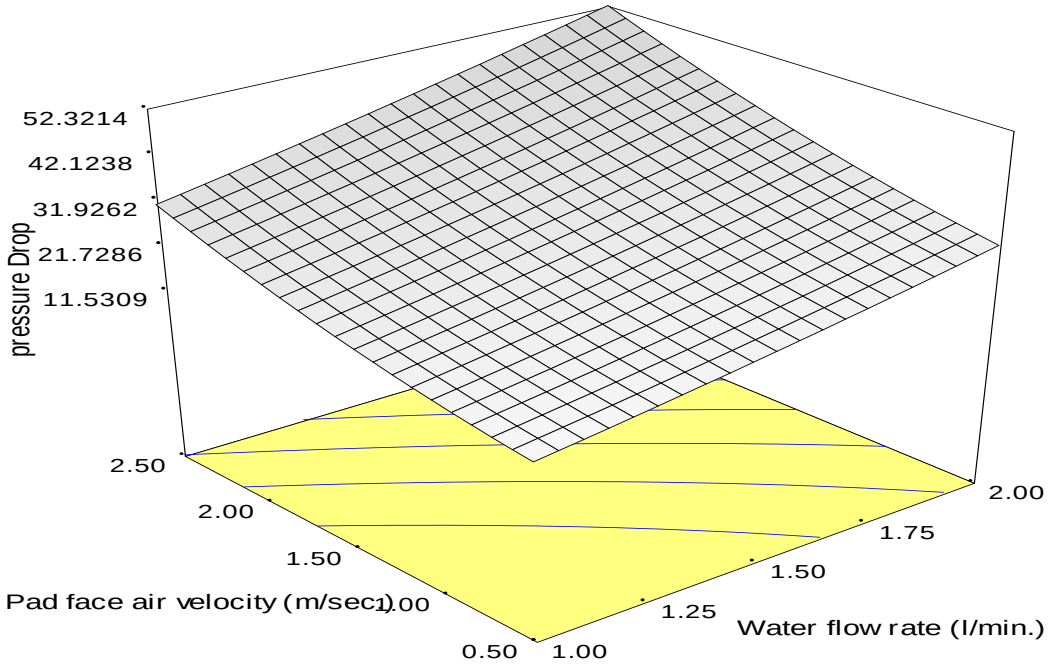

Figure4.15 (c) Response surface plot of the interaction effect of water flow rate and pad face air velocity on the pressure drop of pop sponge pad

4.1.4.4.1 **Optimization of the efficiency and pressure drop ofpopsponge pad**

Table 4.21 Conditions for optimization of efficiency and pressure drop of Pop Sponge

Constraints						
		Lower	Upper	Lower	Upper	
Name	Goal	Limit	Limit	weight	Weight	Importance
Pad thickness	Is in range	50	250	1.0	1.0	3
Water flow rate	Is in range	1.0	2.0	1.0	1.0	3
Air velocity	Is in range	0.5	2.5	1.0	1.0	3
Efficiency	maximize	52.9	70.7	1.0	1.0	3
Pressure drop	minimize	10.6	63.4	1.0	1.0	3

From table 4.21, the pad thickness, water flow rate and pad face air velocity are within range, whereas efficiency and pressure drop are at maximum and minimum respectively.

From the software, the following optimization values were obtained as shown in table 4.22

Table 4.22 Optimization of the sat. efficiency and pressure drop of Pop Sponge pad

No.	Pad thickness (mm)	Water flow rate (l/min)	Pad face air vel. (m/s)	Sat. Efficiency (%)	Pressure drops (Pa)	Desirability
1	184	1	1.3	64.6	18.9	0.745
2	188	1	1.9	66.0	25.0	0.731
3	173	1	1.8	65.4	23.8	0.727
4	170	1	1.9	65.4	23.9	0.725
5	188	1	1.5	65.1	20.5	0.745

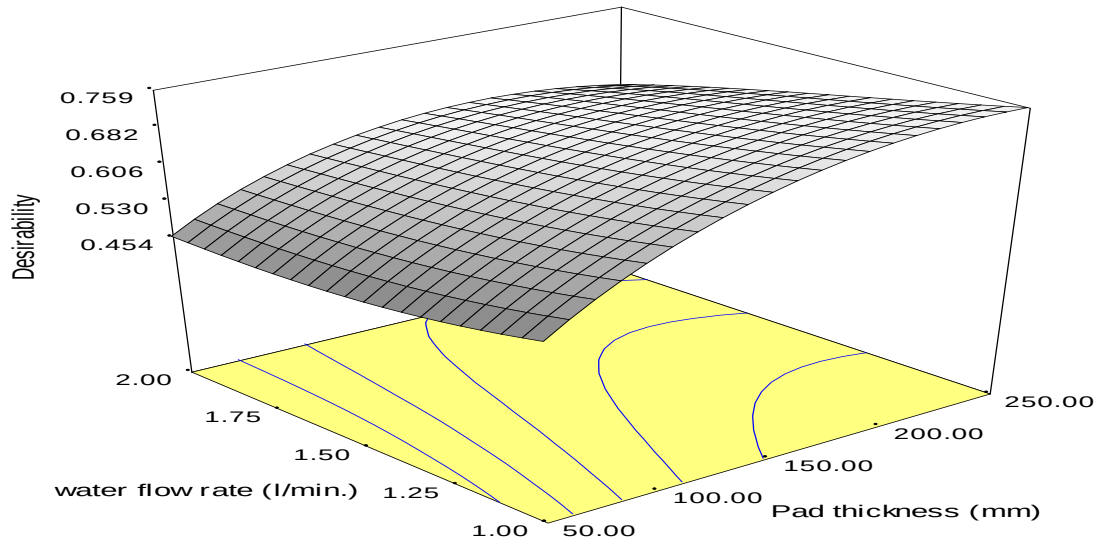

Figure: 4.15 (d)Desirability plot for saturation efficiency of Pop Sponge pad.

A compilation of the best optimization option selected for each of the evaporative cooling pad is presented in table 4.23. From the table the optimum range of the levels of the factors in the study are shown below.

Table 4.23 Summary of optimization for efficiency and pressure drop of various pads.

Pad type	Pad thick-ness (mm)	Water fl-ow rate(l/min)	Pad air vel.(m/s)	Sat. Eff.(%)	Pressure drops(Pa)	Desirability
Celdek	161.0	1.0	0.5	75.6	6.3	0.904
Jute fibre	157.0	1.0	1.5	77.9	35.7	0.789
Coconut fib.	156.0	1.0	1.6	74.1	28.2	0.748
POP sponge	184.0	1.0	1.3	64.6	18.9	0.745

4.1.5 **Tukey's Honestly Significant difference (HSD) Testfor Means Separation.**

4.1.5.1**Saturation efficiency mean separation for pad thickness**

4.1.5.1.1 **Mean separation for celdek pad.**

Table 4.24 Mean values of the saturation efficiency at1.75l/min. for celdek pad

Pad air vel. (m/s)	50mm	100mm	150mm	200mm	250mm
0.5	61.5	71.8	77.9	80.7	79.8
1.0	57.8	68.9	74.8	79.1	78.6
1.5	55.1	66.3	73.3	77.5	77.3
2.0	53.1	64.5	72.6	77.1	76.1
2.5	52.3	63.9	71.4	76.7	76.3
Total	279.8	335.4	370.0	391.1	388.1
Mean	55.86	67.08	74.0	78.22	77.62

Table 4.25Anova summary of saturation efficiency mean separation for celdek

	SS	df	MS	F	P
Treatment	1728.1098	4	432.0274	59.47	<.0001
Error	145.296	20	7.2648		
Total	1873.4056	24			

Tukey HSD test for efficiency

50mm vs 100mm P<.01100mm vs 200mm P<.01

50mm vs 150mm P<.01 100mm vs 250mm P<.01

50mm vs 200mm P<.01 150mm vs 200mm non-significant

50mm vs 250mm P<.01 150mm vs 250mm non-significant

100mm vs 150mm P<.01200mm vs 250mm non-significant

4.1.5.1.2 **Mean separation for jute pad.**

Table 4.26 Mean values of the saturation efficiency at1.75l/min. for jute pad.

Air vel. (m/s)	50mm	100mm	150mm	200mm	250mm
0.5	56.9	63.7	70.7	72.9	73.5
1.0	60.6	67.2	73.8	76.9	77.2
1.5	61.8	71.3	78.0	82.5	80.9
2.0	63.8	73.1	80.3	82.6	82.5
2.5	63.9	74.3	80.7	81.7	82.3
Total	307.0	349.6	383.5	396.6	396.4
Mean	61.4	69.92	76.7	79.32	79.28

Table 4.27Anova summary of saturation efficiency mean separation for jute pad

	SS	df	MS	F	P
Treatment	1182.9616	4	295.7404	18.55	<.0001
Error	318.864	20	15.9432		
Total	1501.8256	24			

Tukey HSD Test for efficiency

50mm vs 100mm P<.05 100mm vs 200mm P<.05

50mm vs 150mm P<.01 100mm vs 250mm P<.05

50mm vs 200mm P<.01 150mm vs 200mm non-significant

50mm vs 250mm P<.01 150mm vs 250mm non-significant

100mm vs 150mm non-significant 200mm vs 250mm non-significant

4.1.5.1.3**Mean separation for coconut pad.**

Table 4.28 Mean values of the saturation efficiency at1.75 l/min. for coconut pad.

air vel. (m/s)	50mm	100mm	150mm	200mm	250mm
0.5	55.8	60.7	66.8	69.2	70.8
1.0	58.6	63.5	69.6	72.6	73.3
1.5	60.5	65.7	72.1	76.3	77.4
2.0	61.2	67.8	75.6	80.3	79.5
2.5	61.7	68.5	76.0	79.9	80.3
Total	297.8	326.2	360.1	378.3	381.3
Mean	59.56	65.24	72.02	75.66	76.26

Table 4.29Anova summary of saturation efficiency mean separation for coconut pad.

	SS	df	MS	F	P
Treatment	1033.1864	4	258.2966	18.21	<.0001
Error	283.716	20	14.1858		
Total	1316.9024	24			

Tukey HSD Test for efficiency

50mm vs 100mm non-significant 100mm vs 200mm P<.05

50mm vs 150mm P<.01 100mm vs 250mm P<.05

50mm vs 200mm P<.01150mm vs 200mm non-significant

50mm vs 250mm P<.01150mm vs 250mm non-significant

100mm vs 150mm non-significant 200mm vs 250mm non-significant

4.1.5.1.4 **Mean separation for popsponge pad.**

Table 4.30 Mean values of the saturation efficiency at1.75l/min. for Sponge pad.

Pad face air vel. (m/s)	50mm	100mm	150mm	200mm	250mm
0.5	50.2	54.1	60.7	62.9	63.4
1.0	51.3	56.9	62.8	65.9	66.5
1.5	53.1	58.9	63.9	66.2	67.3
2.0	56.7	61.5	66.8	70.7	69.3
2.5	57.0	61.3	67.0	70.1	71.6
Total	268.3	292.7	321.2	335.8	338.1
Mean	53.66	58.54	64.24	67.16	67.62

Table 4.31Anova summary of saturation efficiency mean separation for pop sponge pad.

	SS	df	MS	F	P
Treatment	722.2856	4	180.5714	19.45	<.0001
Error	185.716	20	9.2858		
Total	908.0016	24			

Tukey HSD Test for efficiency

50mm vs 100mm non-significant100mm vs 200mm P<.05

50mm vs 150mm P<.01 100mm vs 250mm P<.05

50mm vs 200mm P<.01 150mm vs 200mm non-significant

50mm vs 250mm P<.01 150mm vs 250mm non-significant

100mm vs 150mm non-significant 200mm vs 250mm non-significant

Table 4.32 Summary of tukey's HSD test for pad thickness means separation.

Pad type	Pad thickness (mm)				
	50mm	100mm	150mm	200mm	250mm
Celdek	55.96a	67.08b	74c	78.22c	77.62c
Jute fiber	61.4a	69.92b	76.7bc	79.32c	79.28c
Coconut fiber	59.56a	65.24ab	72.02bc	75.66c	76.26c
Pop sponge	53.66a	58.54ab	64.24bc	67.16c	67.62c

a, b, c. Means with the same letter are not significantly different at 5% level within a row.

Table 4.32shows the summary of tukey's HSD test for pad thickness means separation for the various pad materials.

4.1.5.2 **Saturation efficiency and pressure drop means separation for pad types.**

Saturation efficiency and pressure drop data of various pad materials was understudied using on-line Tukey HSD Test from www.vassarstarts.net/anova1u.html.

Table 4.33 Average mean values of the saturation efficiency and pressure drop at 1.75l/min. water flow rate for various pad thicknesses.

Water flow rate:		1.75 l/min.							
Pad thickness (mm)	Pad face air vel. (m/s)	Saturation Efficiency (%)				Pressure Drop			
		Celdek	Jute	Coconut	Sponge	Celdek	Jute	Coconut	Sponge
50mm	0.5	61.5	56.9	55.8	50.2	5.3	22	16.5	10.5
	1.0	57.8	60.6	58.6	51.3	9.5	31.5	26.3	18.5
	1.5	55.1	61.8	60.5	53.1	13.9	42.4	35.4	25
	2.0	53.1	63.8	61.2	56.7	22.9	57.6	49	36
	2.5	52.3	63.9	61.7	57.0	28	68.7	58.8	45.8
	TOTA	279.8	307.0	297.8	268.3	79.6	222.2	186	135.8
	MEAN	55.96	61.4	59.56	53.66	15.92	44.44	37.2	27.16
100mm	0.5	71.8	63.7	60.7	54.1	6.9	28.6	21.5	13.7
	1.0	68.9	67.2	63.5	56.9	11.9	39.4	32.9	23.1
	1.5	66.3	71.3	65.7	58.9	16.7	50.9	42.5	30.2
	2.0	64.5	73.1	67.8	61.5	27.5	69.1	58.8	43.7
	2.5	63.9	74.3	68.5	61.3	33.6	79	67.6	53.8
	TOTAL	335.4	349.6	326.2	292.7	96.6	267	223.3	164.5
	MEAN	67.08	69.92	65.24	58.54	19.32	53.4	44.68	32.9
150mm	0.5	77.9	70.7	66.8	60.7	9	37.2	28	17.8
	1.0	74.8	73.8	69.6	62.8	14.9	49.3	41.1	28.9
	1.5	73.3	78.0	72.1	63.9	20	61.1	51.1	36.2
	2.0	72.6	80.3	75.6	66.8	31.1	82.9	70.6	52.8
	2.5	71.4	80.7	76.0	67.0	40.3	94.8	81.1	66.1
	TOTAL	370	383.5	360.1	321.2	115.3	325.3	271.9	201.8
	MEAN	74	76.7	72.02	64.24	23.06	65.06	54.38	40.36
200mm	0.5	80.7	72.9	69.2	62.9	11.7	48.4	36.4	23.1
	1.0	79.1	76.9	72.6	65.9	18.6	61.6	49.3	36.1
	1.5	77.5	82.5	76.3	66.2	24	73.3	61.3	43.4
	2.0	77.1	82.6	80.3	70.7	37.3	99.5	84.7	63.4
	2.5	76.7	81.7	79.9	70.1	48.4	113.8	97.3	79.3
	TOTAL	391.1	396.6	378.3	335.8	140	396.6	329	245.3
	MEAN	78.22	79.32	75.66	67.16	28	79.32	65.8	49.06
250mm	0.5	79.8	73.5	70.8	63.4	15.2	62.9	47.3	30.1
	1.0	78.6	77.2	73.3	66.5	23.3	77	61.6	45.1
	1.5	77.3	80.9	77.4	67.3	28.8	90.1	73.6	52.1
	2.0	76.1	82.5	79.5	69.3	44.8	119.4	101.6	76.1
	2.5	76.3	82.3	80.3	71.6	58.1	136.6	116.8	95.2
	TOTAL	388.1	396.4	381.3	338.1	170.2	486	400.9	298.6
	MEAN	77.62	79.28	76.26	67.62	34.04	97.2	80.18	59.72

4.1.5.2.1 **Saturation efficiency means separation of pad types.**

Table 4.34Anova summary of saturationefficiencymean separation for 50mm pad.

	SS	df	MS	F	P
Treatment	182.4335	3	60.8112	6.45	0.004543
Error	150.916	16	9.4322		
Total	333.3495	19			

Tukey HSD test for saturation efficiency of 50mm pad thickness

Celdek vs Jute non-significant Jute vs Coconut non-significant

Celdek vs Coconut non-significantJute vs Sponge P<.01

Celdek vs Sponge non-significantCoconut vs Sponge P<.05

Table 4.35Anova summary ofsaturationefficiencymean separation for100mm pad.

	SS	df	MS	F	P
Treatment	350.8495	3	116.9498	9.35	0.000832
Error	200.2	16	12.5125		
Total	551.0495	19			

Tukey HSD test forsaturation efficiency of 100mm pad thickness

Celdek vs Jute non-significantJute vs Coconut non-significant

Celdek vs Coconut non-significantJute vs Sponge P<.01

Celdek vs Sponge P<.01Coconut vs Sponge P<.05

Table 4.36Anova summary of saturationefficiencymean separation for150mm pad.

	SS	df	MS	F	P
Treatment	430.188	3	143.396	12.03	0.000225
Error	190.78	16	11.9238		
Total	620.968	19			

Tukey HSD test for saturation efficiency of 150mm pad thickness

Celdek vs Jute non-significantJute vs Coconut non-significant

Celdek vs Coconut non-significantJute vs Sponge P<.01

Celdek vs Sponge P<.01Coconut vs Sponge P<.05

Table 4.37Anova summary of Sat.Efficiencymean separation for 200mm pad.

	SS	df	MS	F	P
Treatment	454.498	3	151.4993	11.15	0.000338
Error	217.46	16	13.5913		
Total	671.958	19			

Tukey HSD test for saturation efficiency of 200mm pad thickness

Celdek vs Jute non-significantJute vs Coconut non-significant

Celdek vs Coconut non-significantJute vs Sponge P<.01

Celdek vs Sponge P<.01Coconut vs Sponge P<.05

Table 4.38Anova summary of saturation efficiency mean separation for 250mm pad.

	SS	df	MS	F	P
Treatment	405.4135	3	135.1378	12.41	0.000190
Error	174.236	16	10.8897		
Total	597.6495	19			

Tukey HSD test for saturation efficiency of 250mm pad thickness.

Celdek vs Jute non-significantJute vs Coconut non-significant

Celdek vs Coconut non-significantJute vs Sponge P<.01

Celdek vs Sponge P<.01Coconut vs Sponge P<.05

Table 4.39 Summary of Tukey HSD test for saturation efficiency means separation

Padthickness (mm)	Celdekpad	Jute fibre	Coconut fibre	Pop Sponge
50	55.9ab	61.40a	59.56a	53.66b
100	67.08a	69.92a	65.24a	58.54b
150	74.00a	76.70a	72.02a	64.24b
200	78.22a	79.32a	75.66a	67.16b
250	77.62a	79.28a	76.26a	67.62b

a, b. Mean with same letter are not significantly different at 5% level within the row.

Table 4.39shows the summary of Tukey HSD test for saturation efficiency means separation of pad types at various levels of pad thickness. means separation of pad types.

4.1.5.2.2**Pressure drop mean separation of pad type**

Table 4.40Anova summary of pressure drop mean separation for 50mm pad.

	SS	df	MS	F	P
Treatment	2305.48	3	768.4933	3.3	0.047447
Error	3728.772	16	233.0483		
Total	6034.252	19			

Tukey HSD test for pressure drop of 50mm pad thickness.

Celdekvs Jute P<.05Jute vs Coconut non-significant

Celdekvs Coconut non-significantJute vs Sponge non-significant

Celdek vs Sponge non-significantCoconutvs Sponge non-significant

Table 4.41Anova summary of pressure dropmean separation for100mm pad.

	SS	df	MS	F	P
Treatment	3278.642	3	1092.8807	3.77	0.032023
Error	4637.1	16	289.8188		
Total	7915.742	19			

Tukey HSD test for pressure drop of 100mm pad thickness.

Celdekvs Jute P<.05Jute vs Coconut non-significant
Celdekvs Coconut non-significantJute vs Sponge non-significant
Celdek vs Sponge non-significantCoconutvs Sponge non-significant

Table 4.42Anova summary of pressure dropmean separation for150mm pad.

	SS	df	MS	F	P
Treatment	4956.1815	3	1652.0605	4.25	0.021806
Error	6213.424	16	388.339		
Total	11169.6055	19			

Tukey HSD test for pressure drop of 150mm pad thickness.

Celdekvs Jute P<.05Jute vs Coconut non-significant
Celdekvs Coconut non-significantJute vs Sponge non-significant
Celdek vs Sponge non-significantCoconutvs Sponge non-significant

Table 4.43Anova summary of pressure dropmean separation for 200mm pad.

	SS	df	MS	F	P
Treatment	7355.9895	3	2451.9965	4.74	0.014981
Error	8275.42	16	517.2137		
Total	15631.4095	19			

Tukey HSD test for pressure drop of 200mm pad thickness.

Celdekvs Jute P<.05Jute vs Coconut non-significant
Celdekvs Coconut non-significantJute vs Sponge non-significant
Celdek vs Sponge non-significantCoconutvs Sponge non-significant

Table 4.44Anova summary of pressure dropmean separation for250mm pad.

	SS	df	MS	F	P
Treatment	11113.2375	3	3704.4125	5.48	0.008753
Error	10818.288	16	676.143		
Total	21931.5255	19			

Tukey HSD test for pressure drop of 250mm pad thickness.

Celdekvs Jute P<.05Jute vs Coconut non-significant

Celdekvs Coconut non-significantJute vs Sponge non-significant

Celdek vs Sponge non-significantCoconutvs Sponge non-significant

Table 4.45 Summary of Tukey HSD test for pressure drop mean separation of pad types.

Thickness (mm)	Celdek	Jute fiber	Coconut fiber	Pop Sponge
50	15.92a	44.44b	37.20ab	27.16ab
100	19.32a	53.40b	44.68ab	32.90ab
150	23.06a	65.06b	54.38ab	40.36ab
200	28.00a	77.32b	65.80ab	49.06ab
250	34.02a	97.04b	80.18ab	59.72ab

a, b. Means with same letter are not significantly different at 5% level within a row.

4.1.6**Modeling of Saturation Efficiency and Pressure Drop**

4.1.6.1**Saturation efficiency models**

The model equations of saturation efficiency for the various pad thicknesses were obtained from regression analysis of the various π groups derived from Buckingham π theorem (equations 3.2 - 3.9) using Microsoft office excel package 2007 version. The summary of the model equations obtained from table 4.46 are shown in table 4.47 to 4.50.

Table 4.46 Average values of the ambient conditions, π groups, and saturation efficiency at 1.75 l/min. water flow rate.

Pad Thick-Ness (mm)	Pad Face Vel. (m/s)	AMBIENT CONDITIONS				π GROUPS				SAT. EFFICIENCY (η_{sat}) $=\pi_3$ (%)		
		T_{db}	T_{wb}	H_{v1}	ϑ_{v1}	π_1	π_2	π_4	CEL	JUT	COC	SPO
		(^{0}C)	(^{0}C)	(KJ/Kg)	(M^3/kg)							
50	0.5	34.1	24.3	73.0	0.891	0.467	25	0.713	61.5	56.9	55.8	50.2
	1.0	33.0	23.6	71.5	0.888	0.114	25	0.715	57.8	60.6	58.6	51.3
	1.5	35.0	24.5	74.0	0.895	0.053	25	0.700	55.1	61.8	60.5	53.1
	2.0	34.3	24.1	73.0	0.891	0.029	25	0.703	53.1	63.8	63.2	56.7
	2.5	35.1	24.2	73.0	0.893	0.019	25	0.690	52.3	63.9	63.5	57.0
100	0.5	34.0	24.3	73.5	0.891	7.526	6.25	0.715	71.8	63.7	60.7	54.1
	1.0	34.5	24.2	69.0	0.891	1.766	6.25	0.673	68.9	67.2	63.5	56.9
	1.5	34.2	23.8	72.5	0.890	0.825	6.25	0.696	66.3	71.3	65.7	58.9
	2.0	32.5	23.5	71.0	0.885	0.454	6.25	0.723	64.5	73.1	67.8	61.5
	2.5	36.0	24.0	72.5	0.895	0.297	6.25	0.667	63.9	74.3	68.5	61.3
150	0.5	33.3	23.6	71.5	0.888	37.066	2.78	0.709	77.9	70.7	66.8	60.7
	1.0	33.0	23.7	72.0	0.887	9.331	2.78	0.712	74.8	73.8	69.6	62.8
	1.5	32.5	23.3	69.5	0.885	4.003	2.78	0.717	73.3	78.0	72.1	63.9
	2.0	32.8	23.3	69.5	0.885	2.252	2.78	0.710	72.6	80.3	75.6	66.8
	2.5	36.0	24.0	72.5	0.895	1.503	2.78	0.667	71.4	80.7	76.0	67.0
200	0.5	32.5	23.5	71.0	0.885	116.34	1.563	0.723	80.7	72.9	69.2	62.9
	1.0	35.5	24.8	76.3	0.895	31.253	1.563	0.699	79.1	76.9	72.6	65.9
	1.5	34.4	23.5	70.5	0.890	12.834	1.563	0.683	77.5	82.5	76.3	66.2
	2.0	32.8	23.4	69.5	0.885	7.117	1.563	0.713	77.1	82.6	80.3	70.7
	2.5	34.9	23.8	70.5	0.892	6.402	1.563	0.682	76.7	81.7	79.9	70.1
250	0.5	36.0	24.0	72.5	0.895	289.99	0.25	0.667	79.8	73.5	70.8	63.4
	1.0	35.5	24.8	76.3	0.895	72.500	0.25	0.699	78.6	77.2	73.3	66.5
	1.5	34.1	24.4	73.0	0.891	32.449	0.25	0.715	77.3	80.9	77.4	67.3
	2.0	32.5	23.3	71.0	0.885	17.747	0.25	0.717	76.1	82.5	79.5	69.3
	2.5	33.3	23.6	71.5	0.888	11.440	0.25	0.709	76.3	82.3	80.3	70.1

Table 4.47 Regression analysis of saturation efficiency of Celdek pad for 50mm padthickness

R Square	0.9994					
Adjusted R Square	0.49898					
Standard Error	1.9959					
Observations	5					
ANOVA						
	df	*SS*	*MS*	*F*	*Significance F*	
Regression	3	15706.03	5235.34	1314.13	0.02	
Residual	2	7.97	3.98			
Total	5	15714.00				
	Coefficients	*Standard Error*	*t Stat*	*P-value*	*Lower 95%*	*Upper 95%*
Intercept	0	#N/A	#N/A	#N/A	#N/A	#N/A
π1	19.31	5.74	3.37	0.08	-5.37	44.0
π2	10.76	4.78	2.25	0.15	-9.80	31.3
π4	-20.09	43.40	-0.46	0.69	-206.84	166.7
RESIDUAL OUTPUT				PROBABILITY OUTPUT		
Observation	*Predicted η sat*	*Residuals*	*Standard Residuals*		*Percentile*	*η sat*
1	54.2	-1.95	-1.54		10	52.3
2	53.3	-0.22	-0.17		30	53.1
3	54.3	0.78	0.62		50	55.1
4	56	1.82	1.44		70	57.8
5	61.9	-0.44	-0.35		90	61.5

Table 4.47 shows the regression analysis of saturation efficiency of Celdek pad for 50mm pad thickness obtained byusingMicrosoft office excel package 2007 version. Other tables for other levels of pad thickness and for various pad types are shown in appendices 4.16 to 4.19. From equation (equations 3.2 - 3.9),$\pi 3 = \eta_{sat} = f(\pi_1, \pi_2, \pi_4)$. From table 4.47 the coefficients of the π-group are obtained as +19.31, +10.76 and -20.09 for π1, π2, and π4 respectively. Substituting the dimensionless groups for π_1, π_2, π_4 and their coefficients gives the model equation in equation 4.1. Equations 4.2 to 4.20 are gotten in a similar manner. Tables 4.48, 4.49, 4.50 and 4.51 show the model equations forpredicting saturation efficiency of Celdek, Jute fibre, Coconut fibre, and POP sponge respectively.

Table 4.48 Model equations for predicting saturation efficiency of Celdek pad

Pad Thickness (mm)	Model equation	R^2	No
50	$\eta_{sat}=19.309370\left(\frac{t^4 h_{v1}}{m_a^2 S_v^2}\right)+10.764764\left(\frac{A_2}{t^2}\right)-20.089731\left(\frac{T_{wb}}{T_{db}}\right)$	0.9994	4.1
100	$\eta_{sat}=1.03852\left(\frac{t^4 h_{v1}}{m_a^2 S_v^2}\right)+12.78329\left(\frac{A_s}{t^2}\right)-21.701\left(\frac{T_{wb}}{T_{db}}\right)$	0.9998	4.2
150	$\eta_{sat}=0.14639\left(\frac{t^4 h_{v1}}{m_a^2 S_v^2}\right)+17.18706\left(\frac{A_s}{t^2}\right)+34.98315\left(\frac{T_{wb}}{T_{db}}\right)$	0.9999	4.3
200	$\eta_{sat}=0.032511\left(\frac{t^4 h_{v1}}{m_a^2 S_v^2}\right)+48.26101\left(\frac{A_s}{t^2}\right)+2.36709\left(\frac{T_{wb}}{T_{db}}\right)$	0.9999	4.4
250	$\eta_{sat}=0.003451\left(\frac{t^4 h_{v1}}{m_a^2 S_v^2}\right)+447.0107\left(\frac{A_s}{t^2}\right)-49.0895\left(\frac{T_{wb}}{T_{db}}\right)$	0.9999	4.5

Table 4.49 Model equations for predicting saturation efficiency of Jute fibre pad

Pad Thickness (mm)	Model equation	R^2	No
50	$\eta_{sat}=-11.8748\left(\frac{t^4 h_{v1}}{m_a^2 S_v^2}\right)+4.615423\left(\frac{A_s}{t^2}\right)-74.3809\left(\frac{T_{wb}}{T_{db}}\right)$	0.9999	4.6
100	$\eta_{sat}=-1.37274\left(\frac{t^4 h_{v1}}{m_a^2 S_v^2}\right)+8.642732\left(\frac{A_s}{t^2}\right)+27.19199\left(\frac{T_{wb}}{T_{db}}\right)$	0.9997	4.7
150	$\eta_{sat}=-0.23642\left(\frac{t^4 h_{v1}}{m_a^2 S_v^2}\right)+43.27411\left(\frac{A_s}{t^2}\right)-58.2826\left(\frac{T_{wb}}{T_{db}}\right)$	0.9998	4.8
200	$\eta_{sat}=-0.08756\left(\frac{t^4 h_{v1}}{m_a^2 S_v^2}\right)+48.96336\left(\frac{A_s}{t^2}\right)+8.337848\left(\frac{T_{wb}}{T_{db}}\right)$	0.9998	4.9
250	$\eta_{sat}=-0.00712\left(\frac{t^4 h_{v1}}{m_a^2 S_v^2}\right)-66.0893\left(\frac{A_s}{t^2}\right)+137.4717\left(\frac{T_{wb}}{T_{db}}\right)$	0.9998	4.10

Table 4.50 Model equations for predicting saturation efficiency of coconut fibre pad

Pad Thickness (mm)	Model equation	R^2	No
50	$\eta_{sat} = -10.3713\left(\frac{t^4 h_{v1}}{m_a^2 S_v^2}\right) + 6.354986\left(\frac{A_s}{t^2}\right) - 137.979\left(\frac{T_{wb}}{T_{db}}\right)$	0.9998	4.11
100	$\eta_{sat} = -0.99686\left(\frac{t^4 h_{v1}}{m_a^2 S_v^2}\right) + 8.65482\left(\frac{A_s}{t^2}\right) + 19.16896\left(\frac{T_{wb}}{T_{db}}\right)$	0.9998	4.12
150	$\eta_{sat} = -0.20189\left(\frac{t^4 h_{v1}}{m_a^2 S_v^2}\right) + 43.57408\left(\frac{A_s}{t^2}\right) - 66.6439\left(\frac{T_{wb}}{T_{db}}\right)$	0.9998	4.13
200	$\eta_{sat} = -0.10724\left(\frac{t^4 h_{v1}}{m_a^2 S_v^2}\right) + 21.77886\left(\frac{A_s}{t^2}\right) + 64.7879\left(\frac{T_{wb}}{T_{db}}\right)$	0.9996	4.14
250	$\eta_{sat} = -0.01263\left(\frac{t^4 h_{v1}}{m_a^2 S_v^2}\right) + 21.56496\left(\frac{A_s}{t^2}\right) + 102.5841\left(\frac{T_{wb}}{T_{db}}\right)$	0.9997	4.15

Table 4.51 Model equations for predicting saturation efficiency of Pop sponge pad

Pad Thickness (mm)	Model equation	R^2	No
50	$\eta_{sat} = -6.20867\left(\frac{t^4 h_{v1}}{m_a^2 S_v^2}\right) + 7.217577\left(\frac{A_s}{t^2}\right) - 178.876\left(\frac{T_{wb}}{T_{db}}\right)$	0.9998	4.16
100	$\eta_{sat} = -1.00671\left(\frac{t^4 h_{v1}}{m_a^2 S_v^2}\right) + 6.415152\left(\frac{A_s}{t^2}\right) + 29.70675\left(\frac{T_{wb}}{T_{db}}\right)$	0.9998	4.17
150	$\eta_{sat} = -0.13537\left(\frac{t^4 h_{v1}}{m_a^2 S_v^2}\right) + 35.65733\left(\frac{A_s}{t^2}\right) - 47.4612\left(\frac{T_{wb}}{T_{db}}\right)$	0.9998	4.18
200	$\eta_{sat} = -0.07951\left(\frac{t^4 h_{v1}}{m_a^2 S_v^2}\right) + 9.420884\left(\frac{A_s}{t^2}\right) + 78.86125\left(\frac{T_{wb}}{T_{db}}\right)$	0.9998	4.19
250	$\eta_{sat} = -0.02878\left(\frac{t^4 h_{v1}}{m_a^2 S_v^2}\right) + 413.0803\left(\frac{A_s}{t^2}\right) + -47.7829\left(\frac{T_{wb}}{T_{db}}\right)$	0.9999	4.20

4.1.6.2**Pressure drop models**

The model equations of pressure drop for the various pad thicknesses were obtained from regression analysis of the various π groups derived from Buckingham π theorem (equations 3.10 - 3.17) using Microsoft office excel package 2007 version. The summary of the model equations obtained from table 4.51 are shown in table 4.52 to 4.55.

Table 4.52 Average values of the ambient conditions, π groups, and pressure drop at 1.5 l/min. water flow rate.

Pad Thick-Ness (mm)	Pad Face Vel. (m/s)	AMBIENT CONDITIONS			π GROUPS			PRESSURE DROP (ΔP) = π_3 (pa)			
		T_{db} (^{0}C)	T_{wb} (^{0}C)	ρ_a (kg/m^3)	π_1	π_2	π_4	CEL	JUT	COC	SPO
50	0.5	34.7	23.6	1.122167	876.693	1.40797	7.0135	3.4	15.7	11.8	7.5
	1.0	33.8	23.1	1.126493	3520.286	2.83031	28.1623	6.1	23.9	18.8	13.2
	1.5	34.2	24.0	1.121438	7885.113	4.21065	63.0809	9.3	34.9	27.2	19.2
	2.0	32.8	23.4	1.127943	14099.282	5.66791	112.794	15.3	47.7	39.2	30.4
	2.5	33.3	23.6	1.126493	22015.87	7.08911	176.127	20	58.6	48.7	38.9
100	0.5	34.2	23.8	1.121438	27.37886	0.08796	1.75225	4.4	20.4	15.3	9.8
	1.0	34.8	23.8	1.122157	109.58565	0.17604	7.01348	7.6	29.9	23.5	16.5
	1.5	35.1	24.2	1.118571	245.77976	0.26321	15.7299	11.2	41.9	32.4	23.1
	2.0	33.5	23.4	1.125766	436.94180	0.35321	28.1442	18.4	57.2	47.1	36.5
	2.5	33.0	23.6	1.127218	688.43966	0.44222	44.0460	24.1	67.4	56.1	44.7
150	0.5	35.6	23.8	1.118571	3.5962287	0.01733	7.76778	5.7	26.5	19.9	12.7
	1.0	36.0	24.0	1.116433	14.35742	0.03460	3.10117	9.5	37.4	29.4	20.6
	1.5	34.8	24.5	1.118571	32.366058	0.05199	6.99099	13.4	50.3	38.9	27.7
	2.0	35.5	24.8	1.116433	57.429968	0.06919	12.4047	22.1	68.6	56.5	43.8
	2.5	34.0	24.3	1.122157	90.251678	0.08696	19.4879	28.9	80.9	67.3	53.6
200	0.5	33.5	23.4	1.125404	0.8586151	0.00552	0.43961	7.4	34.4	25.9	16.5
	1.0	34.8	23.8	1.122157	3.4245514	0.01100	1.75337	11.9	46.8	36.8	25.8
	1.5	34.6	23.6	1.122157	7.7052406	0.01650	3.94508	16.1	60.4	46.7	33.2
	2.0	34.2	23.8	1.121438	13.689429	0.02199	7.00899	26.5	82.3	67.8	52.6
	2.5	35.6	23.8	1.118571	21.348705	0.02743	10.9270	34.7	97.1	80.8	64.3
250	0.5	34.6	23.6	1.122157	0.2805393	0.00225	0.28054	9.6	44.7	33.7	21.5
	1.0	35.1	24.2	1.118571	1.1185710	0.00449	1.II8571	14.9	58.5	46.1	32.3
	1.5	32.5	23.5	1.129399	2.5411478	0.00676	2.54115	19.3	72.5	56.1	39.8
	2.0	34.0	24.3	1.122157	4.4886280	0.00901	4.48863	31.8	98.8	81.4	63.1
	2.5	34.6	23.6	1.122157	7.0179706	0.01127	7.01573	41.6	116.5	97	77.2

Table 4.53 Regression analysis of pressure drop of celdek pad for 50mm padthickness

Multiple R	0.9995					
R Square	0.9989					
Adjusted R Square	0.4979					
Standard Error	0.6380					
Observations	5					
ANOVA						
	df	*SS*	*MS*	*F*	*Significance F*	
Regression	3	768.54	256.18	629.4151	0.02929	
Residual	2	0.81	0.41			
Total	5	769.35				
	Coefficients	*tandard Erro*	*t Stat*	*P-value*	*Lower 95%*	*Upper 95%*
Intercept	0	#N/A	#N/A	#N/A	#N/A	#N/A
π1	23.80	22.08	1.08	0.39	-71.19	118.8
π2	1.63	0.26	6.19	0.03	0.50	2.8
π4	-2974.96	2759.54	-1.08	0.39	-14848.31	8898.4
RESIDUAL OUTPUT					PROBABILITY OUTPUT	
Observation	*Predicted (ΔP)*	*Residuals*	*andard Residuals*		*Percentile*	*(ΔP)*
1	2.76	0.64	1.59		10	3.4
2	5.92	0.18	0.45		30	6.1
3	9.87	-0.57	-1.42		50	9.3
4	15.36	-0.06	-0.16		70	15.3
5	19.81	0.19	0.47		90	20

Table 4.53 shows the regression analysis of pressure drop of Celdek pad for 50mm pad thickness obtained byusing Microsoft office excel package 2007 version. Other tables for other levels of pad thickness and for various pad types are shown in appendices 4.20 to 4.23. From equation (equations 3.10 - 3.17), $\pi_3 = \Delta P = f(\pi_1, \pi_2, \pi_4)$. From table 4.53 the coefficients for the π-group are obtained as +23.80, +1.63 and -2974.96 for π_1, π_2 and π_4 respectively. Substituting the dimensionless groups forπ_1, π_2, π_4 and their coefficients gives the model equation in equation 4.21. Equations 4.21 to 4.40 are gotten in a similar manner.

Table 4.54 Model equations for predicting pressure drop of celdek pad material

Pad Thickness (mm)	Model equation	R^2	No
50	$\Delta P = 23.80\left(\frac{L_e \ell_a Q_a^2}{d^5}\right) + 1.63 - \left(\frac{\ell_a Q_a Q_w}{d^4}\right) - 2974.96\left(\frac{V_a \ell_a Q_a}{d^2}\right)$	0.9989	4.21
100	$\Delta P = -0.25\left(\frac{L_e \ell_a Q_a^2}{d^5}\right) + 34.004\left(\frac{\ell_a Q_a Q_w}{d^4}\right) + 4.09\left(\frac{V_a \ell_a Q_a}{d^2}\right)$	0.9986	4.22
150	$\Delta P = 0.07\left(\frac{L_e \ell_a Q_a^2}{d^5}\right) + 201.49\left(\frac{\ell_a Q_a Q_w}{d^4}\right) + 0.25\left(\frac{V_a \ell_a Q_a}{d^2}\right)$	0.9984	4.23
200	$\Delta P = 229.14\left(\frac{L_e \ell_a Q_a^2}{d^5}\right) + 958.87\left(\frac{\ell_a Q_a Q_w}{d^4}\right) - 446.93\left(\frac{V_a \ell_a Q_a}{d^2}\right)$	0.9961	4.24
250	$\Delta P = 1297.85\left(\frac{L_e \ell_a Q_a^2}{d^5}\right) + 3102.7033\left(\frac{\ell_a Q_a Q_w}{d^4}\right) - 1297.3189\left(\frac{V_a \ell_a Q_a}{d^2}\right)$	0.9949	4.25

Table 4.55 Model equations for predicting pressure drop of jute fibre pad material

Pad Thickness (mm)	Model equation	R^2	No
50	$\Delta P = 23.2383\left(\frac{L_e \ell_a Q_a^2}{d^5}\right) + 9.054045\left(\frac{\ell_a Q_a Q_w}{d^4}\right) - 2904.82\left(\frac{V_a \ell_a Q_a}{d^2}\right)$	0.9985	4.26
100	$\Delta P = -0.3498727\left(\frac{L_e \ell_a Q_a^2}{d^5}\right) + 190.70623\left(\frac{\ell_a Q_a Q_w}{d^4}\right) + 5.06899\left(\frac{V_a \ell_a Q_a}{d^2}\right)$	0.9978	4.27
150	$\Delta P = -0.418457\left(\frac{L_e \ell_a Q_a^2}{d^5}\right) + 1120.45433\left(\frac{\ell_a Q_a Q_w}{d^4}\right) + 1.105550\left(\frac{V_a \ell_a Q_a}{d^2}\right)$	0.9995	4.28
200	$\Delta P = 1348.8148\left(\frac{L_e \ell_a Q_a^2}{d^5}\right) + 5209.7247\left(\frac{\ell_a Q_a Q_w}{d^4}\right) - 2639.4489\left(\frac{V_a \ell_a Q_a}{d^2}\right)$	0.9954	4.29
250	$\Delta P = 6970.4888\left(\frac{L_e \ell_a Q_a^2}{d^5}\right) + 16527.095\left(\frac{\ell_a Q_a Q_w}{d^4}\right) - 6982.658\left(\frac{V_a \ell_a Q_a}{d^2}\right)$	0.9937	4.30

Table 4.56 Model equations for predicting pressure drop of coconut fibre pad

Pad Thickness (mm)	Model equation	R^2	No
50	$\Delta P = 33.36702\left(\frac{L_e \ell_a Q_a^2}{d^5}\right) + 6.62305\left(\frac{\ell_a Q_a Q_w}{d^4}\right) - 4170.87\left(\frac{V_a \ell_a Q_a}{d^2}\right)$	0.9987	4.31
100	$\Delta P = -0.592628\left(\frac{L_e \ell_a Q_a^2}{d^5}\right) + 139.42254\left(\frac{\ell_a Q_a Q_w}{d^4}\right) + 9.122674\left(\frac{V_a \ell_a Q_a}{d^2}\right)$	0.9978	4.32
150	$\Delta P = -0.22412379\left(\frac{L_e \ell_a Q_a^2}{d^5}\right) + 829.07222\left(\frac{\ell_a Q_a Q_w}{d^4}\right) + 0.8160106\left(\frac{V_a \ell_a Q_a}{d^2}\right)$	0.9988	4.33
200	$\Delta P = 810.9202\left(\frac{L_e \ell_a Q_a^2}{d^5}\right) + 3806.7850\left(\frac{\ell_a Q_a Q_w}{d^4}\right) - 1586.5034\left(\frac{V_a \ell_a Q_a}{d^2}\right)$	0.9951	4.34
250	$\Delta P = 4590.172\left(\frac{L_e \ell_a Q_a^2}{d^5}\right) + 12159.129\left(\frac{\ell_a Q_a Q_w}{d^4}\right) - 4597.344\left(\frac{V_a \ell_a Q_a}{d^2}\right)$	0.9934	4.35

Table 4.57 Model equations for predicting pressure drop of Pop sponge pad

Pad Thickness (mm)	Model equation	R^2	No
50	$\Delta P = 41.18112\left(\frac{L_e \ell_a Q_a^2}{d^5}\right) + 3.919234\left(\frac{\ell_a Q_a Q_w}{d^4}\right) - 5147.58\left(\frac{V_a \ell_a Q_a}{d^2}\right)$	0.9988	4.36
100	$\Delta P = -0.729352\left(\frac{L_e \ell_a Q_a^2}{d^5}\right) + 85.565213\left(\frac{\ell_a Q_a Q_w}{d^4}\right) + 11.545026\left(\frac{V_a \ell_a Q_a}{d^2}\right)$	0.9982	4.37
150	$\Delta P = -0.003571\left(\frac{L_e \ell_a Q_a^2}{d^5}\right) + 520.39376\left(\frac{\ell_a Q_a Q_w}{d^4}\right) + 0.475674\left(\frac{V_a \ell_a Q_a}{d^2}\right)$	0.9979	4.38
200	$\Delta P = 210.3426\left(\frac{L_e \ell_a Q_a^2}{d^5}\right) + 2293.945\left(\frac{\ell_a Q_a Q_w}{d^4}\right) - 410.833\left(\frac{V_a \ell_a Q_a}{d^2}\right)$	0.9954	4.39
250	$\Delta P = 1882.8012\left(\frac{L_e \ell_a Q_a^2}{d^5}\right) + 7388.353\left(\frac{\ell_a Q_a Q_w}{d^4}\right) - 1884.267\left(\frac{V_a \ell_a Q_a}{d^2}\right)$	0.9939	4.40

4.1.7**Model Validation**

4.1.7.1 **Saturation efficiency model validation**

A plot of the experimental and predicted values of each sample treatment combination for the best saturation efficiency models gave a linear relationship with high coefficient of determination values as illustrated in figures 4.16 to 4.19 and table 4.58.

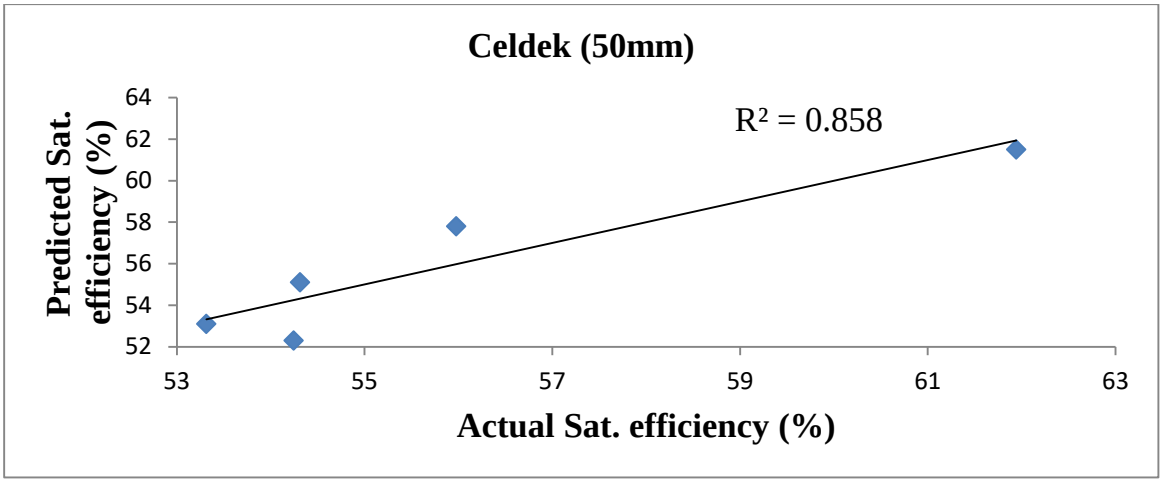

Figure 4.16 Graph of predicted against experimental values for Celdek at 50mm pad thickness and 1.75 l/min. water flow rate.

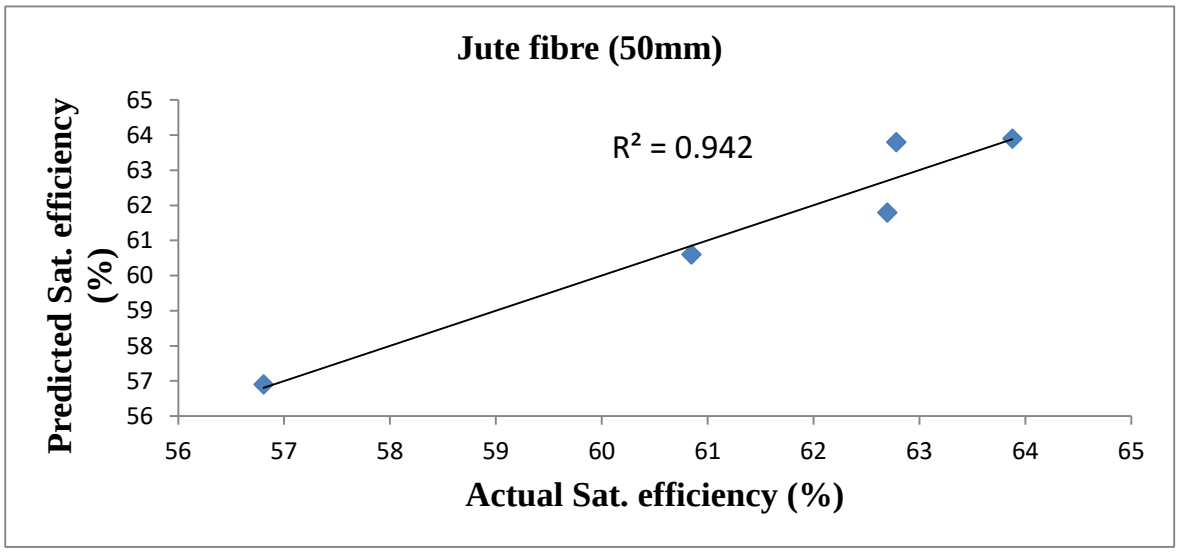

Figure 4.17 Graph of predicted against experimental values for Jute fibre at 50mm pad thickness and 1.75 l/min. water flow rate.

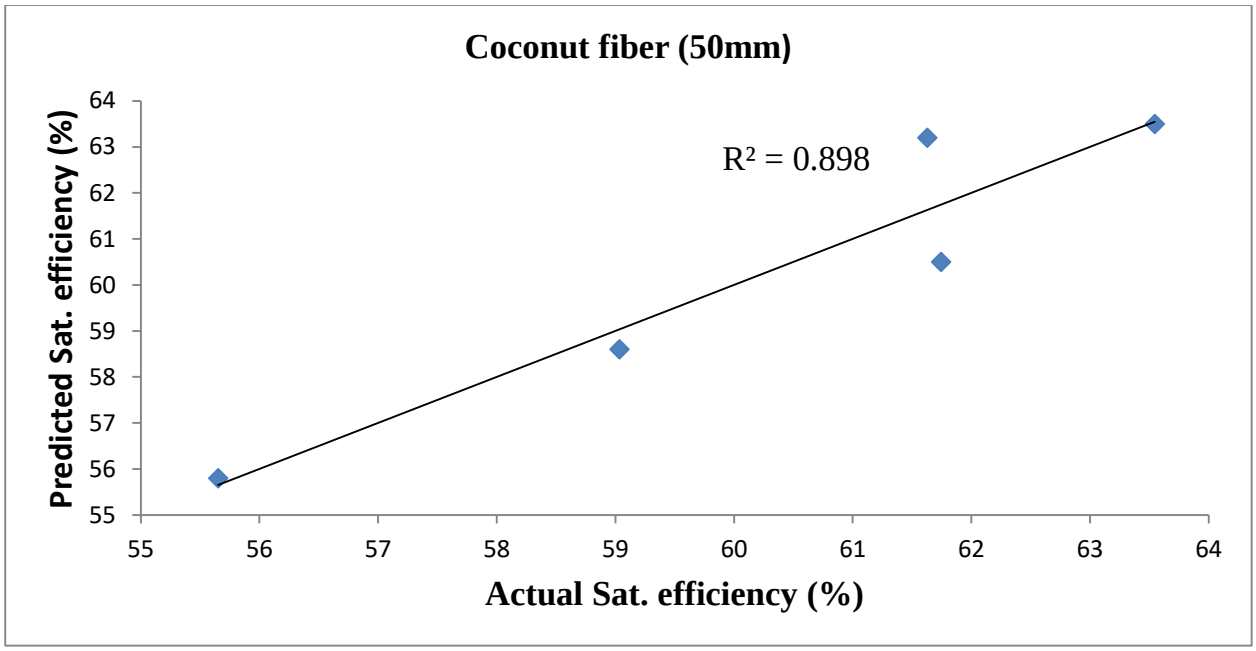

Figure 4.18 Graph of predicted against experimental values for Coconut fibre at 50mm pad thickness and 1.75 l/min. water flow rate.

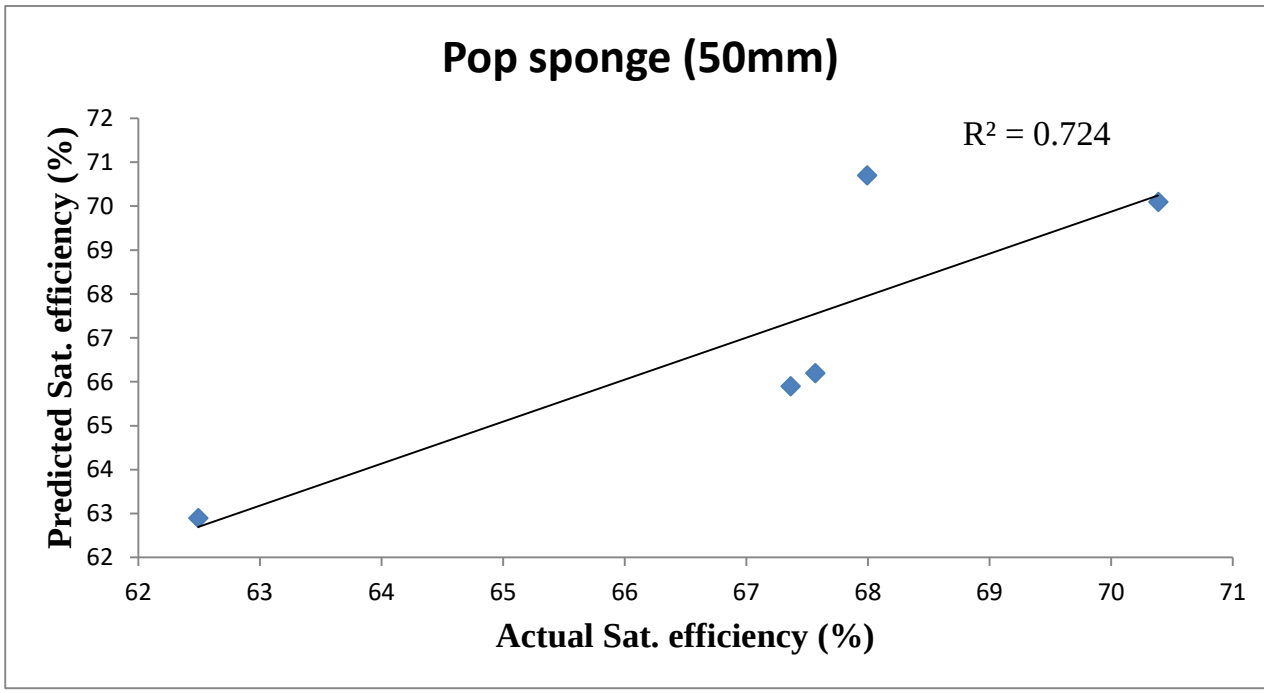

Figure 4.19 Graph of predicted against experimental values for Pop sponge at 50mm pad thickness and 1.75 l/min. water flow rate.

Table 4.58 Summary of saturation efficiency models validation

Pad thick Ness (mm)	Celdek			Jute fiber			Coconut fiber			Pop sponge		
	Pred. Val.	Exp. Val.	R^2	Pred. Val.	Exp. Val	R^2	Pred. Val.	Exp. Val	R^2	Pred. Val.	Exp. Val	R^2
50	54.2	52.3	0.858	56.8	56.9	0.942	55.7	55.8	0.898	62.5	62.9	0.724
	53.3	53.1		60.8	60.6		59.0	58.6		67.4	65.9	
	54,3	55.1		62.7	61.8		61.7	60.5		67.6	66.2	
	55.9	57,8		62.8	63.8		61.6	63.2		70.4	70.1	
	62.0	61.5		63.9	63.9		63.5	63.5		68.0	70.7	
100	65.7	63.9	0.834	63.1	63.7	0.814	60.3	60.7	0.811	53.7	54.1	0.825
	64.7	64.5		69.9	67.2		65.2	63.5		58.3	56.9	
	65.7	66.3		71.8	71.3		66.6	65.7		59.9	58.9	
	67.1	68.9		73.1	73.1		67.5	67.8		61.1	61.3	
	72.2	71.8		71.7	74.3		66.6	68.5		59.6	61.5	
150	71.2	71.4	0.982	70.2	70.7	0.863	66.4	66.8	0.857	60.5	60.7	0.848
	73.0	72.6		76.2	73.8		71.4	69.6		63.8	62.8	
	73.4	73.3		77.6	78.0		72.6	72.1		64.6	63.9	
	74.3	74.8		78.4	80.3		73.3	75.6		65.1	66.8	
	78.0	77.9		81.1	80.7		76.4	76.0		67.3	67.0	
200	77.3	76.7	0.871	72.4	72.9	0.872	68.4	69.2	0.777	62.5	62.9	0.724
	77.4	77.1		79.6	76.9		76.0	72.6		67.4	65.9	
	77.5	77.5		81.1	81.7		76.9	76.3		67.6	66.2	
	78.1	79.1		81.9	82.5		79.5	79.9		70.4	70.1	
	80.9	80.7		81.7	82.6		77.5	80.3		68.0	70.7	
250	77.0	76.1	0.789	73.0	73.5	0.884	70.1	70.8	0.765	63.1	63.4	0.848
	76.6	76.3		79.0	77.2		76.1	73.3		67.8	676.5	
	76.7	77.3		81.6	80.9		78.4	77.4		68.1	67.3	
	77.7	78.6		81.9	82.3		78.7	79.5		68.5	69.3	
	80.0	79.8		80.8	82.5		77.9	80.3		69.1	70.1	

4.1.7.2 **Pressure drop model validation**

A plot of the experimental and predicted values of each sample treatment combination for the best pressure drop models gave a linear relationship with high coefficient of determination values as illustrated in figure 4.20 to 4.23 and table 4.59. Figure 4.24 shows the model validation for the pad types plotted in one graph.

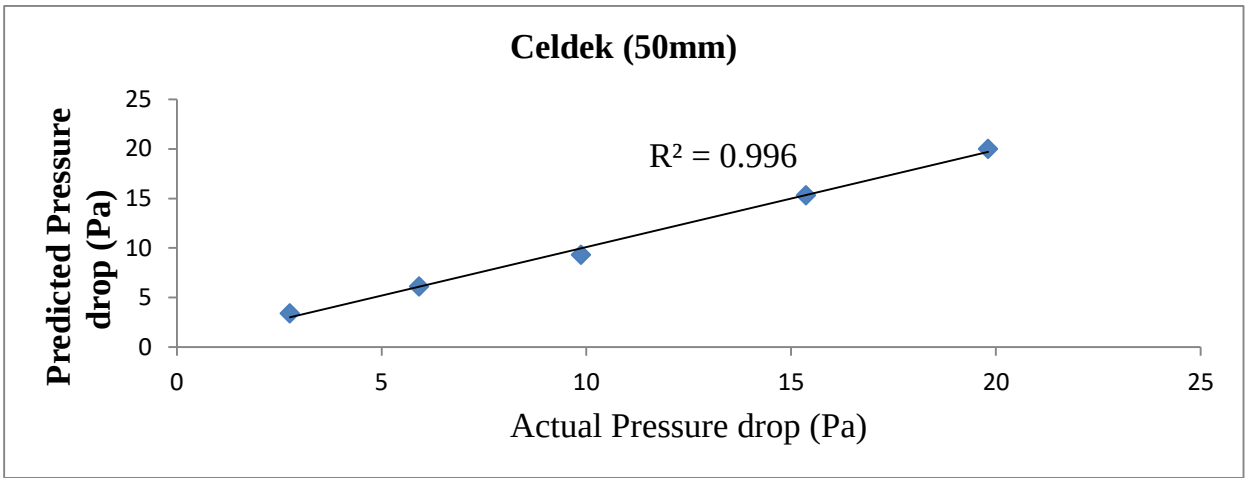

Figure 4.20 Graph of predicted against experimental values of pressure drop for Celdek at 50mm pad thickness and 1.75 l/min. water flow rate.

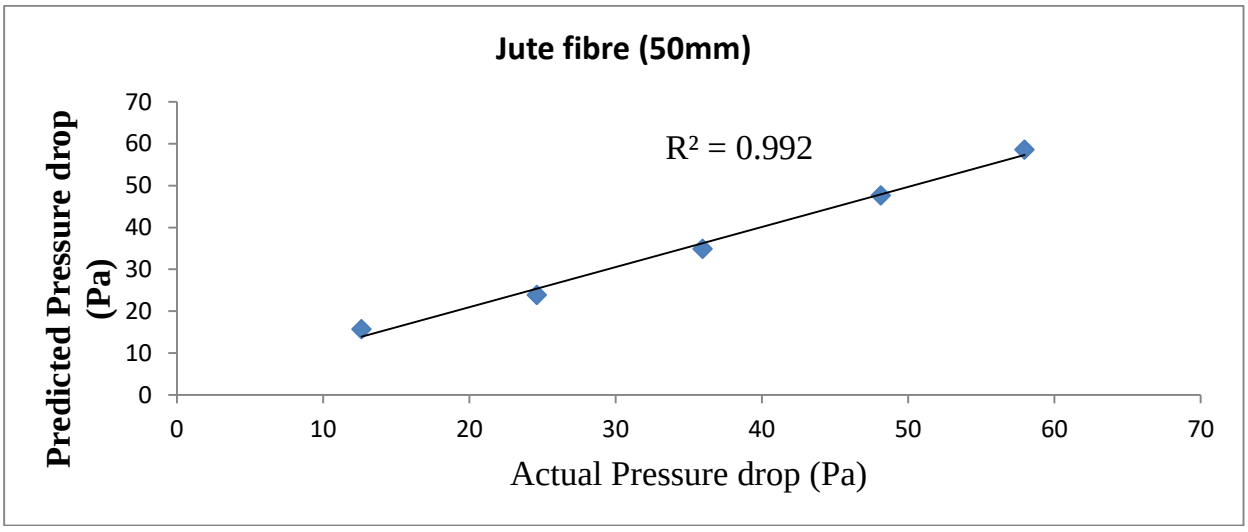

Figure 4.21 Graph of predicted against experimental values of pressure drop for jute fibre at 50mm pad thickness and 1.75 l/min. water flow rate.

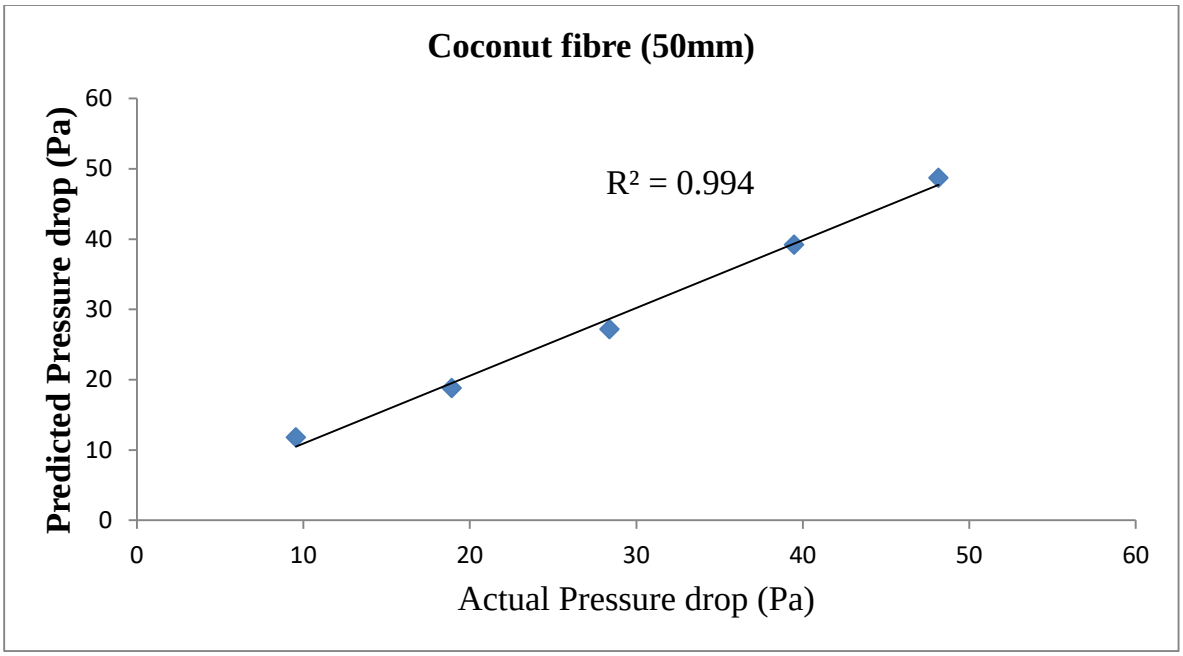

Figure 4.22 Graph of predicted against experimental values of pressure drop for coconut fibre at 50mm pad thickness and 1.75 l/min. water flow rate.

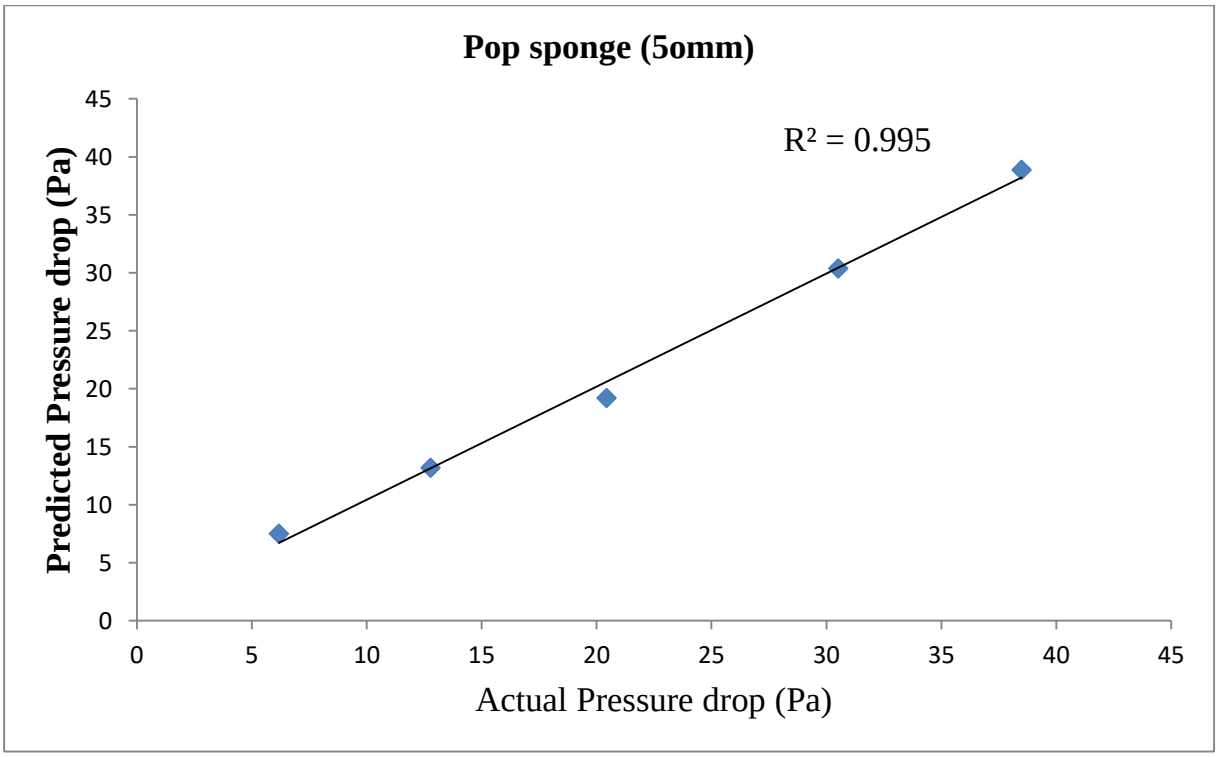

Figure 4.23 Graph of predicted against experimental values of pressure drop for pop sponge at 50mm pad thickness and 1.75 l/min. water flow rate.

Table 4.59 Summary of pressure drop models validation

Pad thick Ness (mm)	Celdek			Jute fiber			Coconut fiber			Pop sponge		
	Pred. Val.	Exp. Val.	R^2	Pred. Val.	Exp. Val	R^2	Pred. Val.	Exp. Val	R^2	Pred. Val.	Exp. Val	R^2
50	2.8	3.4	0.996	12.6	15.7	0.992	9.6	11.8	0.994	6.2	7.5	0.995
	5.9	6.1		24.6	23.9		18.9	18.8		12.8	13.2	
	9.9	9.3		35.9	34.9		28.4	27.2		20.4	19.2	
	15.4	15.3		48.1	47.7		39.5	39.2		30.5	30.4	
	19.8	20.0		58.0	58.6		48.2	48.7		38.5	38.9	
100	3.3	4.4	0.993	16.1	20.4	0.987	12.0	15.3	0.989	7.8	9.8	0.992
	7.4	7.6		30.8	29.9		23.6	23.5		16.1	16.5	
	12.1	11.2		43.9	41.9		34.5	32.4		24.9	23.1	
	18.4	18.4		57.1	57.2		47.1	47.1		36.5	36.5	
	23.9	24.1		66.7	67.4		55.5	56.1		44.2	44.7	
150	5.7	5.7	0.992	26.5	26.5	0.995	19.9	19.9	0.991	12.7	12.7	0.988
	8.8	9.5		36.2	37.4		28.0	29.4		19.4	20.6	
	14.6	13.4		52.4	50.3		41.6	38.9		30.3	27.7	
	21.3	22.1		67.2	68.6		54.6	56.5		41.7	43.8	
	29.1	28.9		81.2	80.9		67.8	67.3		54.2	53.6	
200	5.6	7.4	0.982	26.5	34.4	0.967	19.8	25.9	0.968	12.7	16.5	0.976
	11.6	11.9		48.5	46.8		37.2	36.8		25.2	25.8	
	18.3	16.1		66.1	60.4		52.3	46.7		37.8	33.2	
	25.5	26.5		79.2	82.3		65.0	67.8		50.4	52.6	
	34.7	34.7		97.1	97.1		80.8	80.8		64.3	64.3	
250	7.1	9.6	0.976	33.8	44.7	0.950	25.3	33.7	0.953	16.2	21.5	0.966
	14.5	14.9		60.6	58.5		46.6	46.1		31.5	32.3	
	22.3	19.3		80.8	72.5		64.0	56.1		46.2	39.8	
	30.3	31.8		94.3	98.8		77.4	81.4		60.0	63.1	
	41.6	41.6		116.5	116.5		97.0	97.0		77.2	77.2	

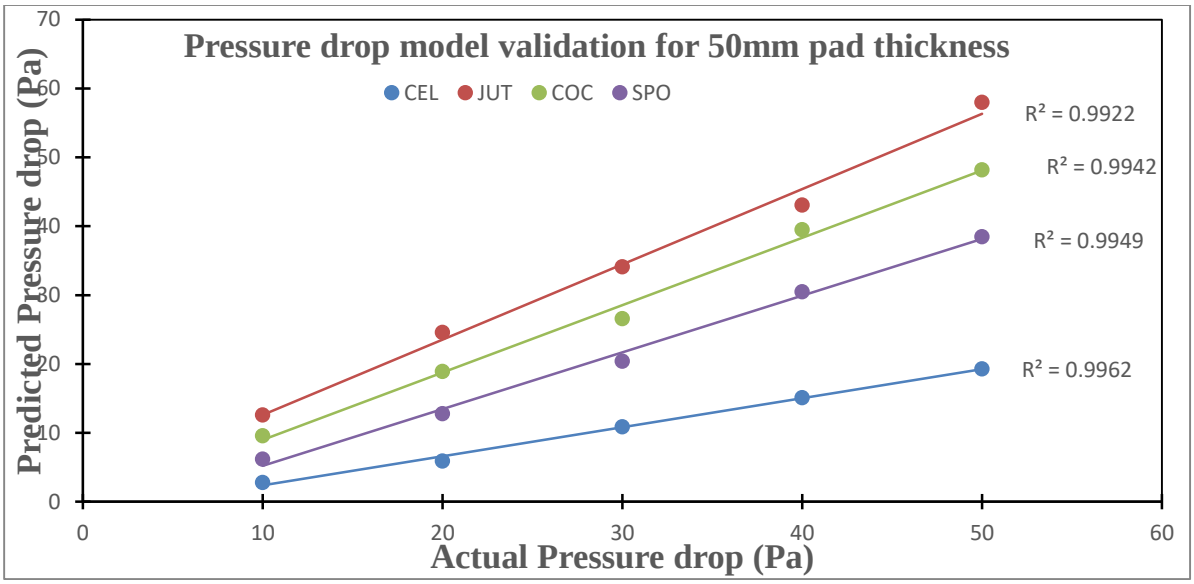

Figure 4.24 Combined graph of predicted against experimental values of pressure drop for pad types at 50mm pad thickness and 1.75 l/min. water flow rate.

4.2 **Discussion**

4.2.1**Discussion on theeffect of pad face air velocity on the saturation efficiency and pressure drop of different pad types**:

Figure 4.1 (a) to (d) show the effect of pad face air velocities at constant pad thickness and 1.75 l/min. water flow rate on saturation efficiency of Celdek, Jute fibre, Coconut fibre and POP Sponge respectively. Saturation efficiency increases with pad-face air velocity for the three local pad materials and decreases slightly withpad-face air velocity for Celdek pad material.At very low pad-face air velocities the air flow tends to be laminar and only the air in the viscous layer surrounding the fibre is saturated with water vapourresulting in low evaporation rate. As pad face air velocity is increased, the flow becomes more turbulent, disrupting the surrounding layer and increasing evaporation and saturation efficiency. The apparent behaviourofCeldek pad material is as a result of the larger pore space between the fibreswhich allows air to pass through the pad with minimal resistance reducing the air-water contact time and decreasing the evaporation rate and saturation efficiency. The behaviour of the efficiency of Celdek pad with air

velocity observed in this study was in agreement with the work done byGunhanetal.(2007).For the local pad materials,the shape of the curves are similar for all the pad materialsbutsaturation efficiency of the jute fibrewasconsistently greater than that of coconut fiber which also wasconsistently greater than that of pop sponge as shown in figure 4.1 (e).Pressure drop increased with increase in pad-face air velocity. The pressure drop of the various pads can be listed from the highest pressure drop to the lowest as follows: Jute fibre > Coconut fibre > Pop sponge > Celdek as shown in figure 4.1 (f).

4.2.2**Discussion on theeffect of pad thickness on the saturation efficiency and pressure drop of pad types:**

Saturation efficiency was found to increase with pad thickness for all the various pad materials as shown in figure 4.1 (g) – (j).As pad thickness is increased, the contact time for air traversingthe pad is increased. The increasedopportunity for evaporation results in higher saturation efficiency. Beyond 200mm the air tends to be saturated with water vapourhence evaporation rate decreases. These results were in agreement withpreviousliterature studies on evaporative cooling pad systems(Dzivama et al., 1999).Generally higherefficiencies are obtained with thicker pads. This result reflects greater evaporativerates as air takes more time to travel through the pad. The saturation efficiencies of the pad materials are in the order: Jute fibre > Celdek > Coconut > POP Sponge as shown in figure 4.1 (k). Pressure drop increased with pad thickness. As pad thickness increases, the resistance to air flow increases resulting in increased pressure drop.The Pressure drop of the pad materials are in the order: Jute fibre > Coconut > POP Sponge > Celdek as shown in figure 4.1 (l).

4.2.3**Discussion on theeffect of water flow rate on the cooling efficiency and pressure drop of pad types:**

As shown in figure 4.1 (m) – (p), the chosen range of water flow rate was found to have little effect on saturation efficiency. Figure 4.2 (b), shows that pressure drop increased

with water flow rate. Water tends to occupy the space between the fibres preventing some of the surface from air contact. This reduced space also restricts air flow, increasing static pressure loss.The saturation efficiency of the pad materials are in the order: Jute fibre > Coconut > Celdek > POP Sponge as shown in figure 4.1 (q). Pressure drop increased with increasing water flow rate for all the pad materials as shown in figure 4.1 (r).

4.2.4**Discussion on thestatisticalanalysis for the effect of pad thickness, water flow rate and pad face air velocity on saturation efficiency and pressure drop.**

4.2.4.1 **Statistical analysis for celdekpadmaterial**

From table 4.4, the model F-value of 92.63 implies that the model is significant. The Prob > F values less than 0.05 indicates model terms that are significant. In this case pad thicknessandair flow rate are the linear and product significant terms whereas water flow rate and the interactions are non-significant. The non-significant terms were expunged from model equation because they have no meaningful impact on the efficiency. The significant terms are primarily responsible for high efficiency of the pad material. Also, the model's high R^2 value of 0.9881 indicates that it captured up to 98.81% of the factor's variations hence the high correlation in the predictions of the efficiency of the pad material. Therefore, the model predictions were reliable hence can be employed in the descriptionof the evaporative cooling process of the Celdek pad material. Consequently, it can be used to predict efficiency of the material. The relationship between the experimental and predicted efficiencies shown in figure 4.2. indicate that the points are close to each other. For the analysis of the pressure drop, from table 4.5, all the factors, their products and interactions are significant as indicated by equation 4.2. This shows that all the factors and their interactions have significant effect on the pressure drop of Celdek pad material. The interaction effects were represented in the response surface plots on figures 4.4 (a) – (c). From the plots it can be seen that pad face air velocity and water flow rate are strong factors than pad thickness.

4.2.4.1.1 **Discussion on theOptimization of the efficiency and pressure drop of celdek**

From table 4.7, the results of the optimization show that option no. 5 tend to be the best due to its relatively lower pressure drop of 6.3Pa and pad thickness of 161mm.Maximum saturation efficiency may not be the optimum operating level, especially if it is obtained at the expense of large static pressure losses. Lower pressure drop means that a more economical suction fans can be used. The lesser the pad thickness, the lower the cost of pad material.

4.2.4.2 **Discussion on theStatistical analysis for jute fibre pad material**

From table 4.9, the model F-value of 184.01 implies that the model is significant. The Prob > F values less than 0.05 indicates model terms that are significant. In this case pad thickness, water flow rate and air flow rate are the linear and product significant terms whereas the interactions are non-significant. The significant terms are primarily responsible for high efficiency of the pad material. Also, the model's high R^2 value of 0.994 indicates that it captured up to 99.4% of the factor's variations hence the high correlation in the predictions of the efficiency of the pad material. Therefore, the model predictions were reliable hence can be employed in the descriptionof the evaporative cooling process of the Jute pad material. Consequently, it can be used to predict efficiency of the material. The relationship between the experimental and predicted efficiencies shown in figure 4.5 indicated that the points are close to each other. For the analysis of the pressure drop, from table 4.10, all the factors, their products and interactions are significant except the product of water flow rate (w x w) as indicated by equation 4.4. This shows that all the factors and their interactions have significant effect on the pressure drop of Jute pad material. The interaction effects were represented in the response surface plots on figures 4.7 (a) – (c). From the plots it can be seen that pad face air velocity and water flow rate are strong factors than pad thickness.

4.2.4.2.1**Discussion onoptimization of the efficiency and pressure drop of jute fibre**

From table 4.12, the results of the optimization show that option no. 4 tend to be the best due to its relatively lower pressure drop of 35.7Pa and pad thickness of

157mm.Maximum saturation efficiency may not be the optimum operating level, especially if it is obtained at the expense of large static pressure losses. Lower pressure drop means that a more economical suction fans can be used. The lesser the pad thickness, the lower the cost of pad material.

4.2.4.3**Discussion on the statistical analysis for coconut fibrepad material**

From table 4.14, the model F-value of 136.11 implies that the model is significant. The Prob > F values less than 0.05 indicates model terms that are significant. In this case pad thickness, and air flow rate are the linear and product significant terms whereas the interactions are non-significant except pad thickness versus pad face velocity. The significant terms are primarily responsible for high efficiency of the pad material. Also, the model's high R^2 value of 0.992 indicates that it captured up to 99.2% of the factors variations hence the high correlation in the predictions of the efficiency of the pad material. Therefore, the model predictions were reliable hence can be employed in the descriptionof the evaporative cooling process of the coconut fibre pad material. Consequently, it can be used to predict efficiency of the material. The relationship between the experimental and predicted efficiencies shown in figure 4.8 indicated that the points are close to each other. The response surface plot of the interaction effect of pad face air velocity and pad thickness on the efficiency of coconut fibre pad shown in figure 4.9 indicated that pad thickness is a stronger factor than pad face air velocity. For the analysis of the pressure drop, from table 4.15, all the factors are significant, while their products and interactions are non-significant as indicated by equation 4.6. This shows that all the factors have significant effect on the pressure drop of coconut fiber pad material.The relationship between the experimental and predicted efficiencies is shown in figure 4.10. The straight line indicates the suitability of the model to describe the Pressure drop of the coconut fibre pad.

4.2.4.3.1**Discussion onoptimization of efficiency and pressure drop of coconut pad**

From table 4.17, the results of the optimization show that option no. 5 tend to be the best due to its relatively lower pressure drop of 28.2Pa and pad thickness of 156mm which

compensated for the relatively lower efficiency of 74.1%.Maximum saturation efficiency may not be the optimum operating level, especially if it is obtained at the expense of large static pressure losses. Lower pressure drop means that a more economical suction fans can be used. The lesser the pad thickness, the lower the cost of pad material.

4.2.4.4**Discussion on thestatistical analysis for pop sponge pad material**

From table 4.19, the model F-value of 229.88 implies that the model is significant. The Prob > F values less than 0.05 indicates model terms that are significant. In this case all the factors and the interaction of water flow rate versus pad thickness are significant terms.The significant terms are primarily responsible for high efficiency of the pad material. Also, the model's high R^2 value of 0.995 indicates that it captured up to 99.1% of the factor's variations hence the high correlation in the predictions of the efficiency of the pad material. Therefore, the model predictions were reliable hence can be employed in the descriptionof the evaporative cooling process of POP sponge pad material. Consequently, it can be used to predict efficiency of the material. The relationship between the experimental and predicted efficiencies shown in figure 4.12 indicates that the points are close to each other. The response surface plot of the interaction effect of water flow rate and pad thickness on the efficiency of POP sponge fibre pad shown in figure 4.13 indicated that pad thickness is a stronger factor than water flow rate. For the analysis of the pressure drop, from table 4.20, their products and interactions are significant terms except product of water flow rate (w x w), as indicated by equation 4.8. This shows that all the factors have significant effect on the pressure drop of POP sponge pad material. The relationship between the experimental and predicted pressure drop is shown in figure 4.14. The straight line indicates the suitability of the model to describe the pressure drop of the POP sponge pad. From figure 4.15 (a) – (c) Pad face air velocity and water flow rate are stronger factors than pad thickness.

4.2.4.4.1Discussion onoptimization of efficiency and pressure drop of pop sponge

From table 4.22, the results of the optimization show that option no. 1 tend to be the best due to its relatively lower pressure drop of 18.9Paand air velocity of 1.3m/s which

compensated for the relatively lower efficiency of 64.6%. The lower the pad face air velocity and pressure drop the lower the suction fan capacity to be used and thus reducing initial and operating cost.

4.2.5 **Discussion onTukey's Honestly Significant Difference (HSD) Testfor Means Separation.**

4.2.5.1**Discussion onsaturation efficiency mean separation for pad thickness**

4.2.5.1.1**Mean separation for celdek pad**.

The test for the saturation efficiencymeans separation of celdek pad material showed significant difference between 50mm versus 100mm,150mm, 200mm and 250mm pad thicknesses and between 100mm versus150mm, 200mm and 250mm pad thicknesses. While non-significant difference exists between 150 mm versus 200mm and 250mm pad thicknesses and between 200mm and 250mm.This shows that 150mm pad thickness can be used in place of 200mm and 250mm pad thickness without any statistical difference in saturation efficiency.

4.2.5.1.2**Mean separation for jute pad**.

The test for the saturation efficiency means separation of Jute fibre pad material showed significant difference between 50mm versus 100mm,150mm, 200mm, 250mm pad thickness and between 100mm versus 200mm, 250mm. While non-significant difference exists between 100mm versus 150 mm, and between 150mm versus 200mm, 250mm and between 200mm versus 250mm. pad thicknesses. This shows that 100mm pad thickness can be used in place of 150mm without any statistical difference in saturation efficiencies. Also, the same can be done with 150mm, 200mm and 250mm pad thicknesses without any statistical difference in their saturation efficiencies.

4.2.5.1.3 **Mean separation for coconut pad**.

The test for the saturation efficiencymeans separation of Coconut fibre pad material showed significant difference between 50mm versus 150mm, 200mm and 250mm pad thicknesses and between 100mm versus 200mm and 250mm. While non-significant difference exists between 50mm and 100mm, between 100mm versus 150 mm, between

150mm versus 200mm, 250mm and between 200mm versus 250mm. pad thicknesses. This shows that 50mm pad thickness can be used in place of 100mm pad thickness, 100mm in place of 150mm and also 150mm in place of 200mm and 250mm pad thicknesses without any statistical difference in their saturation efficiencies.

4.2.5.1.4**Mean separation for popsponge pad**

The test for the saturation efficiency means separation of Pop sponge padmaterial showed significant difference between 50mm versus 150mm, 200mm and 250mm pad thicknesses and between 100mm versus 200mm and 250mm. While non-significant difference exist between 50mm and 100mm, between 100mm versus 150 mm, between 150mm versus 200mm, 250mm and between 200mm versus 250mm. pad thicknesses. This shows that 50mm pad thickness can be used in place of 100mm pad thickness, 100mm in place of 150mm and also 150mm in place of 200mm and 250mm pad thicknesses without any statistical difference in their saturation efficiencies.

4.2.5.2**Discussion onsaturation efficiency and pressure drop means separation**

4.2.5.2.1 **Saturation efficiency means separation of pad types**

Table 4.39 shows the summary of saturation efficiency means separated for the pad types at different levels of pad thicknesses. Within a row, means with the same letter are not significantly different at 5% level. The results of the Tukey HSD test show no significant difference in saturation efficiency between the Celdek, Jute fibre and Coconut fibre pads at all levels of pad thickness. However, there were significant differences in saturation efficiency between the three pads (Celdek, Jute firer, Coconut fibre) and Sponge, except at 50mm thickness where there is no significant difference between Celdek and Sponge.

4.2.5.2.2**Pressure drop means separation of pad-type**

Tukey HSD testwas used to compare means of pressure drop. Table 4.45 shows the summary of pressure drop means separated for pad types at all levels of pad thicknesses. Within a row, means with the same letter are not significantly different at 5% level. The results ofTukey HSD test show no significant difference in the pressure drop between the

Celdek, Coconut fibre and Sponge pads over all levels of pad thicknesses. Also, no significant difference in the pressure drop between the Jute fibre, Coconut fiber and Sponge pad over all levels of pad thickness. However, there are significant differences in pressure drop between Celdek and Jute over all levels of pad thickness.

4.2.6 **Discussion onmodeling of saturation efficiency and pressure drop**

4.2.6.1 **Saturation efficiency models**

From table 4.47, the coefficients of the dimensionless groups π1 ($\frac{t^4 h_{v1}}{m_a^2 S_v^2}$), π2 ($\frac{A_s}{t^2}$), and π4 ($\frac{T_{wb}}{T_{db}}$) are 19.31, 10.76 and -20.09 respectively. This shows that dimensionless group π1 is a stronger factor than dimensionless group π2. While dimensionless group π4 is a weak factor in predicting the saturation efficiency of Celdek pad at 50mm pad thickness. The F value of 1314.13 shows that the model is significant.

4.2.6.2 **Pressure drop models**

From table 4.53, the coefficients of the dimensionless groups π1 ($L_e \rho_a Q_a^2 / d^5$), π2 ($\rho_a Q_w Q_a / d^4$), and π4 ($V_a \rho_a Q_a / d^2$) are 23.8, 1.63 and -2974.96 respectively. This shows that dimensionless group π1 is a stronger factor than dimensionless group π2. While dimensionless group π4 is a weak factor in predicting the Pressure drop of Celdek pad at 50mm pad thickness. The F value of 629.4 shows that the model is significant.

4.2.7 **Discussion onmodel validation**

4.2.7.1 **Saturation efficiency model validation**

From figure 4.16 – 4.19, the closeness of the plotted data to the straight line and the associated high correlation coefficient representing equality between the experimental and predicted illustrates the suitability of the model in describing the saturation efficiency of the pad materials.The significance of the developed saturation efficiency models and their parameters is that the saturation efficiency of the various pad materials at the

various levels of pad thickness and pad face air velocity can be predicted. This is important to evaporative cooler designers as it will enable them predict in advance the expected efficiency when the design parameters are known. Also, for a given saturation efficiency and ambient condition, the pad thickness and pad face air velocity that will give the given efficiency at the given ambient condition can be predicted.

4.2.7.2 **Pressure drop model validation**

From figure 4.20 – 4.23, the closeness of the plotted data to the straight line and the associated high correlation coefficient representing equality between the experimental and predicted illustrates the suitability of the model in describing the pressure drop of the studied pad materials. The high R^2 value of 99.6% indicates close correlation of predicted with experimental data values. It also indicated that a greater percentage of the experimental variability can be explained by the linear model of the graph. TheseR^2 - values show close correlation with pressure drop parameters.From figure 4.24, the parameters of the pressure drop when the celdek material was used had the highest linear correlation followed by the pop sponge and the last , jute fibre.

4.2.8**Summary of discussion**

4.2.8.1 **Design recommendation**

Maximum saturation efficiency may not be the optimum operating level, especially if it is obtained at the expense of large static pressure losses. As shown in figure 4.1(e), an increase in velocity from 0.5m/s to 2.5 m/s increases the saturation efficiency of Jute fibre, Coconut fibre and Pop sponge from 70.7% to 80.7%, 66.8% to 76.0% and 60.7% to 67.0% respectively, while reducing that of Celdek from 77.9% to 71.4%. But, as shown in figure 4.1(f), it also increases the pressure drop of Jute fibre, Coconut fibre, Pop sponge and Celdek from 37.2 to 94.8pa, 28.0 to 81.1pa, 17.8 to 66.1pa and 9.0 to 40.3pa respectively. This improvement in saturation efficiency is gained only through increasing the static pressure drop, substantially increasing initial and operating costs. By limiting the pressure drop a more economical suction fans can be used. Thus, an effective and

economical cooling system would be one that provided high saturation efficiency with minimal pressure drop. As shown in table 4.7, 4.12, 4.17 and 4.22, optimization options nos. 5, 4, 5 and 1 were selected for Celdek, Jute fibre, Coconut fibre and Pop sponge respectively. The chioce for their selection was based mainly on economic reasons rather than technical. The lesser the pad thickness, the lower the cost of pad material. Also, the lower the pad face air velocity and pressure drop the lower the suction fan capacity to be used and thus reducing initial and operating cost. As shown in table 4.23, Celdek has the best optimization, achieving the highest desirability of 0.904 with higher efficiency of 75.6% and lowest pressure drop of 6.3Pa. This optimum performance criteria was achieved at the lowest level of pad face air velocity, lowest level of water flow rate and pad thickness of 161mm. Jute fiber has the highest efficiency of 77.9% at a reasonable reliability of 0.789. However, this high efficiency was achieved at the highest pressure drop and relatively high pad face air velocity of 1.5m/s. This means that a high capacity suction fan will be needed which will increase both the initial and operating cost. Coconut fibre achieved a reliability of 0.748 with a reasonable high efficiency of 74.1% (but lower than that of Jute fibre). This efficiency was realized at a high pad face air velocity of 1.6m/s and high pressure drop of 28.2Pa (lower than that of Jute fibre). This will also require a high capacity suction fan to operate but will be more economical than Jute fibre. POP sponge achieved a reliability of 0.745 with low efficiency of 64.6%. This low efficiency is compensated by relatively low velocity and low pressure drop lowering the initial and operating cost. However, operating at a relatively higher pad thickness will add to the initial cost. But, from table 4.32, the result of the test for the saturation efficiency mean separation of Pop sponge padmaterial shows non-significant difference between 150mm versus 200mm. This shows that 150mm pad of POP sponge material can be used in place of 200mm pad thicknesses without compromising efficiency statistically. Hence, pad thickness may not be a limiting factor for Pop Sponge. In most agricultural buildings where high volume of cool air is needed to displace the warm indoor air, cooling pad materials that offer less resistance to the flow of air is required. In such case POP sponge may be a better option than Jute fibre and coconut fibre.

CHAPTER FIVE

CONCLUSION AND RECOMMENDATIONS

5.1 **Conclusion**

An experimental and numerical evaluation of the cooling process, saturation efficiency and pressure drop of some selected materials to be used as evaporative cooling pad were carried out in a multi-pad evaporative cooler. Also, model equations for predicting the performance criteria of the selected pad materials were carried out. A multi-pad evaporative cooler incorporated with a piece of software known as arduino micro-processor which controls and automates the overall operation of the cooling system through its relay and transducer sensors. Tests were conducted at five (5) levels of each of the three factors (Water flow rate, Pad thickness and Pad face air velocity) in order to evaluate the suitability of these selected materials as cooling pad. Appropriate models for each pad material was developed. Microsoft excel application packages, Central Composite Design in DesignExpert 6.0. statistical software and on-line Tukey's HSD test were extensively used in the analysis of data. It was observed that ambient air temperature and humidity affect the performance of evaporative cooling system. The cooling efficiency and pressure drop of the tested materials was observed to vary with variation of the treatment factors.

The following conclusions are therefore drawn from this study:

1) Arduino micro-processor can be used in the development of a multi-pad evaporative cooling system to automatically and effectively record and store basic cooling parameters with minimum human supervision, thus making the entire cooling operation automated.

(2) The pressure drops increaseswith the increase of air suction velocity, padthickness and water flow rate at significant level. The magnitude of pressure drop values for the four pads are in the order: Jute fibre> Coconut fibre> POP Sponge >Celdek.

(3) The three local pad materials can serve as an alternative pad material depending on application. In most agricultural applications that require large volume of air, saturation efficiency may not be the optimum operating condition. Pads that can offer minimum resistance to the flow of air may be considered first.

(4) The evaporative saturation efficiency increases withthe increase of pad thickness. For instance,at 1.75 l/min.water flow rate and 1.5 m/sec. Pad faceairvelocity, as the pad thickness increases from 50mm to 250mm, evaporative saturation efficiency increased from 55.1% to 77.3%, 61.8% to 80.9%, 60.5% to 77.4% and 53.1% to 67.3% for Celdek, Jute fibre, Coconut fibre and Pop Sponge respectively. No significanteffect of the water flow rate on the saturationefficiency of Celdek and Coconut fibrepads between the limits of the waterflow rates was observed in this study.

(5) The evaporative saturation efficiency increases with the increase of pad faceairvelocity for the three local pad materials and decreases slightly for Celdek pad. For instance at 1.75 l/min.water flow rate and 150mm pad thickness, as the pad face air velocity increases from 0.5 m/s to 2.5 m/s, saturation efficiency increased from 70.7% to 80.7%, 66.8% to 76.0%, and 60.7% to 67.0% for Jute fibre, Coconut fibre and POP Sponge respectively while decreases from 77.9% to 71.4% for Celdek.

(6) Saturation efficiency of the Jute fibreisconsistently greater than that of Coconut fibre which also isconsistently greater than that of POP sponge

(7) The minimum and maximum values of saturation efficiency for Celdek pad, Jute fibre, Coconut fibre and Pop Sponge were: 51.3% and 80.7%; 56.3% and 83.9% ; 54.7% and 80.6% ; 46.8% and 71.9% respectively.The experiment carried out by Al-Sulaiman gave saturation efficiency of 62.1% for jute while this study records maximum efficiency of 83.9%.This shows that jute pad can serve as an alternative cooling pad to the commercial pad.

(8) The semi-experimental models developed to predict the saturation efficiency and resistance to air flow was shown to be reliable as indicated in the validation. The model's high R^2 shows a good agreement between the predicted and experimental data and can be used to simulate the cooling behaviour of the studied pad materials.

(9)The results of the effects of the water flow rate on thesaturation efficiency of pad materials indicated thatthere is no significant effect of the water flow rate chosenin present study on the saturation efficiency of Celdek pad and Coconut fibre.Thisshows that the amount of the water flow rates chosenwere enough to thoroughly wet the two pad materials.

(10) The best combination of factors for optimum performance of the studied pad materials were found to be 1.0 l/min. water flow rate for all the pad, 0.5, 1.5, 1.6, and 1.3 m/s air flow rate and 161, 157, 157 and 184mm pad thickness for Celdek, Jute fibre, Coconut fibre and Pop Sponge respectively.

(11) For Celdek pad, 150mm pad thickness can be used in place of 200mm and 250mm pad thickness without compromising efficiency statistically. Likewise, for Jute fibre,100mm pad thickness can be used in place of 150mm and 150mm,in place of 200mm and 250mm pad thicknesses without any statistical difference in the saturation efficiency. For Coconut fibre and Pop Sponge, 50mm pad thickness can be used in place of 100mm pad thickness, 100mm in place of 150mm and also 150mm in place of 200mm and 250mm pad thicknesses without any statistical difference in their saturation efficiencies.

(12) The high R^2-values of the goodness of fit for each model was good enough to guarantee validity in predicting the cooling parameters (table 4.58 and 4.59)

(13) The minimum and maximum values of pressure drop for Celdek pad, Jute fibre, Coconut fibre and Pop Sponge were: 1.8Pa and 63.2Pa ; 8.5Pa and 150.5Pa ; 6.4Pa and 130.6Pa ; 4.2Pa and 104.7Pa respectively.

5.2 **Recommendations for Further Studies**

The following recommendations are considered for future studies:

1) Further work should be carried out to evaluate other local materials that may be suitable for evaporative cooling pad using the developed multi-pad test rig

2) The same packing density of the pad material was used for the local pads. Experiment should be carried out to determine the optimum packing density of most materials used as cooling pads. In addition, an automated means of packing to ensure uniform arrangement of the pad material should be developed.

3) An automated air conditioning system that incorporates air heaters in addition with desiccant materials should be developed and incorporated to the multi-pad cooler to simulate the ambient air before entering the cooler. This will enable the experiment to be conducted at all climatic conditions.

5.3 **Contributions to Knowledge**

This study has contributed to knowledge in the following ways:

(1)An automated multi-pad evaporative cooler testing rigwassuccessfully constructed.

(2) Models predicting the cooling behaviour of the studied pad materials(celdek pad, jute pad, coconut fibre and POP sponge) have been developed.

(3) The optimum design parameters for the studied pad materials(celdek pad, jute pad, coconut fibre and POP sponge) under the prevailing conditions have been determined

REFERENCES

Abbouda, KS & EA Almuhanna (2012). Improvement of Evaporative Cooling System Efficiency in Greenhouses. *Int. J Latest Trends Agr. Food Sci*. 2(2),83-89

Al-Amri, A.M.S. (2000). Comparative uses of greenhouse cover materials and their effectiveness in evaporative cooling in eastern province of Saudi Arabia. *Agricultural Mechanization in Asia, Africa and Latin America,*31(2), 61–66.

Ali, A. K. A., Al-Haidary, A. A. & Alshaikh, M. A. (1999). The effect of evaporative cooling in alleviating seasonal differences in milk production of Almarai dairy farms in the Kingdom of Saudi Arabia. Asia.*Journal of Animal*, 12(4): 590-600.

Alonso, J. F. S.& Martínez, F. J. R. (1998). Simulation model of an indirect evaporative cooler.*Energy and Buildings*, 29, 23-27.

Al-Sulaiman, F. (2002). Evaluation of the performance of local fibres in evaporative cooling. *Energy Conversion and Management*, 43, 2267-2273.

Amer, O., Boukhanouf, R. &Ibrahim, H. G. (2015) A Review of Evaporative Cooling Technologies. *International Journal of Environmental Science and Development,*6(2), 111-117

Amir, A. Z. & Ali, H. G. (2006). Performance improvement of gas turbine cycle by using desiccant based evaporative cooling system. *Energy Conversion and Management,* 31(14), 2652-2664.

Anyanwu, E.E. (2004). Design and measured performance of a porous evaporative cooler for preservation of fruits and vegetables. *Energy Conversion Management*, 45, 2187–2195.

ASAE(2000). American Society of Agricultural Engineers(ASAE). *Engineering Practice* 406(2), 559-566. ASAE Standards. ASAE, St. Joseph, MI. 49085.

ASHRAE (2007).*American Society of Heating, Refrigeration and Air-conditioning Engineers*.HVAC applications, in evaporative cooling applications. P.52.

Boukhanouf, R.; Alharbi, A.; Ibrahim, G.H. &Kanzari, M.(2014). Investigation of a sub-wet bulb temperature evaporative cooler for buildings. *Journal of Clean Energy Technologies*, 2(3), 221-225.

Chen, C. (2003). Prediction of longitudinal variations in temperature and relative humidity for evaporative cooling greenhouses. *Agricultural Engineering Journal*, 12 (3), 143-164.

Chukwuneke, J. L.; Ajike, C.O.; Achebe, C. H.&Okolie, P. C. (2012), A mathematical model of an evaporative cooling pad using sintered Nigerian clay. *Journal of Minerals and Materials Characterization and Engineering*, 1113-1120.

Coolerado (2006).*Coolerado HMX (Heat and Mass Exchanger) brochure*, C.Corporation. Arvada, Colorado, USA.

Dağtekin, M.; Gürdil, G.A.K., &Yıldız, Y. (1998). Determination of suitable pad material for evaporative cooling of broiler houses in Turkey. *International Conference on Agricultural Engineering*. 271- 272.

Dai, Y. J. & Sumathy, K.(2002). "Theoretical study on across-flow direct evaporative cooler using honeycomb paper as packing material. *Applied Thermal Engineering*, 22, 1417-1430.

Darwesh, M.,Abouzaher, S., Fouda, T. &Helmy, M. (2009). Effect of using pad manufactured fromagricultural residues on the performance of evaporative cooling system. *Jordan Journal of AgriculturalSciences, 5*(2), 111-125.

Delfani, S.; Esmaeelian, J. & Pasdarshahri, H. (2010). Energy saving potential of an indirect evaporative cooler as a pre-cooling unit for mechanical cooling systems in Iran. *Energy and Building*, 42, 2169-2176.

Dzivama, A.U. Bindir, U. B. & Aboaba, F. O. (1999). Evaluation of pad materials in construction of active evaporative cooler for storage of fruits and vegetables in arid environments. *Agricultural Mechanization in Asia, Africa and Latin America*, 30(3), 51–55

Elberling, L. (2006). *Laboratory evaluation of the Colorado cooler-indirect evaporative cooling unit*, Pacific Gas and Electric Company.

El-Dessouky, H.,Ettouney, H. & Al-Zeefari, A. (2004). Performance analysis of two-stage evaporative coolers. *Chemical Engineering Journal*, 102(3), 255-266.

Foster, R. E. (1995). Evaporative air conditioning technologies: Reducing energy and CFC usage nationwide, commercial applications for evaporative cooling systems, Washington State Energy Office, Spokane, Washington.

Franco, A. Valera, D.L.Madueno, A.& Pena, A. (2010).Influence of water and air flow on the performance of cellulose evaporative cooling pads used in Mediterranean greenhouse.*Transactions of the ASABE*, 53, 565-576.

Frank, B. (2011). On-site experimental testing of a novel dew point evaporative cooler. *Energy and Buildings*,43(12), 3475-3483.

Givoni, B. (1994). *Passive and Low-Energy Cooling of Buildings*. Van Nostrand Reinhold.

Groover, M. (2014). *Fundamentals of Modern Manufacturing: Materials, Processes, and Systems.*

Gunhan, T., Demir, V. & Yagciogluinitial, A.K. (2007). Evaluation of the Suitability of Some Local Materials as Cooling Pads. *Biosystems Engineering*, 96 (3),369–377

Ibrahim, E. Shao, L. & Riffat, S.B. (2003). Performance of porous ceramic evaporators for building cooling application. *Energy and Buildings*, 35(9), 941-949.

Jaber, S. & Ajib, S. (2011). Evaporative cooling as an efficient system in Mediterranean region. *Applied Thermal Engineering*, 31, 2590-2596.

Jain, D. & Tiwari, G. (2002). Modeling and optimal design of evaporative cooling system in controlled environment greenhouse. *Energy Conversion and Management*. 43, 2235–2250.

Jiang, Y. & Zhang, X.S.(2006). The research of direct evaporation cooling and its application in air-cooled chiller unit. *Building Energy and Environment*, 25(2), 7-12.

Jiang, Y. (2008).*Chinese building energy consumption situation and energy efficiency strategy*. New Architecture (in Chinese).

Kittas, C; Bartzanas, T. & Jaffrin, A. (2001). Greenhouse evaporative cooling: measurement and data analysis. *Transactions of the ASAE*, 44(3), 683–689.

Kittas, C.; Bartzanas, T. & Jaffarin, A. (2003). Temperature gradients in a partially shaded large greenhouse equipped with evaporative cooling pads. *Bio-systems Engineering*, 85(1), 87-94.

Koca, R.W. Hughes, W.C. & Christianson, L.L. (1991). Evaporative cooling pads: test, procedure and evaluation. *Applied Engineering in Agriculture*, 7(4), 485–490.

Luis, P.L. Jose, O. & Christine, P. (2008). A review on buildings energy consumption information. *Energy and Buildings*, 40(3), 394–398.

Maheshwari, G.P.; Al-Ragom, F. & Suri, R.K. (2001). Energy-saving potential of an indirect evaporative cooler. *Applied Energy*, 69(1), 69–76.

Maisotsenko, V. & Reyzin, I. (2005). The Maisotsenko cycle for electronics cooling. Proceedings of the ASME/Pacific Rim Technical Conference and Exhibition on Integration and Packaging of MEMS, NEMS, and Electronic Systems: Advances in Electronic Packaging, San Francisco, CA, U.S., Pp. 415–424.

Maisotsenko V, G.L., Heaton,T.L.&Gillan, A.D.(2003).Method and plate apparatus for dew pointevaporativecoolerUnited States.

Mekonnen, A. (1996). Effectiveness study of local materials as cooling media for shelters in hot climates. *Agricultural Mechanization in Asia, Africa and Latin America*, 27(2), 64–66.

Muazu, M. (2008).Novel evaporative cooling systemsfor building applications. The University of Nottingham: Nottingham.

Navon, R. & Arkin, H. (1994). Feasibility of direct-indirect evaporative cooling for residences, based on studies with a desert cooler.*Building and Environment*, 29, 393-399.

Ndukwu, M. C. (2011). Development of clay evaporative cooler for fruits and vegetables preservation.*Agricultural Engineering International: CIGR E-Journal,* 13(1), 1-8.

Odesola, I.F. &Onyebuchi, O. (2009). A review of porous evaporative cooling for the preservation of fruits and vegetables. *Pacific Journal of Science Technology*, 10, 935-941.

Ozturk, H.H. (2003). Evaporative cooling efficiency of a fogging system for greenhouses. *Turkish Journal of Agriculture and Forestry*, 27(1), 49–57.

Pérez-Lombard, L. Ortiz, J. & Pout, C. (2008). A review on buildings energy consumption information. *Energy and Buildings*, 40, 394-398.

Rajan, C., Megala, B., Nandhini, A and Rasi, C. (2015). A Review: Comparative Analysis of Arduino Micro Controllers in Robotic Car. *International Journal of Mechanical, Aerospace, Industrial and Mechatronics Engineering*, 9 (2), 365-374.

Renewable-energy-graphical. Retrieved from http://mechanicalinventions. /renewableenergy-sources-graphical.html (December, 2018).

Schiano-Phan, R. (2009). The use of porous ceramic for passiveevaporative cooling in buildings.Retrievedfrom:http://www.phdc.eu/Cooling_with_poro-us_ceramic_on may, 2013.

Sethi, V. P. & S. K. Sharma. (2007a). Survey of cooling technologies for worldwide agricultural greenhouse applications. *Solar Energy*, 81(12), 1447-1459.

Sreeram, V. (2014). Factors affecting the performance characteristics of wet Cooling pads for data center applications. Retrieved From:https://uta-ir.tdl.org/uta-ir/bitstream/handle/Sreeram_uta_2502M_12973.pdf?sequence=1 (Accessed 28th May, 2016).

Steeman, M.;Janssens, A. & Paepe, M.D. (2009).Performance evaluation of indirectevaporative cooling using whole-building hygrothermal simulations. *Applied ThermalEngineering*, (2914-15),2870-2875.

Susan, D. S. & Durward S. (1995). G95-1264 Storing fresh fruits and vegetables. Historical materials from University of Nebraska-Lincoln Extension. Retrieved February, 2017 from the WWW: http://digital commons.unl.edu/extensionhist/1042/.

Tilahun, S.W. (2010). Feasibility and economic evaluation of low-cost evaporative cooling system in fruit and vegetables storage. *African Journal of Food, Agriculture, Nutrition and Development*, 10(8), 2984-2997.

Tinoco, I.F., Figueiredo, J.L., Santos, R.C.; Silva, J.N.; Yanagi, T., Paul, M.O., Puglisi, N.L.; Vigoderis, R.B. & Corderio, M.B. (2001). *Comparison of the cooling effect of different materials used in evaporative pads*. Campinas, Brazil, Pp. 438-442.

Tulsidasani, T. R.; Sawhney, R. L.; Singh, S. P. & Sodha,M. S. (1997). Recent research on an indirect evaporative cooler (IEC) part 2: Thermal performance of a non-conditioned building coupled with an IEC. *International Journal of Energy Research*, 21, 1203-1214.

Ug˘urlu, N & Kara, M. (2000). The cooling performance of wet pads and their effect on reduction of the inside temperature a cage house. *Turkish Journal of Agriculture and Forestry*, 24(1), 79–86.

Velasco, G.E.; Martínez,F.J. R. & González,A. T. (2010).Experimentalcharacterization of the operation and comparative study of two semi-indirectevaporative systems. *Applied Thermal Engineering*,30(11-12),1447-1454.

Vivek, W. K. (2011). Experimental investigation of desert cooler performance using four different cooling pad materials. *American Journal of Scientific and Industrial Research*, 2(3), 418-421.

Wasim, S.; Frank, B. & Steven, T. (2010). Technical research on evaporative air conditioners and feasibility of rating their energy performance. *A Report Prepared For Southern Australian Department of Transport Energy and Infrastructure*.

You, S. J., Zhang, H., Liu, Y.H. & Sun, Z.Q. (1999). Performance of the direct evaporative air humidifier/cooler with aluminum packing and its use in air-cooled chiller units. *HVAC*, 25(5), 41–43.

Zabeltitz, C. V. (2002). Ventilation and cooling of Greenhouses in Hot Arid Climate Presented at Second Protected Agriculture Regional Technical Coordination Meeting, Kuwait.

Zhiyin, D., Changhong, Z., Xingxing, Z., Mahmud, M., Xudong, Z., Behrang, A. & Ala, H. (2012). Indirect evaporative cooling: Past, present and future potentials. *Renewable and Sustainable Energy Reviews*, 6823-6850.

APPENDICES

Appendix 4.1 average values of ambient temperature, cooler temperature, saturation efficiency and pressure drop for 50mm pad thickness

PAD THICK-NESS (mm)	WATER FLOW RATE (L/min)	AIR FLOW RATE (m/s)	AMBIENT TEMP.T (^{0}C)		COOLER TEMP. T_C (^{0}C)				SAT. EFFICIENCY η_{sat} (%)				PRESSURE DROP ΔP (pa)			
			T_{db}	T_{wb}	CE	JU	CO	SP	CE	JU	CO	SP	CE	JU	CO	SP
50	1.0	0.5	34.3	24.1	28.2	28.6	28.1	29.2	60.2	56.3	54.7	46.8	1.4	6.5	4.9	3.2
		1.0	33.4	23.4	27.7	27.5	27.3	28.3	56.9	57.4	55.1	48.2	2.5	11	7.8	5.5
		1.5	35.0	24.6	29.3	28.6	28.8	29.7	54.4	61.3	59.5	50.8	4.1	17.6	12.5	9.4
		2.0	34.2	24.0	28.8	27.8	27.8	28.8	52.6	63.1	62.3	53.1	6.8	26.4	20	15.5
		2.5	35.5	24.8	30.0	28.9	28.7	29.5	51.4	62.0	63.9	55.7	11.1	37	29	24
	1.25	0.5	34.8	23.9	28.2	28.6	28.9	29.4	60.9	56.8	55.1	49.2	2.2	10.1	7.6	5.0
		1.0	32.9	23.6	27.5	27.3	27.5	28.2	57.3	59.9	57.6	50.8	3.9	16.1	12.1	8.5
		1.5	34.7	23.6	28.6	27.8	28.1	28.8	54.8	61.9	59.8	52.9	6.2	24.6	18.1	12.8
		2.0	35.2	24.6	29.6	28.5	28.6	29.3	52.8	63.2	62.5	55.7	10.2	34.8	28	21.7
		2.5	32.5	23.5	27.9	26.8	26.9	27.5	51.3	63.7	62.7	56.1	14.3	46.6	37.7	31.2
	1.50	0.5	34.7	23.6	27.9	28.4	28.5	29.2	61.3	56.9	55.6	49.9	3.4	15.7	11.8	7.5
		1.0	33.8	23.1	27.7	27.3	27.6	28.3	57.4	60.3	58.1	51.2	6.1	23.9	18.8	13.2
		1.5	34.2	24.0	28.6	27.9	28.0	28.8	55.0	61.9	60.3	52.9	9.3	34.9	27.2	19.2
		2.0	32.8	23.4	27.8	26.3	26.4	27.1	53.0	63.5	62.8	56.1	15.3	47.7	39.2	30.4
		2.5	33.3	23.6	28.3	27.1	27.3	27.9	51.7	63.7	62.1	55.9	20	58.6	48.7	38.9
	1.75	0.5	34.1	24.3	28.1	28.5	28.6	29.2	61.5	56.9	55.8	50.2	5.3	22	16.5	10.5
		1.0	33.0	23.6	27.6	27.3	27.5	28.2	57.8	60.6	58.6	51.3	9.5	31.5	26.3	18.5
		1.5	35.0	24.5	29.2	28.5	28.6	29.4	55.1	61.8	60.5	53.1	13.9	42.4	35.4	25
		2.0	34.3	24.1	28.9	27.8	27.9	28.5	53.1	63.8	61.2	56.7	22.9	57.6	49	36
		2.5	35.1	24.2	29.4	28.1	28.2	28.9	52.3	63.9	61.7	57.0	28	68.7	58.8	45.8
	2.00	0.5	35.5	24.8	28.9	29.4	29.5	30.1	61.9	57.1	56.0	50.1	7.4	28.6	23.1	14.7
		1.0	32.5	23.5	27.3	27.1	27.2	27.9	57.9	60.5	58.9	51.4	13.3	40.9	34.2	24.1
		1.5	36.0	24.0	29.3	28.6	28.7	29.6	55.6	62.0	61.0	53.6	18.1	53	42.5	30
		2.0	33.3	23.6	28.1	27.1	27.1	27.9	53.3	64.1	63.8	56.0	27.5	69.1	56.4	41
		2.5	34.1	24.4	29.0	27.9	27.9	28.6	52.9	64.1	63.9	57.2	33.6	79	67.6	52.7

T_{db}= Dry bulb temp. T_{wb}= Wet bulb temp; CE= Celdek; JU= Jute; CO= Coconut; SP = Sponge

Appendix 4.2 average values of ambient temperature, cooler temperature, saturation efficiency and pressure drop for 100mm pad thickness

PAD THICK-NESS (mm)	WATER FLOW RATE (L/min)	AIR FLOW RATE (m/s)	AMBIENT TEMP.T (^{0}C)		COOLER TEMP. T_C (^{0}C)				SAT. EFFICIENCY η_{sat} (%)				PRESSURE DROP ΔP (pa)			
			T_{db}	T_{wb}	CE	JU	CO	SP	CE	JU	CO	SP	CE	JU	CO	SP
100	1.0	0.5	32.5	23.6	26.3	27.0	27.1	27.8	69.8	62.1	60.2	52.5	1.8	8.5	6.4	4.2
		1.0	33.0	23.6	26.6	26.7	27.1	27.9	68.1	66.5	62.8	54.1	3.1	13.8	9.8	6.9
		1.5	34.1	24.4	27.7	2737	27.7	28.6	65.5	69.7	65.6	56.5	4.9	21.1	15	11.3
		2.0	34.7	23.5	27.6	26.8	27.1	28.2	63.8	70.1	67.9	58.3	8.2	31.7	24	18.6
		2.5	35.5	24.8	28.8	28.0	28.2	29.2	62.9	70.3	68.4	58.9	13.3	44.4	34.8	28.8
	1.25	0.5	32.8	23.4	26.2	26.8	27.1	27.6	70.7	64.3	60.7	54.9	2.9	13.1	9.9	6.5
		1.0	33.5	23.4	26.6	26.8	27.0	27.8	68.4	66.8	63.9	56.7	4.9	20.1	15.1	10.6
		1.5	34.0	24.3	27.6	27.2	27.5	28.4	65.8	70.1	67.0	58.1	7.4	29.5	21.7	15.4
		2.0	35.1	24.3	28.2	27.4	27.7	28.5	64.3	71.7	68.9	60.9	12.2	41.8	33.6	26
		2.5	36.0	24.0	28.3	27.4	27.7	28.6	63.8	71.9	69.2	62.0	17.2	55.9	45.2	37.4
	1.50	0.5	34.2	23.8	26.8	27.6	27.9	28.6	71.2	63.8	60.8	54.2	4.4	20.4	15.3	9.8
		1.0	34.8	23.8	27.3	27.4	27.8	28.5	68.5	66.9	63.3	56.9	7.6	29.9	23.5	16.5
		1.5	35.1	24.2	27.9	27.4	27.9	28.7	66.3	70.8	66.2	58.6	11.2	41.9	32.4	23.1
		2.0	33.5	23.4	27.0	26.1	26.5	27.3	64.8	72.9	69.3	61.3	18.4	57.2	47.1	36.5
		2.5	33.0	23.6	27.0	26.1	26.6	27.2	63.5	73.0	68.3	61.7	24.1	67.4	56.1	44.7
	1.75	0.5	34.0	24.3	27.0	27.8	28.1	28.8	71.8	63.7	60.7	54.1	6.9	28.6	21.5	13.7
		1.0	34.5	24.2	27.4	27.6	28.0	28.6	68.9	67.2	63.5	56.9	11.9	39.4	32.9	23.1
		1.5	34.2	23.8	27.3	26.8	27.4	28.1	66.3	71.3	65.7	58.9	16.7	50.9	42.5	30.2
		2.0	32.5	23.5	26.7	25.9	26.4	27.0	64.5	73.1	67.8	61.5	27.5	69.1	58.8	43.7
		2.5	36.0	24.0	28.3	27.1	27.8	28.6	63.9	74.3	68.5	61.3	33.6	79	67.6	53.8
	2.00	0.5	34.2	23.8	26.7	27.6	27.9	28.4	71.9	63.9	61.0	55.3	9.6	37.2	30.1	19.1
		1.0	33.0	23.6	26.5	26.7	27.0	27.6	69.0	67.5	64.1	57.1	16.6	49.1	40.8	28.1
		1.5	36.0	24.0	28.0	27.4	28.1	28.9	66.8	71.5	66.1	59.1	21.7	63.6	51	36.1
		2.0	34.2	23.8	27.4	26.6	27.2	27.8	65.7	73.3	67.5	61.8	33.1	80.9	67.7	50.2
		2.5	35.5	24.8	28.6	27.7	28.3	28.9	64.9	73.2	67.6	61.8	38.6	90.9	77.7	63.2

T_{db}= Dry bulb temp. T_{wb}= Wet bulb temp; CE= Celdek; JU= Jute; CO= Coconut; SP = Sponge

Appendix 4.3 average values of ambient temperature, cooler temperature, saturation efficiency and pressure drop for 150mm pad thickness

PAD THICK-NESS (mm)	WATER FLOW RATE (L/min)	AIR FLOW RATE (m/s)	AMBIENT TEMP.T (^{0}C)		COOLER TEMP. T_C (^{0}C)				SAT. EFFICIENCY η_{sat} (%)				PRESSURE DROP ΔP (pa)			
			T_{db}	T_{wb}	CE	JU	CO	SP	CE	JU	CO	SP	CE	JU	CO	SP
150	1.0	0.5	33.5	23.2	25.7	26.3	26.7	27.4	76.2	69.6	66.3	59.1	2.3	11.1	8.3	5.5
		1.0	34.0	23.1	26.0	26.1	26.6	27.4	73.8	72.6	68.3	60.8	3.9	17.3	12.3	8.6
		1.5	34.5	24.2	27.1	26.6	27.0	27.8	72.1	76.9	73.3	64.8	5.9	25.3	18.1	13.6
		2.0	34.6	23.6	26.8	25.8	26.3	27.4	70.9	80.3	75.8	65.1	9.8	38.1	28.8	22.3
		2.5	34.8	24.5	27.6	26.5	26.9	28.1	69.7	80.5	77.0	65.4	16	53.3	41.8	34.6
	1.25	0.5	35.2	24.0	26.6	27.3	27.8	28.5	76.9	70.3	66.1	59.6	3.8	17	12.9	8.5
		1.0	34.9	23.8	26.7	26.8	27.3	28.0	73.9	73.1	68.9	61.9	6.1	25.1	18.9	13.3
		1.5	34.4	23.5	26.5	26.0	26.5	27.5	72.6	77.5	72.7	63.3	8.9	35.4	26.1	18.5
		2.0	35.0	23.5	26.8	26.0	26.2	27.4	71.5	78.3	76.3	65.8	14.6	50.2	40.3	31.2
		2.5	36.0	24.0	27.6	26.5	27.0	28.1	70.3	78.9	75.8	66.1	20.6	67.1	54.2	44.9
	1.50	0.5	35.6	23.8	26.5	27.2	27.8	28.5	77.3	70.9	66.3	60.1	5.7	26.5	19.9	12.7
		1.0	36.0	24.0	27.0	27.1	27.6	28.5	74.6	73.8	70.0	62.5	9.5	37.4	29.4	20.6
		1.5	34.8	24.5	27.3	26.7	27.2	28.2	72.9	78.6	73.9	63.8	13.4	50.3	38.9	27.7
		2.0	35.5	24.8	27.8	26.8	27.3	28.4	72.1	81.2	76.5	66.2	22.1	68.6	56.5	43.8
		2.5	34.0	24.3	27.1	26.1	26.5	27.5	71.5	81.3	77.0	66.5	28.9	80.9	67.3	53.6
	1.75	0.5	33.3	23.6	25.7	26.4	26.8	27.4	77.9	70.7	66.8	60.7	9	37.2	28	17.8
		1.0	33.0	23.7	26.0	26.1	26.5	27.2	74.8	73.8	69.6	62.8	14.9	49.3	41.1	28.9
		1.5	32.5	23.3	25.8	25.3	25.9	26.6	73.3	78.0	72.1	63.9	20	61.1	51.1	36.2
		2.0	32.8	23.3	25.9	25.2	25.6	26.5	72.6	80.3	75.6	66.8	31.1	82.9	70.6	52.8
		2.5	36.0	24.0	27.4	26.3	26.9	28.0	71.4	80.7	76.0	67.0	40.3	94.8	81.1	66.1
	2.00	0.5	34.0	24.3	26.4	27.1	27.5	28.1	78.1	71.0	67.1	60.9	12.5	48.4	39.1	24.8
		1.0	33.0	23.6	25.9	26.1	26.3	27.1	75.1	73.9	70.9	63.1	20.8	61.4	51	35.1
		1.5	36.0	24.0	27.2	26.6	27.3	28.1	73.5	78.1	72.3	65.8	26	76.3	61.2	43.3
		2.0	34.0	24.3	26.9	26.2	26.7	27.5	72.9	80.5	74.9	67.1	39.7	97.1	81.2	60.2
		2.5	35.5	24.8	27.9	26.9	27.5	28.3	71.2	80.7	75.2	67.3	46.3	109.1	93.2	75.8

T_{db}= Dry bulb temp. T_{wb}= Wet bulb temp; CE= Celdek; JU= Jute; CO= Coconut; SP = Sponge

Appendix 4.4 Average values of ambient temperature, cooler temperature, saturation efficiency and pressure drop for 200mm pad thickness

PAD THICK-NESS (mm)	WATER FLOW RATE (L/min)	AIR FLOW RATE (m/s)	AMBIENT TEMP.T (^{0}C)		COOLER TEMP. T_C (^{0}C)				SAT. EFFICIENCY η_{sat} (%)				PRESSURE DROP ΔP (pa)			
			T_{db}	T_{wb}	CE	JU	CO	SP	CE	JU	CO	SP	CE	JU	CO	SP
200	1.0	0.5	34.5	24.2	26.3	27.0	27.4	28.0	80.0	72.6	69.0	63.0	3	14.4	10.8	7.2
		1.0	35.2	24.0	26.5	26.9	27.1	28.1	77.8	74.5	72.1	63.2	4.9	21.6	15.4	10.8
		1.5	33.5	23.4	25.8	25.2	25.8	26.5	76.3	81.7	76.6	65.7	7.1	30.4	21.7	16.3
		2.0	36.0	24.0	26.9	25.9	26.4	27.8	75.8	83.9	79.9	68.0	11.8	45.7	34.6	26.8
		2.5	35.5	24.8	27.4	26.7	27.0	28.1	75.4	82.7	79.6	68.7	19.2	64	50.2	41.4
	1.25	0.5	34.9	23.8	26.0	26.8	27.2	28.0	80.4	73.0	69.3	62.1	4.9	22.1	16.8	11.1
		1.0	33.5	23.4	25.6	25.9	26.3	27.1	78.1	75.7	71.3	63.4	7.6	31.4	23.6	16.6
		1.5	32.8	23.4	25.6	25.3	25.7	26.5	76.9	79.5	75.2	66.7	10.7	42.5	31.3	22.2
		2.0	34.0	23.1	25.7	25.1	25.4	26.5	76.2	81.3	79.0	68.9	17.5	60.2	48.4	37.4
		2.5	35.1	24.2	26.9	26.1	26.4	27.5	74.9	82.7	79.6	69.3	24.7	80.5	65.1	53.9
	1.50	0.5	33.5	23.4	25.4	26.1	26.5	27.2	80.6	73.6	68.9	62.7	7.4	34.4	25.9	16.5
		1.0	34.8	23.8	26.2	26.4	26.7	27.8	78.5	76.1	73.2	63.9	11.9	46.8	36.8	25.8
		1.5	34.6	23.6	26.1	25.7	26.1	27.4	77.1	81.1	77.3	65.7	16.1	60.4	46.7	33.2
		2.0	34.2	23.8	26.2	25.5	25.9	27.1	76.7	83.5	80.1	68.2	26.5	82.3	67.8	52.6
		2.5	35.6	23.8	26.6	25.7	26.2	27.5	76.2	83.7	79.8	68.5	34.7	97.1	80.8	64.3
	1.75	0.5	32.5	23.5	25.2	25.9	26.3	26.8	80.7	72.9	69.2	62.9	11.7	48.4	36.4	23.1
		1.0	35.5	24.8	27.0	27.3	27.7	28.4	79.1	76.9	72.6	65.9	18.6	61.6	49.3	36.1
		1.5	34.4	23.5	26.0	25.4	26.1	27.2	77.5	82.5	76.3	66.2	24	73.3	61.3	43.4
		2.0	32.8	23.4	25.6	25.0	25.3	26.2	77.1	82.6	80.3	70.7	37.3	99.5	84.7	63.4
		2.5	34.9	23.8	26.4	25.8	26.0	27.1	76.7	81.7	79.9	70.1	48.4	113.8	97.3	79.3
	2.00	0.5	34.2	23.8	25.8	26.6	26.9	27.6	80.7	73.0	70.0	63.1	16.3	62.9	48.9	32.2
		1.0	34.8	24.5	26.7	26.9	27.3	28.1	78.5	77.1	72.9	65.4	26	76.8	63.8	43.9
		1.5	36.0	24.0	26.7	26.2	26.8	27.7	77.2	81.7	76.9	68.8	31.2	91.6	73.4	52
		2.0	34.2	23.8	26.2	25.6	25.8	26.9	77.4	83.5	80.4	70.5	47.6	116.5	97.4	72.2
		2.5	33.0	23.6	25.8	25.2	25.5	26.4	76.9	83.0	79.8	70.3	55.6	130.9	111.8	91

T_{db}= Dry bulb temp. T_{wb}= Wet bulb temp; CE= Celdek; JU= Jute; CO= Coconut; SP = Sponge

Appendix 4. 5 Average values of ambient temperature, cooler temperature, saturation efficiency and pressure drop for 250mm pad thickness

PAD THICK-NESS (mm)	WATER FLOW RATE (L/min)	AIR FLOW RATE (m/s)	AMBIENT TEMP.T (^{0}C)		COOLER TEMP. T_C (^{0}C)				SAT. EFFICIENCY η_{sat} (%)				PRESSURE DROP ΔP (pa)			
			T_{db}	T_{wb}	CE	JU	CO	SP	CE	JU	CO	SP	CE	JU	CO	SP
250	1.0	0.5	36.0	24.0	26.5	27.2	27.6	28.4	79.2	73.2	69.8	63.5	3.9	18.7	14.1	9.4
		1.0	35.6	23.8	26.5	26.7	27.1	27.8	77.5	75.5	72.0	65.7	6.1	27.1	19.3	13.5
		1.5	34.1	24.4	26.1	26.4	26.7	27.4	76.3	79.6	76.1	68.9	8.5	36.5	26.1	19.6
		2.0	33.0	23.6	25.8	25.3	25.5	26.3	76.1	81.8	79.7	71.1	14.2	54.8	41.5	32.2
		2.5	32.8	23.4	25.7	25.1	25.3	26.1	75.8	82.2	80.1	70.8	23.1	76.8	60.2	49.7
	1.25	0.5	34.8	23.8	26.1	26.7	27.1	27.8	79.5	73.9	70.0	63.3	6.4	28.7	21.8	14.3
		1.0	34.9	23.8	26.3	26.5	26.9	27.6	77.6	76.0	72.3	65.9	9.5	39.3	29.5	20.8
		1.5	32.5	23.6	25.7	25.4	25.6	26.3	76.8	80.1	77.0	69.3	12.8	51.1	37.6	26.6
		2.0	35.5	24.8	27.3	26.7	27.0	27.9	76.3	82.3	79.7	70.9	21.1	72.2	58.1	44.9
		2.5	34.8	23.8	26.5	25.7	25.9	26.8	75.6	82.3	80.5	71.2	29.6	96.6	78.1	64.9
	1.50	0.5	34.6	23.6	25.9	26.5	27.0	27.6	79.5	73.9	69.1	63.2	9.6	44.7	33.7	21.5
		1.0	35.1	24.2	26.6	26.8	27.1	27.9	77.9	76.5	73.5	66.2	14.9	58.5	46.1	32.3
		1.5	32.5	23.5	25.6	25.2	25.6	26.5	76.9	80.7	77.1	67.2	19.3	72.5	56.1	39.8
		2.0	34.0	24.3	26.7	26.0	26.3	27.3	75.4	82.1	79.1	68.6	31.8	98.8	81.4	63.1
		2.5	34.6	23.6	26.2	25.5	25.8	27.0	76.0	82.6	80.3	71.5	41.6	116.5	97	77.2
	1.75	0.5	36.0	24.0	26.4	27.2	27.5	28.4	79.8	73.5	70.8	63.4	15.2	62.9	47.3	30.1
		1.0	35.5	24.8	27.1	27.2	27.7	28.4	78.6	77.2	73.3	66.5	23.3	77	61.6	45.1
		1.5	34.1	24.4	26.6	26.3	26.6	27.6	77.3	80.9	77.4	67.3	28.8	90.1	73.6	52.1
		2.0	32.5	23.3	25.5	24.9	25.2	26.1	76.1	82.5	79.5	69.3	44.8	119.4	101.6	76.1
		2.5	33.3	23.6	25.9	25.3	25.5	26.4	76.3	82.3	80.3	71.6	58.1	136.6	116.8	95.2
	2.00	0.5	32.5	23.5	25.3	25.9	26.1	26.8	80.2	73.6	70.9	63.6	21.2	75.5	58.7	38.6
		1.0	35.2	24.0	26.4	26.5	26.9	27.7	78.6	78.1	73.8	66.9	32.5	92.2	76.6	50.7
		1.5	34.9	23.8	26.3	25.9	26.4	27.4	77.6	81.0	76.8	67.8	40.7	109.9	88.1	62.4
		2.0	36.0	24.0	26.8	26.1	26.3	27.7	76.5	82.8	81.0	69.5	51.1	133.9	109.1	83.1
		2.5	34.8	24.5	26.8	26.4	26.5	27.4	77.2	82.0	80.6	71.9	63.2	150.5	130.6	104.7

T_{db}= Dry bulb temp. T_{wb}= Wet bulb temp; CE= Celdek; JU= Jute; CO= Coconut; SP = Sponge

Appendix 4.6 Average Values of Saturation Efficiency And Pressure Drop For Various Pad Materials at 1.0 L/Min Pad Water Flow Rate .

Water Flow Rate:		1.0 l/min							
Pad Thick-ness (mm)	Pad Face Air Velocity (m/sec.)	SATURATION EFFICIENCY				PRESSURE DROP			
		CELDEK	JUTE FIBER	COCONUT FIBER	POP SPONGE	CELDEK	JUTE FIBER	COCONUT FIBER	POP SPONGE
50	0.5	60.2	56.3	54.7	46.8	1.4	6.5	4.9	3.2
	1.0	56.9	57.4	55.1	48.2	2.5	11	7.8	5.5
	1.5	54.4	61.3	59.5	50.8	4.1	17.6	12.5	9.4
	2.0	52.6	63.1	62.3	53.1	6.8	26.4	20	15.5
	2.5	51.4	62.0	63.9	55.7	11.1	37	29	24
100	0.5	69.8	62.1	60.2	52.5	1.8	8.5	6.4	4.2
	1.0	68.1	66.5	62.8	54.1	3.1	13.8	9.8	6.9
	1.5	65.5	69.7	65.6	56.5	4.9	21.1	15	11.3
	2.0	63.8	70.1	67.9	58.3	8.2	31.7	24	18.6
	2.5	62.9	70.3	68.4	58.9	13.3	44.4	34.8	28.8
150	0.5	76.2	69.6	66.3	59.1	2.3	11.1	8.3	5.5
	1.0	73.8	72.6	68.3	60.8	3.9	17.3	12.3	8.6
	1.5	72.1	76.9	73.3	64.8	5.9	25.3	18.1	13.6
	2.0	70.9	80.3	75.8	65.1	9.8	38.1	28.8	22.3
	2.5	69.7	80.5	77.0	65.4	16	53.3	41.8	34.6
200	0.5	80.0	72.6	69.0	63.0	3	14.4	10.8	7.2
	1.0	77.8	74.5	72.1	63.2	4.9	21.6	15.4	10.8
	1.5	76.3	81.7	76.6	65.7	7.1	30.4	21.7	16.3
	2.0	75.8	83.9	79.9	68.0	11.8	45.7	34.6	26.8
	2.5	75.4	82.7	79.6	68.7	19.2	64	50.2	41.4
250	0.5	79.2	73.2	69.8	63.5	3.9	18.7	14.1	9.4
	1.0	77.5	75.5	72.0	65.7	6.1	27.1	19.3	13.5
	1.5	76.3	79.6	76.1	68.9	8.5	36.5	26.1	19.6
	2.0	76.1	81.8	79.7	71.1	14.2	54.8	41.5	32.2
	2.5	75.8	82.2	80.1	70.8	23.1	76.8	60.2	49.7

Appendix 4.7 Average Values of Saturation Efficiency And Pressure Drop For Various Pad Materials at 1.25 L/Min Pad Water Flow Rate .

Water Flow Rate:		1.25 l/min							
Pad Thick-ness (mm)	Pad Face Air Velocity (m/sec.)	SATURATION EFFICIENCY				PRESSURE DROP			
		CELDEK	JUTE FIBER	COCONUT FIBER	POP SPONGE	CELDEK	JUTE FIBER	COCONUT FIBER	POP SPONGE
50	0.5	60.9	56.8	55.1	49.2	2.2	10.1	7.6	5.0
	1.0	57.3	59.9	57.6	50.8	3.9	16.1	12.1	8.5
	1.5	54.8	61.9	59.8	52.9	6.2	24.6	18.1	12.8
	2.0	52.8	63.2	62.5	55.7	10.2	34.8	28	21.7
	2.5	51.3	63.7	62.7	56.1	14.3	46.6	37.7	31.2
100	0.5	70.7	64.3	60.7	54.9	2.9	13.1	9.9	6.5
	1.0	68.4	66.8	63.9	56.7	4.9	20.1	15.1	10.6
	1.5	65.8	70.1	67.0	58.1	7.4	29.5	21.7	15.4
	2.0	64.3	71.7	68.9	60.9	12.2	41.8	33.6	26
	2.5	63.8	71.9	69.2	62.0	17.2	55.9	45.2	37.4
150	0.5	76.9	70.3	66.1	59.6	3.8	17	12.9	8.5
	1.0	73.9	73.1	68.9	61.9	6.1	25.1	18.9	13.3
	1.5	72.6	77.5	72.7	63.3	8.9	35.4	26.1	18.5
	2.0	71.5	78.3	76.3	65.8	14.6	50.2	40.3	31.2
	2.5	70.3	78.9	75.8	66.1	20.6	67.1	54.2	44.9
200	0.5	80.4	73.0	69.3	62.1	4.9	22.1	16.8	11.1
	1.0	78.1	75.7	71.3	63.4	7.6	31.4	23.6	16.6
	1.5	76.9	79.5	75.2	66.7	10.7	42.5	31.3	22.2
	2.0	76.2	81.3	79.0	68.9	17.5	60.2	48.4	37.4
	2.5	74.9	82.7	79.6	69.3	24.7	80.5	65.1	53.9
250	0.5	79.5	73.9	70.0	63.3	6.4	28.7	21.8	14.3
	1.0	77.6	76.0	72.3	65.9	9.5	39.3	29.5	20.8
	1.5	76.8	80.1	77.0	69.3	12.8	51.1	37.6	26.6
	2.0	76.3	82.3	79.7	70.9	21.1	72.2	58.1	44.9
	2.5	75.6	82.3	80.5	71.2	29.6	96.6	78.1	64.9

Appendix 4.8 Average Values of Saturation Efficiency And Pressure Drop For Various Pad Materials at 1.5 L/Min Pad Water Flow Rate .

Water Flow Rate:		1.5 l/min							
Pad Thick-ness (mm)	Pad Face Air Velocity (m/sec.)	SATURATION EFFICIENCY				PRESSURE DROP			
		CELDEK	JUTE FIBER	COCONUT FIBER	POP SPONGE	CELDEK	JUTE FIBER	COCONUT FIBER	POP SPONGE
50	0.5	61.3	56.9	55.6	49.9	3.4	15.7	11.8	7.5
	1.0	57.4	60.3	58.1	51.2	6.1	23.9	18.8	13.2
	1.5	55.0	61.9	60.3	52.9	9.3	34.9	27.2	19.2
	2.0	53.0	63.5	62.8	56.1	15.3	47.7	39.2	30.4
	2.5	51.7	63.7	62.1	55.9	20	58.6	48.7	38.9
100	0.5	71.2	63.8	60.8	54.2	4.4	20.4	15.3	9.8
	1.0	68.5	66.9	63.3	56.9	7.6	29.9	23.5	16.5
	1.5	66.3	70.8	66.2	58.6	11.2	41.9	32.4	23.1
	2.0	64.8	72.9	69.3	61.3	18.4	57.2	47.1	36.5
	2.5	63.5	73.0	68.3	61.7	24.1	67.4	56.1	44.7
150	0.5	77.3	70.9	66.3	60.1	5.7	26.5	19.9	12.7
	1.0	74.6	73.8	70.0	62.5	9.5	37.4	29.4	20.6
	1.5	72.9	78.6	73.9	63.8	13.4	50.3	38.9	27.7
	2.0	72.1	81.2	76.5	66.2	22.1	68.6	56.5	43.8
	2.5	71.5	81.3	77.0	66.5	28.9	80.9	67.3	53.6
200	0.5	80.6	73.6	68.9	62.7	7.4	34.4	25.9	16.5
	1.0	78.5	76.1	73.2	63.9	11.9	46.8	36.8	25.8
	1.5	77.1	81.1	77.3	65.7	16.1	60.4	46.7	33.2
	2.0	76.7	83.5	80.1	68.2	26.5	82.3	67.8	52.6
	2.5	76.2	83.7	79.8	68.5	34.7	97.1	80.8	64.3
250	0.5	79.5	73.9	69.1	63.2	9.6	44.7	33.7	21.5
	1.0	77.9	76.5	73.5	66.2	14.9	58.5	46.1	32.3
	1.5	76.9	80.7	77.1	67.2	19.3	72.5	56.1	39.8
	2.0	75.4	82.1	79.1	68.6	31.8	98.8	81.4	63.1
	2.5	76.0	82.6	80.3	71.5	41.6	116.5	97	77.2

Appendix 4.9 Average Values of Saturation Efficiency And Pressure Drop For Various Pad Materials at 2.0 L/Min Pad Water Flow Rate .

Water Flow Rate:		2.0 l/min							
Pad Thick-ness (mm)	Pad Face Air Velocity (m/sec.)	SATURATION EFFICIENCY				PRESSURE DROP			
		CELDEK	JUTE FIBER	COCONUT FIBER	POP SPONGE	CELDEK	JUTE FIBER	COCONUT FIBER	POP SPONGE
50	0.5	61.9	57.1	56.0	50.1	7.4	28.6	23.1	14.7
	1.0	57.9	60.5	58.9	51.4	13.3	40.9	34.2	24.1
	1.5	55.6	62.0	61.0	53.6	18.1	53	42.5	30
	2.0	53.3	64.1	63.8	56.0	27.5	69.1	56.4	41
	2.5	52.9	64.1	63.9	57.2	33.6	79	67.6	52.7
100	0.5	71.9	63.9	61.0	55.3	9.6	37.2	30.1	19.1
	1.0	69.0	67.5	64.1	57.1	16.6	49.1	40.8	28.1
	1.5	66.8	71.5	66.1	59.1	21.7	63.6	51	36.1
	2.0	65.7	73.3	67.5	61.8	33.1	80.9	67.7	50.2
	2.5	64.9	73.2	67.6	61.8	38.6	90.9	77.7	63.2
150	0.5	78.1	71.0	67.1	60.9	12.5	48.4	39.1	24.8
	1.0	75.1	73.9	70.9	63.1	20.8	61.4	51	35.1
	1.5	73.5	78.1	72.3	65.8	26	76.3	61.2	43.3
	2.0	72.9	80.5	74.9	67.1	39.7	97.1	81.2	60.2
	2.5	71.2	80.7	75.2	67.3	46.3	109.1	93.2	75.8
200	0.5	80.7	73.0	70.0	63.1	16.3	62.9	48.9	32.2
	1.0	78.5	77.1	72.9	65.4	26	76.8	63.8	43.9
	1.5	77.2	81.7	76.9	68.8	31.2	91.6	73.4	52
	2.0	77.4	83.5	80.4	70.5	47.6	116.5	97.4	72.2
	2.5	76.9	83.0	79.8	70.3	55.6	130.9	111.8	91
250	0.5	80.2	73.6	70.9	63.6	21.2	75.5	58.7	38.6
	1.0	78.6	78.1	73.8	66.9	32.5	92.2	76.6	50.7
	1.5	77.6	81.0	76.8	67.8	40.7	109.9	88.1	62.4
	2.0	76.5	82.8	81.0	69.5	51.1	133.9	109.1	83.1
	2.5	77.2	82.0	80.6	71.9	63.2	150.5	130.6	104.7

Appendix 4.10Average values of saturation efficiency and pressure drop for various pad materials at 50mm pad thicknesses,.

pad thicknesses:		50mm							
pad face air vel. (m/s)	Water flow rate (L/min)	Saturation Efficiency (%)				Pressure Drop (Pa)			
		Celdek	Jute	Coconut	Sponge	Celdek	Jute	Coconut	Sponge
0.5	1.0	60.2	56.3	54.7	46.8	1.4	6.5	4.9	3.2
	1.25	60.9	56.8	55.1	49.2	2.2	10.1	7.6	5.0
	1.5	61.3	56.9	55.6	49.9	3.4	15.7	11.8	7.5
	1.75	61.5	56.9	55.8	50.2	5.3	22	16.5	10.5
	2.0	61.9	57.1	56.0	50.1	7.4	28.6	23.1	14.7
1.o	1.0	56.9	57.4	55.1	48.2	2.5	11	7.8	5.5
	1.25	57.3	59.9	57.6	50.8	3.9	16.1	12.1	8.5
	1.5	57.4	60.3	58.1	51.2	6.1	23.9	18.8	13.2
	1.75	57.8	60.6	58.6	51.3	9.5	31.5	26.3	18.5
	2.0	57.9	60.5	58.9	51.4	13.3	40.9	34.2	24.1
1.5	1.0	54.4	61.3	59.5	50.8	4.1	17.6	12.5	9.4
	1.25	54.8	61.9	59.8	52.9	6.2	24.6	18.1	12.8
	1.5	55.0	61.9	60.3	52.9	9.3	34.9	27.2	19.2
	1.75	55.1	61.8	60.5	53.1	13.9	42.4	35.4	25
	2.0	55.6	62.0	61.0	53.6	18.1	53	42.5	30
2.0	1.0	52.6	63.1	62.3	53.1	6.8	26.4	20	15.5
	1.25	52.8	63.2	62.5	55.7	10.2	34.8	28	21.7
	1.5	53.0	63.5	62.8	56.1	15.3	47.7	39.2	30.4
	1.75	53.1	63.8	61.2	56.7	22.9	57.6	49	36
	2.0	53.3	64.1	63.8	56.0	27.5	69.1	56.4	41
2.5	1.0	51.4	62.0	63.9	55.7	11.1	37	29	24
	1.25	51.3	63.7	62.7	56.1	14.3	46.6	37.7	31.2
	1.5	51.7	63.7	62.1	55.9	20	58.6	48.7	38.9
	1.75	52.3	63.9	61.7	57.0	28	68.7	58.8	45.8
	2.0	52.9	64.1	63.9	57.2	33.6	79	67.6	52.7

Appendix 4.11 Average values of saturation efficiency and pressure drop for various pad materials at 100mm pad thicknesses

pad thicknesses:		100mm							
pad face air vel. (m/s)	Water flow rate (L/min)	Saturation Efficiency (%)				Pressure Drop (Pa)			
		Celdek	Jute	Coconut	Sponge	Celdek	Jute	Coconut	Sponge
0.5	1.0	69.8	62.1	60.2	52.5	1.8	8.5	6.4	4.2
	1.25	70.7	64.3	60.7	54.9	2.9	13.1	9.9	6.5
	1.5	71.2	63.8	60.8	54.2	4.4	20.4	15.3	9.8
	1.75	71.8	63.7	60.7	54.1	6.9	28.6	21.5	13.7
	2.0	71.9	63.9	61.0	55.3	9.6	37.2	30.1	19.1
1.o	1.0	68.1	66.5	62.8	54.1	3.1	13.8	9.8	6.9
	1.25	68.4	66.8	63.9	56.7	4.9	20.1	15.1	10.6
	1.5	68.5	66.9	63.3	56.9	7.6	29.9	23.5	16.5
	1.75	68.9	67.2	63.5	56.9	11.9	39.4	32.9	23.1
	2.0	69.0	67.5	64.1	57.1	16.6	49.1	40.8	28.1
1.5	1.0	65.5	69.7	65.6	56.5	4.9	21.1	15	11.3
	1.25	65.8	70.1	67.0	58.1	7.4	29.5	21.7	15.4
	1.5	66.3	70.8	66.2	58.6	11.2	41.9	32.4	23.1
	1.75	66.3	71.3	65.7	58.9	16.7	50.9	42.5	30.2
	2.0	66.8	71.5	66.1	59.1	21.7	63.6	51	36.1
2.0	1.0	63.8	70.1	67.9	58.3	8.2	31.7	24	18.6
	1.25	64.3	71.7	68.9	60.9	12.2	41.8	33.6	26
	1.5	64.8	72.9	69.3	61.3	18.4	57.2	47.1	36.5
	1.75	64.5	73.1	67.8	61.5	27.5	69.1	58.8	43.7
	2.0	65.7	73.3	67.5	61.8	33.1	80.9	67.7	50.2
2.5	1.0	62.9	70.3	68.4	58.9	13.3	44.4	34.8	28.8
	1.25	63.8	71.9	69.2	62.0	17.2	55.9	45.2	37.4
	1.5	63.5	73.0	68.3	61.7	24.1	67.4	56.1	44.7
	1.75	63.9	74.3	68.5	61.3	33.6	79	67.6	53.8
	2.0	64.9	73.2	67.6	61.8	38.6	90.9	77.7	63.2

Appendix 4.12 Average values of saturation efficiency and pressure drop for various pad materials at 150mm pad thicknesses

pad thicknesses:		150mm							
pad face air vel. (m/s)	Water flow rate (L/min)	Saturation Efficiency (%)				Pressure Drop (Pa)			
		Celdek	Jute	Coconut	Sponge	Celdek	Jute	Coconut	Sponge
0.5	1.0	76.2	69.6	66.3	59.1	2.3	11.1	8.3	5.5
	1.25	76.9	70.3	66.1	59.6	3.8	17	12.9	8.5
	1.5	77.3	70.9	66.3	60.1	5.7	26.5	19.9	12.7
	1.75	77.9	70.7	66.8	60.7	9	37.2	28	17.8
	2.0	78.1	71.0	67.1	60.9	12.5	48.4	39.1	24.8
1.o	1.0	73.8	72.6	68.3	60.8	3.9	17.3	12.3	8.6
	1.25	73.9	73.1	68.9	61.9	6.1	25.1	18.9	13.3
	1.5	74.6	73.8	70.0	62.5	9.5	37.4	29.4	20.6
	1.75	74.8	73.8	69.6	62.8	14.9	49.3	41.1	28.9
	2.0	75.1	73.9	70.9	63.1	20.8	61.4	51	35.1
1.5	1.0	72.1	76.9	73.3	64.8	5.9	25.3	18.1	13.6
	1.25	72.6	77.5	72.7	63.3	8.9	35.4	26.1	18.5
	1.5	72.9	78.6	73.9	63.8	13.4	50.3	38.9	27.7
	1.75	73.3	78.0	72.1	63.9	20	61.1	51.1	36.2
	2.0	73.5	78.1	72.3	65.8	26	76.3	61.2	43.3
2.0	1.0	70.9	80.3	75.8	65.1	9.8	38.1	28.8	22.3
	1.25	71.5	78.3	76.3	65.8	14.6	50.2	40.3	31.2
	1.5	72.1	81.2	76.5	66.2	22.1	68.6	56.5	43.8
	1.75	72.6	80.3	75.6	66.8	31.1	82.9	70.6	52.8
	2.0	72.9	80.5	74.9	67.1	39.7	97.1	81.2	60.2
2.5	1.0	69.7	80.5	77.0	65.4	16	53.3	41.8	34.6
	1.25	70.3	78.9	75.8	66.1	20.6	67.1	54.2	44.9
	1.5	71.5	81.3	77.0	66.5	28.9	80.9	67.3	53.6
	1.75	71.4	80.7	76.0	67.0	40.3	94.8	81.1	66.1
	2.0	71.2	80.7	75.2	67.3	46.3	109.1	93.2	75.8

Appendix 4.13 Average values of saturation efficiency and pressure drop for various pad materials at 200mm pad thicknesses

pad thicknesses:200mm									
pad face air vel. (m/s)	Water flow rate (L/min)	Saturation Efficiency (%)				Pressure Drop (Pa)			
		Celdek	Jute	Coconut	Sponge	Celdek	Jute	Coconut	Sponge
0.5	1.0	80.0	72.6	69.0	63.0	3	14.4	10.8	7.2
	1.25	80.4	73.0	69.3	62.1	4.9	22.1	16.8	11.1
	1.5	80.6	73.6	68.9	62.7	7.4	34.4	25.9	16.5
	1.75	80.7	72.9	69.2	62.9	11.7	48.4	36.4	23.1
	2.0	80.7	73.0	70.0	63.1	16.3	62.9	48.9	32.2
1.o	1.0	77.8	74.5	72.1	63.2	4.9	21.6	15.4	10.8
	1.25	78.1	75.7	71.3	63.4	7.6	31.4	23.6	16.6
	1.5	78.5	76.1	73.2	63.9	11.9	46.8	36.8	25.8
	1.75	79.1	76.9	72.6	65.9	18.6	61.6	49.3	36.1
	2.0	78.5	77.1	72.9	65.4	26	76.8	63.8	43.9
1.5	1.0	76.3	81.7	76.6	65.7	7.1	30.4	21.7	16.3
	1.25	76.9	79.5	75.2	66.7	10.7	42.5	31.3	22.2
	1.5	77.1	81.1	77.3	65.7	16.1	60.4	46.7	33.2
	1.75	77.5	82.5	76.3	66.2	24	73.3	61.3	43.4
	2.0	77.2	81.7	76.9	68.8	31.2	91.6	73.4	52
2.0	1.0	75.8	83.9	79.9	68.0	11.8	45.7	34.6	26.8
	1.25	76.2	81.3	79.0	68.9	17.5	60.2	48.4	37.4
	1.5	76.7	83.5	80.1	68.2	26.5	82.3	67.8	52.6
	1.75	77.1	82.6	80.3	70.7	37.3	99.5	84.7	63.4
	2.0	77.4	83.5	80.4	70.5	47.6	116.5	97.4	72.2
2.5	1.0	75.4	82.7	79.6	68.7	19.2	64	50.2	41.4
	1.25	74.9	82.7	79.6	69.3	24.7	80.5	65.1	53.9
	1.5	76.2	83.7	79.8	68.5	34.7	97.1	80.8	64.3
	1.75	76.7	81.7	79.9	70.1	48.4	113.8	97.3	79.3
	2.0	76.9	83.0	79.8	70.3	55.6	130.9	111.8	91

Appendix 4.14 Average values of saturation efficiency and pressure drop for various pad materials at 250mm pad thicknesses

pad thicknesses:250mm									
pad face air vel. (m/s)	Water flow rate (L/min)	Saturation Efficiency (%)				Pressure Drop (Pa)			
		Celdek	Jute	Coconut	Sponge	Celdek	Jute	Coconut	Sponge
0.5	1.0	79.2	73.2	69.8	63.5	3.9	18.7	14.1	9.4
	1.25	79.5	73.9	70.0	63.3	6.4	28.7	21.8	14.3
	1.5	79.5	73.9	69.1	63.2	9.6	44.7	33.7	21.5
	1.75	79.8	73.5	70.8	63.4	15.2	62.9	47.3	30.1
	2.0	80.2	73.6	70.9	63.6	21.2	75.5	58.7	38.6
1.o	1.0	77.5	75.5	72.0	65.7	6.1	27.1	19.3	13.5
	1.25	77.6	76.0	72.3	65.9	9.5	39.3	29.5	20.8
	1.5	77.9	76.5	73.5	66.2	14.9	58.5	46.1	32.3
	1.75	78.6	77.2	73.3	66.5	23.3	77	61.6	45.1
	2.0	78.6	78.1	73.8	66.9	32.5	92.2	76.6	50.7
1.5	1.0	76.3	79.6	76.1	68.9	8.5	36.5	26.1	19.6
	1.25	76.8	80.1	77.0	69.3	12.8	51.1	37.6	26.6
	1.5	76.9	80.7	77.1	67.2	19.3	72.5	56.1	39.8
	1.75	77.3	80.9	77.4	67.3	28.8	90.1	73.6	52.1
	2.0	77.6	81.0	76.8	67.8	40.7	109.9	88.1	62.4
2.0	1.0	76.1	81.8	79.7	71.1	14.2	54.8	41.5	32.2
	1.25	76.3	82.3	79.7	70.9	21.1	72.2	58.1	44.9
	1.5	75.4	82.1	79.1	68.6	31.8	98.8	81.4	63.1
	1.75	76.1	82.5	79.5	69.3	44.8	119.4	101.6	76.1
	2.0	76.5	82.8	81.0	69.5	51.1	133.9	109.1	83.1
2.5	1.0	75.8	82.2	80.1	70.8	23.1	76.8	60.2	49.7
	1.25	75.6	82.3	80.5	71.2	29.6	96.6	78.1	64.9
	1.5	76.0	82.6	80.3	71.5	41.6	116.5	97	77.2
	1.75	76.3	82.3	80.3	71.6	58.1	136.6	116.8	95.2
	2.0	77.2	82.0	80.6	71.9	63.2	150.5	130.6	104.7

Appendix 4.15 Regression Analysis of Saturation Efficiency for Celdek Pad

CELDEK (50mm)

R Square	0.999492951
Adjusted R Square	0.498985903
Standard Error	1.99596641
Observations	5

ANOVA

	df	SS	MS	F	Significance F
Regression	3	15706.03224	5235.344079	1314.13134	0.020274804
Residual	2	7.967763822	3.983881911		
Total	5	15714			

	Coefficients	Standard Error	t Stat	P-value	Lower 95%	Upper 95%	.ower 95.0%	Jpper 95.0%
Intercept	0	#N/A	#N/A	#N/A	#N/A	#N/A	#N/A	#N/A
π1	19.30936998	5.735677188	3.366537088	0.0780441	-5.369257129	43.98799709	-5.36926	43.988
π2	10.76476481	4.77869748	2.252656683	0.15306848	-9.796310944	31.32584057	-9.79631	31.32584
π4	-20.08973151	43.40278695	-0.462867316	0.68894043	-206.8368513	166.6573882	-206.837	166.6574

RESIDUAL OUTPUT

Observation	Predicted ηsat	Residuals	Standard Residuals
1	54.24684821	-1.946848206	-1.542229007
2	53.31672883	-0.216728827	-0.171685436
3	54.31500878	0.784991219	0.621844181
4	55.97842756	1.821572436	1.44298967
5	61.94298662	-0.442986623	-0.350919408

PROBABILITY OUTPUT

Percentile	ηsat
10	52.3
30	53.1
50	55.1
70	57.8
90	61.5

CELDEK(100mm)

SUMMARY OUTPUT

Regression Statistics	
Multiple R	0.999843
R Square	0.999685
Adjusted R	0.49937
Standard E	1.883677
Observatio	5

ANOVA

	df	SS	MS	F	ignificance F
Regression	3	22534.5	7511.501	2116.966	0.015975
Residual	2	7.096476	3.548238		
Total	5	22541.6			

	Coefficients	andard Erro	t Stat	P-value	Lower 95%	Upper 95%	.ower 95.0%	Jpper 95.0%
Intercept	0	#N/A	#N/A	#N/A	#N/A	#N/A	#N/A	#N/A
π1	1.038521	0.335665	3.093922	0.090509	-0.40573	2.48277	-0.40573	2.48277
π2	12.78329	4.516932	2.830082	0.105468	-6.6515	32.21808	-6.6515	32.21808
π4	-21.701	41.02371	-0.52899	0.649656	-198.212	154.8097	-198.212	154.8097

RESIDUAL OUTPUT

Observation	redicted ηsa	Residuals	ndard Residuals
1	65.73591	-1.83591	-1.54104
2	64.67543	-0.17543	-0.14726
3	65.65047	0.649527	0.545206
4	67.13605	1.763955	1.480646
5	72.20214	-0.40214	-0.33755

PROBABILITY OUTPUT

Percentile	ηsat
10	63.9
30	64.5
50	66.3
70	68.9
90	71.8

CELDEK(150mm)

SUMMARY OUTPUT

Regression Statistics	
Multiple R	0.999992
R Square	0.999984
Adjusted R	0.499967
Standard E	0.473003
Observatio	5

ANOVA

	df	*SS*	*MS*	*F*	*ignificance F*
Regression	3	27404.61	9134.871	40829.48	0.003638
Residual	2	0.447464	0.223732		
Total	5	27405.06			

	Coefficients	*andard Erro*	*t Stat*	*P-value*	*Lower 95%*	*Upper 95%*	*ower 95.0%*	*Jpper 95.0%*
Intercept	0	#N/A	#N/A	#N/A	#N/A	#N/A	#N/A	#N/A
π1	0.14639	0.016262	9.002089	0.012116	0.076421	0.216359	0.076421	0.216359
π2	17.18706	2.877685	5.972533	0.026908	4.805388	29.56874	4.805388	29.56874
π4	34.98315	11.41413	3.064897	0.092001	-14.1279	84.0942	-14.1279	84.0942

RESIDUAL OUTPUT

Observation	*redicted ηsa*	*Residuals*	*ıdard Residuals*
1	71.32336	0.076641	0.256193
2	72.96167	-0.36167	-1.20897
3	73.44541	-0.14541	-0.48608
4	74.27093	0.529069	1.768552
5	77.99863	-0.09863	-0.32969

PROBABILITY OUTPUT

Percentile	*ηsat*
10	71.4
30	72.6
50	73.3
70	74.8
90	77.9

CELDEK(200mm)

SUMMARY OUTPUT

Regression Statistics	
Multiple R	0.999977
R Square	0.999954
Adjusted R	0.499907
Standard E	0.841743
Observatio	5

ANOVA

	df	*SS*	*MS*	*F*	*ignificance F*
Regression	3	30601.43	10200.48	14396.63	0.006126
Residual	2	1.417064	0.708532		
Total	5	30602.85			

	Coefficients	*andard Erro*	*t Stat*	*P-value*	*Lower 95%*	*Upper 95%*	*ower 95.0%*	*Jpper 95.0%*
Intercept	0	#N/A	#N/A	#N/A	#N/A	#N/A	#N/A	#N/A
π1	0.032511	0.012815	2.537021	0.126539	-0.02263	0.087649	-0.02263	0.087649
π2	48.26107	14.57284	3.311714	0.080344	-14.4408	110.9629	-14.4408	110.9629
π4	2.36709	32.98506	0.071762	0.949321	-139.556	144.2903	-139.556	144.2903

RESIDUAL OUTPUT

Observation	*redicted ηsa*	*Residuals*	*ıdard Residuals*
1	77.25431	-0.55431	-1.04122
2	77.35117	-0.25117	-0.47179
3	77.46603	0.03397	0.06381
4	78.10271	0.99729	1.873319
5	80.92579	-0.22579	-0.42412

PROBABILITY OUTPUT

Percentile	*ηsat*
10	76.7
30	77.1
50	77.5
70	79.1
90	80.7

CELDEK (250mm)

SUMMARY OUTPUT

Regression Statistics	
Multiple R	0.999968
R Square	0.999936
Adjusted R	0.499872
Standard E	0.980483
Observatio	5

ANOVA

	df	*SS*	*MS*	*F*	*ignificance F*
Regression	3	30132.27	10044.09	10447.94	0.007192
Residual	2	1.922693	0.961346		
Total	5	30134.19			

	Coefficients	*andard Erro*	*t Stat*	*P-value*	*Lower 95%*	*Upper 95%*	*ower 95.0%*	*Jpper 95.0%*
Intercept	0	#N/A	#N/A	#N/A	#N/A	#N/A	#N/A	#N/A
π1	0.003451	0.017784	0.194079	0.86404	-0.07307	0.079968	-0.07307	0.079968
π2	447.0107	288.9463	1.547038	0.261919	-796.225	1690.246	-796.225	1690.246
π4	-49.0895	100.9129	-0.48645	0.67473	-483.283	385.1038	-483.283	385.1038

RESIDUAL OUTPUT

Observation	*redicted ηsa*	*Residuals*	*ıdard Residuals*
1	77.00247	-0.70247	-1.13281
2	76.6217	-0.5217	-0.84131
3	76.74117	0.558828	0.901173
4	77.70902	0.890985	1.436813
5	80.02564	-0.22564	-0.36387

PROBABILITY OUTPUT

Percentile	*ηsat*
10	76.1
30	76.3
50	77.3
70	78.6
90	79.8

Appendix 4.16 Regression Analysis of Saturation Efficiency for Jute Pad

JUTE FIBER(50mm)

Multiple R	0.999949
R Square	0.999899
Adjusted R	0.499797
Standard E	0.977814
Observatio	5

ANOVA

	df	*SS*	*MS*	*F*	*ignificance F*
Regression	3	18880.95	6293.649	6582.482	0.00906
Residual	2	1.912242	0.956121		
Total	5	18882.86			

	Coefficients	*andard Erro*	*t Stat*	*P-value*	*Lower 95%*	*Upper 95%*	*ower 95.0%*	*Jpper 95.0%*
Intercept	0	#N/A	#N/A	#N/A	#N/A	#N/A	#N/A	#N/A
π1	-11.8748	3.337247	-3.55826	0.070707	-26.2338	2.484216	-26.2338	2.484216
π2	4.615423	1.697793	2.718484	0.112864	-2.68959	11.92044	-2.68959	11.92044
π4	-74.3809	60.6912	-1.22556	0.345096	-335.514	186.7522	-335.514	186.7522

RESIDUAL OUTPUT

Observation	*redicted ηsa*	*Residuals*	*ıdard Residuals*
1	56.80408	0.095916	0.155097
2	60.84475	-0.24475	-0.39577
3	62.69433	-0.89433	-1.44614
4	62.77881	1.021191	1.65128
5	63.87803	0.021973	0.035531

PROBABILITY OUTPUT

Percentile	*ηsat*
10	56.9
30	60.6
50	61.8
70	63.8
90	63.9

JUTE FIBER(100mm)

SUMMARY OUTPUT

Regression Statistics	
Multiple R	0.999708
R Square	0.999415
Adjusted R	0.498831
Standard E	2.677272
Observatio	5

ANOVA

	df	*SS*	*MS*	*F*	*ignificance F*
Regression	3	24506.98	8168.995	1139.682	0.021771
Residual	2	14.33557	7.167784		
Total	5	24521.32			

	Coefficients	*andard Erro*	*t Stat*	*P-value*	*Lower 95%*	*Upper 95%*	*ower 95.0%*	*Jpper 95.0%*
Intercept	0	#N/A	#N/A	#N/A	#N/A	#N/A	#N/A	#N/A
π1	-1.37274	0.477081	-2.87737	0.10254	-3.42545	0.679973	-3.42545	0.679973
π2	8.642732	6.41992	1.346237	0.310515	-18.98	36.26542	-18.98	36.26542
π4	27.19199	58.30704	0.466359	0.686823	-223.683	278.0669	-223.683	278.0669

RESIDUAL OUTPUT

Observation	*redicted ηsc*	*Residuals*	*ıdard Residuals*
1	63.1194	0.580597	0.342888
2	69.87888	-2.67888	-1.58209
3	71.80761	-0.50761	-0.29978
4	73.05583	0.044168	0.026085
5	71.73827	2.561727	1.512901

PROBABILITY OUTPUT

Percentile	*ηsat*
10	63.7
30	67.2
50	71.3
70	73.1
90	74.3

JUTE FIBER(150mm)

SUMMARY OUTPUT

Regression Statistics	
Multiple R	0.999826
R Square	0.999653
Adjusted R	0.499306
Standard E	2.26201
Observatio	5

ANOVA

	df	*SS*	*MS*	*F*	*ignificance F*
Regression	3	29479.28	9826.426	1920.466	0.016772
Residual	2	10.23338	5.116688		
Total	5	29489.51			

	Coefficients	*andard Erro*	*t Stat*	*P-value*	*Lower 95%*	*Upper 95%*	*ower 95.0%*	*Jpper 95.0%*
Intercept	0	#N/A	#N/A	#N/A	#N/A	#N/A	#N/A	#N/A
π1	-0.23642	0.077767	-3.04006	0.093305	-0.57102	0.098188	-0.57102	0.098188
π2	43.27411	13.76174	3.144523	0.087989	-15.9379	102.4861	-15.9379	102.4861
π4	-58.2826	54.58498	-1.06774	0.397446	-293.143	176.5777	-293.143	176.5777

RESIDUAL OUTPUT

Observation	*redicted ηsc*	*Residuals*	*ıdard Residuals*
1	70.23419	0.465809	0.3256
2	76.23742	-2.43742	-1.70375
3	77.57294	0.427055	0.298511
4	78.36579	1.93421	1.352008
5	81.08965	-0.38965	-0.27237

PROBABILITY OUTPUT

Percentile	*ηsat*
10	70.7
30	73.8
50	78
70	80.3
90	80.7

JUTE FIBER(200mm)

SUMMARY OUTPUT

Regression Statistics	
Multiple R	0.999838
R Square	0.999676
Adjusted R	0.499353
Standard E	2.258967
Observatio	5

ANOVA

	df	*SS*	*MS*	*F*	*ignificance F*
Regression	3	31521.71	10507.24	2059.059	0.016198
Residual	2	10.20586	5.102932		
Total	5	31531.92			

	Coefficients	*andard Erro*	*t Stat*	*P-value*	*Lower 95%*	*Upper 95%*	*ower 95.0%*	*Jpper 95.0%*
Intercept	0	#N/A	#N/A	#N/A	#N/A	#N/A	#N/A	#N/A
π1	-0.08756	0.034391	-2.54599	0.12581	-0.23553	0.060413	-0.23553	0.060413
π2	48.96336	39.10878	1.251979	0.337146	-119.308	217.2348	-119.308	217.2348
π4	8.337848	88.52123	0.09419	0.933545	-372.538	389.2139	-372.538	389.2139

RESIDUAL OUTPUT

Observation	*redicted ηsa*	*Residuals*	*ıdard Residuals*
1	72.37156	0.528436	0.369873
2	79.62146	-2.72146	-1.90486
3	81.10074	1.399258	0.979395
4	81.85148	0.748525	0.523922
5	81.65475	0.045245	0.031669

PROBABILITY OUTPUT

Percentile	*ηsat*
10	72.9
30	76.9
50	81.7
70	82.5
90	82.6

JUTE FIBER(250mm)

SUMMARY OUTPUT

Regression Statistics	
Multiple R	0.999897
R Square	0.999795
Adjusted R	0.499589
Standard E	1.797834
Observatio	5

ANOVA

	df	*SS*	*MS*	*F*	*ignificance F*
Regression	3	31479.98	10493.33	3246.489	0.012901
Residual	2	6.464415	3.232208		
Total	5	31486.44			

	Coefficients	*andard Erro*	*t Stat*	*P-value*	*Lower 95%*	*Upper 95%*	*ower 95.0%*	*Jpper 95.0%*
Intercept	0	#N/A	#N/A	#N/A	#N/A	#N/A	#N/A	#N/A
π1	-0.00712	0.032608	-0.21831	0.84744	-0.14742	0.133184	-0.14742	0.133184
π2	-66.0893	529.818	-0.12474	0.912137	-2345.71	2213.534	-2345.71	2213.534
π4	137.4717	185.0361	0.742946	0.534929	-658.674	933.6178	-658.674	933.6178

RESIDUAL OUTPUT

Observation	*redicted ηsa*	*Residuals*	*ıdard Residuals*
1	73.06569	0.434315	0.381966
2	78.99933	-1.79933	-1.58245
3	81.60771	-0.70771	-0.62241
4	81.90483	0.595173	0.523436
5	80.82246	1.477543	1.299453

PROBABILITY OUTPUT

Percentile	*ηsat*
10	73.5
30	77.2
50	80.9
70	82.3
90	82.5

Appendix 4.17 Regression Analysis of Saturation Efficiency for Coconut Fiber Pad

COCONUT FIBER(50mm)

Regression Statistics	
Multiple R	0.999884
R Square	0.999768
Adjusted R	0.499536
Standard E	1.454491
Observatio	5

ANOVA

	df	*SS*	*MS*	*F*	*ignificance F*
Regression	3	18230.11	6076.703	2872.407	0.013715
Residual	2	4.231087	2.115544		
Total	5	18234.34			

	Coefficients	*andard Erro*	*t Stat*	*P-value*	*Lower 95%*	*Upper 95%*	*ower 95.0%*	*Upper 95.0%*
Intercept	0	#N/A	#N/A	#N/A	#N/A	#N/A	#N/A	#N/A
π1	-10.3713	4.964128	-2.08924	0.171882	-31.7302	10.98764	-31.7302	10.98764
π2	6.354986	2.525453	2.516374	0.12824	-4.51116	17.22113	-4.51116	17.22113
π4	-137.979	90.27767	-1.52838	0.266011	-526.412	250.4547	-526.412	250.4547

RESIDUAL OUTPUT

Observation	*redicted ηsc*	*Residuals*	*ıdard Residuals*
1	55.65031	0.149686	0.16272
2	59.03334	-0.43334	-0.47108
3	61.74397	-1.24397	-1.35229
4	61.62791	1.572087	1.708974
5	63.54446	-0.04446	-0.04833

PROBABILITY OUTPUT

Percentile	*ηsat*
10	55.8
30	58.6
50	60.5
70	63.2
90	63.5

COCONUT FIBER(100mm)

SUMMARY OUTPUT

Regression Statistics	
Multiple R	0.999818
R Square	0.999636
Adjusted R	0.499273
Standard E	1.969015
Observatio	5

ANOVA

	df	*SS*	*MS*	*F*	*ignificance F*
Regression	3	21314.57	7104.855	1832.556	0.01717
Residual	2	7.754039	3.87702		
Total	5	21322.32			

	Coefficients	*andard Erro*	*t Stat*	*P-value*	*Lower 95%*	*Upper 95%*	*ower 95.0%*	*Upper 95.0%*
Intercept	0	#N/A	#N/A	#N/A	#N/A	#N/A	#N/A	#N/A
π1	-0.99686	0.350872	-2.84111	0.104775	-2.50654	0.512815	-2.50654	0.512815
π2	8.65482	4.721567	1.83304	0.20825	-11.6604	28.97008	-11.6604	28.97008
π4	19.16896	42.88225	0.447014	0.698611	-165.338	203.6764	-165.338	203.6764

RESIDUAL OUTPUT

Observation	*redicted ηsc*	*Residuals*	*ıdard Residuals*
1	60.28988	0.410117	0.329328
2	65.22289	-1.72289	-1.3835
3	66.60999	-0.90999	-0.73073
4	67.50073	0.299273	0.240319
5	66.5765	1.923496	1.544586

PROBABILITY OUTPUT

Percentile	*ηsat*
10	60.7
30	63.5
50	65.7
70	67.8
90	68.5

COCONUT FIBER(150mm)

SUMMARY OUTPUT

Regression Statistics	
Multiple R	0.99983
R Square	0.999661
Adjusted R	0.499321
Standard E	2.100454
Observatio	5

ANOVA

	df	*SS*	*MS*	*F*	*ignificance F*
Regression	3	25987.35	8662.449	1963.424	0.016588
Residual	2	8.823818	4.411909		
Total	5	25996.17			

	Coefficients	*andard Erro*	*t Stat*	*P-value*	*Lower 95%*	*Upper 95%*	*ower 95.0%*	*Jpper 95.0%*
Intercept	0	#N/A	#N/A	#N/A	#N/A	#N/A	#N/A	#N/A
π1	-0.20189	0.072213	-2.79574	0.107669	-0.5126	0.108819	-0.5126	0.108819
π2	43.57408	12.77886	3.409856	0.076293	-11.4089	98.55709	-11.4089	98.55709
π4	-66.6439	50.68646	-1.31483	0.319096	-284.73	151.4423	-284.73	151.4423

RESIDUAL OUTPUT

Observation	*redicted ηsa*	*Residuals*	*ıdard Residuals*
1	66.42226	0.377744	0.284351
2	71.38841	-1.78841	-1.34625
3	72.55082	-0.45082	-0.33936
4	73.33755	2.262453	1.703085
5	76.40096	-0.40096	-0.30183

PROBABILITY OUTPUT

Percentile	*ηsat*
10	66.8
30	69.6
50	72.1
70	75.6
90	76

COCONUT FIBER (200mm)

SUMMARY OUTPUT

Regression Statistics	
Multiple R	0.999674
R Square	0.999349
Adjusted R	0.498698
Standard E	3.057288
Observatio	5

ANOVA

	df	*SS*	*MS*	*F*	*ignificance F*
Regression	3	28694.5	9564.832	1023.304	0.022975
Residual	2	18.69402	9.347008		
Total	5	28713.19			

	Coefficients	*andard Erro*	*t Stat*	*P-value*	*Lower 95%*	*Upper 95%*	*ower 95.0%*	*Jpper 95.0%*
Intercept	0	#N/A	#N/A	#N/A	#N/A	#N/A	#N/A	#N/A
π1	-0.10724	0.046544	-2.30394	0.147749	-0.3075	0.093029	-0.3075	0.093029
π2	21.77886	52.92984	0.411467	0.720634	-205.96	249.5176	-205.96	249.5176
π4	64.7879	119.8047	0.540779	0.642833	-450.69	580.2659	-450.69	580.2659

RESIDUAL OUTPUT

Observation	*redicted ηsa*	*Residuals*	*ıdard Residuals*
1	68.40639	0.793608	0.41043
2	75.97573	-3.37573	-1.74583
3	76.91422	-0.61422	-0.31766
4	79.47096	0.829044	0.428757
5	77.5327	2.367296	1.224296

PROBABILITY OUTPUT

Percentile	*ηsat*
10	69.2
30	72.6
50	76.3
70	79.9
90	80.3

COCONUT FIBER(250mm)

SUMMARY OUTPUT

Regression Statistics	
Multiple R	0.999732
R Square	0.999463
Adjusted R	0.498926
Standard E	2.797131
Observatio	5

ANOVA

	df	*SS*	*MS*	*F*	*ignificance F*
Regression	3	29128.98	9709.661	1241.019	0.020863
Residual	2	15.64788	7.82394		
Total	5	29144.63			

	Coefficients	*andard Erro*	*t Stat*	*P-value*	*Lower 95%*	*Upper 95%*	*ower 95.0%*	*Jpper 95.0%*
Intercept	0	#N/A	#N/A	#N/A	#N/A	#N/A	#N/A	#N/A
π1	-0.01263	0.050733	-0.24896	0.826626	-0.23092	0.205657	-0.23092	0.205657
π2	21.56496	824.3086	0.026161	0.981504	-3525.15	3568.279	-3525.15	3568.279
π4	102.5841	287.8854	0.356337	0.755669	-1136.09	1341.255	-1136.09	1341.255

RESIDUAL OUTPUT

Observation	*redicted ηsc*	*Residuals*	*ıdard Residuals*
1	70.12126	0.678738	0.383671
2	76.14077	-2.84077	-1.6058
3	78.38029	-0.98029	-0.55413
4	78.7096	0.790396	0.446788
5	77.94808	2.351924	1.329476

PROBABILITY OUTPUT

Percentile	*ηsat*
10	70.8
30	73.3
50	77.4
70	79.5
90	80.3

Appendix 4.18 Regression Analysis of Saturation Efficiency for Pop Sponge Pad

POP SPONGE(50mm)

SUMMARY OUTPUT

Regression Statistics	
Multiple R	0.999807
R Square	0.999614
Adjusted R	0.499228
Standard E	2.088343
Observatio	5

ANOVA

	df	*SS*	*MS*	*F*	*ignificance F*
Regression	3	22585.44	7528.479	1726.25	0.017691
Residual	2	8.722353	4.361177		
Total	5	22594.16			

	Coefficients	*andard Erro*	*t Stat*	*P-value*	*Lower 95%*	*Upper 95%*	*ower 95.0%*	*Jpper 95.0%*
Intercept	0	#N/A	#N/A	#N/A	#N/A	#N/A	#N/A	#N/A
π1	-0.07951	0.031793	-2.50093	0.129533	-0.21631	0.057282	-0.21631	0.057282
π2	9.420884	36.15482	0.260571	0.818799	-146.141	164.9825	-146.141	164.9825
π4	78.86125	81.83505	0.963661	0.436893	-273.247	430.969	-273.247	430.969

RESIDUAL OUTPUT

Observation	*redicted ηsc*	*Residuals*	*ıdard Residuals*
1	62.49117	0.408826	0.309533
2	67.3639	-1.4639	-1.10835
3	67.5666	-1.3666	-1.03469
4	70.38704	0.312963	0.236952
5	67.99129	2.108712	1.596561

PROBABILITY OUTPUT

Percentile	*ηsat*
10	62.9
30	65.9
50	66.2
70	70.1
90	70.7

POP SPONGE(100mm)

SUMMARY OUTPUT

Regression Statistics	
Multiple R	0.99982
R Square	0.99964
Adjusted R	0.499281
Standard E	1.757045
Observatio	5

ANOVA

	df	*SS*	*MS*	*F*	*ignificance F*
Regression	3	17167.4	5722.465	1853.605	0.017072
Residual	2	6.174416	3.087208		
Total	5	17173.57			

	Coefficients	*andard Erro*	*t Stat*	*P-value*	*Lower 95%*	*Upper 95%*	*ower 95.0%*	*Jpper 95.0%*
Intercept	0	#N/A	#N/A	#N/A	#N/A	#N/A	#N/A	#N/A
π1	-1.00671	0.313099	-3.21531	0.08463	-2.35387	0.340446	-2.35387	0.340446
π2	6.415152	4.213278	1.522604	0.267295	-11.7131	24.54342	-11.7131	24.54342
π4	29.70675	38.26586	0.776325	0.518792	-134.938	194.3515	-134.938	194.3515

RESIDUAL OUTPUT

Observation	*redicted ησα*	*Residuals*	*ıdard Residuals*
1	53.74919	0.350806	0.315685
2	58.29423	-1.39423	-1.25465
3	59.93719	-1.03719	-0.93335
4	61.1182	0.381803	0.343579
5	59.60119	1.698807	1.528731

PROBABILITY OUTPUT

Percentile	*ησατ*
10	54.1
30	56.9
50	58.9
70	61.3
90	61.5

POP SPONGE(150mm)

SUMMARY OUTPUT

Regression Statistics	
Multiple R	0.999894
R Square	0.999787
Adjusted R	0.499575
Standard E	1.481801
Observatio	5

ANOVA

	df	*SS*	*MS*	*F*	*ignificance F*
Regression	3	20658.39	6886.13	3136.14	0.013126
Residual	2	4.391468	2.195734		
Total	5	20662.78			

	Coefficients	*andard Erro*	*t Stat*	*P-value*	*Lower 95%*	*Upper 95%*	*ower 95.0%*	*Jpper 95.0%*
Intercept	0	#N/A	#N/A	#N/A	#N/A	#N/A	#N/A	#N/A
π1	-0.13537	0.050944	-2.65727	0.117234	-0.35457	0.083822	-0.35457	0.083822
π2	35.65733	9.015064	3.955306	0.058379	-3.13135	74.44602	-3.13135	74.44602
π4	-47.4612	35.75762	-1.3273	0.315654	-201.314	106.3915	-201.314	106.3915

RESIDUAL OUTPUT

Observation	*redicted ησα*	*Residuals*	*ıdard Residuals*
1	60.47402	0.225981	0.241131
2	63.7776	-0.9776	-1.04314
3	64.56064	-0.66064	-0.70492
4	65.10619	1.693807	1.807357
5	67.28155	-0.28155	-0.30042

PROBABILITY OUTPUT

Percentile	*ησατ*
10	60.7
30	62.8
50	63.9
70	66.8
90	67

POP SPONGE(200mm)

SUMMARY OUTPUT

Regression Statistics	
Multiple R	0.999807
R Square	0.999614
Adjusted R	0.499228
Standard E	2.088343
Observatio	5

ANOVA

	df	*SS*	*MS*	*F*	*ignificance F*
Regression	3	22585.44	7528.479	1726.25	0.017691
Residual	2	8.722353	4.361177		
Total	5	22594.16			

	Coefficients	*andard Erro*	*t Stat*	*P-value*	*Lower 95%*	*Upper 95%*	*ower 95.0%*	*Jpper 95.0%*
Intercept	0	#N/A	#N/A	#N/A	#N/A	#N/A	#N/A	#N/A
π1	-0.07951	0.031793	-2.50093	0.129533	-0.21631	0.057282	-0.21631	0.057282
π2	9.420884	36.15482	0.260571	0.818799	-146.141	164.9825	-146.141	164.9825
π4	78.86125	81.83505	0.963661	0.436893	-273.247	430.969	-273.247	430.969

RESIDUAL OUTPUT

Observation	*redicted ησα*	*Residuals*	*ıdard Residuals*
1	62.49117	0.408826	0.309533
2	67.3639	-1.4639	-1.10835
3	67.5666	-1.3666	-1.03469
4	70.38704	0.312963	0.236952
5	67.99129	2.108712	1.596561

PROBABILITY OUTPUT

Percentile	*ησατ*
10	62.9
30	65.9
50	66.2
70	70.1
90	70.7

POP SPONGE(250mm)

SUMMARY OUTPUT

Regression Statistics	
Multiple R	0.999907
R Square	0.999815
Adjusted R	0.499629
Standard E	1.450118
Observatio	5

ANOVA

	df	*SS*	*MS*	*F*	*ignificance F*
Regression	3	22683.39	7561.131	3595.671	0.012258
Residual	2	4.205686	2.102843		
Total	5	22687.6			

	Coefficients	*andard Erro*	*t Stat*	*P-value*	*Lower 95%*	*Upper 95%*	*ower 95.0%*	*Jpper 95.0%*
Intercept	0	#N/A	#N/A	#N/A	#N/A	#N/A	#N/A	#N/A
π1	-0.02878	0.026302	-1.09404	0.388117	-0.14194	0.084392	-0.14194	0.084392
π2	413.0803	427.3469	0.966616	0.435715	-1425.64	2251.805	-1425.64	2251.805
π4	-47.7829	149.2486	-0.32016	0.779203	-689.948	594.382	-689.948	594.382

RESIDUAL OUTPUT

Observation	*redicted ησα*	*Residuals*	*ıdard Residuals*
1	63.06853	0.331475	0.361424
2	67.80276	-1.30276	-1.42047
3	68.14769	-0.84769	-0.92428
4	68.50386	0.796144	0.868077
5	69.07716	1.022836	1.115251

PROBABILITY OUTPUT

Percentile	*ησατ*
10	63.4
30	66.5
50	67.3
70	69.3
90	70.1

Appendix 4.19 Validation of Saturation Efficiency Model Equations for Celdek

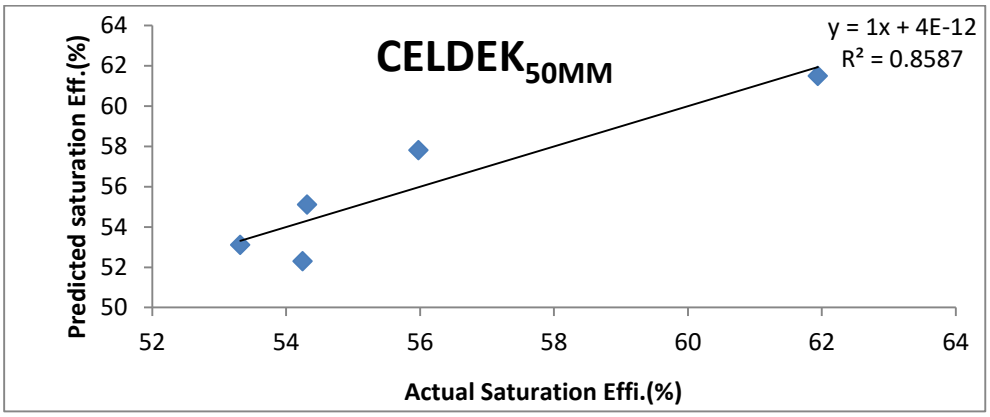

Graph of predicted against experimental data for equation 4.1

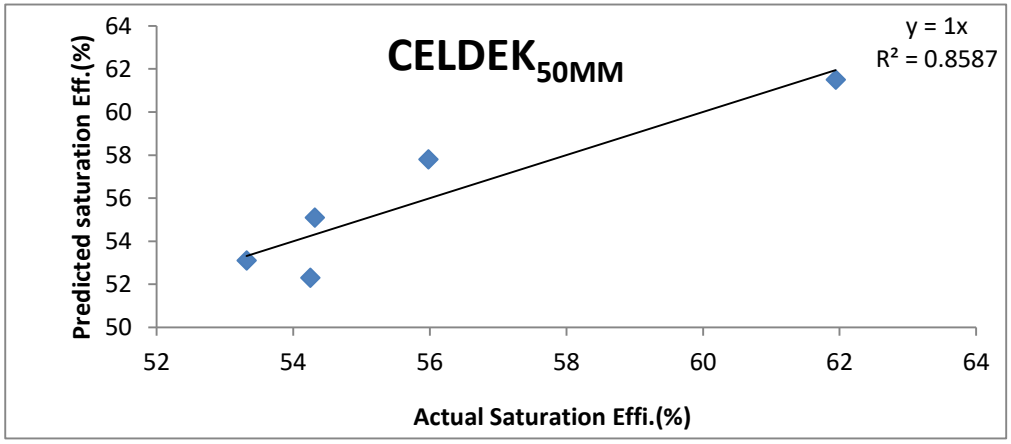

Graph of predicted against experimental data for equation 4.2

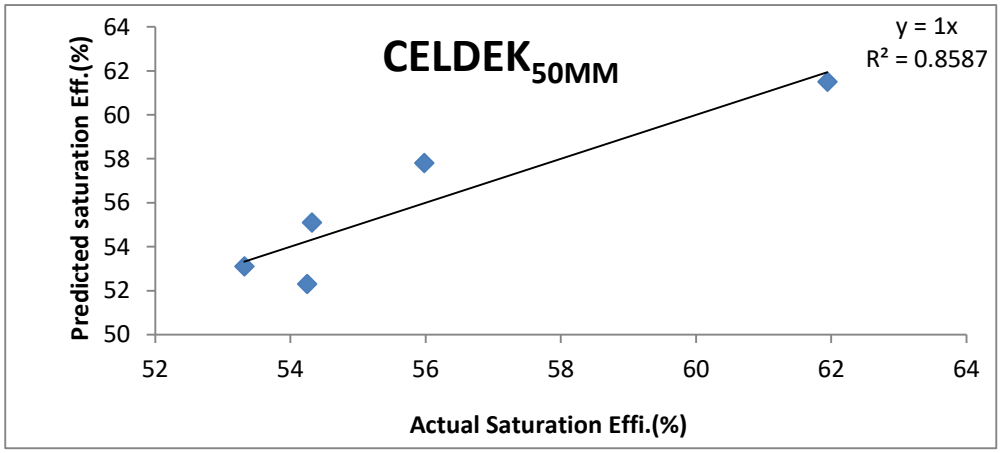

Graph of predicted against experimental data for equation 4.3

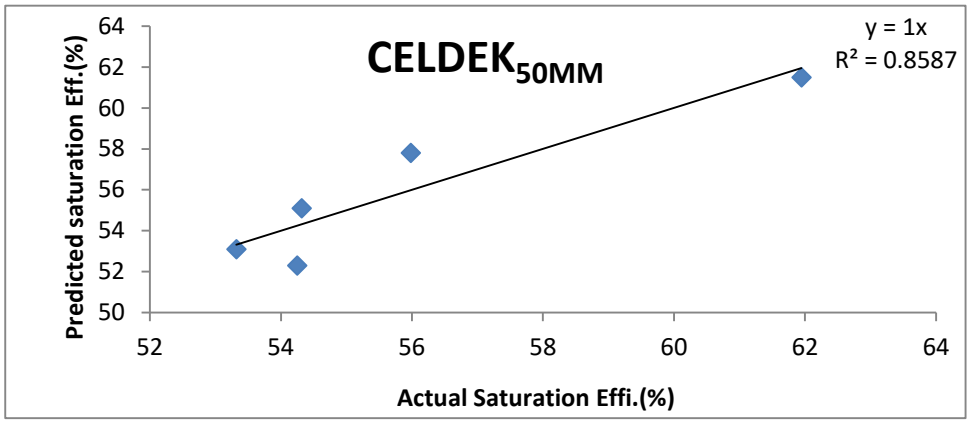

Graph of predicted against experimental data for equation 4.4

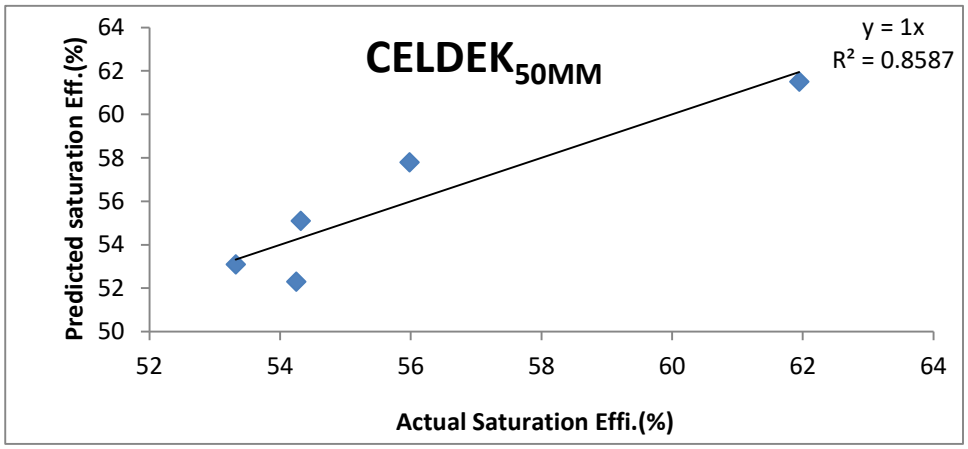

Graph of predicted against experimental data for Equation 4.5

Appendix 4.20 Validation Of Saturation Efficiency Model for Jute pad

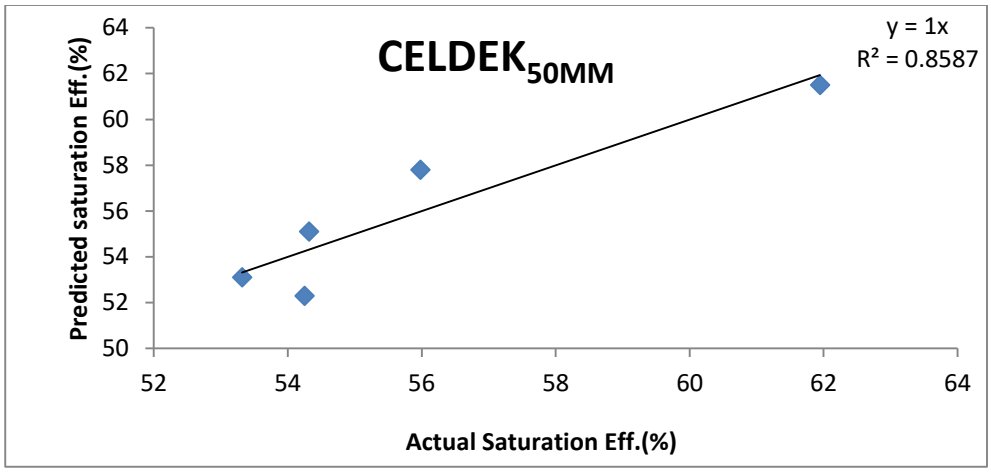

Graph of predicted against experimental data for equation 4.6

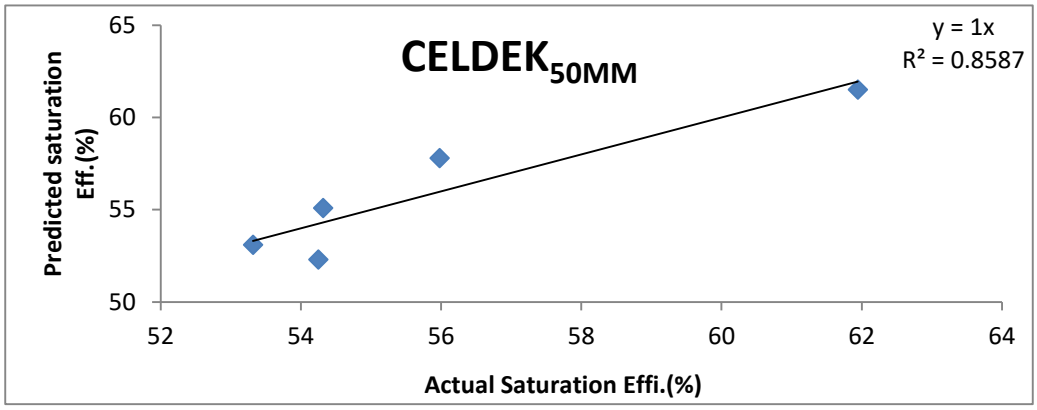

Graph of predicted against experimental data for equation 4.7

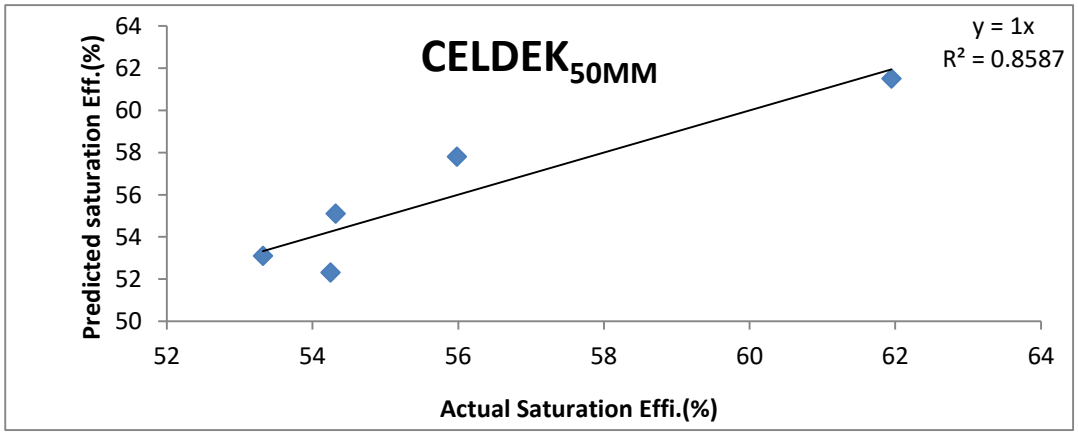

Graph of predicted against experimental data for equation 4.8

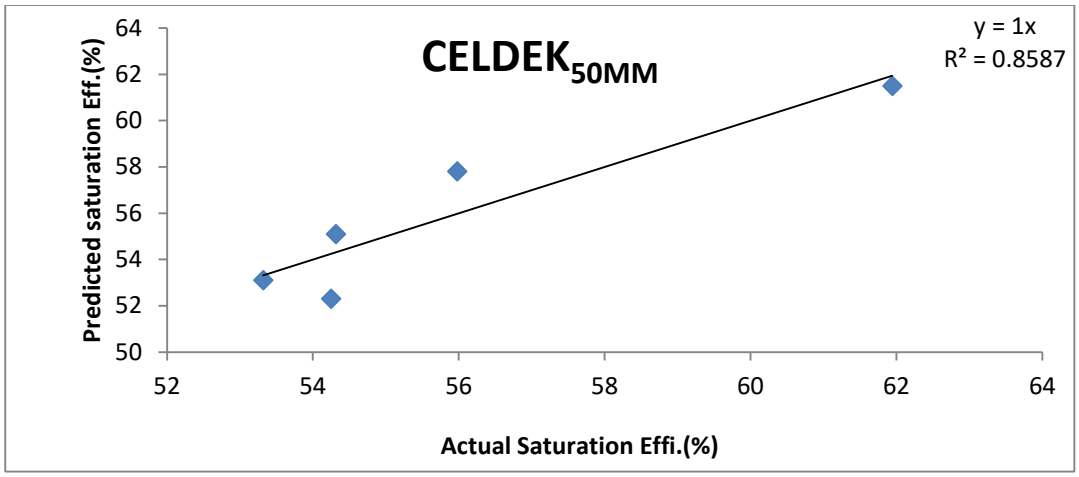

Graph of predicted against experimental data for equation 4.9

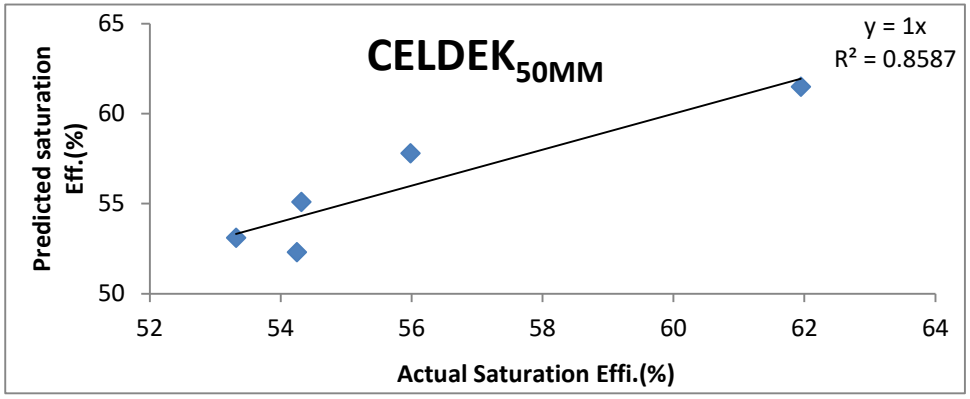

Graph of predicted against experimental data for equation 4.10

Appendix 4.21 Validation Of Saturation Efficiency Model Equations for Coconut

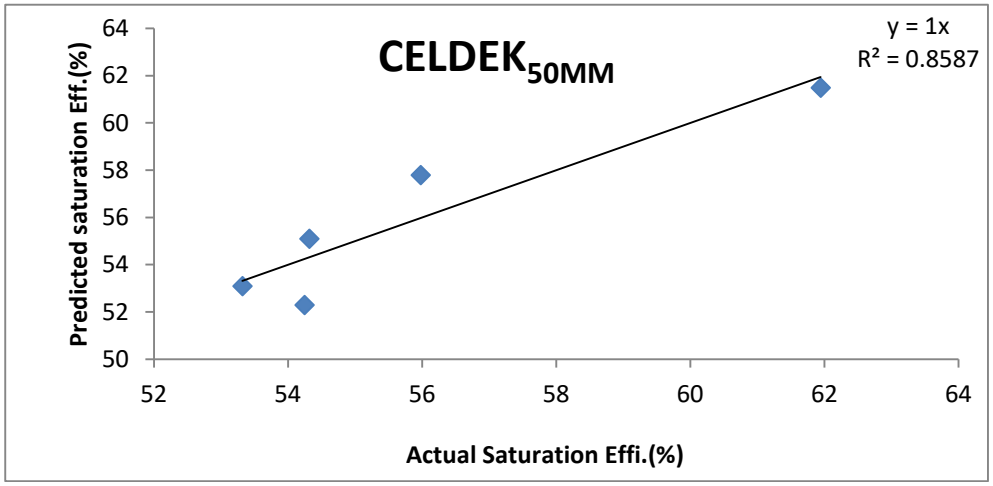

Graph of predicted against experimental data for equation 4.11

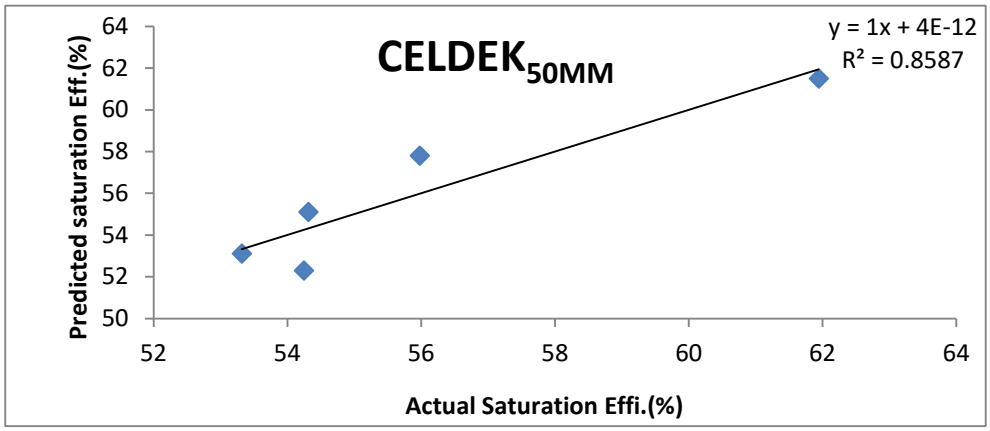

Graph of predicted against experimental data for equation 4.12

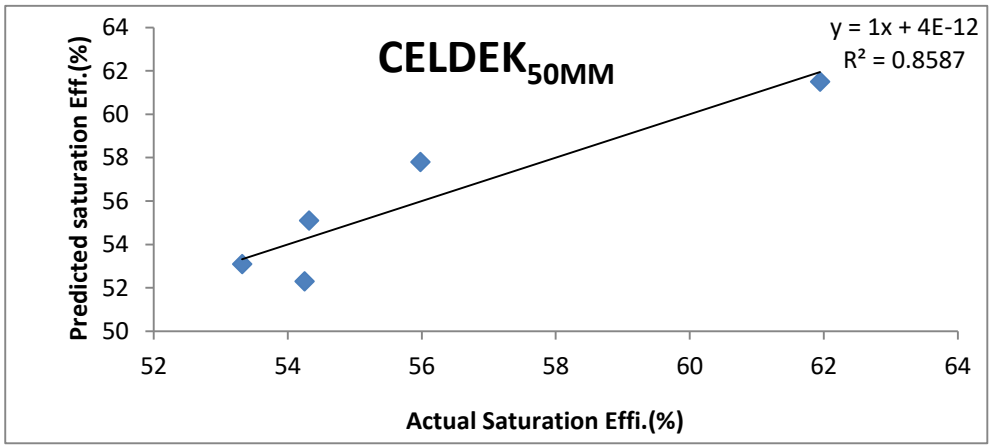

Graph of predicted against experimental data for equation 4.13

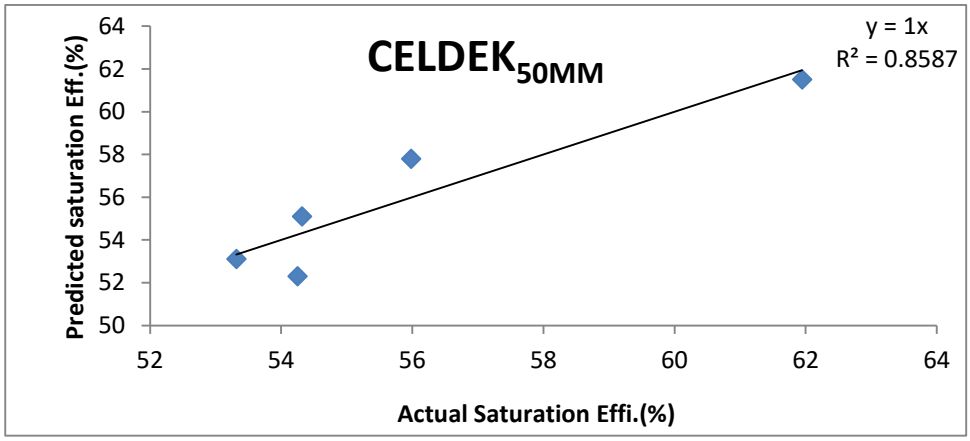

Graph of predicted against experimental data for equation 4.14

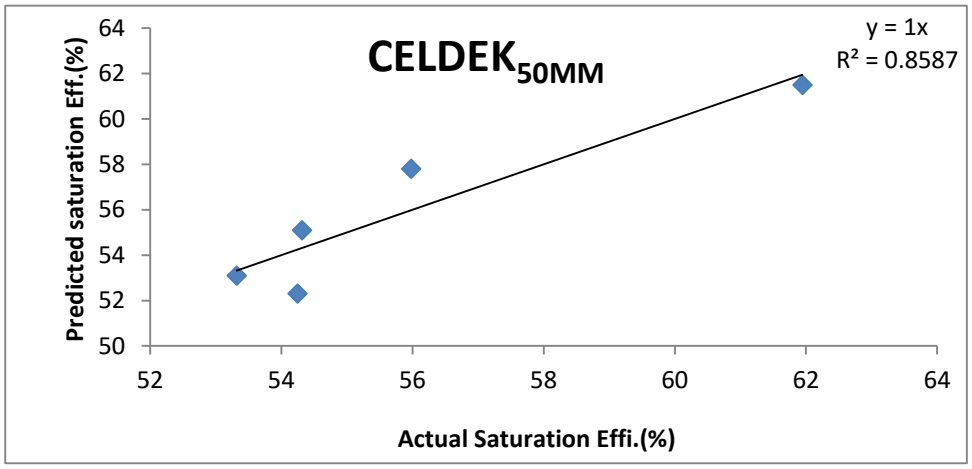

Graph of predicted against experimental data for equation 4.15

Appendix 4.22 Validation Of Saturation Efficiency Models for Pop Sponge

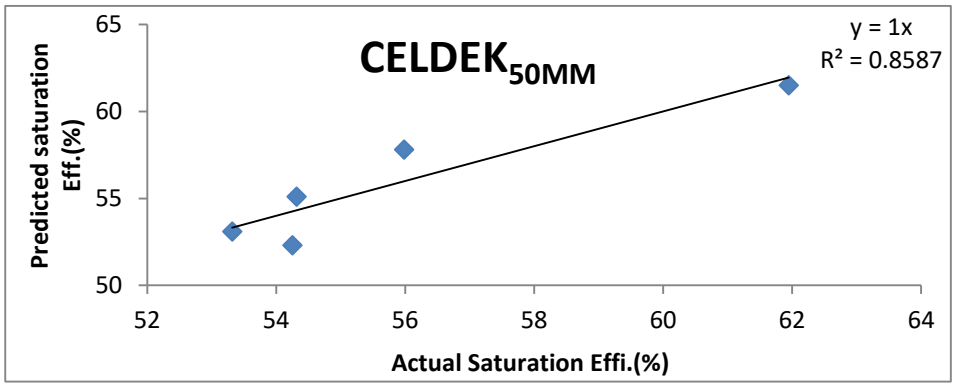

Graph of predicted against experimental data for equation 4.16

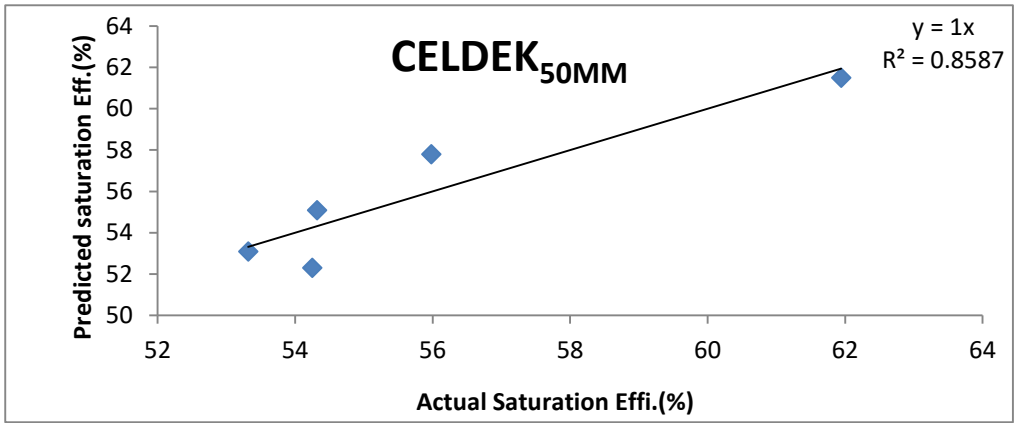

Graph of predicted against experimental data for equation 4.17

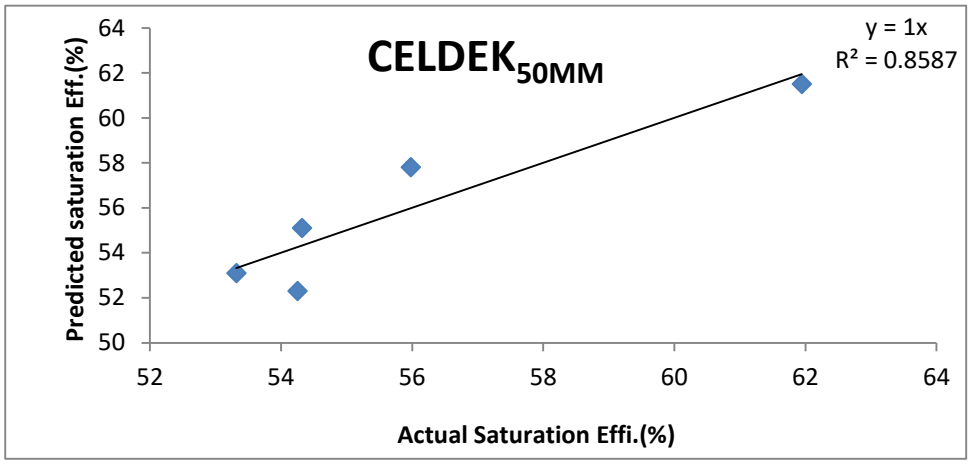

Graph of predicted against experimental data for equation 4.18

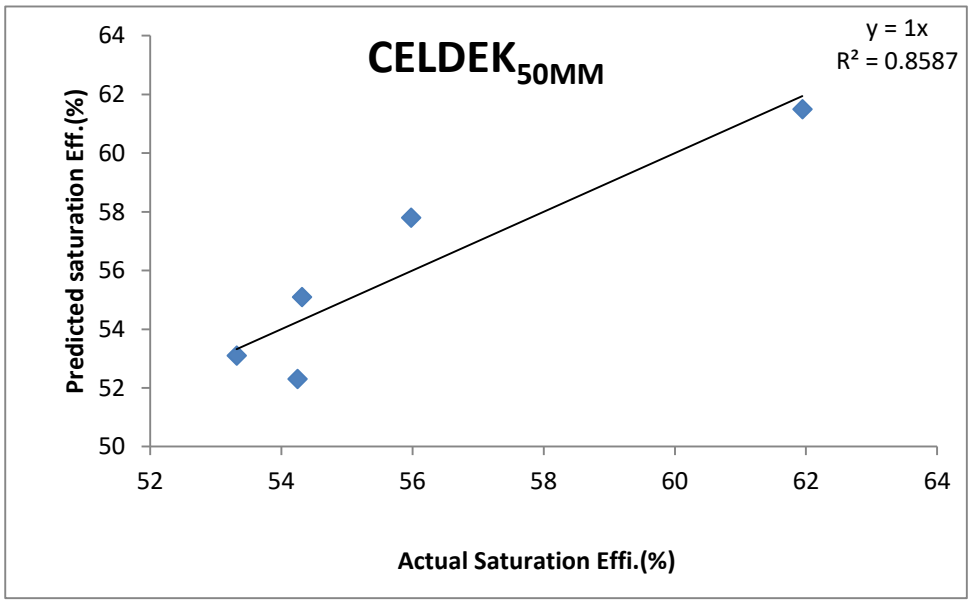

Graph of predicted against experimental data for equation 4.19

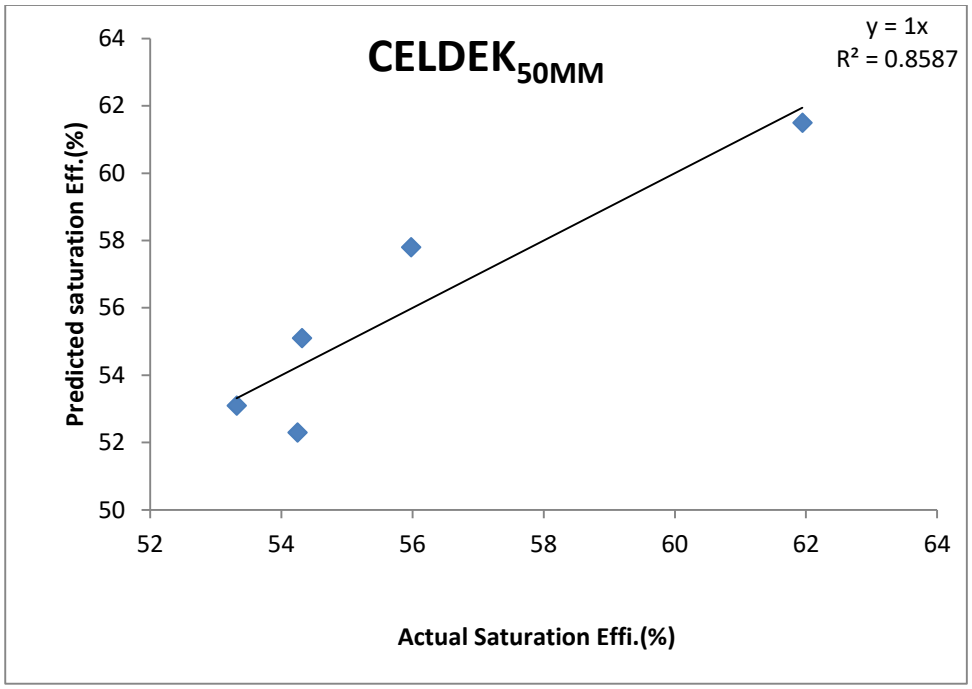

Graph of predicted against experimental data for equation 4.20

Appendix 4.23 Regression Analysis of Pressure Drop for Celdek Pad

CELDEK(50mm)

SUMMARY OUTPUT

Regression Statistics	
Multiple R	0.999471
R Square	0.998942
Adjusted R	0.497884
Standard E	0.637974
Observatio	5

ANOVA

	df	*SS*	*MS*	*F*	*ignificance F*
Regression	3	768.536	256.1787	629.4151	0.029291
Residual	2	0.814021	0.407011		
Total	5	769.35			

	Coefficients	*andard Erro*	*t Stat*	*P-value*	*Lower 95%*	*Upper 95%*	*ower 95.0%*	*Jpper 95.0%*
Intercept	0	#N/A	#N/A	#N/A	#N/A	#N/A	#N/A	#N/A
π1	23.80006	22.07636	1.078079	0.393749	-71.1868	118.787	-71.1868	118.787
π2	1.630368	0.263379	6.190194	0.025118	0.497139	2.763597	0.497139	2.763597
π4	-2974.96	2759.542	-1.07806	0.393755	-14848.3	8898.391	-14848.3	8898.391

RESIDUAL OUTPUT

Observation	*edicted (ΔP*	*Residuals*	*ıdard Residuals*
1	2.759708	0.640292	1.586883
2	5.917089	0.182911	0.453322
3	9.874569	-0.57457	-1.424
4	15.36263	-0.06263	-0.15522
5	19.80885	0.191151	0.473745

PROBABILITY OUTPUT

Percentile	*(ΔP)*
10	3.4
30	6.1
50	9.3
70	15.3
90	20

CELDEC(100mm)

SUMMARY OUTPUT

Regression Statistics	
Multiple R	0.999081369
R Square	0.998163583
Adjusted R	0.496327166
Standard E	1.014970811
Observatio	5

ANOVA

	df	*SS*	*MS*	*F*	*ignificance F*
Regression	3	1119.87	373.2899	362.3591	0.038593
Residual	2	2.060331	1.030166		
Total	5	1121.93			

	Coefficients	*andard Erro*	*t Stat*	*P-value*	*Lower 95%*	*Upper 95%*	*ower 95.0%*	*Upper 95.0%*
Intercept	0	#N/A	#N/A	#N/A	#N/A	#N/A	#N/A	#N/A
π1	-0.248752491	0.414122	-0.60067	0.609062	-2.03058	1.533072	-2.03058	1.533072
π2	34.00437269	6.544967	5.195499	0.035107	5.843652	62.16509	5.843652	62.16509
π4	4.088255136	6.479498	0.630952	0.592561	-23.7908	31.96728	-23.7908	31.96728

RESIDUAL OUTPUT

Observation	*Predicted (ΔP)*	*Residuals*	*ndard Residuals*
1	3.344110047	1.05589	1.644883
2	7.399321941	0.200678	0.31262
3	12.11980776	-0.91981	-1.43289
4	18.38099333	0.019007	0.029609
5	23.85761881	0.242381	0.377586

PROBABILITY OUTPUT

Percentile	*(ΔP)*
10	4.4
30	7.6
50	11.2
70	18.4
90	24.1

CELDEK(150mm)

SUMMARY OUTPUT

Regression Statistics	
Multiple R	0.999186728
R Square	0.998374117
Adjusted R	0.496748235
Standard E	1.14968584
Observatio	5

ANOVA

	df	*SS*	*MS*	*F*	*ignificance F*
Regression	3	1623.276	541.0921	409.367	0.036313
Residual	2	2.643555	1.321778		
Total	5	1625.92			

	Coefficients	*andard Erro*	*t Stat*	*P-value*	*Lower 95%*	*Upper 95%*	*ower 95.0%*	*Upper 95.0%*
Intercept	0	#N/A	#N/A	#N/A	#N/A	#N/A	#N/A	#N/A
π1	0.074108139	0.046538	1.592419	0.252295	-0.12613	0.274345	-0.12613	0.274345
π2	201.4916506	40.40185	4.987189	0.037933	27.65652	375.3268	27.65652	375.3268
π4	0.249981139	0.181785	1.375148	0.302865	-0.53218	1.032138	-0.53218	1.032138

RESIDUAL OUTPUT

Observation	*Predicted (ΔP)*	*Residuals*	*ndard Residuals*
1	5.700158614	-0.00016	-0.00022
2	8.810846798	0.689153	0.947778
3	14.62175488	-1.22175	-1.68025
4	21.29817639	0.801824	1.102731
5	29.08170528	-0.18171	-0.2499

PROBABILITY OUTPUT

Percentile	*(ΔP)*
10	5.7
30	9.5
50	13.4
70	22.1
90	28.9

CELDEK(200mm)

SUMMARY OUTPUT

Regression Statistics	
Multiple R	0.998033226
R Square	0.996070319
Adjusted R Sc	0.492140639
Standard Erro	2.154250567
Observations	5

ANOVA

	df	*SS*	*MS*	*F*	*ignificance F*
Regression	3	2352.638409	784.2128	168.9824	0.056475
Residual	2	9.281591007	4.640796		
Total	5	2361.92			

	Coefficients	*Standard Error*	*t Stat*	*P-value*	*Lower 95%*	*Upper 95%*	*ower 95.0%*	*Upper 95.0%*
Intercept	0	#N/A	#N/A	#N/A	#N/A	#N/A	#N/A	#N/A
π1	229.1452958	707.9454274	0.323676	0.776895	-2816.9	3275.189	-2816.9	3275.189
π2	958.8657834	295.3616178	3.246413	0.083212	-311.973	2229.704	-311.973	2229.704
π4	-446.925887	1383.572613	-0.32302	0.777323	-6399.96	5506.107	-6399.96	5506.107

RESIDUAL OUTPUT

Observation	*Predicted (ΔP)*	*Residuals*	*ıdard Residuals*
1	5.567461026	1.832538974	1.345015
2	11.64092474	0.259075264	0.190151
3	18.2825438	-2.1825438	-1.6019
4	25.45464368	1.045356319	0.767252
5	34.69784381	0.002156187	0.001583

PROBABILITY OUTPUT

Percentile	*(ΔP)*
10	7.4
30	11.9
50	16.1
70	26.5
90	34.7

CELDEK(250mm)

SUMMARY OUTPUT

Regression Statistics	
Multiple R	0.997442611
R Square	0.994891762
Adjusted R Sc	0.489783525
Standard Erro	2.959171179
Observations	5

ANOVA

	df	*SS*	*MS*	*F*	*ignificance F*
Regression	3	3410.946612	1136.982	129.8415	0.064402
Residual	2	17.51338813	8.756694		
Total	5	3428.46			

	Coefficients	*Standard Error*	*t Stat*	*P-value*	*Lower 95%*	*Upper 95%*	*ower 95.0%*	*Upper 95.0%*
Intercept	0	#N/A	#N/A	#N/A	#N/A	#N/A	#N/A	#N/A
π1	1297.849956	3005.57556	0.431814	0.707971	-11634.1	14229.8	-11634.1	14229.8
π2	3102.703313	998.8449281	3.106291	0.089883	-1194.98	7400.386	-1194.98	7400.386
π4	-1297.31894	3007.448892	-0.43137	0.708247	-14237.3	11642.69	-14237.3	11642.69

RESIDUAL OUTPUT

Observation	*Predicted (ΔP)*	*Residuals*	*ıdard Residuals*
1	7.12914494	2.47085506	1.320223
2	14.52511598	0.374884018	0.200307
3	22.32080818	-3.02080818	-1.61407
4	30.33629152	1.463708485	0.782086
5	41.6008876	-0.000887603	-0.00047

PROBABILITY OUTPUT

Percentile	*(ΔP)*
10	9.6
30	14.9
50	19.3
70	31.8
90	41.6

Appendix 4.24 Regression Analysis of Pressure Drop for Jute Fiber Pad

JUTE FIBER(50mm)

SUMMARY OUTPUT

Regression Statistics	
Multiple R	0.999249
R Square	0.998499
Adjusted R	0.496997
Standard E	2.411186
Observatio	5

ANOVA

	df	*SS*	*MS*	*F*	*ignificance F*
Regression	3	7733.332	2577.777	443.3882	0.034893
Residual	2	11.62763	5.813816		
Total	5	7744.96			

	Coefficients	*andard Erro*	*t Stat*	*P-value*	*Lower 95%*	*Upper 95%*	*ower 95.0%*	*Jpper 95.0%*
Intercept	0	#N/A	#N/A	#N/A	#N/A	#N/A	#N/A	#N/A
π1	23.23827	83.43632	0.278515	0.806772	-335.759	382.2358	-335.759	382.2358
π2	9.054045	0.995426	9.095646	0.011873	4.771071	13.33702	4.771071	13.33702
π4	-2904.82	10429.53	-0.27852	0.806769	-47779.5	41969.83	-47779.5	41969.83

RESIDUAL OUTPUT

Observation	*redicted (ΔP*	*Residuals*	*ıdard Residuals*
1	12.632	3.067997	2.011844
2	24.61261	-0.71261	-0.46729
3	35.94376	-1.04376	-0.68445
4	48.14296	-0.44296	-0.29047
5	57.95072	0.649279	0.425766

PROBABILITY OUTPUT

Percentile	*(ΔP)*
10	15.7
30	23.9
50	34.9
70	47.7
90	58.6

JUTE FIBER(100mm)

SUMMARY OUTPUT

Regression Statistics	
Multiple R	0.998893654
R Square	0.997788532
Adjusted R	0.495577063
Standard E	3.468545458
Observatio	5

ANOVA

	df	*SS*	*MS*	*F*	*ignificance F*
Regression	3	10856.32	3618.773	300.7922	0.042354
Residual	2	24.06162	12.03081		
Total	5	10880.38			

	Coefficients	*andard Erro*	*t Stat*	*P-value*	*Lower 95%*	*Upper 95%*	*ower 95.0%*	*Jpper 95.0%*
Intercept	0	#N/A	#N/A	#N/A	#N/A	#N/A	#N/A	#N/A
π1	-0.349872667	1.415215	-0.24722	0.827799	-6.43905	5.739306	-6.43905	5.739306
π2	190.7062268	22.36667	8.526358	0.013478	94.47022	286.9422	94.47022	286.9422
π4	5.06898928	22.14293	0.228921	0.840208	-90.2044	100.3423	-90.2044	100.3423

RESIDUAL OUTPUT

Observation	*Predicted (ΔP)*	*Residuals*	*ıdard Residuals*
1	16.07754141	4.322459	1.970396
2	30.7821555	-0.88216	-0.40213
3	43.93886036	-2.03886	-0.92942
4	57.14800168	0.051998	0.023703
5	66.73658969	0.66341	0.302416

PROBABILITY OUTPUT

Percentile	*(ΔP)*
10	20.4
30	29.9
50	41.9
70	57.2
90	67.4

JUTE FIBER(150mm)

SUMMARY OUTPUT

Regression Statistics	
Multiple R	0.99974566
R Square	0.999491385
Adjusted R	0.498982771
Standard E	2.009695645
Observatio	5

ANOVA

	df	*SS*	*MS*	*F*	*ignificance F*
Regression	3	15873.79	5291.264	1310.083	0.020306
Residual	2	8.077753	4.038877		
Total	5	15881.87			

	Coefficients	*andard Erro*	*t Stat*	*P-value*	*Lower 95%*	*Upper 95%*	*ower 95.0%*	*Upper 95.0%*
Intercept	0	#N/A	#N/A	#N/A	#N/A	#N/A	#N/A	#N/A
π1	-0.418457231	0.08135	-5.14389	0.035778	-0.76848	-0.06843	-0.76848	-0.06843
π2	1120.454334	70.62401	15.86506	0.003949	816.5837	1424.325	816.5837	1424.325
π4	1.105549789	0.317767	3.479121	0.07361	-0.26169	2.472791	-0.26169	2.472791

RESIDUAL OUTPUT

Observation	*Predicted (ΔP)*	*Residuals*	*ıdard Residuals*
1	26.50027325	-0.00027	-0.00021
2	36.18825159	1.211748	0.95335
3	52.43749735	-2.1375	-1.68169
4	67.20626347	1.393737	1.09653
5	81.21308537	-0.31309	-0.24632

PROBABILITY OUTPUT

Percentile	*(ΔP)*
10	26.5
30	37.4
50	50.3
70	68.6
90	80.9

JUTE FIBER(200mm)

SUMMARY OUTPUT

Regression Statistics	
Multiple R	0.997709868
R Square	0.99542498
Adjusted R Sq	0.49084996
Standard Erro	7.288614242
Observations	5

ANOVA

	df	*SS*	*MS*	*F*	*ignificance F*
Regression	3	23117.2122	7705.737	145.0522	0.060943
Residual	2	106.2477951	53.1239		
Total	5	23223.46			

	Coefficients	*Standard Error*	*t Stat*	*P-value*	*Lower 95%*	*Upper 95%*	*ower 95.0%*	*Upper 95.0%*
Intercept	0	#N/A	#N/A	#N/A	#N/A	#N/A	#N/A	#N/A
π1	1348.814834	2395.237214	0.563124	0.630061	-8957.06	11654.69	-8957.06	11654.69
π2	5209.72465	999.3159234	5.213291	0.03488	910.0153	9509.434	910.0153	9509.434
π4	-2639.448887	4681.130045	-0.56385	0.62965	-22780.7	17501.83	-22780.7	17501.83

RESIDUAL OUTPUT

Observation	*Predicted (ΔP)*	*Residuals*	*ıdard Residuals*
1	26.54233844	7.857661563	1.704584
2	48.46220429	-1.662204293	-0.36059
3	66.06626248	-5.666262478	-1.2292
4	79.19589486	3.104105144	0.673382
5	97.09474976	0.005250243	0.001139

PROBABILITY OUTPUT

Percentile	*(ΔP)*
10	34.4
30	46.8
50	60.4
70	82.3
90	97.1

JUTE FIBER(250mm)

SUMMARY OUTPUT

Regression Statistics	
Multiple R	0.99686306
R Square	0.99373596
Adjusted R Squa	0.487471919
Standard Error	10.32089539
Observations	5

ANOVA

	df	*SS*	*MS*	*F*	*ignificance F*
Regression	3	33797.23824	11265.75	105.7609	0.071331
Residual	2	213.0417631	106.5209		
Total	5	34010.28			

	Coefficients	*Standard Error*	*t Stat*	*P-value*	*Lower 95%*	*Upper 95%*	*ower 95.0%*	*Upper 95.0%*
Intercept	0	#N/A	#N/A	#N/A	#N/A	#N/A	#N/A	#N/A
π1	6970.488837	10482.74299	0.664949	0.574498	-38133.1	52074.09	-38133.1	52074.09
π2	16527.09528	3483.736961	4.744071	0.041674	1537.785	31516.41	1537.785	31516.41
π4	-6982.658314	10489.27673	-0.66569	0.574107	-52114.4	38149.06	-52114.4	38149.06

RESIDUAL OUTPUT

Observation	*Predicted (ΔP)*	*Residuals*	*ıdard Residuals*
1	33.76705991	10.93294009	1.674903
2	60.59423355	-2.09423355	-0.32083
3	80.78336207	-8.28336207	-1.26899
4	94.2709071	4.529092897	0.693847
5	116.5006749	-0.00067489	-0.0001

PROBABILITY OUTPUT

Percentile	*(ΔP)*
10	44.7
30	58.5
50	72.5
70	98.8
90	116.5

Appendix 4.25 Regression Analysis of Pressure Drop for **Co**conut Fiber Pad

COCONUT FIBER(50mm)

SUMMARY OUTPUT

Regression Statistics	
Multiple R	0.999336
R Square	0.998673
Adjusted R	0.497346
Standard E	1.846881
Observatio	5

ANOVA

	df	*SS*	*MS*	*F*	*ignificance F*
Regression	3	5134.028	1711.343	501.7176	0.032804
Residual	2	6.821936	3.410968		
Total	5	5140.85			

	Coefficients	*tandard Erro*	*t Stat*	*P-value*	*Lower 95%*	*Upper 95%*	*ower 95.0%*	*Upper 95.0%*
Intercept	0	#N/A	#N/A	#N/A	#N/A	#N/A	#N/A	#N/A
π1	33.36702	63.90919	0.5221	0.653667	-241.612	308.3461	-241.612	308.3461
π2	6.62305	0.76246	8.686417	0.012995	3.342447	9.903652	3.342447	9.903652
π4	-4170.87	7988.642	-0.5221	0.653667	-38543.2	30201.48	-38543.2	30201.48

RESIDUAL OUTPUT

Observation	*edicted (ΔP*	*Residuals*	*ıdard Residuals*
1	9.56329	2.23671	1.914877
2	18.91494	-0.11494	-0.0984
3	28.39616	-1.19616	-1.02405
4	39.48656	-0.28656	-0.24533
5	48.15876	0.541241	0.463364

PROBABILITY OUTPUT

Percentile	*(ΔP)*
10	11.8
30	18.8
50	27.2
70	39.2
90	48.7

COCONUT FIBER(100mm)

SUMMARY OUTPUT

Regression Statistics	
Multiple R	0.998909018
R Square	0.997819225
Adjusted R	0.495638451
Standard E	2.802260537
Observatio	5

ANOVA

	df	*SS*	*MS*	*F*	*ignificance F*
Regression	3	7186.015	2395.338	305.0351	0.042059
Residual	2	15.70533	7.852664		
Total	5	7201.72			

	Coefficients	*tandard Erro*	*t Stat*	*P-value*	*Lower 95%*	*Upper 95%*	*ower 95.0%*	*Upper 95.0%*
Intercept	0	#N/A	#N/A	#N/A	#N/A	#N/A	#N/A	#N/A
π1	-0.592628343	1.143361	-0.51832	0.655876	-5.51212	4.326859	-5.51212	4.326859
π2	139.4225415	18.07018	7.715615	0.016386	61.67284	217.1722	61.67284	217.1722
π4	9.122673728	17.88942	0.509948	0.660791	-67.8493	86.09464	-67.8493	86.09464

RESIDUAL OUTPUT

Observation	*Predicted (ΔP)*	*Residuals*	*ndard Residuals*
1	12.02332336	3.276677	1.848822
2	23.58207181	-0.08207	-0.04631
3	34.54010081	-2.1401	-1.20752
4	47.05169508	0.048305	0.027255
5	55.48386866	0.616131	0.347644

PROBABILITY OUTPUT

Percentile	*(ΔP)*
10	15.3
30	23.5
50	32.4
70	47.1
90	56.1

COCONUT FIBER(150mm)

SUMMARY OUTPUT

Regression Statistics	
Multiple R	0.999390697
R Square	0.998781765
Adjusted R	0.49756353
Standard Er	2.528391078
Observatior	5

ANOVA

	df	*SS*	*MS*	*F*	*ignificance F*
Regression	3	10482.334	3494.111	546.5731	0.03143
Residual	2	12.785523	6.392761		
Total	5	10495.12			

	Coefficients	*tandard Erro*	*t Stat*	*P-value*	*Lower 95%*	*Upper 95%*	*ower 95.0%*	*Upper 95.0%*
Intercept	0	#N/A	#N/A	#N/A	#N/A	#N/A	#N/A	#N/A
π1	-0.22412379	0.1023467	-2.18985	0.159949	-0.66449	0.216238	-0.6645	0.216238
π2	829.0722163	88.851821	9.330954	0.011291	446.7737	1211.371	446.774	1211.371
π4	0.816010595	0.3997816	2.041141	0.178018	-0.90411	2.536132	-0.9041	2.536132

RESIDUAL OUTPUT

Observation	*Predicted (ΔP)*	*Residuals*	*ıdard Residuals*
1	19.90041187	-0.000412	-0.00026
2	27.99864684	1.4013532	0.876341
3	41.55418277	-2.654183	-1.6598
4	54.61445105	1.885549	1.179135
5	67.77090446	-0.470904	-0.29448

PROBABILITY OUTPUT

Percentile	*(ΔP)*
10	19.9
30	29.4
50	38.9
70	56.5
90	67.3

COCONUT FIBER(200mm)

SUMMARY OUTPUT

Regression Statistics	
Multiple R	0.997521101
R Square	0.995048346
Adjusted R Squ	0.490096692
Standard Error	6.161001695
Observations	5

ANOVA

	df	*SS*	*MS*	*F*	*ignificance F*
Regression	3	15255.5041	5085.168	133.9685	0.063406
Residual	2	75.9158838	37.95794		
Total	5	15331.42			

	Coefficients	*Standard Erro*	*t Stat*	*P-value*	*Lower 95%*	*Upper 95%*	*ower 95.0%*	*Upper 95.0%*
Intercept	0	#N/A	#N/A	#N/A	#N/A	#N/A	#N/A	#N/A
π1	810.9202372	2024.67301	0.400519	0.727507	-7900.54	9522.385	-7900.54	9522.385
π2	3806.785006	844.712986	4.506602	0.045876	172.2784	7441.292	172.2784	7441.292
π4	-1586.503375	3956.91817	-0.40094	0.72724	-18611.7	15438.74	-18611.7	15438.74

RESIDUAL OUTPUT

Observation	*Predicted (ΔP)*	*Residuals*	*ıdard Residuals*
1	19.83906516	6.06093484	1.555458
2	37.18524628	-0.3852463	-0.09887
3	52.26475354	-5.5647535	-1.42812
4	64.95992474	2.84007526	0.728867
5	80.79465814	0.00534186	0.001371

PROBABILITY OUTPUT

Percentile	*(ΔP)*
10	25.9
30	36.8
50	46.7
70	67.8
90	80.8

COCONUT FIBER(250mm)

SUMMARY OUTPUT

Regression Statistics	
Multiple R	0.996691987
R Square	0.993394916
Adjusted R Squ	0.486789833
Standard Error	8.609249565
Observations	5

ANOVA

	df	*SS*	*MS*	*F*	*ignificance F*
Regression	3	22294.83164	7431.611	100.2657	0.073251
Residual	2	148.2383561	74.11918		
Total	5	22443.07			

	Coefficients	*Standard Error*	*t Stat*	*P-value*	*Lower 95%*	*Upper 95%*	*ower 95.0%*	*Upper 95.0%*
Intercept	0	#N/A	#N/A	#N/A	#N/A	#N/A	#N/A	#N/A
π1	4590.171787	8744.255913	0.524936	0.652014	-33033.3	42213.67	-33033.3	42213.67
π2	12159.1291	2905.984393	4.184169	0.052649	-344.313	24662.57	-344.313	24662.57
π4	-4597.34376	8749.706084	-0.52543	0.651727	-42244.3	33049.6	-42244.3	33049.6

RESIDUAL OUTPUT

Observation	*Predicted (ΔP)*	*Residuals*	*ıdard Residuals*
1	25.3428019	8.357198101	1.534848
2	46.57212806	-0.472128061	-0.08671
3	63.96055382	-7.860553824	-1.44364
4	77.35223735	4.047762652	0.743395
5	97.00149409	-0.001494088	-0.00027

PROBABILITY OUTPUT

Percentile	*(ΔP)*
10	33.7
30	46.1
50	56.1
70	81.4
90	97

Appendix 4.26 Regression Analysis of Pressure Drop for Pop Sponge Fiber Pad

SPONGE(50mm

SUMMARY OUTPUT

Regression Statistics	
Multiple R	0.999403
R Square	0.998807
Adjusted R	0.497614
Standard E	1.345939
Observatio	5

ANOVA

	df	*SS*	*MS*	*F*	*ignificance F*
Regression	3	3032.877	1010.959	558.062	0.031105
Residual	2	3.623106	1.811553		
Total	5	3036.5			

	Coefficients	*andard Erro*	*t Stat*	*P-value*	*Lower 95%*	*Upper 95%*	*ower 95.0%*	*Upper 95.0%*
Intercept	0	#N/A	#N/A	#N/A	#N/A	#N/A	#N/A	#N/A
π1	41.18112	46.5747	0.884195	0.469867	-159.214	241.5759	-159.214	241.5759
π2	3.919234	0.555653	7.053378	0.019514	1.52845	6.310018	1.52845	6.310018
π4	-5147.58	5821.832	-0.88419	0.469871	-30196.9	19901.74	-30196.9	19901.74

RESIDUAL OUTPUT

Observation	*edicted (ΔP*	*Residuals*	*ıdard Residuals*
1	6.179507	1.320493	1.551246
2	12.77698	0.423022	0.496944
3	20.43422	-1.23422	-1.44989
4	30.52505	-0.12505	-0.1469
5	38.4981	0.401902	0.472133

)

PROBABILITY OUTPUT

Percentile	*(ΔP)*
10	7.5
30	13.2
50	19.2
70	30.4
90	38.9

POP SPONGE(100mm)

SUMMARY OUTPUT

Regression Statistics	
Multiple R	0.99911
R Square	0.99822
Adjusted R	0.49644
Standard E	1.940731
Observatio	5

ANOVA

	df	*SS*	*MS*	*F*	*ignificance F*
Regression	3	4224.707	1408.236	373.8906	0.037994
Residual	2	7.532876	3.766438		
Total	5	4232.24			

	Coefficients	*andard Erro*	*t Stat*	*P-value*	*Lower 95%*	*Upper 95%*	*ower 95.0%*	*Jpper 95.0%*
Intercept	0	#N/A	#N/A	#N/A	#N/A	#N/A	#N/A	#N/A
π1	-0.72935	0.791845	-0.92108	0.454245	-4.13639	2.677684	-4.13639	2.677684
π2	85.56521	12.51467	6.837194	0.020729	31.71894	139.4115	31.71894	139.4115
π4	11.54503	12.38948	0.931841	0.449791	-41.7626	64.85267	-41.7626	64.85267

RESIDUAL OUTPUT

Observation	*edicted (ΔP*	*Residuals*	*ıdard Residuals*
1	7.78726	2.01274	1.639805
2	16.10719	0.392809	0.320027
3	24.86375	-1.76375	-1.43695
4	36.46361	0.036386	0.029644
5	44.23599	0.464011	0.378036

PROBABILITY OUTPUT

Percentile	*(ΔP)*
10	9.8
30	16.5
50	23.1
70	36.5
90	44.7

P0OP SPONGE150 POP SPONGE(200mm)

SUMMARY OUTPUT

Regression Statistics	
Multiple R	0.997686
R Square	0.995378
Adjusted R	0.490756
Standard E	4.54577
Observatio	5

ANOVA

	df	*SS*	*MS*	*F*	*ignificance F*
Regression	3	8900.052	2966.684	143.5676	0.061256
Residual	2	41.32806	20.66403		
Total	5	8941.38			

	Coefficients	*andard Erro*	*t Stat*	*P-value*	*Lower 95%*	*Upper 95%*	*ower 95.0%*	*Jpper 95.0%*
Intercept	0	#N/A	#N/A	#N/A	#N/A	#N/A	#N/A	#N/A
π1	210.3426	1493.864	0.140804	0.900926	-6217.24	6637.921	-6217.24	6637.921
π2	2293.945	623.2544	3.680593	0.066536	-387.702	4975.593	-387.702	4975.593
π4	-410.833	2919.532	-0.14072	0.900986	-12972.6	12150.9	-12972.6	12150.9

RESIDUAL OUTPUT

Observation	*edicted (ΔP*	*Residuals*	*ıdard Residuals*
1	12.65972	3.84028	1.335751
2	25.2206	0.579398	0.20153
3	37.82232	-4.62232	-1.60777
4	50.39121	2.208785	0.768274
5	64.29543	0.004571	0.00159

PROBABILITY OUTPUT

Percentile	*(ΔP)*
10	16.5
30	25.8
50	33.2
70	52.6
90	64.3

POP SPONGE(200mm)

SUMMARY OUTPUT

Regression Statistics	
Multiple R	0.997686
R Square	0.995378
Adjusted R	0.490756
Standard E	4.54577
Observatio	5

ANOVA

	df	*SS*	*MS*	*F*	*ignificance F*
Regression	3	8900.052	2966.684	143.5676	0.061256
Residual	2	41.32806	20.66403		
Total	5	8941.38			

	Coefficients	*andard Erro*	*t Stat*	*P-value*	*Lower 95%*	*Upper 95%*	*ower 95.0%*	*Jpper 95.0%*
Intercept	0	#N/A	#N/A	#N/A	#N/A	#N/A	#N/A	#N/A
π1	210.3426	1493.864	0.140804	0.900926	-6217.24	6637.921	-6217.24	6637.921
π2	2293.945	623.2544	3.680593	0.066536	-387.702	4975.593	-387.702	4975.593
π4	-410.833	2919.532	-0.14072	0.900986	-12972.6	12150.9	-12972.6	12150.9

RESIDUAL OUTPUT

Observation	*edicted (ΔP*	*Residuals*	*ıdard Residuals*
1	12.65972	3.84028	1.335751
2	25.2206	0.579398	0.20153
3	37.82232	-4.62232	-1.60777
4	50.39121	2.208785	0.768274
5	64.29543	0.004571	0.00159

PROBABILITY OUTPUT

Percentile	*(ΔP)*
10	16.5
30	25.8
50	33.2
70	52.6
90	64.3

POP SPONGE(250mm)

SUMMARY OUTPUT

Regression Statistics	
Multiple R	0.996947839
R Square	0.993904994
Adjusted R Sq	0.487809987
Standard Erro	6.301754222
Observations	5

ANOVA

	df	*SS*	*MS*	*F*	*ignificance F*
Regression	3	12951.60579	4317.202	108.7125	0.07036
Residual	2	79.42421255	39.71211		
Total	5	13031.03			

	Coefficients	*Standard Error*	*t Stat*	*P-value*	*Lower 95%*	*Upper 95%*	*ower 95.0%*	*Jpper 95.0%*
Intercept	0	#N/A	#N/A	#N/A	#N/A	#N/A	#N/A	#N/A
π1	1882.801158	6400.575474	0.294161	0.796355	-25656.7	29422.25	-25656.7	29422.25
π2	7388.352933	2127.107511	3.473427	0.073825	-1763.85	16540.56	-1763.85	16540.56
π4	-1884.266931	6404.564862	-0.29421	0.796325	-29440.9	25672.35	-29440.9	25672.35

RESIDUAL OUTPUT

Observation	*Predicted (ΔP)*	*Residuals*	*ıdard Residuals*
1	16.21126794	5.288732061	1.326967
2	31.53413254	0.765867464	0.19216
3	46.21637242	-6.41637242	-1.6099
4	59.9859778	3.114022196	0.781322
5	77.20186819	-0.001868188	-0.00047

PROBABILITY OUTPUT

Percentile	*(ΔP)*
10	21.5
30	32.3
50	39.8
70	63.1
90	77.2

Appendix 4.27 Validation of Pressure Drop Models for Celdek Pad

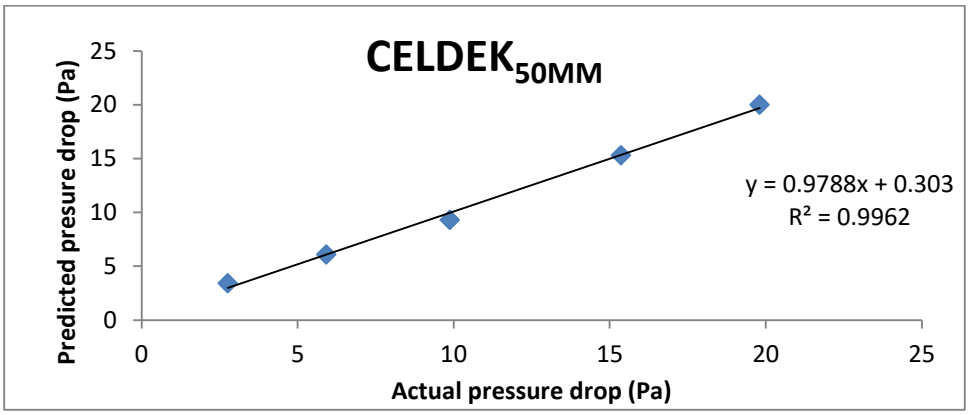

Graph of predicted against experimental data for equation 4.21

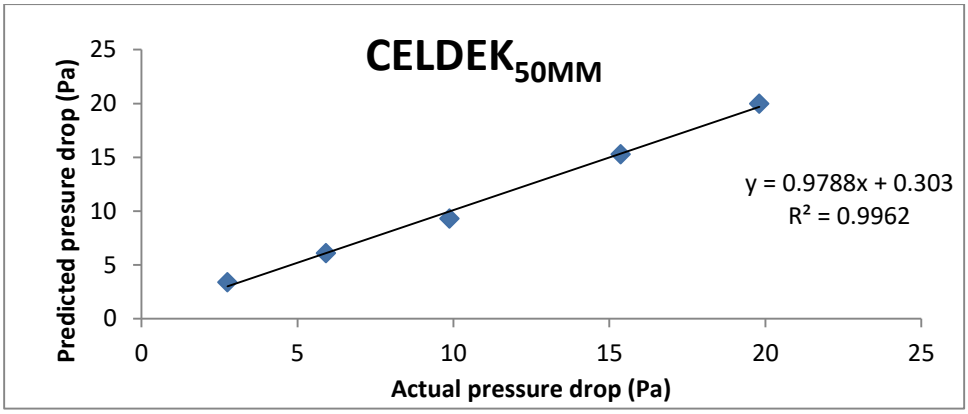

Graph of predicted against experimental data for equation 4.22

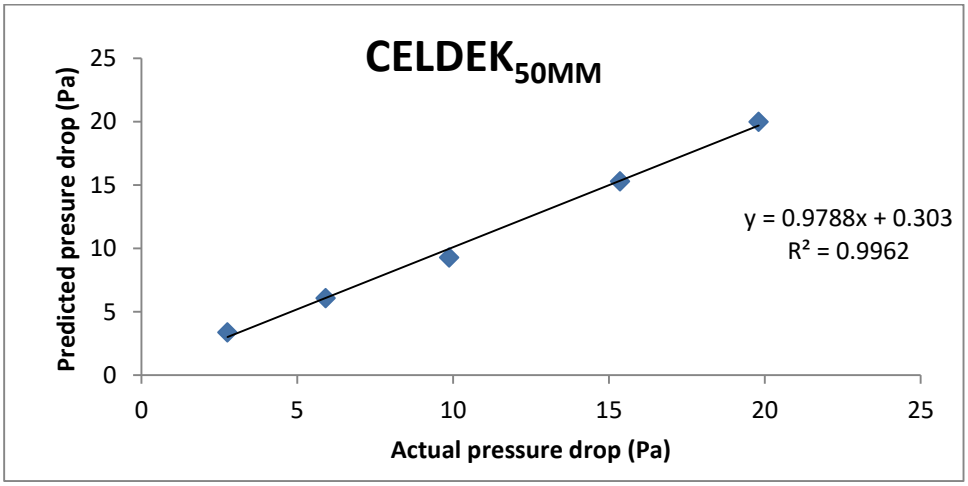

Graph of predicted against experimental data for equation 4.23

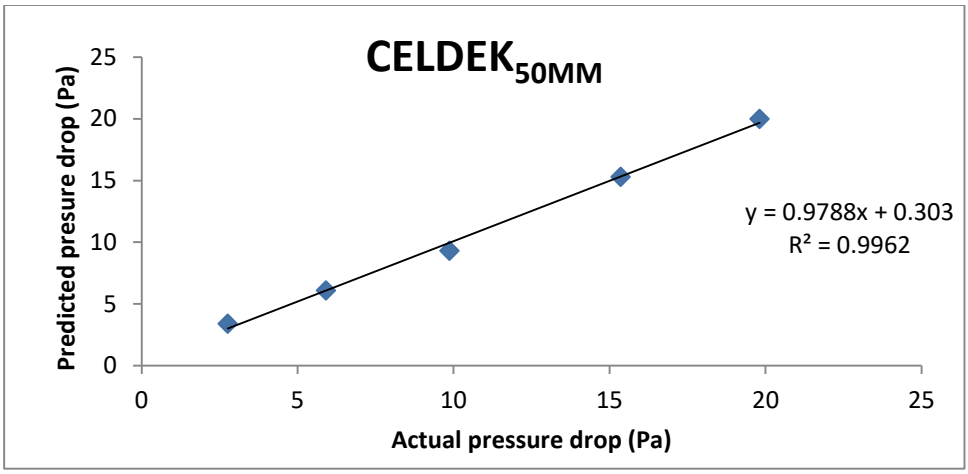

Graph of predicted against experimental data for equation 4.24

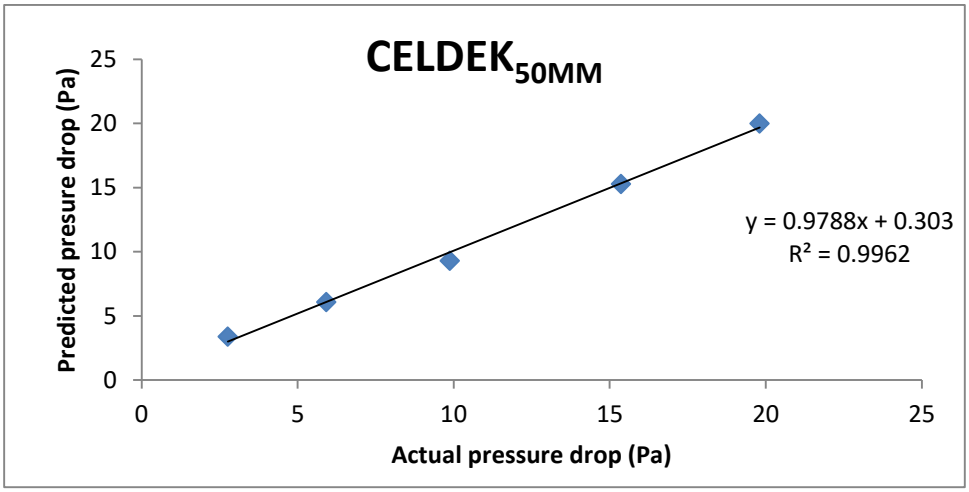

Graph of predicted against experimental data for equation 4.25

Appendix 4.28 Validation of Pressure Drop Models for Jute Fiber Pad

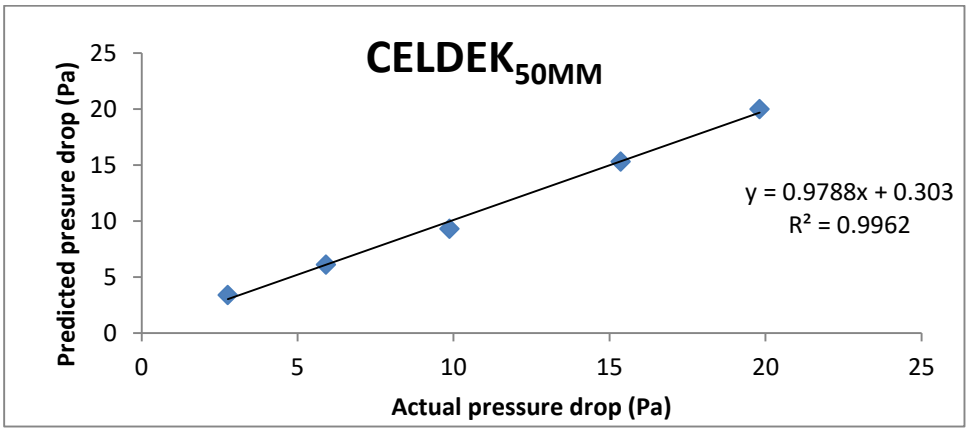

Graph of predicted against experimental data for equation 4.26

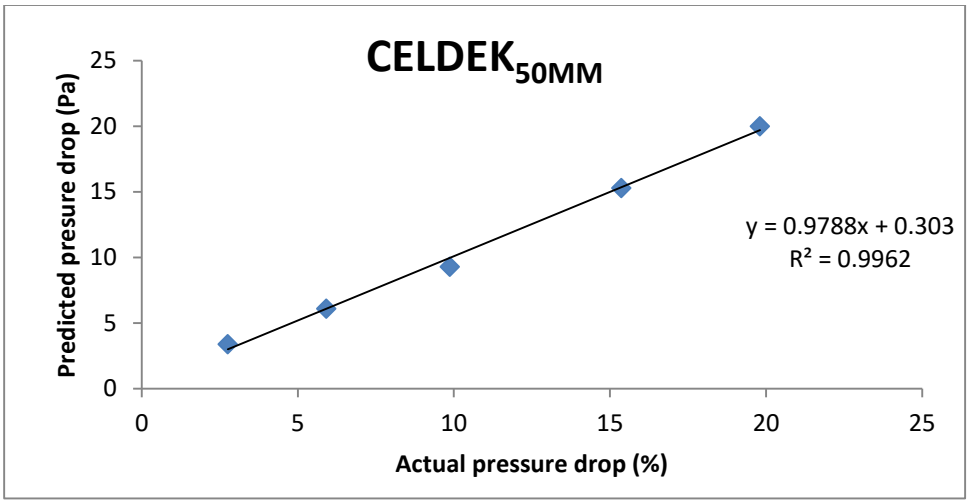

Graph of predicted against experimental data for equation 4.27

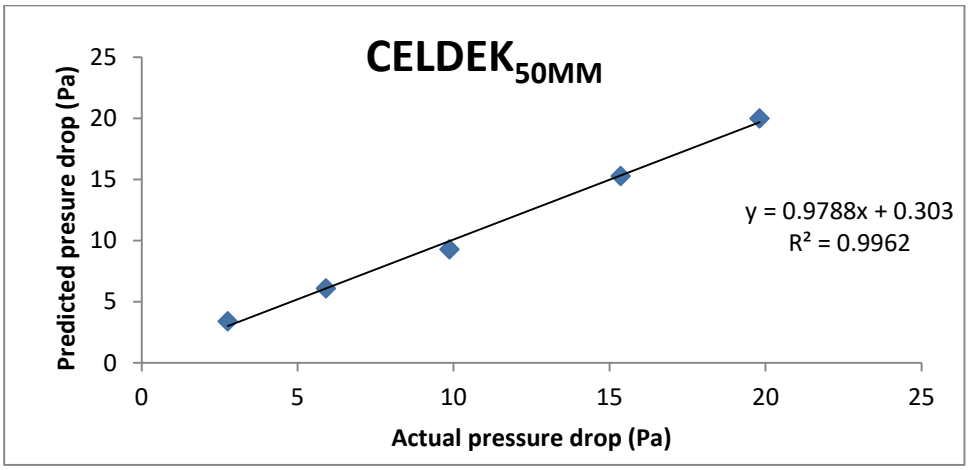

Graph of predicted against experimental data for equation 4.28

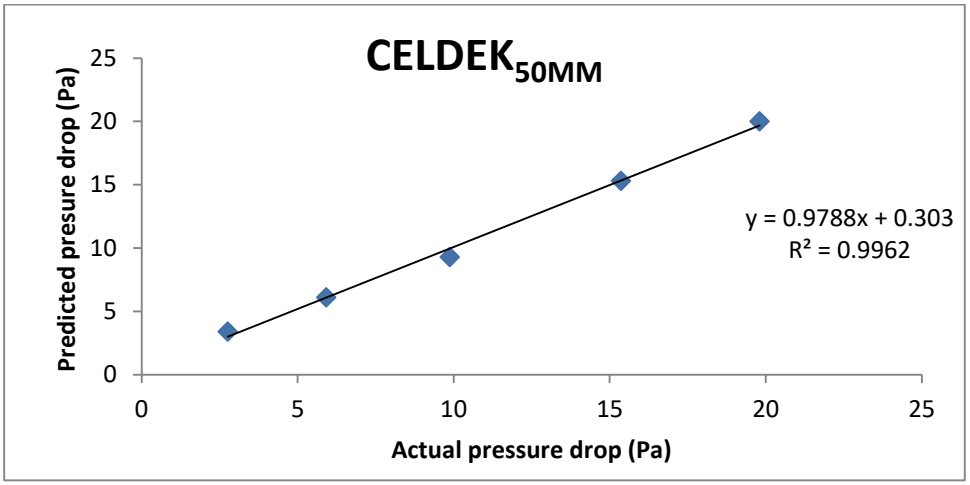

Graph of predicted against experimental data for equation 4.29

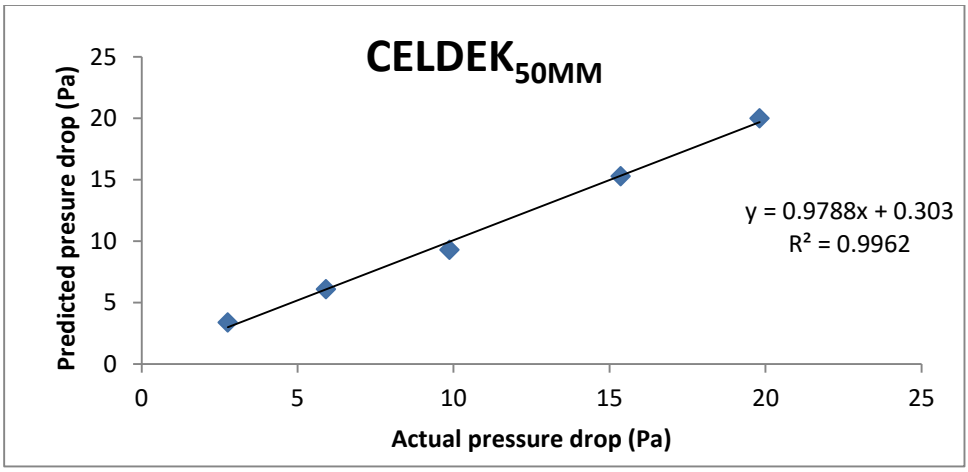

Graph of predicted against experimental data for equation 4.30

Appendix 4.29 Validation of Pressure Drop Models for Coconut Fiber Pad

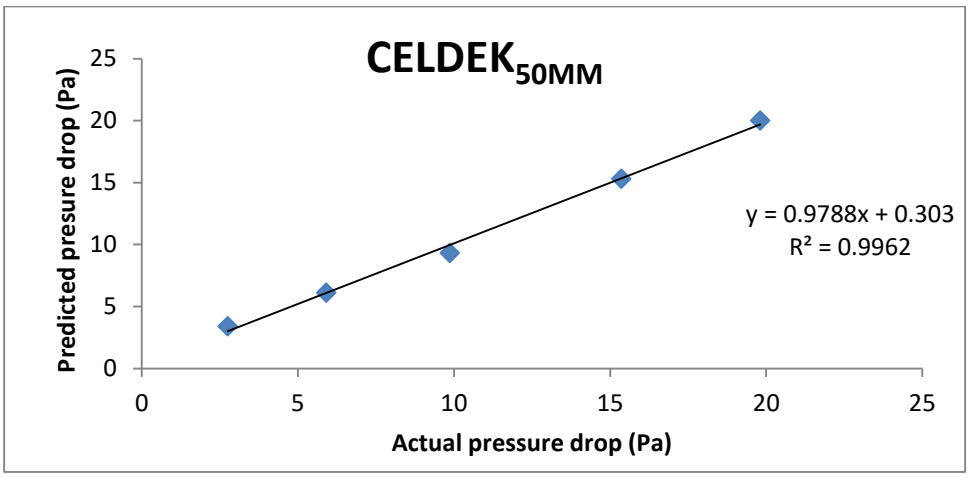

Graph of predicted against experimental data for equation 4.31

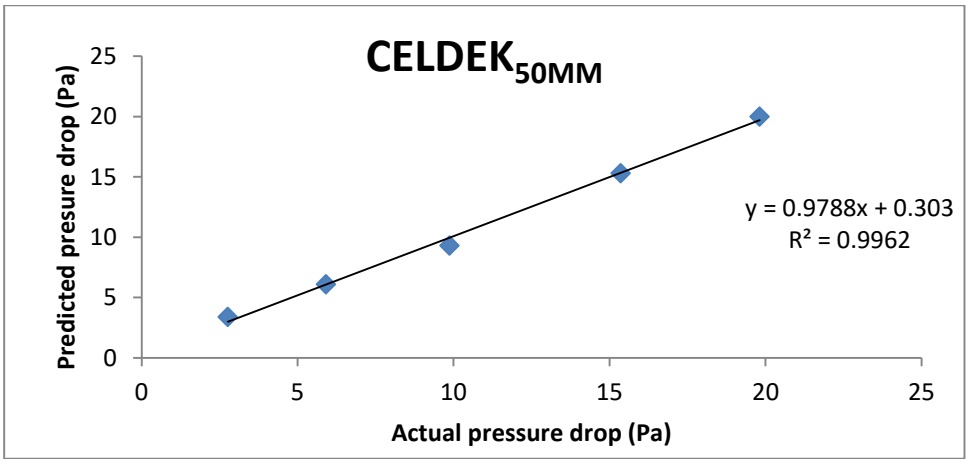

Graph of predicted against experimental data for equation 4.32

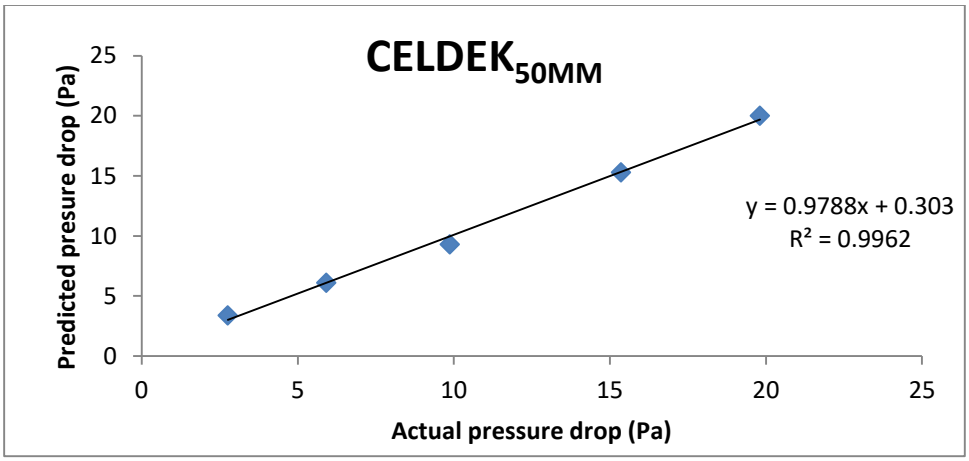

Graph of predicted against experimental data for equation 4.33

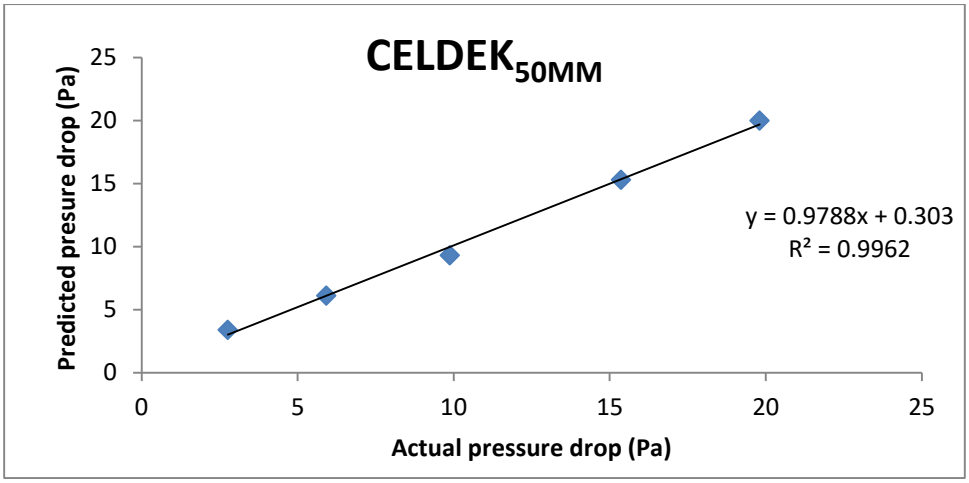

Graph of predicted against experimental data for equation 4.34

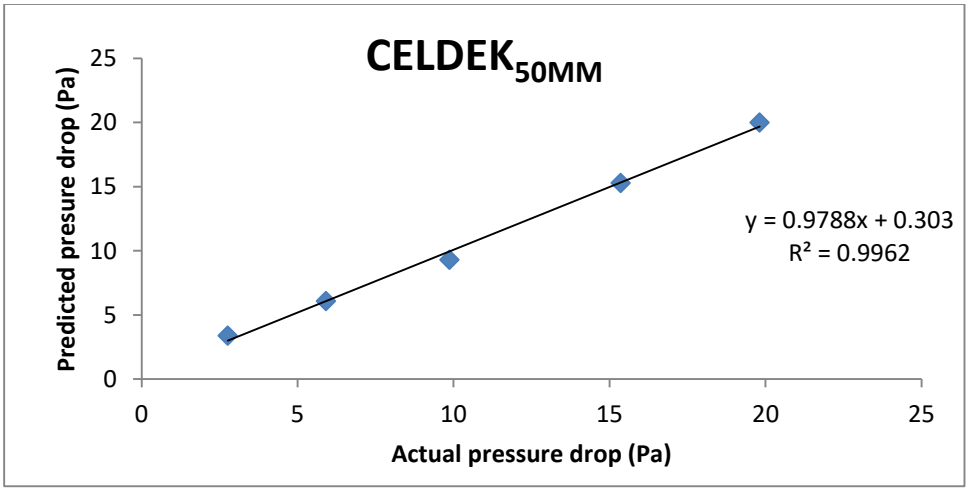

Graph of predicted against experimental data for equation 4.35

Appendix 4.30 Validation of Pressure Drop Models for Pop Sponge Pad

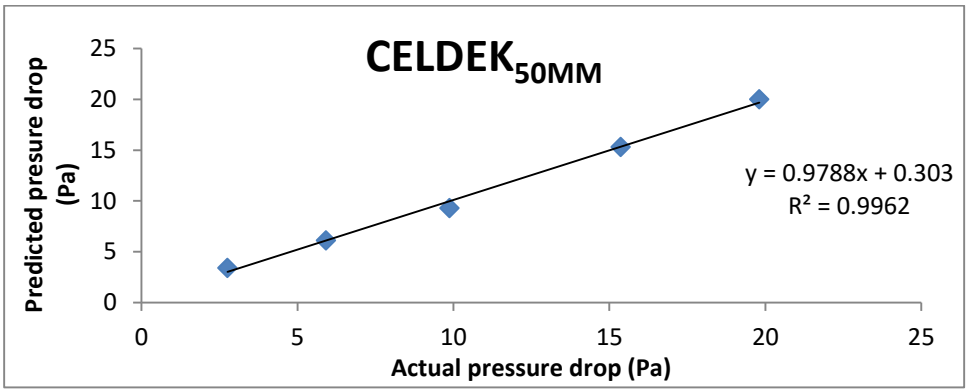

Graph of predicted against experimental data for equation 4.36

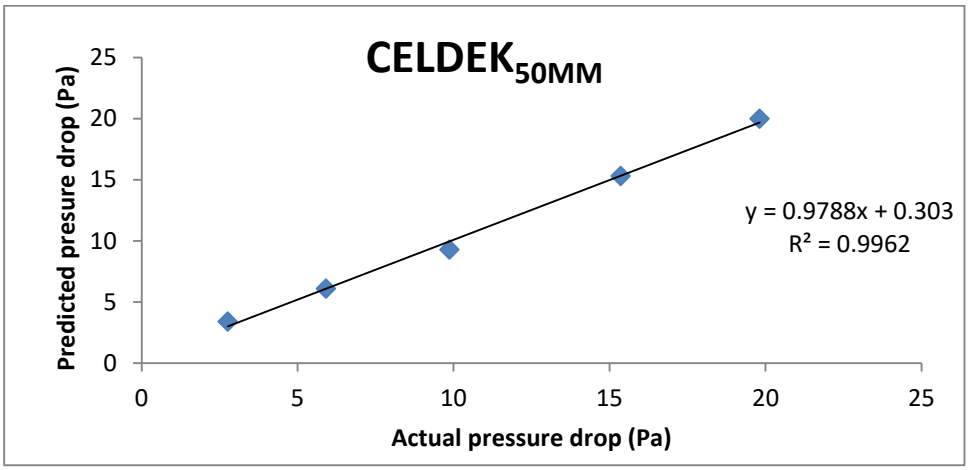

Graph of predicted against experimental data for equation 4.37

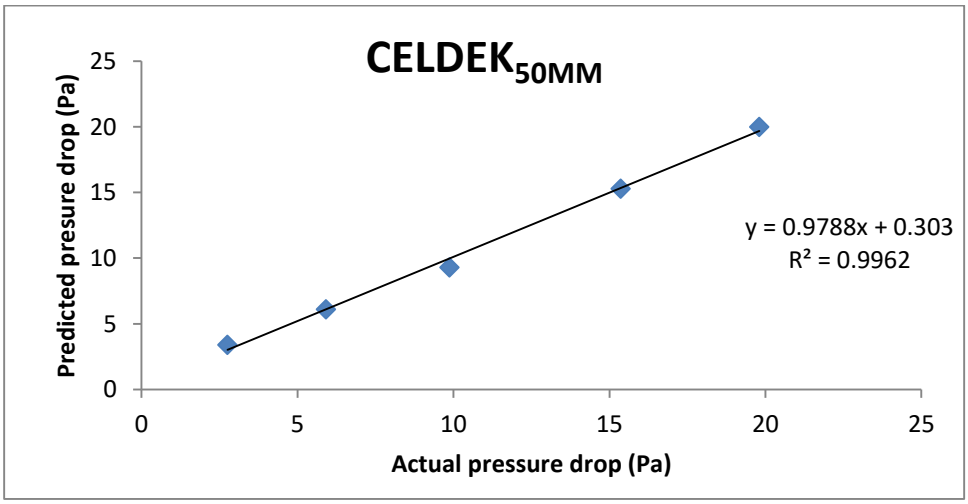

Graph of predicted against experimental data for equation 4.38

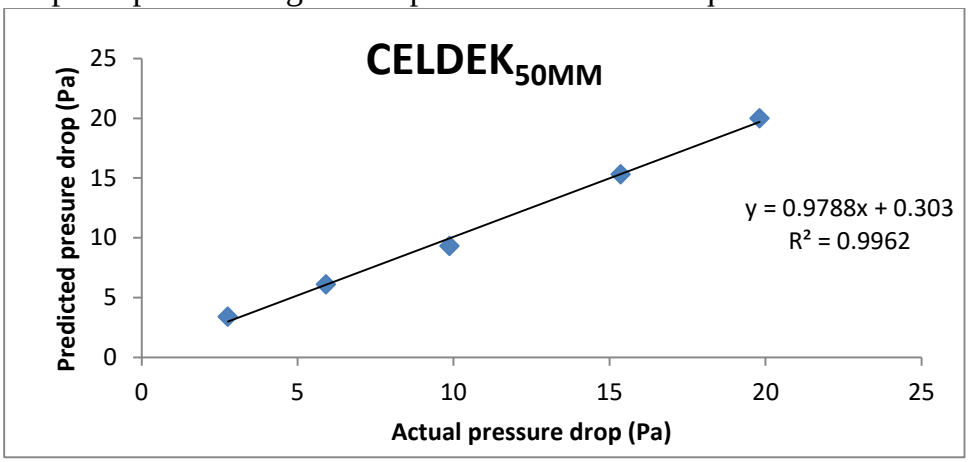

Graph of predicted against experimental data for equation 4.39

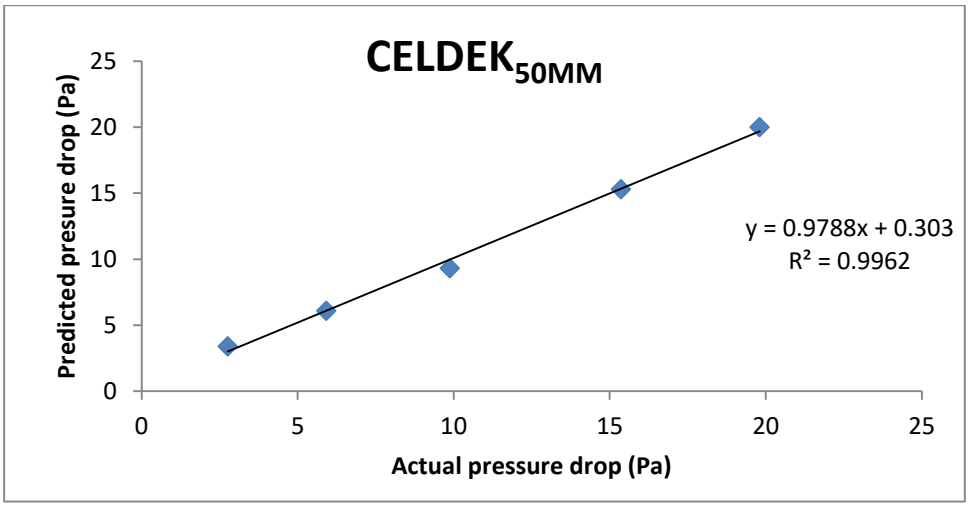

Graph of predicted against experimental data for equation 4.40